Deciphering the oxylipin signaling pathways during defense responses in brown macroalgae

Qikun Xing

Sorbonne Université

Ecole doctorale 227 - Sciences de la Nature et de l'Homme : Ecologie et Evolution

Laboratoire de Biologie Intégrative des Modèles Marins UMR8227

Equipe Biologie des algues et interactions avec l'environnement

Deciphering the oxylipin signaling pathways during defense responses in brown macroalgae

Par Qikun Xing

Thèse de doctorat en Biologie Marine

Dirigée par Catherine Leblanc

Présentée et soutenue publiquement le 25 juin 2021

Devant un jury composé de :

Dr. Debora Gasperini	Leibniz Institute of Plant Biochemistry, Halle	Rapportrice
Prof. Emmanuel Gaquerel	IBMP, Strasbourg	Rapporteur
Dr. Gwenaël Piganeau	Observatoire Océanologique de Banyuls	Examinatrice
Prof. Georg Pohnert	Friedrich-Schiller-Universität Jena	Examinateur
Prof. Claire Gachon	MNHN, Paris	Examinatrice
Dr. Catherine Leblanc	Station Biologique de Roscoff	Directrice de thèse
Dr. Gabriel Markov	Station Biologique de Roscoff	Membre invité

Acknowledgements

First of all, I would like to thank my supervisor Catherine Leblanc. I am very lucky to have you as my supervisor. During my PhD, you trained me to think like a researcher and gave me enough freedom to design experiments for my own project. You are very patient and considerate to me. Last year, due to the COVID-19 pandemic, I cannot go back to China to celebrate new year with my family. You invited me to spend Chrimas with your family. It means a lot to me and I will never forget it. After spending three years with you, I have become a better man. Thank you !

I would also like to thank Philippe Potin and Gabriel Markov. You have provided incredible help with designing experiments and interpretation of results. I also appreciate your efforts on reading and correcting my thesis manuscript. I would not have been able to finish this project on time without you!

Erwan Corre gave me a lot of advises on transcriptomic analysis, which helped me to improve my bioinformatic analysis skills. And Cédric Leroux helped me to perform the metabolic profiling.Thank you very much!

Thanks also to Miriam Bernard, Sylvie Rousvoal and Murielle Jam for helping me with my experiments in the lab, which was difficult for me at the beginning.

Furthermore, I am very grateful for valuable discussions of my work with the members of my thesis committee and with the ABIE team. Your suggestions are very helpful to my work.

I want to thank all of the jury members for agreeing to review my thesis. Thanks for your patience and I wish you to enjoy reading my manuscript!

A special thanks goes to Eugenie Grigorian : You are a perfect office mate and I really enjoy the tea breaks and our conversation. And thanks for your help in my daily life.

I want to thank my friends I met in Roscoff : Marieke, Rik, Maeva, Giannis, Cedric, Haiqin, Hetty and Miriam for all the amazing moments I shared with you.

Looking back into the past, this thesis would not have happened without the supervisor of my master, Yunxiang Mao. You recommanded station biologique de Roscoff as a good place to start my PhD. And you really aroused my love for algae. Thank you!

在这里我要感谢我的父母，他们给予了我生命并且不辞辛劳地培养了我。没有你们对于我的学业的全力的支持，也不会有我今天所获得的一切成就。这些恩情我会用余生来报答！同时也要感谢一路走来关心和帮助我的亲朋好友，谢谢你们！

我还要感谢我的女朋友郭静，谢谢这三年来对我的理解。一人独在异乡倍感孤独，尤其在遇到困难的时候更加难熬。感谢你每天和我聊天交流，我有些不能和父母说的话也只能和你说，谢谢你一起陪我度过开心和难过的时刻。

最后我想感谢我自己，感谢自己在经历过许多挫折和苦难之后仍然对科研充满热情。正是这份热情支撑着我走到今天。同时也希望自己在未来一直保持这份热情，不改初心！

Table of contents

General Introduction

1. Evolutionary context and multiple origins of eukaryotic algae

Algae are ubiquitous and important primary producers in all aquatic environments, which cover over 70% of the Earth's surface. In total, 40% of global photosynthesis is contributed by both micro- and macroalgae (Metting, 1996). The algae are tremendously diverse and include at least seven distinct phylogenetic lineages that arose independently during geological time and that evolved at different rates. According to the plastid endosymbiosis theory, the eukaryotic cells obtained the light-harvesting capabilities from the ancestors of modern cyanobacteria through the process of endosymbiosis (Gould et al., 2008, Reyes-Prieto et al., 2007). During this so-called primary endosymbiosis, the engulfed cyanobacterium was transformed as a primary plastid with two membranes, and this can be considered as the beginning of eukaryotic photosynthesis (Archibald, 2009). The primary plastids are found in land plants and green algae, red algae and glaucophyte algae. Then the primary plastids have kept co-evolving with their hosts and were diverse in form and functions.

After the primary endosymbiosis, a flagellate unicell, also called ancestral green flagellate, is believed to evolve and form the green lineage (Leliaert et al., 2012). The green lineage is divided into two big group: Chlorophyta and Streptophyta. Chlorophyta includes most described species of green algae. The other group Streptophyta is considered as one of the deepest branches of the green lineage, including the charophyte green algae from which the land plants evolved.

As members of the same superkingdom, Archaeplastida, red algae form an independent sister lineage from the Glaucophyte algal lineage and green algae, belonging to the green lineage (Figure 1). Once the primary plastids established in ancestral unicellular green or red unicellular algae, they have later spread into numerous eukaryotic lineages through secondary or tertiary endosymbiosis events. Among algal lineages with red-algal-derived plastids, the most abundant and species-rich groups are the Haptophytes, Stramenopiles and Dinoflagellates (Not et al., 2012). Haptophytes consist of unicellular biflagellate algae with a flagellum-like protrusion of ambiguous function (Andersen, 2004).

Stramenopiles form an independent, well-separated superkingdom (Figure 1). Unlike Archaeplastida, it not only includes photosynthetic organisms, but also oomycetes, a group of heterotrophic organisms. Stramenopiles exhibit a remarkable variation in morphology, which ranges from unicellular diatoms to the largest marine brown algae, such as the giant kelps with length more than 40 meters.

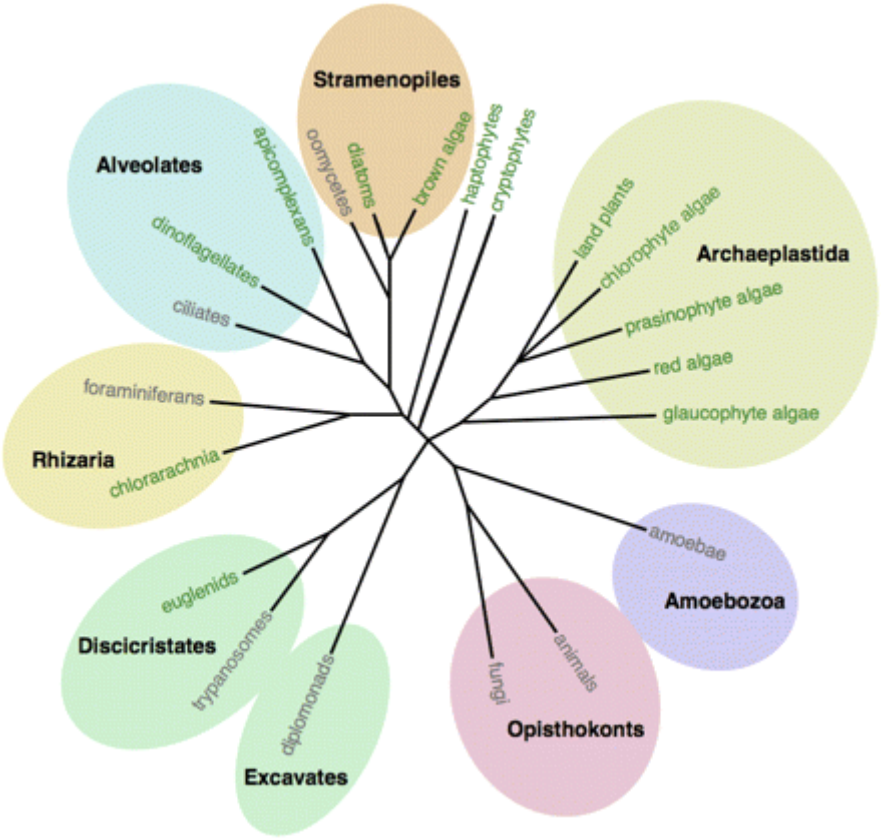

Fig 1: Eukaryotic tree of life (Cock & Coelho, 2011)

In this evolutionary context, eukaryotic algae refer to a large group of photosynthetic organisms with high diversity. Each independently evolved lineage has developed unique metabolic systems (Cock & Coelho, 2011). However, some ancestral traits related to basic or essential biological functions involved in the responses against biotic and abiotic stress have been shown being shared in algal lineages and other non-photosynthetic eukaryotic lineages, such as that grouping animals and fungi, the Opisthokonts (Cock & Coelho, 2011). Besides, the conservation of some specific metabolic pathways could also be observed between two close lineages due to the plastid transmission and evolution, such as those of red and brown algae.

2. Defense responses in algae against biotic stresses

2.1. Recognition of the attacker or the *non-se* perception

As already shown in other eukaryotes lineages, such as animals or land plants, the induction of innate immunity, including specific defense responses, is based on the early and efficient recognition of the attacker to stop it before irreversible damages (Weinberger, 2007). During biotic interactions, defense responses in host are usually induced by the perception of some compounds which are defined as elicitors (Conrath et al., 2002). Elicitors are mainly classified into two categories: Microbe-Associated Molecular Patterns (MAMPs) and Microbe-Induced Molecular Patterns (MIMPs), according to their biosynthesis origin. MAMPs are highly conserved and specific in major microorganism pathogenic groups, and are linked to the components of microbial cell envelope or cell wall (Weinberger, 2007). For example, lipopolysaccharides (LPS) from the outer cell envelope of Gram-negative bacteria can strongly induce some early events of defense responses in the brown alga *Laminaria digitata*, such as the oxidative burst, the release of free saturated and unsaturated fatty acids (FFAs) and the accumulation of oxylipins (Küpper et al., 2006). In another brown alga *Saccharina japonica*, a conserved peptide in the N-terminal part of bacterial flagellin, flg22, can also induce the oxidative burst in the gametophytic stage, suggesting its role as MAMPs elicitor in algae (Wang et al., 2013).

In addition to MAMPs, some endogenous compounds can also induce defense responses in algae. These compounds are breakdown products of cell wall and cell membrane following the biotic attack and thus they are named as Microbe-Induced Molecular Patterns elicitors. For instance, oligoguluronates are MIMPs that have been extensively studied in brown algae. As one major component of brown algal cell wall, alginate is a linear binary copolymer of two different monomers: β-D-mannuronate (M) and α-L-guluronate (G). Three combination of these two monomers have been found in alginate: homopolymeric guluronate blocks (GG), homopolymeric mannuronate blocks (MM) and alternating mannuronate and guluronate blocks (MG) (Figure 2), which have different physical and chemical characteristics (Paredes Juárez et al., 2014). In brown algae, only the guluronate-containing alginate fragments can be recognized as elicitor. Indeed, purified GG blocks can induce a much stronger oxidative burst than MG blocks, when MM blocks and alginate polymers are not perceived by algae (Küpper et al., 2001). Besides the oxidative burst, a GG treatment also induces the production of some volatile aldehydes and the expression of some stress-related genes (Goulitquer et al., 2009, Cosse et al., 2009).

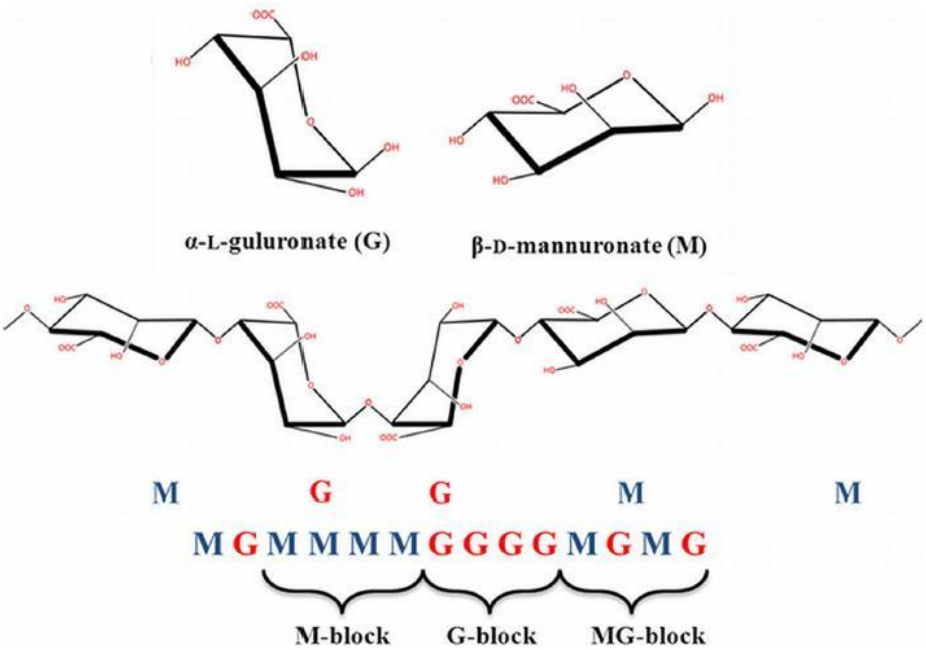

Fig 2: Chemical structure of alginate. Linear block polymers of β-D-mannuronate (M) and α-L-guluronate (G) with a variation in composition and sequential arrangements (Paredes Juárez et al., 2014).

2.2. Oxidative burst and early local signaling

As the earliest defense response in innate immunity process, an oxidative burst is rapidly induced following the recognition of the attack(er), producing massive amounts of reactive oxygen species (ROS), such as superoxide ions (O^{2-}•), hydrogen peroxide (H_2O_2), or hydroxyl radicals (OH•), by NADPH oxidases located at the plasma membrane (Weinberger & Friedlander, 2000, Küpper et al., 2001) or by various oxidases and peroxidases (Potin, 2008). In brown alga *Laminaria digitata*, a strong release of H_2O_2 was monitored in the surrounding seawater within 2-3 minutes after the treatment with GG. In immunity responses, the oxidative burst is highly conserved among eukaryotes, from animals to terrestrial plants and marine macroalgae (Halliwell & Gutteridge, 1985). The production of extracellular ROS has been widely observed in the chlorophytes, heterokonts (Stramenopiles), rhodophytes, haptophytes and alveolates lineages (Marshall et al., 2005). Since many algal genomes were sequenced, some NADPH oxidase-like genes have been reported in green algae, such as *Chlamydomonas reinhardtii* and in red macroalgae, such as *Chondrus crispus* (Hervé et al., 2006, Allen et al., 2007). Similarly, to what have been observed in land plants, the inhibition of NADPH oxidase-like enzymes by diphenylene iodonium (DPI)

suppressed the oxidative burst in algae (Potin, 2008, Kustka et al., 2005, Coelho et al., 2008), indicating the key role of these enzymes in production of extracellular ROS.

The extracellular ROS released by host are cytotoxic to bacteria or microbes attached to the algal surface, and can help to control and suppress the growth of pathogen (Weinberger & Friedlander, 2000). ROS are also a key element in defense responses against some eukaryotic potential pathogens such as algal endophytes. The gametophytes of the red alga *Chondrus crispus* are naturally resistant to the green algal endophyte *Acrochaete operculata,* generating a much stronger oxidative burst after the treatment by the endophyte extract than the sporophytes, which are susceptible to the endophyte infection. The inhibition of H_2O_2 generation by DPI in *C. crispus* gametophytes resulted in the loss of resistance to the endophyte (Bouarab et al., 1999). Besides the direct cytotoxic effect on the endophytes, the authors hypothesized that ROS also act as signaling molecules to induce some systemic acquired resistance in algae.

ROS could also participate in other signaling pathways during defense responses. For example, membrane lipids are chemically converted, in the presence of ROS, into oxylipins, which are also intracellular signaling compounds. The nonenzymatic lipid oxidation is usually considered as deleterious. However, recent evidence suggests that lipid peroxidation can eventually benefit cells under oxidative stress (Farmer & Mueller, 2013).

2.3. Defensive chemicals

In addition to broad spectrum of defense responses, such as massive ROS production, each algal species also has specific defense features related to the biosynthesis of particular defense compounds. In past decades, several bioactive secondary metabolites have been identified in macro-algae as actors of inducible defense responses. In a recent example, a defense compound (1,1,3,3-tetrabromo-2-heptanone), found in the red alga *Bonnemaisonia hamifera,* significantly decreases bacterial colonization on algal surface (Nylund et al., 2013). Similarly, dimethylsulphopropionate (DMSP) and proline extracted from the surface of the brown alga *Fucus vesiculosus* were able to inhibit the growth of several bacterial strains (Saha et al., 2012). In brown algae, chemical studies have mainly identified compounds involved in defenses against

grazers. As a product of DMSP cleavage, dimethylsulfide (DMS) was emitted by algae during grazing and acted as an herbivore deterrent (Van Alstyne & Houser, 2003). Another antiherbivore chemicals, dopamine, was identified in the green alga *Ulvaria obscura.* Dopamine is a catecholamine that acts as a neurotransmitter in animals. The result demonstrated that dopamine decreased algal consumption by sea urchins (*Strongylocentrotus droebachiensis*), snails (*Littorina sitkana*) and isopods (*Idotea wosnesenskii*) (Van Alstyne et al., 2006). Additionally, some fatty-acid-derived C_{11} hydrocarbons and C_{11} sulfur metabolites have also been identified as defensive compounds against herbivores in the brown alga *Dictyopteris membranacea* (Schnitzler et al., 2001).

In unicellular algae, a wide range of secondary metabolites are produced and released into the environment, and a large number of those compounds have biological functions in the interactions between organisms. The most studied compounds are polyunsaturated aldehydes (PUA) produced in diatoms and some of them have been shown to be toxic to a wide range of organisms, from bacteria to invertebrates (Ribalet et al., 2007). They are often considered as defensive metabolites which are produced immediately from polyunsaturated fatty acids through oxylipin pathway after cell damages. Ribalet *et al*. (2008) tested the effect of three diatom-produced PUAs (2E,4E-decadienal, 2E,4E-octadienal and 2E,4E-heptadienal) on growth of 33 marine bacteria. The effect of these PUAs was variable between different bacterial strains, indicating the possible capability of these compounds to shape the structure of associated bacterial communities (Ribalet et al., 2008). The same PUAs have also been tested on six marine phytoplankton species, which belong to different taxonomic groups representing the marine phytoplankton diversity. A stronger reduction effect on growth rate was observed in all plankton species treated with long-chained aldehydes than those treated with short-chained aldehydes, suggesting their important role in the interactions with other phytoplankton cells (Ribalet et al., 2007). During the interactions with herbivores, unlike in macroalgae, defensive chemicals produced by diatoms, such as non-volatile oxylipins, were proposed to negatively impact their egg-hatching rate instead of having a direct deterring effect (Ianora et al., 2015).

In addition to inhibition of microbial growth and herbivore deterrence, several defensive metabolites are capable of interfering with the bacterial quorum sensing (QS) systems (Egan et al., 2014). In the brown alga *Laminaria digitata*, production of hypobromous acid resulted in

deactivation of acylated homoserine-lactone (AHL) signals, which are involved in QS-regulated gene expression in bacteria (Borchardt et al., 2001). Several compounds interfering in different ways with AHL signals have been also found in red algae, which are therefore able to control the bacterial biofilm at their surface. Halogenated furanones produced by the red macroalga *Delisea pulchra* mimicked AHL signal and repressed bacterial gene expression (Harder et al., 2012). Another red alga *Ahnfeltiopsis flabelliformis* released betonicine, floridoside and isethionic acids to compete with AHL signals for modulating gene expression (Kim et al., 2007).

2.4. Transcriptomic regulations

The regulation of gene expression plays a key role in the response of organisms to biotic and abiotic stress (Shinozaki & Yamaguchi-Shinozaki, 2007). In 1995, gene expression was analysis for the first time in the plant model *Arabidopsis*, using a microarray approach, which was based on the hybridization of transcripts and gene probes (Schena et al., 1995). Since 2006, RNA sequencing has been widely used to study the transcriptome-wide gene expression. The development of high-throughput RNA sequencing technologies has further promoted the increase of studies on transcriptomic regulation in plant and animal biological researches (Lowe et al., 2017).

In macroalgae, however, there has been a significant delay in the study of transcriptomic regulation comparing to plant and animal models. The first study of transcriptome-wide gene expression analysis in algae was performed in *C. crispus* in 2007, demonstrating multiple transcriptomic regulations in response to abiotic stresses, such as temperature, light and osmotic stress, in this red macroalga (Collén et al., 2007). In the past decade, the amount of transcriptomic regulation studies has been rapidly increasing in the algal research field. Most of those studies focused on transcriptomic responses to abiotic stress, such as light, temperature and desiccation stress. (Deng et al., 2012, Liu et al., 2014, Heinrich et al., 2015, Lee et al., 2017) and only few studies reported on the gene regulations in macroalgae submitted to biotic stresses, such as grazing pressure or pathogen infection. Comparing to abiotic stress, the interactions with pathogens or herbivores seem to only induce a small number of specific genes that are identified as differentially expressed. For example, in the brown alga *Fucus vesiculosus*, 1.7% of total genes were differentially expressed in response to grazing by *Littorina obtusata* (Flöthe et al., 2014).

The transcriptomic analysis of two other brown algae, *L. digitata* and *Lessonia spicata*, showed only 0.8% of total genes were induced upon grazing by herbivores (Ritter et al., 2017a). However, due to the low annotation rate of algal genes, around 40%, the functions of most genes induced by biotic stress are still unclear.

When the red seaweed *Laurencia dendroidea* was challenged with the bacterial pathogen *Vibrio madracius*, de Oliveira et al. (2017) also observed a slight change in global transcriptomic regulation (1.8% of total genes). The differential expressed genes include genes encoding for functions usually involved in general stress responses such as transcription factors, signaling pathways, ROS metabolism and vesicle trafficking. Additionally, some genes putatively involved in the biosynthesis of terpenes, which are considered as important defensive compounds against bacterial colonization, were upregulated in response to the infection of *V. madracius* (de Oliveira et al., 2017).

In the diatom, *Pseudo-nitzschia*, the incubation with predator cues induced the differential expression of 1128 genes in total (1.6% of total genes). Genes involved in methyl-erythritol phosphate metabolic (MEP) pathway and proline metabolism were upregulated, and were considered as candidate genes for the biosynthesis of a known defense compound, the domoic acid. Moreover, 13 upregulated genes with unknown function were suggested to be specifically involved in diatom responses to grazers (Harðardóttir et al., 2019).

Similarly, Cosse et al. (2009) incubated *L. digitata* sporophytes with GG for analyzing transcriptomic responses to biotic stress, as GG blocks are likely to be endogenous elicitor signals, released from the broken cell wall during biotic interactions with alginolytic bacteria or endophytes. After GG elicitation, fifty upregulated genes were detected over a 24-h time-course, which include genes related to oxidative stress responses. Among those upregulated genes, a vanadium-dependent haloperoxidase (vHPO) gene specific of iodide oxidation was characterized, showing the activation of defense-related iodine metabolism. Furthermore, several genes coding for C5 epimerases, which convert MM-rich alginates into GG-rich polysaccharides, were upregulated, suggesting the occurrence of cell wall strengthening as mechanical protection against pathogens or biotic aggressors (Cosse et al., 2009). In another brown alga, *F. vesiculosus*, a

targeted approach on phlorotannin biosynthesis upon grazing by herbivores has recently revealed the up-regulation of a cytochrome P450 homologous gene, which might be involved in oxylipin synthesis (Emeline et al., 2021). However, the number of genes used to analyze the transcriptional regulations in previous studies was limited and the global metabolic regulations upon biotic stress remain poorly understood in brown macroalgal models, especially those related to oxylipins pathway induction. A transcriptome-wide gene regulation analysis is necessary and it will provide more information about the molecular mechanisms of defense response in kelps during biotic interactions.

2.5. Systemic responses and distance signaling

When land plants are attacked by grazers, their defense responses may not only occur locally, but also be induced in the whole plant by signal transduction in order to protect healthy, undamaged tissues (Dempsey & Klessig, 2012). Salicylic acid (SA) has been proved to act as an important signal to trigger systemic defense responses in plants (Heil, 2008, Conrath, 2009). However, SA is not crucial for systemic defense induction (Heil, 2008). Some oxylipin-derived compounds, such as 12-oxo-phytodienoic acid (12-OPDA) and α-ketol of octadecadienoic acid (KODA), are also able to induce the expression of defense-related genes and increase resistance in distal plant parts (Wang et al., 2020). In some studies, it has been demonstrated that the release of volatile organic compounds (VOCs) is also a strategy of signal transduction towards some distal plant parts which lack vascular connection with damaged parts (Heil, 2008, Heil, 2010). As airborne chemical cues, VOCs also participate in the plant-plant communication and affect the resistance of the neighboring conspecifics (Beckers & Conrath, 2007, Heil, 2010).

In the brown alga, *L. digitata*, both GG elicitation and abiotic stress during low tide induced release of various volatile aldehydes, such as (*E*)-4-hydroxyhex-2-enal (4-HHE), (*E*)-4-hydroxynon-2-enal (4-HNE) and 4-hydroxydodeca-2,6-dienal (4-HDDE). Then the putative signaling role of those aldehydes were tested on *L. digitata*. Only treatment with 4-HHE induced the increased release of an oxylipin, 13s-hydroxy-9Z,11E,15Z-octadecatrienoic acid (13S)-HOTrE), suggesting that 4-HHE could activate the oxylipin pathway leading to defense mechanisms in *L. digitata* (Goulitquer et al., 2009). Some preliminary results further suggested that the treatment with 4-HHE could protect young plantlets of *L. digitata* from grazers in a laboratory bioassay (Cabioch et al., unpublished data), suggesting an ecological role of aldehydes

during biotic interactions in kelps beds. In addition, Thomas et al. showed that waterborne cues released by GG-elicited *L. digitata* sporophyte shaped the responses of neighboring conspecifics, indicating the existence of chemical communication between kelps (Thomas et al., 2011). A GG elicitation experiment in *L. digitata* showed that oxidative responses were triggered at distant parts of thallus after the elicitation. A pharmacological approach suggested that *L. digitata* systemic signal transduction might rely on the translocation of free fatty acid and their oxidative derivatives from the site of elicitation (Thomas et al., 2014). However, the role of systemic responses and distance signaling during biotic interactions remains to be studied, as well as the chemical nature of the involved signals.

3. **Oxylipin biosynthesis**

The term oxylipin was introduced to describe oxygenated substances derived from unsaturated fatty acids by chemical reactions (Frankel, 1980). Oxylipins have been found ubiquitously in many organisms, from prokaryotic organisms to eukaryotic land plants. In cyanobacteria, oxylipin molecules are formed by one or two metabolic steps. More than 500 different related molecules were identified in different eukaryotes, suggesting that complex oxylipin synthesis pathways have evolved in the different eukaryotic lineages (Andreou et al., 2009).

3.1. Oxylipin biosynthesis pathways and biological roles in prokaryotes

Since the discovery of the first two prokaryotic lipoxygenase (LOX) sequences in 2002, the information about enzymes involved in oxylipin pathways in bacteria has been steadily increasing. Till now, approximately 30 putative LOXs have been identified in prokaryotic organisms and mostly characterized in cyanobacteria. In the cyanobacterium *Nostoc punctiforme*, two additional prokaryotic LOXs were identified as being linoleate (13S)-LOXs (Koeduka et al., 2007, Lang & Feussner, 2007). Non-esterified 13-LOX products was shown to accumulate in response to the wounding of *N. punctiforme* cell, indicating that LOX might play a role in stress response. Besides the 13-LOXs, two (9R)-hydroperoxy C-18 PUFAs were detected in the cyanobacterium *Anabaena flosaquae*, suggesting the presence of a linoleate (9R)-LOX pathway in cyanobacteria (Murakami et al., 1992). Then a dual function LOX gene (*NspLOX*) has been identified in closely related cyanobacterium *Nostoc (Anabaena)* sp. PCC 7120 (Schneider et al., 2007). The protein sequence analysis revealed the catalase-LOX fusion structure of NspLOX-encoding gene: The C-

terminal domain of NspLOX have the full function of linoleate (9R)-LOX, which can convert linoleic acid (LA), α-linolenic acid (ALA) and arachidonic acid (ARA) to (9R)-HPODE, (9R)-HPOTE and (11R)-HPETE, respectively (Figure 3) (Lang et al., 2008). Then (9R)-HPODE and (9R)-HPOTE can be catalyzed into two unstable allylic epoxides by the catalase-related domain, thus behaving as an allene oxide synthase (AOS) (Figure 3A). In *Pseudomonas aeruginosa*, the function of one LOX (*loxA*) was validated as enzyme catalyzing arachidonic acid into 15-HETE, which could play a regulatory role in host-pathogen interaction (Vance et al., 2004). Besides LOX, it has been also revealed that prokaryotic enzyme with hydroperoxide lyase (HPL) activity is present in the cyanobacterium *Oscillatoria* sp. In this organism, an unspecific LOX converted LA to 9-HPODE and 13-HPODE (Andrianarison et al., 1989). Then 13-HPODE was cleaved into 13-oxo-trideca-9, 11-dienoic acid and pentanol by HPL enzyme (Fig. 3B). The alphaproteobacterium *Methylobacterium nodulans*, which is involved in root-nodule symbiosis in land plants, also has a protein showing HPL activity (Lee et al., 2008).

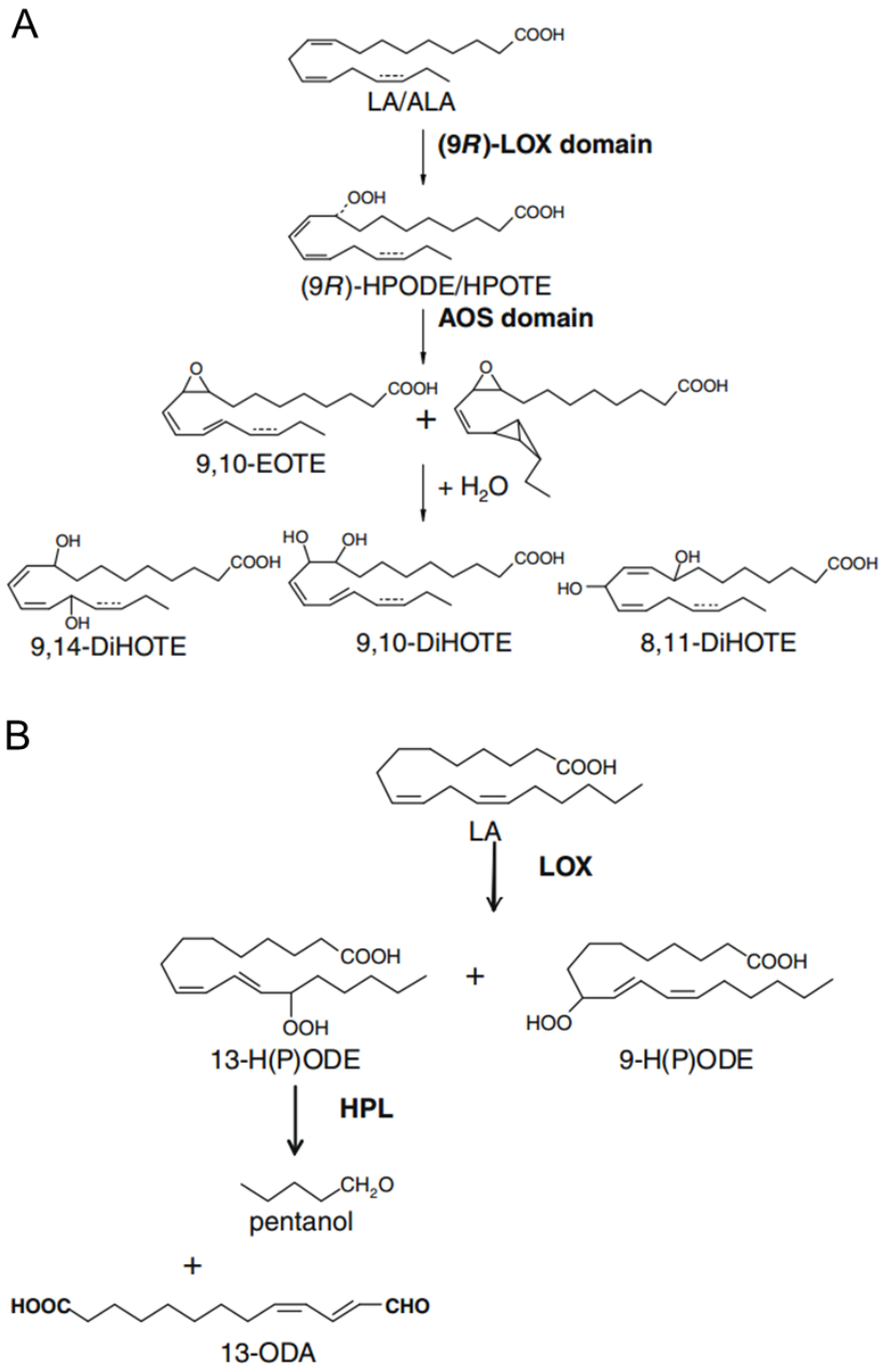

Fig 3: A. Proposed metabolism of ALA by the cyanobacterium *Nostoc sp.* **B.** Proposed LOX/HPL metabolism from cyanobacterium *Oscillatoria sp.* (Andreou et al., 2009)

3.2. Oxylipin biosynthesis pathways and biological roles in Opisthokonts

3.2.1. Fungi

During evolution, fungi emerged as a sister group of animals in the eukaryotic tree of life, forming the non-photosynthetic superkingdom Opisthokonts (Figure 1). The enzymes involved in oxylipin formation in different fungi have been studied for almost three decades (Hamberg, 1986, Matsuda et al., 1976). With numerous fungal genomes being published in the past few years, the potential oxylipin biosynthesis pathways can therefore be predicted in a number of fungal species by homology searches in protein sequence databases.

The occurrence of prostaglandins has been widely reported in pathogenic and non-pathogenic fungal species. The pathogenic yeasts, *Candida albicans* and *Cryptococcus neoformans*, were able to produce prostaglandins *de novo*, using exogenous arachidonic acid (ARA) (Noverr et al., 2001). In later studies, various prostaglandins have been found in fungal species. Prostaglandin E_2 and $F_{2\alpha}$ were identified in *Mortierella* and *Cunninghamella* (Lamacka & Sajbidor, 1998). Yeasts of the Lipomycetaceae family and *Saccharomyces cerevisiae* were also able to synthesize prostaglandin F2 and prostaglandin F2-lactone (Kock et al., 2003, Noverr et al., 2003). However, the enzymes involved in the formation of prostaglandins in fungi remain unidentified. The available fungal genomes did not include any sequences homologous to known prostaglandin H synthases (PGHS). Unlike mammals, the prostaglandin E_2 biosynthesis in fungus *C. albicans* was not repressed by the selective PGHS-2 inhibitor CAY10404, but was affected by non-selective mammalian PGHS inhibitors and NDGA LOX inhibitor (Erb-Downward & Noverr, 2007). These results suggest that the enzymes responsible for prostaglandin E_2 in fungi are distinct from mammalian PGHS, but might contain some similar features with PGHS and LOX. In addition to PGHS, several enzymes were also shown being involved in the prostaglandin E_2 formation, such as fatty acid desaturase homolog Ole2 and a putative multicopper oxidase or laccase homolog Fet3 (Erb-Downward & Noverr, 2007). The function of prostaglandins has also been tested in several plant pathogen fungal species. The results of these studies showed that prostaglandins can affect growth and maturation of fungi as well as fungal pathogenesis. For example, in *C. albicans*, adding exogenous prostaglandin E_2 promoted the formation of germ tubes (Noverr et al., 2001) and increased the biofilm formation (Alem & Douglas, 2004), which are two important processes associated with fungal infection and colonization.

The identification and characterization of LOX have contributed to the characterization of oxylipins biosynthesis pathways in fungi. The first fungal LOX was isolated from the ascomycete *Fusarium oxysporum* in 1975 (Yuzuru et al., 1978, Matsuda et al., 1978). This enzyme converted linoleic acid to a mixture of (10E,12E)-9-hydroperoxyoctadeca-10,12-dienoic acid (9-HPODE) and (9Z,11E)-13-hydroperoxyoctadeca-9,11-dienoic acid (13-HPODE) (Matsuda et al., 1978). Moreover, a special LOX, manganese LOX (MnLOX), has been found in the fungus of wheat *Gaeumannomyces graminis*. Unlike other known LOXs, this enzyme contains manganese in catalytic center instead of iron (Su & Oliw, 1998), and that significantly affects the catalytic mechanism and the chemical types of oxygenated products. When linoleic acid was the substrate, MnLOX oxidized linoleic acid on C-11 and C-9 instead of C-13 and could isomerise the intermediate 13-hydroperoxide products to epoxy alcohols and keto compounds (Figure 4) (Cristea & Oliw, 2006). The role of Mn-LOX-derived oxylipins is still not clear, it has been reported that those compounds might cause oxidative damages to cells during the plant penetration of *G. graminis* (Oliw, 2002). Additionally, there are accumulating evidences to support the hypothesis that LOX products might be involved in the population density-dependent transitions of dimorphic fungi. For example, it has been shown that inhibition and deletion of LOX in fungi affect their development by being involved in quorum sensing (Jensen et al., 1992, Brown et al., 2008).

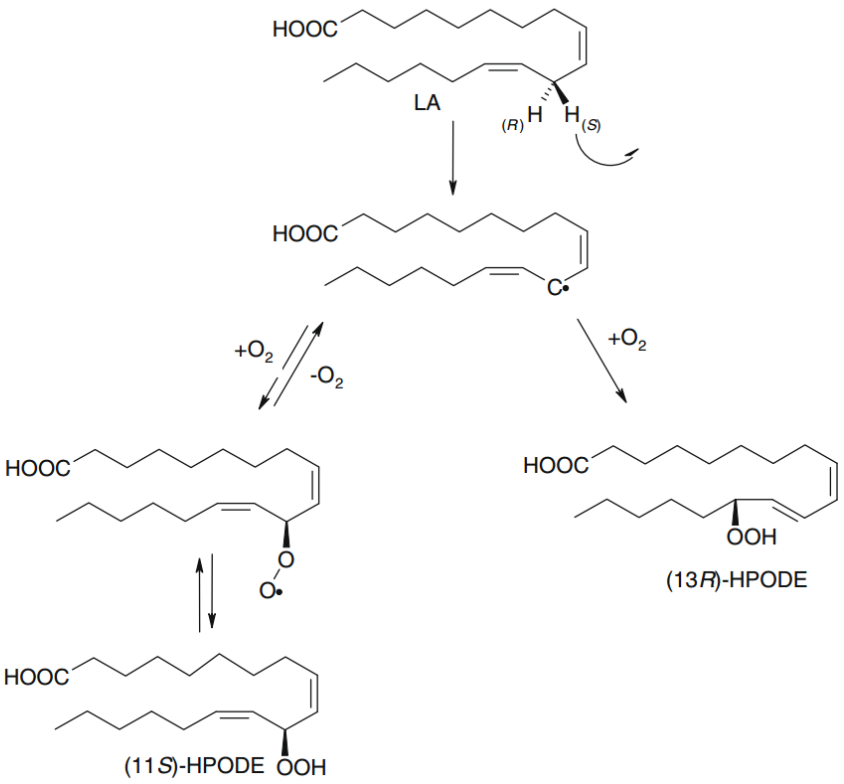

Fig 4: Reaction mechanism of MnLOX from *G. graminis* (Andreou et al., 2009). The abstraction of the pro-S-hydrogen from linoleic acid at the C-11 displays the initial reaction step and leads to formation of a delocalized linoleoyl radical. Dioxygen attacks reversibly the radical at the C-11 in a suprafacial way and thus (11S)-HPODE is formed that may be isomerised into (13S)-HPODE. Dioxygen attacks alternatively directly the radical at the C-13 in a suprafacial way resulting in the irreversible formation of (13R)-HPODE.

In addition to LOX, other oxylipin-forming enzymes have been identified in fungi. In *G. graminis*, a 7,8-linoleate diol synthase (7,8-LDS) has been characterized as a heme- containing bifunctional enzyme, which firstly converted linoleic acid to (8R)-HPODE and then isomerised this intermediate product to (7S,8S)-DiHODE (Su & Oliw, 1996, Su et al., 1998, Hamberg et al., 1994). Its cDNA sequence analysis demonstrated that this enzyme shares 23-24% identity with mammalian PGHS-2 and further studies showed that it might use a similar reaction mechanism as mammalian PGHS (Hörnsten et al., 1999). In *Cercospora zeae-maydis*, the LDS homolog expression was correlated with the accumulation of mycotoxin cercosporin, suggesting a potential role of this enzyme in pathogenesis (Shim & Dunkle, 2002). Later a protein named Spore-Specific protein 1 (Ssp1) was identified in *Ustilago maydis* and shared 33% identity with the 7,8-LDS. The localization and expression analysis of this enzyme suggested that it might have similar function with LDS enzyme as a fatty acid dioxygenase. Moreover, three homolog genes (*ppoA*, *ppoB* and *ppoC*) have been found in the genome of *Aspergillus nidulans.* The results of linoleic acid metabolism analysis in knock out strains suggested that ppoA might catalyze the synthesis of (8R)-hydroperoxides and ppoC might code for a linoleate (10R)-dioxygenase (10-DOX) (Garscha et al., 2007).

In addition to the oxylipins mentioned above, there are many other oxylipins for which biosynthesis pathways are still not clear. In the basidiomycete *Gomphus floccosus*, three oxylipins, (9S)-HODE, 13-oxo-9E,11Z-octadecadienoic acid and 9-oxo-10E,12E-octaddecadienoic acid, were identified and validated to have anti-fungal bioactivity against plant pathogens (Cantrell et al., 2008). Furthermore, a C-20 PUFA was also shown to have antifungal bioactivity in *Entomocorticium* sp., which is a symbiotic fungus in the beetle *Dendroctonus frontalis* (Scott et al., 2008).

Signal transduction through oxylipins has been proven to go through transmembrane G-protein coupled receptors in *Aspergillus* (Affeldt et al., 2012). The signal tranduction cascade also involves a transcription factor and induces, among other biological effects, hyphal branching (Niu et al., 2020).

3.2.2. Animals

As suggested with the fragmentary data available in corals, mammals may not be good representatives of oxylipin signaling across all animals, having secondarily lost the AOS enzyme, for example (Lee et al., 2008). However, they are the group where the larger amount of functional data is available.

In animal lineages, the oxylipins are mainly derived from eicosanoids, i.e. from arachidonic acid (AA), a C20 fatty acid, and three main biosynthesis pathways have been characterized, mainly in mammals, which are catalyzed by three types of enzyme: cyclooxygenases (COXs), lipoxygenases (LOXs) and cytochrome P450 epoxygenases (CYP450s) (Figure 5).

In the COX pathway, AA is firstly converted into prostaglandin G_2 and then to prostaglandin H_2 in the present of COX. After that, prostaglandin H_2 is converted into various downstream eicosanoids, such as PGD_2, PGE_2, $PGF_{2\alpha}$ and thromboxane A (TXA) by tissue-specific isomerases (Smith et al., 2011). Prostaglandins (PGs) and thromboxanes (TXs), also known as prostanoids, represent the oldest known and most abundant group of eicosanoids (Capra et al., 2013). They activate the downstream pathways by combining to specific receptors, such as G protein-coupled receptors (GPCRs). Nine GPCRs have been identified as the targets of prostanoids (Smith et al., 2011).

The LOX pathways in mammals contain three main branches, which are catalyzed by three different LOX isoforms, 5-, 12- and 15-LOX. The products of these pathways, 5-, 12- and 15-HpETE are the initial precursors of a number of bioactive compounds. For example, leukotrienes, the 5-HpETE-derived products, are further cyclized by 5-LOX into LTA_4. LTA_4 can serve as the substrate of either LTA_4 hydrolase for LTB_4 formation or LTC_4 synthase for conjugation to cysteine (Peters-Golden et al., 2006). In 12-LOX branch, 12-HpETE can be converted to its hydroxyl analogue (12-HETE), which can be further oxidized to 12-oxoeicosatetraenoates (12-oxoETEs), or it can be used to produce hepoxilin A and B (Powell & Rokach, 2015). Moreover, the product of 15-LOX,15-HpETE, can be catalyzed to lipoxins (LXA4 and LXB4) in the presence of 5-LOX (Romano et al., 2015). Similarly to prostanoids, LOX-derived oxylipins can also combine with GPCRs. For instance, two GPCRs were identified as the targets of LTB_4, namely BLT1 and BLT2, and two additional receptors, CysLTR1 and CysLTR2, were revealed to be the targets of cysLTs (Yokomizo et al., 2018).

The products of CYP450s represent the minority of AA-derived oxylipins. Among those metabolites, epoxyeicosatetraenoids (EETs) are produced by CYP2C and CYP2J, while 20-HETE is generated by CYP4A and CYP4F (Fan & Roman, 2017). The CYP-derived compounds are very unstable, and can be further catalyzed by other enzymes, such as LOX, COX, epoxide hydrolases and phase II enzymes, to less active or inactive products.

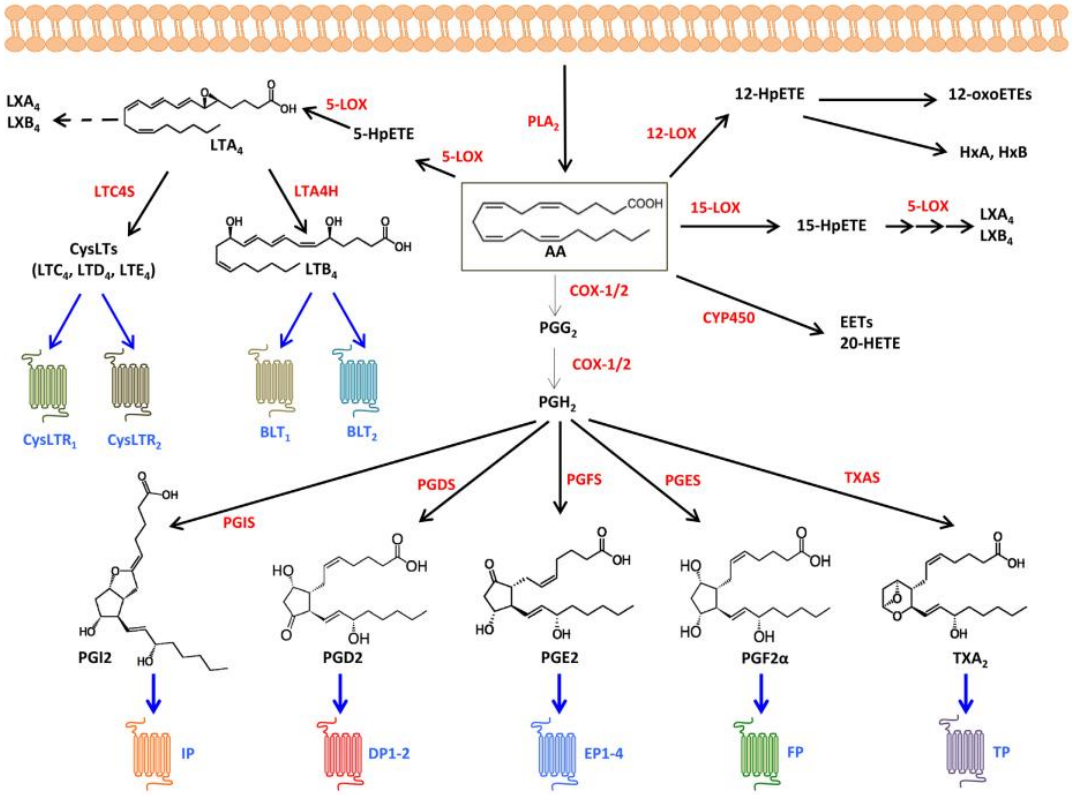

Fig 5: Biosynthetic pathways and known receptors of arachidonic acid -derived bioactive lipids in mammals (Leuti et al., 2020). AA: arachidonic acid; BLT: leukotriene B receptor; COX: cyclooxygenase; CYP450: cytochrome P450; CysLT: cysteinyl leukotriene; DP: prostaglandin D receptor; EP: prostaglandin E receptor; FP: prostaglandin F receptor; HpETE: hydroperoxy eicosatetraenoic acid; Hx: hepoxilyn; IP: prostaglandin I receptor; LOX: lipoxygenase; LT: leukotriene; LTA4H: leukotriene A4 hydrolase; LTC4S: leukotriene C4 synthase; LX: lipoxin; oxoETE; oxo-eicosatetraenoic acid; PG: prostaglandin; PGDS: prostaglandin D synthase; PGES: prostaglandin E synthase; PGFS: prostaglandin F synthase; PGIS: prostaglandin I synthase; PLA: phospholipase A TP: thromboxane receptor TXAS: thromboxane A synthase.

Strikingly, animals and fungi share oxylipin signaling through membrane receptors while in plants, the most of experimental data available are related to ligand binding of intracellular cofactors of transcription factors (like coi1 featured, see later on Figure 6).

3.3. Oxylipin biosynthesis pathways and biological roles in Archaeplastida

3.3.1. Land plants

In the past few decades, oxylipins have also been widely studied in land plants. Numerous enzymes have been identified and used to reconstruct complex pathways of oxylipin biosynthesis. The oxylipin biosynthesis pathways are triggered by the release of free fatty acids. Until now, only one specific acyl-lipid hydrolase was shown to provide free fatty acids that initiate jasmonate biosynthesis in *Arabidopsis* (Ishiguro et al., 2001). After released from cell membrane, free fatty acids are further converted to fatty acid hydroperoxides. Unlike in mammals, LOXs seem to be the most prevalent enzymes of the initial steps in oxylipin pathways in land plants. Plant LOX are subdivided into two groups, 9-LOX and 13-LOX, based on the position where the molecular oxygen is introduced on C18 fatty acids. Comparing to 9-LOX, 13-LOX are able to accept complex lipids as substrate due to their special structure of active site (Newcomer & Brash, 2015). Fatty acid hydroperoxides produced by LOX may serve as signal molecules or be catalyzed into oxylipins and aldehydes by downstream enzymes, such as Allene oxide synthase (AOS), hydroperoxide lyase/isomerase (HPL), epoxyalcohol synthase (EAS), and divinyl ether synthase (DES). Most of those enzymes belong to the CYP74 family of cytochrome P450 enzymes and, unlike other members of the cytochrome P450 family, they are able to catalyze reactions without molecular oxygen or NAD(P)H-dependent cytochrome P450 reductases as a cofactor. The structure analysis showed the close relationships of all those four enzymes and there are only very few amino acid differences between them in their active sites (Scholz et al., 2012, Toporkova et al., 2013, Toporkova et al., 2008).

Jasmonic acid (JA) biological roles and its biosynthesis pathway have been well studied in land plants (Wasternack & Feussner, 2018, Ray et al., 2019). JA participates in the physiological responses to various processes, including development, biotic and abiotic stress acclimation of plants. The JA biosynthesis is a downstream pathway of so-called octadecanoid pathway. After the reaction catalyzed by 13-AOS, the unstable products, allylic epoxides, are spontaneously hydrolyzed by water to α-ketols and γ-ketols and cyclized to a racemic mixture of cis-(+) and cis-(−)-enantiomers (González-Pérez et al., 2017). Then allene oxide cyclase (AOC) catalyzes the formation of the cis-(+)-isomer of oxo-phytodienoic acid (OPDA) in the chloroplast. As a key enzyme in JA biosynthesis, the overexpression of AOC led to the accumulation of JA, which increased the tolerance to salinity in wheat (Zhao et al., 2014). The next step is the transportation of the cis-(+)-isomer of OPDA from chloroplast to peroxisomes where the other enzymes of JA

synthesis, such as acyl-CoA synthetases, 12-oxophytodienoic acid reductase3 (OPR3) and β-oxidation enzymes are located. The knockout of OPR3 led to JA deficient and accumulation of OPDA, indicating the ability of OPR3 to convert OPDA for JA synthesis (Sanders et al., 2000, Stintzi, 2000). In the later step, the fatty acid β-oxidation machinery shortens the carboxyl side chain of JA. Moreover, many studies have also investigated the role of JA metabolism in the signaling transduction and 12 different pathways of JA metabolism have been established until now (Figure 6). Among those pathways, JA conjugation with the amino acid isoleucine is the best-studied process in land plant. The conjugation product, (+)-7-iso-JA-Ile, is the most bioactive JA-derived compound, which serves as the signal molecule during defense and other stress responses (Fonseca et al., 2009). The hydroxylation catalyzed by CYP94 genes inactivates JA-Ile by converting it to 12-OH-JA-Ile. It has been proven that the overexpression of CYP94 gene family members turned off JA-Ile signaling during herbivory and pathogen attack by *Botrytis cinerea* (Heitz et al., 2012, Koo et al., 2011). Additionally, JA methylation also plays an important role in herbivore resistance and plant development (Luo et al., 2016). Across land plants, there are some variations in the signaling molecules, with the JA precursor dinor-OPDA being the main signal molecule in the bryophyte *Marchantia polymorpha* (Monte et al., 2018).

Metabolites derived from other enzymes in plant oxylipin pathways have also been studied for their biological functions(Wasternack & Feussner, 2018). The HPL branch of oxylipin pathway provides various volatile compounds that are involved in plant defense responses. During the wounding responses of *Arabidopsis*, the dominant HPL volatile product, hexenyl acetate, attracts the natural enemies of the herbivores as indirect defense strategies (Chehab et al., 2008). HPL-derived volatile compounds can also directly affect the attacker and protect plants from grazing. Other products, such as the alcohol (3Z)-hexenal and (3Z)-hexenol, served as signal molecules to induce defense responses in the undamaged neighboring plants (Sugimoto et al., 2014). In addition, 9-LOX-derived fatty acid hydroxides were likely used to regulate the defense reactions by the crosstalk with other signaling pathways in *Arabidopsis*, such as those involving mitogen-activated protein kinases, MPK3 and MPK6, and salicylic acid (SA)(Montillet et al., 2013). Similarly, linoleic acid and its hydroperoxides, such as 9- and 13-HPODE, were also associated with the regulation of stomatal closure in *Arabidopsis* (Montillet et al., 2013). Jasmonate precursors, such as OPDA, also play a role in long-distance signaling during *Arabidopsis* growth response to wounding (Schulze et al., 2019).

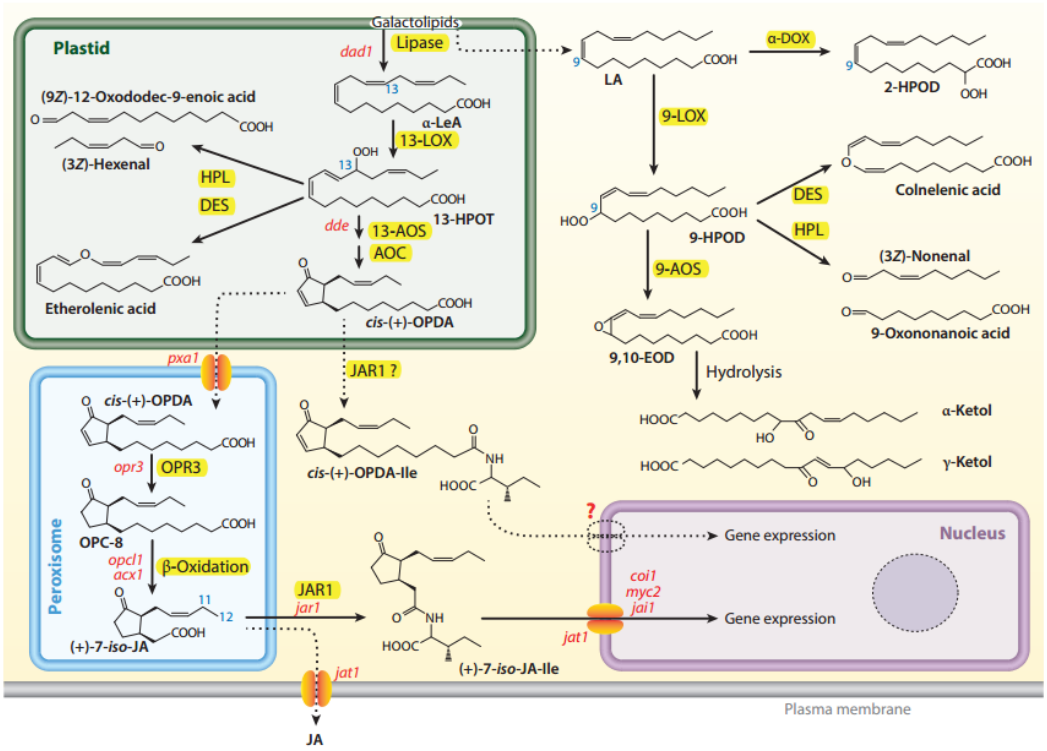

Fig 6: Synthesis of oxylipins and their intracellular transport in land plants (Wasternack & Feussner, 2018). Mutants known for *Arabidopsis* and tomato are indicated in red and enzyme names are highlighted in yellow. Abbreviations for compounds: α-LeA, α-linolenic acid; HPOD, hydroperoxy octadecatrienoic acid; 13-HPOT, (13S)-hydroperoxy octadecatrienoic acid; cis-(+)-OPDA, cis-(+)-12-oxo-phytodienoic acid; cis-(+)-OPDA-Ile, cis-(+)-12-oxo-phytodienoic acid isoleucine conjugate; JA, jasmonic acid; JA-Ile, jasmonic acid isoleucine conjugate; OPC-8, 3-oxo-2-(2-pentenyl)-cyclopentane-1-octanoic acid. Abbreviations for enzymes/proteins/mutants: α-DOX, α-dioxygenase; acx1, acyl CoA-oxidase1; AOC, allene oxide cyclase; AOS, allene oxide synthase; coi1, coronatine insensitive1; dad1, delayed anther dehiscence1; dde, delayed dehiscence1; DES, divinyl ether synthase; EOD, epoxy octadecaenoic acid; HPL, hydroperoxide lyase; jai1, jasmonic acid insensitive1; JAR1, jasmonoyl amino acid conjugate synthase; jat1, JA/JA-Ile transporter1; LOX, lipoxygenase; myc2, bHLHzip transcription factor MYC2; opcl1, 3-oxo-2-(2-[Z]–pentenyl)-cyclopentane-1-octanoic acid ligase; OPR3, 12-oxo-phytodienoic acid reductase3; pxa1, ATP-binding cassette (ABC) transporter (also known as COMATOSE).

3.3.2. Green algae

As the main primary producers in coastal zones of the ocean, green, red and brown algae can produce diverse PUFA, such as the human-essential linoleic and α-linolenic acids, as well as stearidonic, eicosapentaenoic and docosahexaenoic acids (Kumari et al., 2013). PUFA are not only the key components of cell membrane, but also participate in some regulation processes by being the substrate of oxylipin pathways (Gerwick et al., 1991, Gerwick, 1996). Due to their evolution positions, the different algal lineages have evolved independently than other well-known eukaryotic lineages such as animals, fungi or land plants, and have developed unique oxylipin biosynthetic pathways, which lead to the formation of numerous oxylipins with novel

structure and biological effects (Barbosa et al., 2016). Therefore, the algal oxylipins have been recently targets of lipid research and, many oxylipins have been identified and characterized in different algal species. Additionally, some nonenzymatically-derived oxylipins, such as phytoprostanes, were also found to have potential biological activities in algae (Barbosa et al., 2016). However, this chapter will focus on knowledge about enzymatic pathways.

Like land plants, the members of Chlorophyta are typically rich in C_{18} PUFA (Barbosa et al., 2016). The C_{18} oxylipin pathway enzymes, such as 9-LOX, 13-LOX and HPL, and their products have been reported in several green macroalgae (Andreou et al., 2009). In *Acrosiphonia coalita*, a large variety of 9-LOX-derived oxylipins were identified, together with aldehydes derived from these oxylipins, like coalital, which served as an antifungal compound against the pathogenic yeast *Candida albicans* (Bernart et al., 1993). HPL cleavage activity has also been detected in another green alga *Cladophora columbiana*, which used an α-linolenic acid derivative, 9-hydroperoxyoctadecatrienoic acid (9-HpOTrE), as substrate (Gerwick et al., 1993b). Then the enzymatic activity of LOX has been studied in several *Ulva* species. After arachidonic acid treatment, the formation of 15-HETE and 12-hydroxyeicosatetraenoic acid (12-HETE) has been observed in *Ulva intestinalis*, suggesting the existence of 12- and 15-LOX in this green alga (Kuo et al., 1996). In the green alga *Ulva lactuca*, a multifunctional LOX was isolated and purified, and this enzyme can cleave different PUFA substrates into several hydroxy-fatty acids, including 9-hydroxyoctadecadienoic acid (9-HODE), 13-HODE, 9-hydroxyoctadecatrienoic acid (9-HOTrE), 12-HETE, 15-HETE, 12-hydroxyeicosapentaenoic acid (12-HEPE), and 14-hydroxydocosahexaenoic acid (14-HDoHE) (Kuo et al., 1997). More recently, the content of oxylipins was determined in different macroalgal species. The result showed that Chlorophyta species were richer in those oxylipins comparing to red and brown alga species (Kumari et al., 2014b). Nowadays, the genus *Ulva* has become a model for investigating complex metabolic networks. In this regard, many studies have focused on the lipidomic changes during various stress conditions in *U. lactuca* (Kumar et al., 2010, Kumar et al., 2011, Kumari et al., 2014a). For example, the shift of PUFA and their derivatives was observed during nitrate and phosphate nutritional stress, which was considered as a strategy to balance the lack of nutrients in macroalgae (Kumari et al., 2014a). More generally, the accumulation of hydroxy-oxylipin compounds was also involved in the defense responses against Cd^{2+} induced oxidative stress conditions in green macroalgae (Kumar et al., 2010, Kumar et al., 2011).

3.3.3. Red algae

Unlike green algae in which C_{18} PUFA and their derivatives are the main components of oxylipins pathway, red algae have been shown to be the source of a larger chemical diversity of oxylipins as their LOX-derived metabolism can utilize both C_{20} and C_{18} PUFA as substrates (Gerwick, 1994, Bouarab et al., 2004). Until now, the most abundant oxylipin structures identified in red macroalgae are the 12-LOX-derived compounds of C_{20} PUFA metabolism (Barbosa et al., 2016).

Several novel oxylipins have been characterized in red algae. For instance, a novel oxylipin, hybridalactone, was isolated in *Laurencia hybrida* and the characterization of its structure by spectroscopic methods showed the existence of a cyclopropane and a macrolactone ring in this compound (Higgs & Mulheirn, 1981). In a later work, the intermediate product, 12S-hydroxyeicopentaenoic acid (12S-HEPE), was also identified in *L. hybrida*, indicating the biosynthesis reaction of hybridalactone via 12-LOX activity (Bernart & Gerwick, 1988).

12S-HEPE was also discovered in two other red algal species, *Platysiphonia miniata* and *Gracilariopsis lemaneiformis* (Moghaddam et al., 1989, Jiang & Gerwick, 1991). The biological functions of 12S-HEPE were investigated in *Murrayella periclados* and they included the inhibition of phospholipase A_2 (PLA_2) and ATPases, such as Na^+/K^+ ATPase and H^+/K^+ ATPase (Bernart & Gerwick, 1994). Besides 12S-HEPE, two fatty acid derivatives, leukotriene B_4 and hepoxilin B_3, were isolated from the red alga *M. periclados*, and showed very high similarities to oxylipins from mammals (Bernart & Gerwick, 1994). In humans, hepoxilins are able to regulate the permeability of skin plasma and induce the release of arachidonic acid (Antón et al., 2002).

Although the occurrence of methyl jasmonate in macroalgae is still not clear, similar to land plants, methyl jasmonate can trigger the oxylipin pathways in red algae. In *Chondrus crispus*, the treatment using exogenous methyl jasmonate induced a cascade of PUFA oxidation, which resulted in the formation of 13-hydroxyoctadecadienoic acid (13-HODE) and 13-oxo-octadecadienoic acid (13-oxo-ODE) (Gaquerel et al., 2007). Furthermore, methyl jasmonate elicitation induced a strong oxidative burst in *G racilaria dura* thalli and the upregulation of 13-

LOX pathway, as well as the formation and accumulation of several hydro-oxylipins (Kumari et al., 2015).

The function of other LOXs, such as arachidonate 5R-, 8R-, and 15S-LOX, as well as linoleate 9S- and 13S-LOX, were also revealed in red algae. 5R-LOX-derived oxylipins, 5-hydroxyeicosatetraenoic acid (5-HETE) and 5-hydroxyeicosapentaenoic acid (5-HEPE), as well as two vicinal diol-fatty acids, 5,6-dihydroxyeicosatetraenoic acid (5,6-diHETE) and 5,6-dihydroxyeicosapentaenoic acid (5,6-diHEPE) were detected in lipid extracts of *Rhodymenia pertusa* (Jiang et al., 2000). 8-LOX activities have also been widely reported in Rhodophyta species, including *Sarcodiotheca gaudichaudii*, *Agardhiella subulata*, *Gracilaria chilensis* and *Gracilaria vermiculophylla* (Proteau, 1993, Graber et al., 1996, Lion et al., 2006, Nylund et al., 2011). The production of 8-LOX-derived metabolites, such as 8-HETE and 7,8-diHETE, was induced by mechanically wounding in two red algae, *G. vermiculophylla* and *G. chilensis* (Nylund et al., 2011, Lion et al., 2006). Additionally, the release of novel conjugated lactones and leukotriene B_4 were also involved in the wounding response in *G. vermiculophylla*. The similar oxylipin regulation during the wounding response in both species suggests that the metabolism of arachidonic acid might play important roles in the defense responses against herbivory in red macroalgae. Moreover, the occurrence of 9S-hydroxyeicosatetraenoic acid (9S-HETE) in the extracts of *Polyneura latissima* supported the hypothesis that a simple peroxidase-type reduction of 9S-hydroperoxyeicosatetraenoic acid (9S-HpETE) might exist in this alga (Jiang & Gerwick, 1997). 9,15-dihydroxyeicosatetraenoic acid (9,15-diHETE) were also identified in the extract, suggesting the involvement of 15-LOX activity (Jiang & Gerwick, 1997).

In addition to LOX, other enzyme involved in oxylipin pathways were also discovered in red algae. An AOS was reported in *G. lemaneiformis*, which converts 12-HpETE into 12R and 13S-diHETE (Hamberg & Gerwick, 1993). In the red alga *C. crispus*, Gaquerel et al. described a new enzyme with the activity of catalyzing the regio- and stereoselective bisallylic (omega-7)-hydroxylation of C_{18} to C_{22} PUFA (Gaquerel et al., 2007) and a similar activity was previously observed during the analysis of crude protein extracts from *Lithothamnion corallioides* (Hámberg et al., 1992, Gerwick et al., 1993a).

As well-known oxylipins in animals, prostaglandins have been also detected in several red algal species. Two prostaglandins, prostaglandin E2 (PGE_2) and prostaglandin $F_{2\alpha}$ ($PGF_{2\alpha}$), were firstly identified in *Gracilaria lichenoides* (Gregson et al., 1979). Soon afterwards, more prostaglandin homologs, such as PGA_2, PGE_2 and 15-keto-PGE_2, were found in other species of *Gracilaria* genus (Nylund et al., 2011, Rempt et al., 2012, Imbs et al., 2001, Lee et al., 2010). In *C. crispus*, the methyl jasmonate treatment induced the formation of prostaglandin A_2 (PGA_2) and 15-keto-PGE2 (Gaquerel et al., 2007). Furthermore, the first non-mammal prostaglandin endoperoxide H synthase (PGHS) was identified in *G. vermiculophylla* and its involvement in the production of $PGF_{2\alpha}$, was validated using a prokaryotic expression system (Kanamoto et al., 2011).

3.4. Oxylipins biosynthesis pathways and biological roles in Stramenopiles

3.4.1. Oomycetes

Oomycetes are the only non-photosynthetic group in Stramenopiles and they are widespread all over the world. As the major pathogen of plants and animals, many studies have illustrated the regulation of host oxylipin pathway during the oomycete infection. However, only few studies focused on the oxylipin pathway in oomycetes. In the oomycete *Saprolegnia parasitica,* a LOX was shown to have not only the activities of LOX but also EAS, which isomerised its intermediate product 15-Hydroperoxyarachidonic acid (15-HPETE) into (11S,12R)-epoxy-(15S)-hydroperoxy-(5Z,8Z,13E)-eicosatrienoic acid and (13R,14R)-epoxy-(15S)-hydorperoxy-(5Z,8Z,11Z)-eicosatrienoic acid (Herman & Hamberg, 1987, Hamberg, 1986). Later, a phospholipase-like enzyme and a prostaglandin-like synthase, homologous to vertebrate proteins involved in the prostaglandin biosynthesis pathway, were found in the genome of *S. parasitica* (Belmonte et al., 2014). And *S. parasitica* was capable of producing PGE2 during the infection, which increased the inflammatory response in fish and repressed the expression of genes involved in cellular immunity (Belmonte et al., 2014).

3.4.2. Diatoms

Diatoms are ones of major primary producers in the ocean. The chemical ecology of diatoms has been widely studied and discussed, since the discovery of secondary metabolites which negatively affect the reproduction of marine invertebrates (Miralto et al., 1999). Among those secondary

metabolites, oxylipins have been well-studied and documented about their biosynthesis process and biological functions.

The chemical profiling analysis indicated a huge diversity of oxylipin pathways in different diatom species, based on the occurrence of diverse LOX activities (Lamari et al., 2013). The most conserved pathway among the diatom species is the 15S-LOX pathway (Ruocco et al., 2020a). Other LOX activities, such as 5-LOX, 8-LOX, 9S-LOX, 11-LOX, 12-LOX and 14-LOX, have been also found in various diatoms (Fontana et al., 2007b, Fontana et al., 2007a, Ruocco et al., 2020b, Lamari et al., 2013, d'Ippolito et al., 2005, d'Ippolito et al., 2009, Nanjappa et al., 2014). Recently, a survey of oxylipins showed that three fatty acids, hexadecatrienoic, eicosapentaenoic (EPA) and docosahexaenoic (DHA) acids, were mostly used as substrates of oxylipin pathways in diatoms (Russo et al., 2020).

In the past decade, several commercially available oxylipins found in diatom, including five polyunsaturated aldehydes (PUAs), 2E,4E-heptadienal (HD), 2E,4E-octadienal (OD), 2E,4E,7Z-octatrienal (OT), 2E,4E-decadienal (DD) and 2E,4E,7Z-decatrienal (DT), as well as four oxygenated fatty acids, 5-hydroxy-6E,8Z,11Z,14Z,17Z-eicosapentaenoic acid (5-HEPE), 9-hydroxy-5Z,7E,11Z,14Z,17Z-eicosapentaenoic acid (9-HEPE), 11-hydroxy-5Z,8Z,12E,14Z,17Z-eicosapentaenoic acid (11-HEPE) and 15-hydroxy-5Z,8Z,11Z,13E,17Z-eicosapentaenoic acid (15-HEPE), have been tested in laboratory conditions on the biology and reproduction of marine invertebrates. In these studies, both morphological and molecular effects have been reported, which is summarized in Table.1, suggesting significant ecological roles of these oxylipins during interactions with herbivores and marine invertebrates.

Table 1. Species, oxylipins, concentrations tested and morphological and molecular effects reported in the literature on marine invertebrates during 2010–2020 (Ruocco et al., 2020a). Abbreviations: DD, 2E,4E-decadienal; HD, 2E,4E-heptadienal; OD, 2E,4E-octadienal; OT, 2E,4E,7Z-octatrienal; 5-HEPE, 5-hydroxy-6E,8Z,11Z,14Z,17Z-eicosapentaenoic acid; 9-HEPE, 9-hydroxy-5Z,7E,11Z,14Z,17Z-eicosapentaenoic acid; 11-HEPE, 11-hydroxy-5Z,8Z,12E, 14Z,17Z-eicosapentaenoic acid; 15-HEPE, 15-hydroxy-5Z,8Z,11Z,13E,17Z-eicosapentaenoic acid.

Species	Oxylipins (µM)	Morphological Effects	Molecular Effects
Paracentrotus lividus	DD, HD, OD and OT (0.658–32)	Cleavage inhibition; Malformed plutei with decadienal	Not detected

Paracentrotus lividus	DD (0.002–0.03)	Increase of endogenous NO levels and consequently apoptosis induction	Upregulation of hsp70 and caspase-8; downregulation of NOS
Paracentrotus lividus	DD (0.001–0.0023)	Differentially expressed genes with dose dependent effect	Upregulation of hsp70, hsp56, hsp60, hat, BP10, 14-3-3", p38 MAPK, GS and MTase; downregulation of sox9, uni, SM30, Nec and SM50
Paracentrotus lividus	DD (0.5–2.5), HD (1.0–6.0) and OD (2.0–9.0	Dose-dependent malformations of sea urchin plutei	Upregulation of hsp70, hat; downregulation of SM50, Wnt6, MT4 and MT6
Echinometra mathaei	DD (0.4–1.2), HD (0.5–1.5) and OD (0.6–1.7)	Dose-dependent malformations of sea urchin plutei	Not detected
Paracentrotus lividus	5-, 9-, 11-, 15-HEPE (100), DD (3.3), HD (9.0) and OD (11.0)	Impairment at blastula and pluteus stage with PUAs and HEPEs	Activation of caspase-8 and caspase-3/7
Paracentrotus lividus	DD (1.0–2.3), HD (2.0–6.0) and OD (2.5–8.0)	Not detected	Upregulation of MTase and p38 MAPK; downregulation of MT6, CAT Alix and SM50
Paracentrotus lividus	5- and 15-HEPE (6–30)	Dose-dependent malformations of sea urchin plutei	Upregulation of hsp70, hsp56, 14-3-3", Blimp and MT5; downregulation of HIF1A and SM50
Paracentrotus lividus	DD (1.6), HD (3.0) and OD (4.5)	Not detected	Upregulation of Jun and Foxo
Paracentrotus lividus	Mixture of 5-, 9-, 11-, 15-HEPEs (1.0–7.0)	Synergic effect of HEPEs	Downregulation of MAPK and Alix MTase, p38
Paracentrotus lividus	Mixture of PUAs (DD 0.3, HD 0.7 and OD 1) and HEPEs (1.6)	Higher morphological effects than those detected with individual oxylipins and PUAs/HEPEs mixtures	Upregulation of ADMP2, Delta, Goosecoid, KIF19, jun and CAT; downregulation of ARF1, GS, HIF1A and sox9
Temora stylifera	15-HEPE, DD and HD (1.0 to 20 µg/mL)	Reduction of egg production, naupliar and female survival	Not detected
Temora stylifera	DD (0.5 to 2 µg/mL)	Reduction of egg production, hatching success and increase of mortality	Not detected
Pseudodiaptomus annandalei	DD (0.75 to 4.5 µM)	Dose-dependent reduction of female survival and nauplii production	Not detected
Acartia clausi *Calanus helgolandicus*	PUAs (0.97 µg/mg protein in 2004 and 1.2 µg/mg protein in 2005) and oxygenated fatty acids (3.6 µg/mg protein in 2004 and14 µg/mg protein in 2005)	Reduction of egg production and hatching success	Not detected
Calanus helgolandicus	oxygenated fatty acids (0.001 to 1389.13 ng/mg)	Reduction of egg production and hatching success	Upregulation of ALDH8, ALDH7, ALDH6, CAT, GST, HSP40, HSP70; downregulation of CAS, CARP, BTUB, ATUB, ALDH3, SOD, CYP

Oxylipins produced by diatoms also served as chemical regulators within the phytoplankton communities. For instance, 2E,4E-decadienal was employed to control the population density by triggering the programmed cell death (PCD) in diatom cells (Vardi et al., 2006). Similarly, allelopathy was also observed when 2E,4E-heptadienal and 2E,4E-octadienal were tested on the prymnesiophyte *Isochrysis galbana*, the chlorophyte *Tetraselmis suecica* and the diatom *S. marinoi* (Ribalet et al., 2007). Furthermore, these oxylipins were also involved in the interaction between bacteria and phytoplankton. The accumulation of HEPEs, especially 15-HEPE, were detected during the co-cultivation of a diatom species, *Chaetoceros didymus*, with an algicidal bacteria, *Kordia algicida*, which might play a key role in the defense responses of phytoplankton (Meyer et al., 2018). Several PUAs, such as 2E,4E-decadienal, 2E,4E-heptadienal and 2E,4E-octadienal have been shown to selectively inhibit the growth of bacteria (Ribalet et al., 2008).

3.4.3. Brown algae

Similarly to red algae, brown algae have complex oxylipin metabolism, which utilizes both C_{18} and C_{20} PUFA as substrates for oxylipin biosynthesis (Figure 7). In the studies of oxylipins in brown macroalgae, 12- and 15-LOX-derived metabolites, such as hydroxylated fatty acid derivatives, short chain aldehydes, and carboxylic oxylipins, were mostly reported.

Brown algae contain a number of structurally unique oxylipins produced through novel pathways (Barbosa et al., 2016). Among those metabolites, many cyclic oxylipins have been found. Ecklonialactones A and B were discovered in the brown alga *Ecklonia stolonifera* and these two tricyclic compounds with a backbone of 18 carbon atoms were revealed to have antifeedant activity against the abalone *Haliotis discus* (Kurata et al., 1989). Afterwards, more homologous ecklonialactones (C-F) were isolated in *E. stolonifera* (Kurata et al., 1993). The same metabolites were also reported in other brown algal species, such as *Cymathaere triplicata*, *Egregia menziesii*, *Laminaria sinclairii* and *Eisenia bicyclis* (Proteau & Gerwick, 1992, Proteau et al., 1994, Todd et al., 1994, Kousaka et al., 2003).

Moreover, several prostanoid-like cyclic oxylipins have been identified in the edible kelp *C. triplicata*. For instance, the occurrence of cymathere ether A and B was reported and 10S-

hydroxyoctadecatetraenoic acid (10S-HODTA) was considered as the intermediate in the biosynthesis of these two bicyclic oxylipins (Proteau & Gerwick, 1992). In a later study, a combination of spectroscopic techniques and synthetic derivatization was performed to elucidate the structure of some new oxylipins, such as cymatherelactone and cymatherols A-C, which contain cyclopentyl, cyclopropyl, epoxyde, and lactone rings (Choi et al., 2012). These metabolites were suggested to derive from the C_{18} PUFA stearidonic acid, except cymatherol C, which was likely produced from eicosapentaenoic acid (Choi et al., 2012). The biological function of cymatherelactone was further validated as being a regulator of sodium channel (Choi et al., 2012).

Another class of cyclic oxylipins, which contain a chloride or an iodide, was discovered in brown algae. Among those halogenated oxylipins, three homologous egregiachlorides (A-C) were firstly identified in *E. menziesii* and this study revealed a cyclopentyl ring with an adjacent chlorine functionality in the structure of these oxylipins (Todd et al., 1993). Afterwards, Kousaka et al. reported that another brown alga, *E. bicyclis*, produced not only egregiachlorides A and B, but also novel ecklonialactone derivatives such as eiseniachlorides and eiseniaiodides (Kousaka et al., 2003). Those halogenated oxylipins were derived from C18 PUFA through 13-LOX oxidation and a number of rearrangements and showed antibacterial activities against two bacterial strains, *Bacillus subtilis Cohn* and *Staphylococcus aureus Rosenbach* (Kousaka et al., 2003).

In addition to those structurally unique oxylipins, brown algae also contain a number of known hydroxylated fatty acid derivatives. The targeted metabolic analysis in three brown algal species, *Laminaria sinclairii*, *Laminaria setchellii* and *Saccharina latissima*, revealed the occurrence of 13- and 15-LOX-derived oxylipins (Proteau, 1993). In *L. augustata,* Boonprab et al. found some evidences supporting the existence of the C_6 and C_9 aldehydes biosynthesis pathways (Boonprab et al., 2003). In these pathways, C_9 aldehydes, 3Z-nonenal and 2E-nonenal, were synthesized exclusively from C_{20} PUFA in the presence of LOX and HPL activities, while C_6 aldehydes n-hexanal derived either from C_{18} or from C_{20} fatty acids (Boonprab et al., 2003). A pathway of producing a C_{10} aldehyde, 2(E),4(E)-decadienal, was discovered in *L. augustata*, in which arachidonic acid was catalyzed by 11-LOX and HPL into 2(E),4(E)-decadienal, with 11-hydroperoxyeicosatetraenoic acid (11-HPETE) being produced as an intermediate. These short-chain aldehydes seem to play important roles in the chemical defense responses (Boonprab et al.,

2004). In brown algae *Laminaria digitata* and *Ectocarpus siliculosus*, copper stress induced oxylipins derived from C18 and C20 pathways, as well as from non-enzymatic reactions (Figure 7) (Ritter et al., 2008, Ritter et al., 2014). Moreover, isoprostanoids in macroalgae submitted to copper stress increased after 24 h of exposure corroborating the existence of concomitant non-enzymatic reactions (Vigor et al., 2018).

Several studies focusing on the defense responses provided evidence supporting the crucial roles of different oxylipins in brown algae. During the defense reactions induced by bacterial lipopolysaccharides, a rapid release of PUFAs and the accumulation of oxylipins, such as 13-hydroxyoctadecatrienoic (13-HOTrE) and 15-hydroxyeicosapentaenoic (15-HEPE) acid, were observed following an oxidative burst in *L. digitata* sporophytes (Küpper et al., 2006). Later, an endogenous elicitor, oligoguluronate (GG), was also used to induce the defense reactions in *L. digitata,* and triggered a rapid release of a number of aldehydes, such as 4-hydroxy-2-hexenal (4HHE), 4-Hydroxynonenal (4HNE) and dodecadinal (Goulitquer et al., 2009). In this study, the authors also tested the ability of all identified aldehydes to trigger the oxylipin production in *L. digitata.* Among those aldehydes, only 4HHE can induce the later accumulation of (13S)-HOTrE (Goulitquer et al., 2009). Similarly, some PUFA and oxylipin-derived compounds, such as methyl jasmonate, were also reported to activate the fatty acid oxidation pathways (Küpper et al., 2009). Also, a divergent ortholog of the CYP74 family was experimentally demonstrated to be involved in epoxidation of Hydroperoxi-fatty acids in *E. siliculosus* (Toporkova et al., 2017).

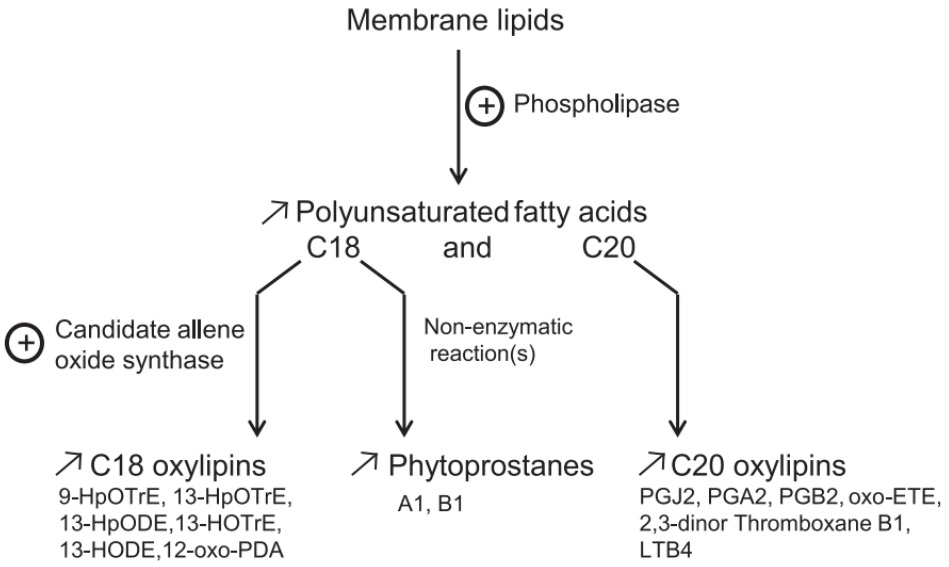

Fig 7: model of oxylipin pathways in brown algae (Ritter et al., 2014). 9-HpOTrE, 9-hydroperoxy-10,12,15-octadecatrienoic acid; 13-HpOTrE, 13S-hydroperoxy-9Z,11E,15Z-octadecatrienoic acid; 13-HpODE, 13-hydroperoxy-9Z,11E-octadecadienoic acid; 13-HOTrE, 13S-hydroxy-9Z,11E,15Z-octadecatrienoic acid; 13-HODE, 13-hydroxy-9Z,11E-octadecadienoic acid; 12-oxo-PDA, 12-oxophytodienoic acid; PGJ2, prostaglandin J2; PGA2, prostaglandin A2; PGB2, prostaglandin B2; oxo-ETE, oxo-6E,8Z,11Z,14Z-eicosatetraenoic acid; LTB4, leukotriene B4.

4. Thesis project and outline

Brown algal kelps are key components of marine forests in rocky zones of and potential sources of temperate and cold waters ecologically important chemical compounds. Some species, such as *Saccharina japonica*, are exploited for alginate extraction or as food sources, and extensively cultured in Asian countries. In European coastal marine habitats, both kelps, *Laminaria digitata* and *Saccharina latissima* have also great ecological and economic values, and *S. latissima* is becoming an important emerging species for aquaculture. As mentioned in previous sections, many evidences have shown that, similarly to land plants and animals, kelps produce polyunsaturated fatty acid, oxidized derivatives from both C18- and C20- PUFAs, and aldehydes. This feature constitutes a conserved innate immune trait with other well-studied eukaryotic lineages, where oxylipins play a pivotal role as stress-related signaling molecules. The access to genomic data in few brown algal species, first in *Ectocarpus* (Cock et al., 2010) and later in *S. japonica* (Ye et al., 2015), has allowed to analyze the phylogeny of two key gene families, encoding lipoxygenases (Teng et al., 2017) and cytochromes P450 (Teng et al., 2019), showing a large diversity of homologous enzymes, with unknown biochemical functions in Stramenopiles. In the brown algal lineage, their biosynthesis pathway of oxylipins has been hardly explored neither their biological and ecological roles during defense and interactions with the marine environment. In this context, my thesis focuses on the biological functions of PUFA derived compounds, their biosynthesis pathways and they regulation during biotic interactions in kelps, by combining transcriptomic and metabolomic approaches.

With the development of high-throughput sequencing technologies, RNA-seq has become an efficient method to obtain genome-wide gene expression data (Wang et al., 2009b). Wide transcriptomic studies have been mostly conducted in brown algal species submitted to various abiotic stresses, such as salinity or copper stress in *Ectocarpus* (Dittami et al., 2009, Ritter et al., 2014), acidification in *S. japonica* (Xu et al., 2019, Lu et al., 2020) , or temperature, salinity and

light stress in *S. latissima* (Heinrich et al., 2015, Li et al., 2020a, Li et al., 2020b). Due to the availability of its genome in the near future (included in the Phaeoexplorer project, France Genomic) and increasing amount of RNA-seq data of abiotic stress, we chose *S. latissima* as the main model species for studying the oxylipins pathway in a context of biotic interactions.

Only few studies focused on molecular defense responses related to biotic attack in large brown algae and it is still necessary to develop suitable bioassays in Laminariales species for controlled laboratory studies. Grazing by herbivores was shown to induce the release of free fatty acids and oxylipins in *L. digitata*, indicating the participation of oxylipins in the brown algal defense response (Ritter et al., 2017a). Furthermore, during the thesis of Léa cabioch, it has also been reported that some products of oxylipin pathways could induce the production of oxylipins in *L. digitata* and later protect this species against herbivores (Cabioch, 2016), but the molecular mechanisms of the induction are still unclear. The interactions between herbivores and kelps seem to be interesting for studying oxylipins biological roles. During my thesis, I first tried to adapt a bioassay using kelp specific grazers, i.e. helcions *Patella pellucida*, and *S. latissima* cultures. However, this bioassay was very difficult to standardize, as grazer individuals were only sampled in the wild, seasonally, and featured important biological and eating behavior variability. I therefore chose to use two other bioassays, mimicking biotic interactions, for which larger scale experiments in laboratory-controlled conditions would be possible.

In *S. latissima* and *L. digitata*, a bioassay of co-cultivation with endophytic brown algae was established by Miriam Bernard during her PhD project at Roscoff (Bernard, 2018) and will be useful for exploring the transcriptome-wide gene regulations in kelp hosts during endophytic infection.

Previous studies have used GG to induce the production of oxylipins and aldehydes in *L. digitata* (Goulitquer et al., 2009) and to have a first view of gene regulation after defense elicitation (Cosse et al., 2009). Although these studies revealed the existence of C18 and C20 oxylipin pathways in kelps, the global regulation of genes involved in kelp oxylipin pathways have been hardly explored in kelps. GG elicitation seems to be an interesting approach for studying, in a global way, the induction of genes related to oxylipin pathways. In addition, GG application is known to

induce an oxidative burst in *S. latissima*, but nothing is known about global transcriptomic regulation upon elicitation and putative molecular bases of innate immunity in this species.

To obtain a better understanding of the oxylipin pathways and their regulations in kelps on a molecular level, I therefore combined global and targeted methodological approaches during my thesis:

One first challenge of using *S. latissima* was the lack of reliable reference genes for real time quantification PCR (RT-qPCR). RT-qPCR is widely applied for targeted gene expression due to its advantage of sensitivity, specificity, and rapid execution (Pombo et al., 2017a). The accuracy of relative quantification mode in RT-qPCR is based on the expression stability of reference genes. However, up to now, there was no study about the identification and validation of RT-qPCR reference genes in *S. latissima*. In chapter I, I performed a transcriptome-wide identification and validation of reference genes with stable expression level in *S. latissima*, submitted to abiotic or biotic stress conditions. Three genes were chosen as reference genes for further gene expression analysis of targeted genes.

In Chapter II, I compared the physiological and transcriptomic responses of *S. latissima* and *L. digitata*, to the infection of a brown algal endophyte *Laminarionema elsbetiae*. I analyzed the transcriptomic regulations in the two different kelp hosts, and these results provide new insights into the gene regulation during defense responses in kelps and into the specificity of host-endophyte interactions.

In chapter III, I performed a large-scale transcriptomic analysis over four time points, 0.5h, 1h, 4.5h and 12h after GG treatment in *S. latissima*, to study the dynamics of gene regulation upon elicitation. In that dataset, genes involved in the oxylipin pathways were identified for further targeted gene expression analysis. In parallel, I combined metabolomic analysis with gene expression data to explore the regulation of oxylipin pathways in kelps.

In chapter IV, I compared the transcriptomic responses to 4-HHE and GG in *L. digitata*, building on the results from the PhD work of Lea Cabioch on the potential bioactivity of 4-HHE. At the same time, I tested several oxylipins and aldehydes using LOX and CYP genes to screen compounds that can induce the oxylipin pathways in kelps. The results help us to better understand the oxylipin pathways in kelps.

Chapter I

Transcriptome-wide identification and evaluation of optimal reference genes for RT-qPCR expression analysis of *Saccharina latissima* responses to biotic and abiotic stress

Chapter I. Transcriptome-wide identification and evaluation of optimal reference genes for RT-qPCR expression analysis of *Saccharina latissima* responses to biotic and abiotic stress

As a kelp species with huge ecological and economic value, *Saccharina latissima* has become a model for studying biotic and abiotic stress responses in brown macro-algae. To better understand physiological responses of *S. latissima* under different stress conditions, gene expression analysis has been widely performed to explore the metabolic pathway regulations. Until now, several studies used RNA sequencing to perform the transcriptome-wide untargeted gene expression analysis in *S. latissima* under different abiotic stresses. With the upcoming release of its genome in the context of Phaeoexplorer project (https://phaeoexplorer.sb-roscoff.fr/) and the increasing of transcriptomic information in *S. latissima*, there will be more applications of targeted gene expression analysis in this species, especially in a context of both fundamental and applied research. As a powerful and rapid method for targeted gene expression analysis, real-time quantitative polymerase chain reaction (RT-qPCR) needs reliable reference genes with stable expression level to obtain accurate results. However, when I started my PhD, there was no study about the reference genes for RT-qPCR in *S. latissima* yet. In this methodological chapter, we selected eight candidate reference genes based on in silico analysis of available transcriptome data. Those candidate genes were validated under biotic and abiotic stress conditions in the laboratory. In the end, two sets of the most stable reference gene combinations were chosen for biotic and abiotic stress. The validated reference genes will be suitable internal standards to further explore the gene regulation related to stress acclimation and adaptation in *S. latissima* using RT-qPCR. The reference genes were later used for targeted gene expression analysis of candidate genes related to defense responses and oxylipins pathways in *S. latissima* plantlets (see Chapter IV).

Article published online in Journal of Applied Phycology – 2021, 33 :617–627.

doi.org/10.1007/s10811-020-02279-x

Transcriptome-wide identification and evaluation of optimal reference genes for RT-qPCR expression analysis of *Saccharina latissima* responses to biotic and abiotic stress

Qikun Xing, Sylvie Rousvoal, Catherine Leblanc *

Sorbonne Université, CNRS, UMR 8227, Integrative Biology of Marine Models, Station Biologique de Roscoff, Roscoff, France

* corresponding author

Abstract

- **Background:** *Saccharina latissima*, known as sugar kelp, is a brown macroalga with huge ecological and economic values. In marine intertidal environment, *S. latissima* has to cope with both biotic and abiotic stress, which can cause the reduction of the yield during cultivation. To better understand physiological responses of *S. latissima* under different stress conditions, large-scale transcriptomic analyses are useful to explore global metabolic pathway regulations. In addition, real-time quantitative polymerase chain reaction (RT-qPCR) is a powerful and rapid method for further quantifying changes in gene expression, and for targeting specific defense-related gene pathways. However, its level of accuracy is highly related to the expression stability of selected reference genes used for normalization.
- **Results:** In this study, we experimentally tested eight candidate reference genes identified from *in silico* screening of public transcriptomic datasets of *S. latissima* from different abiotic and biotic stress treatments. The stability analysis using complementary statistical approaches showed that: *EIF5B* and *ATPase* are the most stable reference genes under biotic stress, whereas under temperature and light stress, their combination with *NDH* gene is the best choice for RT-qPCR normalization.
- **Conclusions:** The selected reference genes were used to monitor the expression of target genes, related to oxidative responses, such as those involved in oxylipin pathways, in *S. latissima* plantlets submitted to different stress in laboratory controlled conditions.

Keywords: *Saccharina latissima*, reference gene, real time PCR, environmental stress, gene expression, RNA-Seq

1. Introduction

Saccharina latissima, known as the sugar kelp, is a seaweed of great ecological and economic values (Bartsch et al., 2008, Lüning & Mortensen, 2015). The underwater forests formed by *S. latissima* and other kelp species provide habitats and food, and play a significant role in primary production of coastal area. In their natural environment, kelps are exposed to biotic aggressions by a high number of potentially harmful organisms such as grazers, fungi, bacteria or endophytic algae (Potin et al., 2002). In the intertidal area, kelps have also to cope with multiple abiotic stress such as fluctuations of temperature and light intensity. The molecular mechanisms of acclimation and adaptation in kelp species are fundamental open questions. In this context, several studies have explored the global transcriptomic regulations in several kelp species under different stress conditions, including the combination of temperature and light stress (Heinrich et al., 2015, Heinrich et al., 2012) and osmotic and temperature stress (Li et al., 2020a) and also along a geographical gradient in *S. latissima* (Monteiro et al., 2019b), and under copper stress and ocean acidification in *Saccharina japonica* (Zhang et al., 2019, Xu et al., 2019), during interactions with herbivores in *Laminaria digitata* and *Lessonia spicata* (Ritter et al., 2017b) and under light, temperature and nutrients stress in the giant kelp *Macrocystis pyrifera* (Konotchick et al., 2013).

To further understand the stress-tolerance mechanisms in specific algae, targeted gene expression analysis by RT-qPCR is widely applied due to its advantage of sensitivity, specificity and rapid execution (Pombo et al., 2017b). However, given the potential biases introduced by reverse-transcription step and PCR amplification, the relative quantification mode is based on the normalization by transcript level of reference genes, for which the expression is considered as stable or constitutive. The choice of reference genes is therefore particularly important, as small variation in the expression of reference gene could lead to significant changes in target gene expression (Dheda et al., 2005). An ideal reference gene should have minimal or no fluctuation in different tissues, developmental stages and diverse stress conditions. Housekeeping genes generally refer to a small set of highly conserved genes which are essential for basic biological functions in organisms (Fiume & Fletcher, 2012), and were considered having a stable expression level through all conditions and tissues. However, some traditionally used housekeeping genes have shown variable expression in different physiological conditions. For example, in the plant model *Arabidopsis thaliana*, the genes coding for tubulin 6 (*TUB6*), elongation factor-1alpha (*EF1*α), actin 2 (*ACT2*), and *glyceraldehyde 3-phosphate dehydrogenase* (*GAPDH*) display

strongly reduced expressions in pollen samples, and the expressions of *ACT2* and *GAPDH* are also reduced in seed samples (Czechowski et al., 2005). In addition, *GAPDH* and alpha-tubulin (*TubA*) were proved to be the least stable reference genes in the fish *Odontesthes humensis* in different ages and tissues (Silveira et al., 2018). For each target species and each condition to be studied, it is therefore essential to validate the expression stability of reference genes in order to improve the reliability and accuracy of RT-qPCR expression analyses.

With the development of high-throughput sequencing technologies, RNA-seq has become an efficient method to obtain genome-wide gene expression data (Wang et al., 2009c). This method is mainly applied for the analysis of global transcriptomic regulation and the identification of differential expressed genes, when comparing different tissues, treatments or stress conditions. The available transcriptomic data also constitute an interesting resource of constitutively expressed genes for identifying novel stable reference genes instead of only relying on available candidate genes. Recently, RNA-seq data have been used for the selection and validation of suitable reference genes in some land plant species such as *Lycoris aurea* (Ma et al., 2016) and *Oxytropis ochrocephala Bunge* (Fu et al., 2015). In marine macroalgae, some housekeeping genes have been validated as reference genes in few model species such as *Ectocarpus siliculosus* (Le Bail et al., 2008), *Chondrus crispus* (Kowalczyk et al., 2014), *Heterosigma akashiwo* (Koeduka et al., 2015), and *Pyropia yezoensis* (Gao et al., 2018). However, up to now, there is no study about the identification of RT-qPCR reference genes in *S. latissima* yet, when this kelp is becoming an important model species for studying molecular responses to environmental changes (Li et al., 2020a, Monteiro et al., 2019b).

In order to conduct studies on the expression regulation of targeted metabolic pathways, we looked for putative stable reference genes in RNA-seq datasets of this species, obtained from both biotic and abiotic stress experiments, using *in silico* analyses. Subsequently, the expression stability of selected genes was further validated using RT-qPCR under different light, temperature and endophyte co-cultivation conditions as those used to generate RNA-seq data and following defense elicitation using endogenous elicitor, oligo-guluronates (GG) treatment. Indeed, GG applications have shown to induce rapid oxidative bursts in kelps (Küpper et al., 2001, Küpper et al., 2002) and later metabolic regulations (Goulitquer et al., 2009), including conserved defense and signaling pathways, such as the release of free fatty acids and oxylipins. In order to validate RTqPCR normalization in *S. latissima* in a physiological context of both abiotic and biotic stress,

all selected reference genes were then re-assessed to monitor the expression of two target genes encoding a lipoxygenase (*LOX*) and a glutathione s-transferase (*GST*), which are involved in oxylipin pathway and oxidative stress responses, respectively. The validated reference genes will be suitable internal standards to further explore gene expression regulations related to stress responses and resistance in *S. latissima* using RT-qPCR.

2. Results

2.1. *In silico S. latissima* transcriptome-wide selection of candidate reference genes

A total of 23,049 unigenes from *S. latissima* was analyzed based on RNAseq and microarray datasets: the dispersion measure (DPM) was calculated to evaluate their expression variability according to different experimental conditions, using PaGeFinder. The DPM value of 3,641 unigenes in biotic stress data, i.e. co-cultivation datasets including corresponding control datasets, and 2,576 unigenes in abiotic stress data, i.e. temperature, light stress and control conditions, were lower than 0.3 and were first selected as a pool of most stable transcripts. Among them, the unigenes without any function annotation or whose expression level was too low (TPM<10) were removed, leading to 225 and 788 remaining candidate genes. Finally, eight genes were selected based on the combination of genes with low DPM values, either in biotic stress datasets only, or in abiotic stress datasets only or in all datasets.

PCR amplification and melting curve analysis were performed to confirm the specificity of the eight designed primer pairs, i.e. presenting a single band of amplification at the expected size (Sup. Fig.1) and a single peak of the melting curve of the PCR product (Sup. Fig.2). The mean amplification efficiency of each gene ranged from 1.95 to 2.03 (Table 1).

Table 1 Description of the candidate reference genes

Gene symbol	NR description	DPM* (abiotic stress)	DPM* (biotic stress)	Primer sequence : Forward Reverse	RT-qPCR efficiency[a]	Error[b]
60S	60S ribosomal protein L10A [Ectocarpus siliculosus]	0.2596	0.1423	TACAAAATAATAGCCCAGCACG CAGAGTTACATTACACCCAGGAG	1.99	0.01

ACT	beta-actin [Fucus vesiculosus]	0.2919	0.0947	CACATTATTCTCGCACACAACAG TAAAGAACACGCACACTTAGCAG	2.006	0.167
ATM1	iron-sulfur clusters transporter atm1, mitochondrial precursor [Ectocarpus siliculosus]	0.1947	>0.3	GTTTTTGTCGGATAGAGTGAATGG TCAAACAGACGCACGCTACG	2.039	0.0019
ATPase	F-type H-ATPase beta subunit [Ectocarpus siliculosus]	0.2469	0.1222	TTGCTGTCGGTTCTGCTGG TGGCGGTGTGGAAGTGG	1.963	0.108
EIF5B	EIF5B, eukaryotic translation initiation factor 5B [Ectocarpus siliculosus]	0.2807	0.1015	GAGGTGACGAGCGATTGA TCTTTCGGCGACGGGTT	2.002	0.0484
LISK	LISK family protein kinase [Ectocarpus siliculosus]	0.2482	0.1149	CCGCTTCTTCCTGTTCTGG GCTTGATGGCTGCCTACGA	1.953	0.0255
NDH	ND11 homolog, NADH dehydrogenase (ubiquinone) subunit 11 [Ectocarpus siliculosus]	0.2593	0.0807	GGAGGAGATGGAGGAGCGTGTG GGCGTCCGTGCGGTAGAAGT	1.962	0.116
TUBD	Tubulin folding cofactor D [Ectocarpus siliculosus]	0.1985	>0.3	AGGTCAGCATCGGTTTAC TTTGGTTCGGCTGTCGTAG	1.961	0.046

* DPM: the dispersion measure

[a] The PCR amplification efficiency for each primers pair was determined by LightCycler®480 gene scanning software (version 1.5)

[b] The Error value of amplification efficiency for each primers pair was determined by LightCycler®480 gene scanning software (version 1.5) with an acceptable value < 0.2.

2.2. RT-qPCR expression profiles of candidate reference genes

The expression levels of the eight candidate genes were monitored by RT-qPCR in all *S. latissima* RNA samples, obtained from biotic and abiotic stress experiments, including corresponding control conditions. For each gene primer set amplification, the quantification cycle (Cq) value was reported in each RNA sample and the mean Cq value was calculated by pooling either all the Cq values derived from biotic conditions, or from abiotic conditions or from all tested conditions (Fig. 1). Globally the eight tested genes featured a relatively wide expression range, from 19.62 to 30.65 Cq and showed a very similar expression profiles between the two treatment conditions. Since the Cq values are negatively correlated to the transcript levels, the *LISK* was the highest expressed gene and the 60S ribosomal protein encoding gene was the lowest expressed gene. Whatever the analyzed datasets (biotic, abiotic and all stress together), the *ACT* gene displayed the largest expression variation (Fig. 1). In biotic experimental conditions (Fig. 1A), the *LISK*

gene exhibited the smallest expression variation, whereas in abiotic ones (Fig. 1B) and all stress conditions (Fig. 1C), it was the *ATPase* gene.

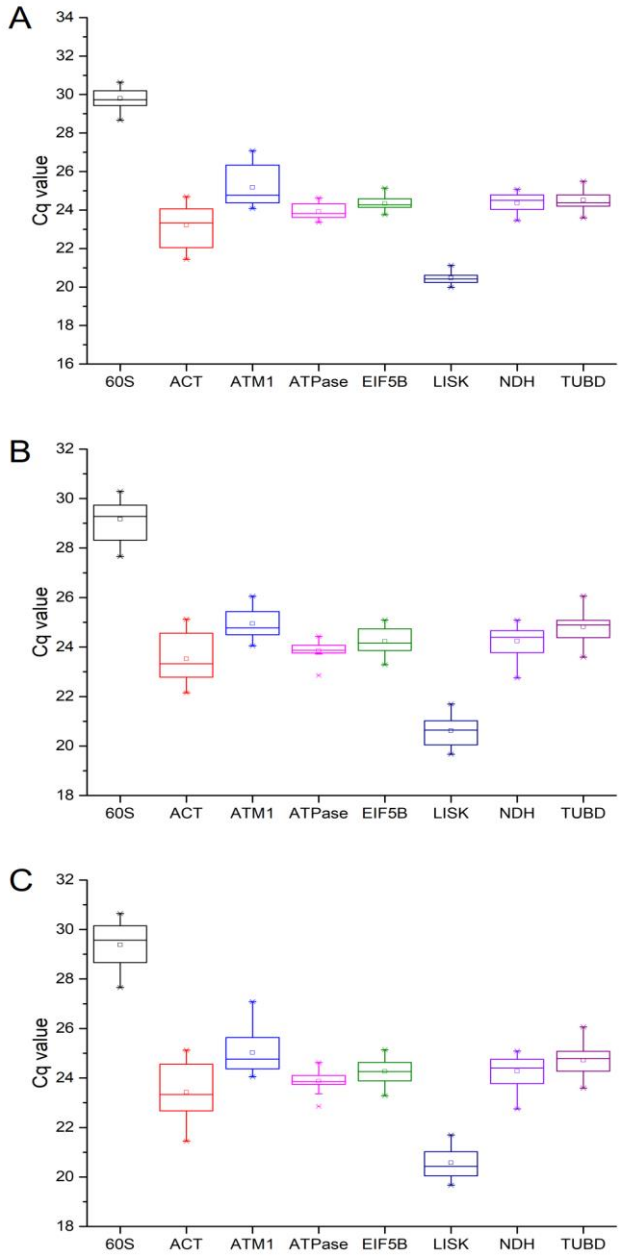

Figure 1. Box-plots of Cq values obtained for the 8 candidate reference genes in (A) Biotic stress (n=16), (B) Temperature and light stress (n=20), and (C) All tested conditions (n=36). Central lines in the boxes correspond to the median values.

2.3. Computational analysis of candidate gene expression stability

The Cq values of the eight candidate genes were then used to evaluate their expression stability under different experimental conditions using four computational algorithms, namely geNorm, NormFinder, BestKeeper and the comparative ΔCt method.

The geNorm analysis showed that expression stability value (M) of all the candidate genes ranged from 0.16 to 0.80 under all conditions, demonstrating that their expression could be considered as relatively stable, as M was always under 1.5 (Sup. Table 1). Under temperature and light stress, the *ACT* and *NDH* genes were predicted as the most stable reference genes, with the lowest M value, when the *ATPase* and *EIF5B* genes exhibited the lowest M value in biotic stress conditions. Comprehensive analysis combining all the conditions together showed the M-value-based ranking of all candidate genes, from the most (the lowest M value) to the least (the highest M value) constitutively expressed, was: *EIF5B*, *NDH*, *ATPase*, *LISK*, *TUBD*, *ATM1*, *60S* and *ACT* (Sup. Table 1). In addition, the pairwise variation analysis suggested that the combination of three reference genes was suitable for the light and temperature treatment group, as the V3/V4 value was the first one lower than 0.15 (Sup. Fig. 3). Using the co-cultivation and GG treatment group, the V2/V3 value was the first one lower than 0.15 (Sup. Fig. 3), indicating that two reference genes were sufficient for RT-qPCR normalization.

Based on Normfinder analysis, the most stable genes in term of expression were *NDH* followed by *EIF5B*, both being considered as suitable reference genes, in temperature and light stress conditions and when considering all conditions together (Sup. Table 2). However, the two most stable expressed genes were *ATPase* and *EIF5B*, in the biotic stress conditions.

In the Bestkeeper analysis, only the SD value of the *ACT* gene in biotic stress conditions was bigger than one (Sup. Table 3), and its expression should be considered as relatively unstable. Among all the other genes, Bestkeeper identified two most stable genes, *ATPase* and *EIF5B*, considering all the sample sets or only the light and temperature stress related samples. Under biotic stress, the *EIF5B* and *LISK* genes were predicted as the two most stable expressed genes.

The comparative delta Ct method identified the *ATPase* and *EIF5B* genes as the two most stable genes during biotic stress experiments (Sup. Table 4). When analyzing the light and temperature stress conditions or all conditions together, the expression stability was the strongest for the *NDH* and *EIF5B* genes.

2.4. Integrating computational methods for a comprehensive ranking of candidate reference genes

Based on these analyses, the prediction of the most stable genes revealed some variations according to experimental conditions tested and methods used (Fig. 2). Some overall trends appear such as the relatively bad ranking of the *ACT* gene as potential reference gene, except for one method (delta Ct) in abiotic conditions (Fig. 2B). Indeed, the final ranks of the eight candidate reference genes were sometimes very different as observed for the *LISK* gene, classified from 1 to 4 in biotic conditions (Fig. 2A) or for the *ATPase* gene, ranked from 1 to 6 in abiotic conditions (Fig. 2B). Therefore, RefFinder, an online software based on statistical approaches, was used to compare these data and establish a comprehensive ranking of all candidate genes (Sup. Table 5). Our results showed that *ATPase* and *EIF5B* were the two most stable reference genes under biotic stress, i.e. for co-cultivation or elicitation experimental conditions (Fig. 2). While under light and temperature stress, the predictive reference genes were *NDH* and *EIF5B.* In the end, the overall ranking of the eight genes considering all conditions from the most stable to the least stable expressed was: *NDH* > *EIF5B* > *ATPase* > *TUBD* > *LISK* > *ATM1* > *60S* > *ACT* (Fig. 2; Sup. Table 5).

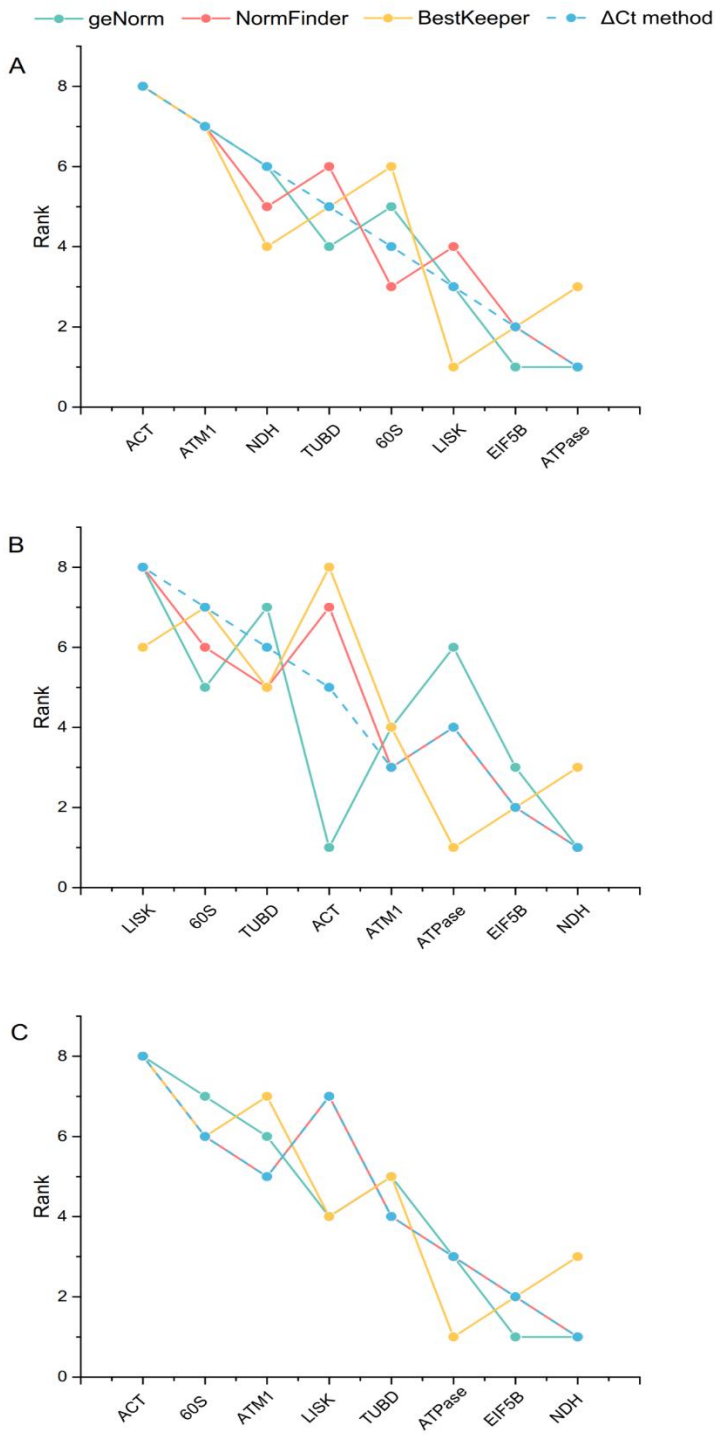

Figure 2. Comparison of ranking of 8 candidate reference genes using geNorm, NormFinder, Delta Ct, and BestKeeper under (A) biotic stress, (B) light and temperature stress, and (C) the combination of all stresses. The ordering of genes on X axis indicates the comprehensive ranking obtained with RefFinder (see Sup. Table 5), from the least to the most stable genes.

2.5. RT-qPCR reference gene validation

To further validate the reliability of the reference gene selection when studying gene regulation during either abiotic or biotic stress conditions, the expression levels of two target genes, *LOX* and *GST*, were monitored and normalized using the three best reference gene combination, the most stable reference gene or the least stable reference gene, predicted previously (Fig. 2A, 2B). Under light and temperature stress conditions, compared to control conditions, the *LOX* relative expression calculations appeared differently affected by the three normalization modes, depending on stress treatment (Fig. 3). For instance, no significant difference of the fold-change expression levels was detected under high temperature and low light treatment for the *LOX* gene. When comparing all conditions, the *LOX* expression always featured down-regulated patterns, when using the least stable reference gene (*LISK*) or the most stable reference gene (*NDH*) for normalization. Interestingly, this expression pattern was much more contrasted using the best reference gene combination (*NDH, EIF5B* and *ATPase*) as calibrator, and changed from 0.12-fold in high temperature and high light conditions to 1.53-fold, appearing up-regulated in low temperature and low light conditions (Fig.3). Interestingly, when comparing these results with the fold change value obtained from the RNA-seq data, the best reference gene combination as calibrators resulted in a similar expression pattern, with a down-regulation in high temperature stresses and an induction under low light and temperature stress conditions. In this later condition, the relative expression levels of *LOX* seem to be significantly underestimated, when using the most stable reference gene (*NDH*). While using the least stable reference gene (LISK), the expression fold changes showed significant differences in two conditions out of four tested (Fig. 3), confirming the low-quality prediction of this gene as reference gene.

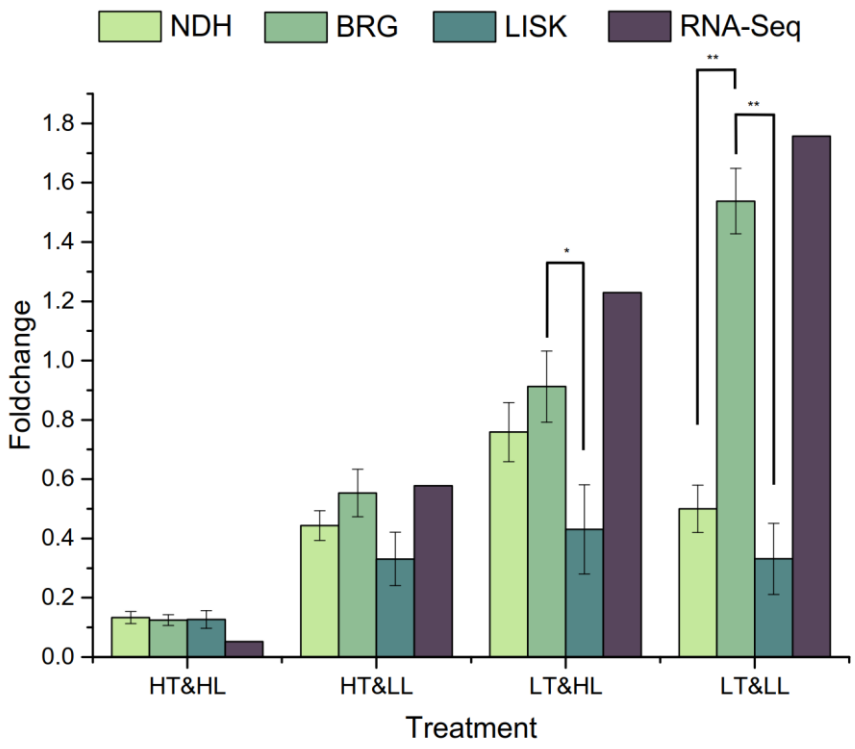

Figure 3. Relative expression levels of LOX gene, normalized by the most stable reference gene, NDH; the best reference gene combination, BRG (NDH, ATPase and EIF5B); the least stable reference gene, LISK, in temperature and light stress compared to control condition. HT: high temperature; LT: low temperature; HL: high light; LL: low light. Error bars indicate standard errors (n=4). The statistical significance between normalization modes is indicated by one or two asterisks (*, P value < 0.05; **, P value < 0.01; t-test).

In *S. latissima* samples cultivated with endophytes for two days, the *GST* expression levels showed strong up-regulations, 5.73-fold and 9.41-fold changes, respectively, when using the most stable reference gene (*ATPase*) and the best reference gene combination (*ATPase* and *EIF5B*) as calibrators. These expression patterns were in agreement with that obtained from RNA-seq datasets (Fig.4). The use of the least stable reference gene (*ACT*) for normalization significantly affect the calculation of the relative expression level, leading to a much lower value (2.39-fold change). A similar under-estimation bias of the *GST* relative expression level was found in the GG treated samples, where the best reference gene combination (11.31-fold) and *ATPase* (6.66-fold) normalization showed the highest upregulation shifts, compared to the expression results normalized by *ACT*. In that case, however, we couldn't compare these results with the corresponding GG RNA-seq datasets as reference.

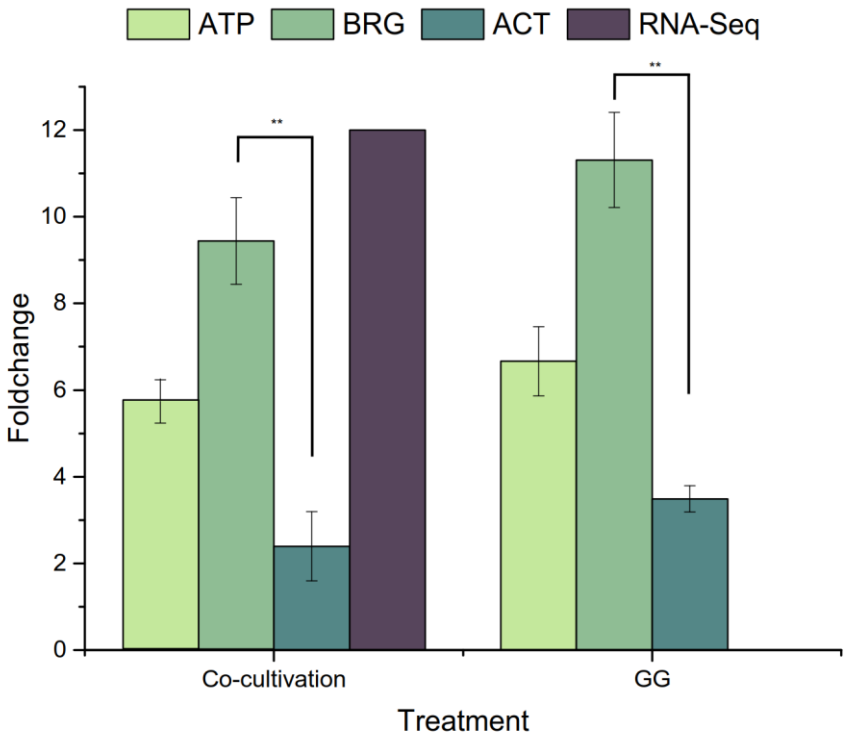

Figure 4. Relative expression levels of GST gene, normalized by the most stable reference gene, ATPase; the best reference gene combination, BRG (ATPase and EIF5B); the least stable reference gene, ACT, in biotic stress. GG: oligoguluronates elicitation. Error bars indicate standard errors (n=4). The statistical significance between normalization modes is indicated by one or two asterisks (*, P value < 0.05; **, P value < 0.01; t-test).

3. Discussion

RT-qPCR has been widely used for many purposes such as the quantification of target gene expression because of its specificity and high sensitivity of detection. However, the choice of internal standard genes has a huge effect on the normalization step and the final accuracy of RT-qPCR results. Using inappropriate reference genes as calibrators will result in significant differences of target transcript quantification as shown in the strong biases observed using different sets of genes for normalization (Fig. 3 and 4). Reference genes were generally selected from housekeeping genes, but recent studies have shown that some classic housekeeping genes do not present a stable expression under variable conditions, or not sufficiently stable to be used for RT-qPCR normalization (Czechowski et al., 2005, Silveira et al., 2018). In agreement with these results, our study also showed that a classic housekeeping gene coding for actin (*ACT*), which has been widely used as reference gene in numerous species by the past, did not exhibit

high stability in any of the six experimental conditions analyzed, covering both abiotic and biotic stress conditions (Fig. 1). Therefore, it is not only necessary to select reference genes for each studied species, but they also need to be adapted to each experimental set-up, by validating the absence of variability of their expression in corresponding physiological conditions.

As an important source of transcriptomic information, RNA-seq analysis has been performed to explore suitable reference genes for specific experimental conditions (Zhan et al., 2019, Liu et al., 2018). In this study, we analyzed RNA-seq datasets related to biotic (co-cultivation with endophyte) and abiotic stress (light and temperature) in *S. latissima*. Eight candidate reference genes were selected considering credible protein annotation (Nr database), appropriate expression levels (TPM>10) and a low dispersion measure (DPM $\leq$ 0.3), and their expression stability was further validated by RT-qPCR in *S. latissima* plantlets submitted to different stress treatments carried out in laboratory controlled conditions. These treatments were chosen to cover a range of different physiological conditions, such as temperature and light environmental changing parameters, which could be encountered during intertidal exposures. For biotic stress validation, plantlets were cultivated with their natural endophyte *Laminarionema elsbetiae* (Bernard et al., 2019) using laboratory-controlled bioassays. In addition, oligo-guluronate elicitation was performed as previous studies indicated that this chemical treatment was able to induce an oxidative burst in *S. latissima* (Küpper et al., 2002) and transcriptomic and metabolic defense regulations in another closely-related Laminariales, *L. digitata* (Cosse et al., 2009, Goulitquer et al., 2009). GG elicitation is therefore expected to mimic the damages of cell wall caused by numerous biotic agents and induced defense-related pathways in *S. latissima*.

Based on RT-qPCR expression data, the comprehensive ranking of candidate genes by RefFinder led to the identification of two optimal combinations of reference genes, according to experimental conditions (Fig 2, Sup. Table 5). For biotic stress conditions, it was the two genes, *EIF5B* and *ATPase*. *ATPase* encodes the mitochondrial and chloroplast synthases, which use a proton gradient produced by electron transfer reactions to drive the synthesis of ATP. This gene has also been validated as the best internal standard in *Coleomegilla maculate* under different developmental stage (Yang et al., 2015). However, its use as reference gene is not ubiquity, as in a dinoflagellate microalga, *Alexandrium catenella*, *ATPase* was predicted as the least stable gene across different nutritional conditions (Niaz et al., 2019). Unlike *ATPase*, the *EIF5B* gene is rarely

used as reference gene in other species. *EIF5B* belongs to the translation initiation factor family and is an essential initiation factor catalyzing the second GTP-dependent step in eukaryotic translation initiation (Lee et al., 2002). The other members of translation initiation factor gene family have been widely used as constitutively reference gene in some macroalgal species. In the red alga *C. crispus,* the expression stability of the gene coding for the translation initiation factor 4A-1 has been validated under light, osmotic and heavy metal stress (Kowalczyk et al., 2014). In our study, *EIF5B* also exhibited a high stability of expression in all the experimental setup tested, including biotic, abiotic and control conditions. For the light and temperature treatment group, three reference genes, including *EIF5B*, *ATPase* and *NDH,* were predicted to be the best combination in these physiological conditions. The *NDH* gene encodes NADH dehydrogenase located on the inner membrane of mitochondrial, transferring electron from NADH to coenzyme Q10. *NDH* was the best ranked reference gene under temperature and light stress conditions (Fig. 2). However, it wasn't the case in the biotic treatment group (Fig. 2), therefore its use should be adapted to physiological studies upon changing abiotic parameters or further validated using other experimental conditions. The actin (*ACT*) gene, a traditional used as reference gene for qPCR normalization, was validated in strawberry under light and temperature stress conditions according to its stable expression level (Zhang et al., 2018). However, in our study, *ACT* was the least stable reference gene across all conditions we tested, as also observed in the brown alga *Ectocarpus siliculosus,* under multiple stress conditions (Le Bail et al., 2008).

The *LOX* gene is involved in the oxylipin synthesis pathway, which plays an important role in the signal transduction under stress conditions (López et al., 2011, Lim et al., 2015). According to the RNA-Seq dataset analysis, the *LOX* gene was significantly up-regulated under light and temperature stress conditions and *GST* was up-regulated under co-cultivation stress. Therefore, these two target genes were used to validate the use of selected reference genes for normalizing their expression. In light and temperature stress, the results showed that, the expression normalized by the least stable gene *LISK* was significantly underestimated comparing to the one normalized by the best reference gene combination (BRG), including the three genes, *NDH*, *ATPase* and *EIF5B.* It is worth noting that the normalization by a single reference gene, even if being the most stable one, *NDH,* also conducted to a significant underestimation compared to the normalization by the BRG, indicating the necessity of using multiple reference gene combination as a calibrator. The strong correlation observed with the expression pattern derived from the RNA-

Seq data further supports the validity of this combination to be used in physiological experiments related to different abiotic conditions. Similarly, the *GST* expression analysis under biotic stress showed the same trend: the use of two reference gene combination (*ATPase* and *EIF5B*) led to an accurate expression quantification, compared to RNA-seq results, at the contrary of the actin gene normalization, which has to be avoid in such conditions.

4. Conclusions

In this study, eight candidate genes with low expression variance were screened using large transcriptomic datasets generated in the kelp *S. latissima* under biotic and abiotic stress conditions. Among these genes, two combinations of reference genes were identified according to their expression stability under the different physiological conditions tested: *EIF5B* and *ATPase* are the best adapted reference genes under biotic stress related conditions, while *NDH*, *ATPase* and *EIF5B* are the optimal combination for RT-qPCR normalization under temperature and light stress. Moreover, our study clearly showed that a commonly used reference gene, coding for Actin, is not suitable to normalize RT-qPCR gene expression under the different physiological conditions in *S. latissima*, its expression being too much variable. This result further illustrates the importance of conducting specific experimental validation, before selecting accurate reference gene in RT-qPCR. The two validated reference gene combinations are expected to be further used as reliable calibrators for targeted gene expression analysis by RT-qPCR in *S. latissima* upon both abiotic and biotic environmental conditions.

5. Methods

5.1. Algal material and treatments

Fertile sporophytes of the kelp *Saccharina latissima* were collected at Roscoff (Perharidy, 48.73° N, 4.00° W), cleaned and cut into small pieces for spores release using the hanging-drop technique (WYNNE, 1969). Lab-grown gametophytes were kept for several weeks in Provasoli-enriched, filtrated and autoclaved natural seawater (FSW), under 12°C and 20 µmol photons m^{-2} s^{-1} with a 12 h light/dark cycle. After self-fertilization, the developing sporophytes were grown in petri dishes in the same culture conditions (10 mL Provasoli solution/L FSW, (Provasoli, 1968)). After 4 weeks, the sporophytes were detached from the cover slips and transferred to 10 L bottles connected to an aeration system. The culture medium (FSW enriched with Provasoli) was weekly

changed. The kelp cultures were maintained under 12°C and 20 µmol photons m^{-2} s^{-1} with a 12 h light/dark cycle. The brown filamentous alga *Laminarionema elsbetiae strain* was maintained in petri dishes in the same culture medium conditions, except the photon rate at 5µmol photons m^{-2} s^{-1}.

The laboratory-grown sporophytes of *S. latissima* (~5 cm length) and its natural endophyte *Laminarionema elsbetiae* were co-cultivated in 2 L bottles filled with 1.5 L sterile Provasoli enriched FSW and connected to an aeration system. The co-cultivation experiment was performed for 2 days, and control cultures of *S. latissima* without endophytes were conducted in the same time, in the same conditions. In parallel, the GG elicitation was performed on *S. latissima* sporophytes, by adding 150 µg/mL of oligo-guluronates blocks (GG, prepared from *L. hyperborea* according to Haug et al. 1974) (Haug et al., 1974) in small glass bakers filled with 30 mL FWS, under shaking for 1 hour. All the co-cultivation tests, including GG treatments and corresponding control experiments, were conducted under the same conditions: 12°C and 20µmol photons m^{-2} s^{-1} with a 12 h light/dark cycle.

For subjecting sporophytes to various abiotic stress, laboratory-grown sporophytes were transferred in 30 mL FSW glass bakers and maintained for two days in four different temperature and light culture conditions as already conducted in (Heinrich et al., 2012): high temperature and high light (HT&HL, 17°C & 107.8±5 µmol photons m^{-2} s^{-1}), high temperature and low light (HT&LL, 17°C & 23.8±3.2 µmol photons m^2 s^{-1}), low temperature and high light (LT&HL, 2°C & 107.8±5 µmol photons m^2 s^{-1}) and low temperature and low light (LT&LL, 2°C & 23.8±3.2 µmol photons m^2 s^{-1}). Three biological replicates were collected for each treatment. They were flash frozen in liquid nitrogen and kept at -80°C until RNA extraction.

5.2. RNA isolation and cDNA synthesis

Total RNA was extracted using a combination of a classical CTAB-based method and of the RNeasy Mini kit (QIAGEN, Hilden, Germany), as described in Heinrich *et al.* (Heinrich et al., 2012). Compared to this protocol, before the use of the purification kit, an additional ethanol precipitation step was conducted to remove polysaccharides, and RNA was separated from DNA

and major contaminants by precipitation in 3M LiCl solution and 1% 2-mercaptoethanol, at -20°C overnight. After RNA extraction, a treatment with RNAse-free DNAse I (Turbo DNAse, Ambion) was performed to eliminate residual genomic DNA. The quality and quantity of total RNA were tested on a NanoDrop™ spectrophotometer (Thermo Fisher Scientific Inc., Waltham, US) and further checked on a 2% agarose gel. RNA samples with concentrations above 100 ng/µL and A260/A280 ratio of 1.8–2.0 were used for cDNA synthesis. The RNA was reverse-transcribed to cDNA using the ImProm-II™ Reverse Transcription System (Promega).

5.3. Bioinformatic selection of candidate reference genes

Different RNA-seq data sets were used to screen for potential candidate reference genes. RNA sequencing of control and co-cultured samples were previously performed using Illumina Hi-Seq™ 3000 platform (Bernard, Xing, et al. unpublished data; ENA at the EBI; ID: PRJEB37483). After transcriptome assembly and annotation, the reads were mapped on the transcriptome using bowtie2 (Langmead & Salzberg, 2012). The read counts were calculated by RSEM (Li & Dewey, 2011b) and converted into transcripts per million (TPM) for each unigene. The microarray data of *S. latissima* under abiotic stress (control, high temperature & high light, high temperature & low light, low temperature & high light and low temperature & low light) were downloaded from EMBL database (ArrayExpress at the EBI; http://www.ebi.ac.uk/microarray-as/ae/; ID: E-MEXP-3450) and the probes of each gene were mapped to the reference transcriptome to link the expression of probes with unigenes.

The expression stability of all unigenes in two datasets were calculated and ranked separately by the Pattern Gene Finder (PaGeFinder). PaGeFinder is a web-based server for the on-line detection of gene expression patterns from serial transcriptomic data generated by high-throughput technologies like microarray or next-generation sequencing. In PaGeFinder, the dispersion measure (DPM) was calculated to evaluate the variability of gene expression profiles. A value of DPM close to 0 suggests a similar expression level of a gene over all RNAseq samples, and then a strong stability of its expression whatever the treatments. In the end, genes with putative and reliable protein annotation (Nr databases), appropriate expression levels (TPM> 10), and a low dispersion measure (DPM ≤0.3) were selected as candidate genes to be further tested as RT-qPCR reference genes.

5.4. RT-qPCR and Data Analysis

For each reference candidate gene and stress-related target genes, a pair of specific primers was designed in the 3' end coding region of sequences using Primer5 software (Table 1). Primers were designed to have a melting temperature around 60°C, a length between 18–26 nucleotides, a GC content between 40–60%, avoiding secondary structures and self- and cross-annealing. The specificity of each primer was tested *in silico,* using BLASTN search on the reference transcriptome of *S. latissima.*

The RT-qPCR reactions were performed in 384-well plates in a LightCycler®480 (Roche Molecular Biochemicals, Mannheim, Germany) with LightCycler®480 SYBR Green I Master kit (Roche, Germany). The protocol was: 95 °C for 5 min, followed by 55 cycles of 95 °C for 10 s, 60 °C for 10 s, and 72 °C for 20 s. Four biological replicates were performed for each treatment. The specificity of the amplification was verified with a dissociation curve obtained by heating the samples from 65°C to 95°C. A 1:5 dilution series of the *S. latissima* cDNA was prepared and tested for each gene to determine the amplification efficiency of the selected primers pairs, which was calculated by the LightCycle®480 gene scanning software (version 1.5), using the Fit-points method. These amplification tests on cDNA dilution series are also important to set the linearity limits of the amplification.

The gene expression level was determined by the number of amplification cycles (Cq), which was extracted from the raw fluorescence data of the RT-qPCR curve. Four statistical methods (NormFinder, geNorm, BestKeeper and comparative delta Ct method) were used to evaluate the expression stability of selected reference genes. Bestkeeper is an Excel-based tool that analyzes absolute raw Cq values directly using pairwise correlations. It calculates three variables related to the expression level of genes: the standard deviation (SD), the coefficient of correlation (r), and the coefficient of variance (CV). The gene with the lowest CV ± SD is considered as the most stable transcript gene. In other three methods, the Cq value is converted into relative quantities according to the formula: $2^{-\Delta Ct}$ (ΔCt= the corresponding Cq value−minimum Cq). In geNorm, the M-values are calculated to evaluate the expression stability of genes. The most stable expressed gene exhibits the lowest M-value. In NormFinder, the genes are ranked according to their stability

value (SV) which is calculated using an ANOVA model based on ΔCt values. A lower SV is correlated with a higher expression stability. The last method is based on the pairwise comparisons of ΔCt, ranking the genes from the most to the least stable transcripts, based on the average standard deviations, the lowest average SD corresponding to the most stable. Finally, an online software, RefFinder (http://leonxie.esy.es/RefFinder/) was used to obtain the overall final ranking of all candidate genes based on results of the four computational programs, NormFinder, BestKeeper, GeNorm, and comparative ΔCt.

For target genes, the raw data were divided by the Cq value of corresponding reference genes as a normalization step. And then the relative expression level of treated samples versus control samples was calculated by comparing the normalized Cq of treatment and control samples according to the formula: $2^{-\Delta\Delta Ct}$ (ΔΔCt= normalized Cq value of treated sample−normalized Cq value of control sample).

Authors' contributions.

QX and CL conceived the experiments. QX and SR processed algal and RNA samples, and QX performed the in silico and RTqPCR analyses, and interpreted the data. QX wrote the first draft of the manuscript and SR and CL contributed substantially to the revisions. All authors read and approved the final manuscript.

Acknowledgements

We would like to thank L. Dartevelle and E. Rolland from the LBI2M's Algal Culture facilities for technical support. This work has also benefited from the computational resources of the ABiMS bioinformatics platform (FR 2424, CNRS-Sorbonne Université, Roscoff), which are part of the Biogenouest core facility network.

6. Supplementary Material

Supplementary Table 1 geNorm ranking and M values for the 8 candidate reference genes

Rank	All stress		Light & temperature stress		Biotic stress	
	Gene	M value	Gene	M value	Gene	M value
1	EIF5B	0.48	ACT	0.46	ATPase	0.16
2	NDH	0.48	NDH	0.46	EIF5B	0.16
3	ATPase	0.55	EIF5B	0.58	LISK	0.25
4	LISK	0.61	ATM1	0.63	TUBD	0.31
5	TUBD	0.65	60S	0.69	60S	0.40
6	ATM1	0.71	ATPase	0.73	NDH	0.47
7	60S	0.74	TUBD	0.77	ATM1	0.56
8	ACT	0.77	LISK	0.80	ACT	0.70

Supplementary Table 2 Ranking and expression stability of the 8 candidate reference genes calculated by NormFinder

Rank	All stress		Light & temperature stress		Biotic stress	
	Gene	Stability	Gene	Stability	Gene	Stability
1	NDH	0.33	NDH	0.31	ATPase	0.22
2	EIF5B	0.39	EIF5B	0.45	EIF5B	0.33
3	ATPase	0.43	ATM1	0.45	60S	0.35
4	TUBD	0.57	ATPase	0.52	LISK	0.44
5	ATM1	0.61	TUBD	0.675	NDH	0.5
6	60S	0.62	60S	0.69	TUBD	0.52
7	LISK	0.65	ACT	0.69	ATM1	0.68
8	ACT	0.73	LISK	0.74	ACT	0.97

Supplementary Table 3 Ranking and expression stability of the 8 candidate reference genes calculated by BestKeeper

Rank	All stress			Light & temperature stress			Biotic stress		
	Gene	SD	CV	Gene	SD	CV	Gene	SD	CV

1	ATPase	0.30	1.25	ATPase	0.21	0.89	EIF5B	0.30	1.24
2	EIF5B	0.40	1.64	EIF5B	0.39	1.60	LISK	0.29	1.46
3	NDH	0.43	1.76	NDH	0.42	1.71	ATPase	0.36	1.54
4	60S	0.58	1.97	ATM1	0.48	1.93	60S	0.54	1.82
5	TUBD	0.51	2.07	60S	0.58	1.99	NDH	0.47	1.96
6	LISK	0.47	2.25	TUBD	0.50	2.02	TUBD	0.48	1.96
7	ATM1	0.73	2.91	LISK	0.50	2.42	ATM1	0.96	3.81
8	ACT	0.73	3.19	ACT	0.69	2.96	ACT	1.03	4.45

Supplementary Table 4 Ranking and expression stability of the 8 candidate reference genes calculated by ΔCt method

Rank	All stress		Light & temperature stress		Biotic stress	
	Gene	MeanSD	Gene	MeanSD	Gene	MeanSD
1	NDH	0.67	NDH	0.67	ATPase	0.51
2	EIF5B	0.69	EIF5B	0.74	EIF5B	0.55
3	ATPase	0.71	ATM1	0.75	LISK	0.61
4	TUBD	0.79	ATPase	0.79	60S	0.63
5	ATM1	0.82	ACT	0.87	TUBD	0.66
6	60S	0.83	TUBD	0.87	NDH	0.70
7	LISK	0.83	60S	0.88	ATM1	0.88
8	ACT	0.89	LISK	0.91	ACT	1.14

Supplementary Table 5 Comprehensive ranking of the expression stability of the 8 candidate reference genes

Method	1	2	3	4	5	6	7	8
RANKING ORDER UNDER ALL STRESS								
geNorm	EIF5B|NDH		ATPase	LISK	TUBD	ATM1	60S	ACT
NormFinder	NDH	EIF5B	ATPase	TUBD	ATM1	60S	LISK	ACT
BestKeeper	ATPase	EIF5B	NDH	LISK	TUBD	60S	ATM1	ACT
ΔCt method	NDH	EIF5B	ATPase	TUBD	ATM1	60S	LISK	ACT
Comprehensive ranking	NDH	EIF5B	ATPase	TUBD	LISK	ATM1	60S	ACT
RANKING ORDER UNDER TEMPERATURE AND LIGHT STRESS								
geNorm	ACT|NDH		EIF5B	ATM1	60S	ATPase	TUBD	LISK
NormFinder	NDH	EIF5B	ATM1	ATPase	TUBD	60S	ACT	LISK
BestKeeper	ATPase	EIF5B	NDH	ATM1	TUBD	LISK	60S	ACT
ΔCt method	NDH	EIF5B	ATM1	ATPase	ACT	TUBD	60S	LISK
Comprehensive ranking	NDH	EIF5B	ATPase	ATM1	ACT	TUBD	60S	LISK

	RANKING ORDER UNDER BIOTIC STRESS							
geNorm	EIF5B| ATPase		LISK	TUBD	60S	NDH	ATM1	ACT
NormFinder	ATPase	EIF5B	60S	LISK	NDH	TUBD	ATM1	ACT
BestKeeper	LISK	EIF5B	ATPase	NDH	TUBD	60S	ATM1	ACT
ΔCt method	ATPase	EIF5B	LISK	60S	TUBD	NDH	ATM1	ACT
Comprehensive ranking	ATPase	EIF5B	LISK	60S	TUBD	NDH	ATM1	ACT

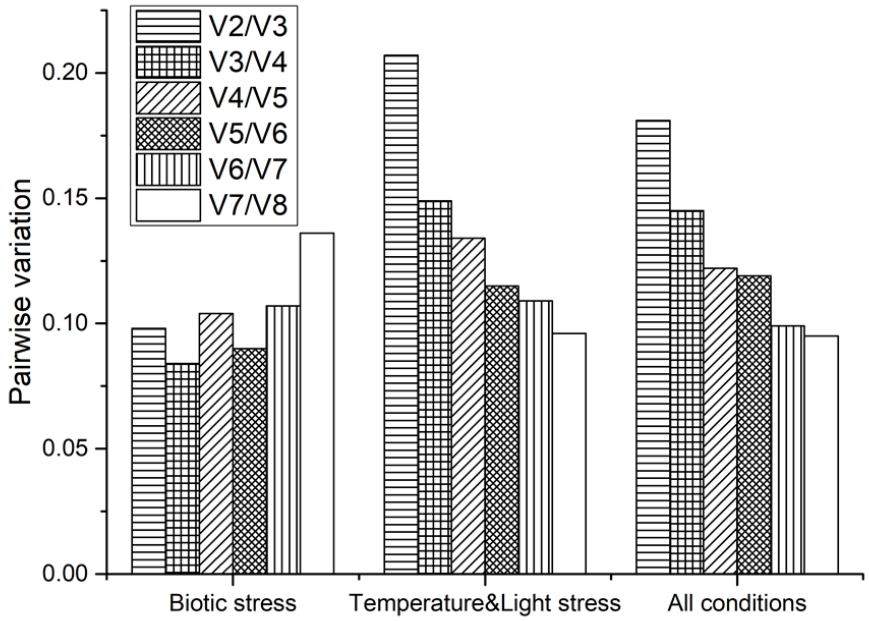

Supplementary Figure 1. Pairwise variation (V) of the candidate reference genes calculated by geNorm to establish the optimal number of reference genes according to stress condition.

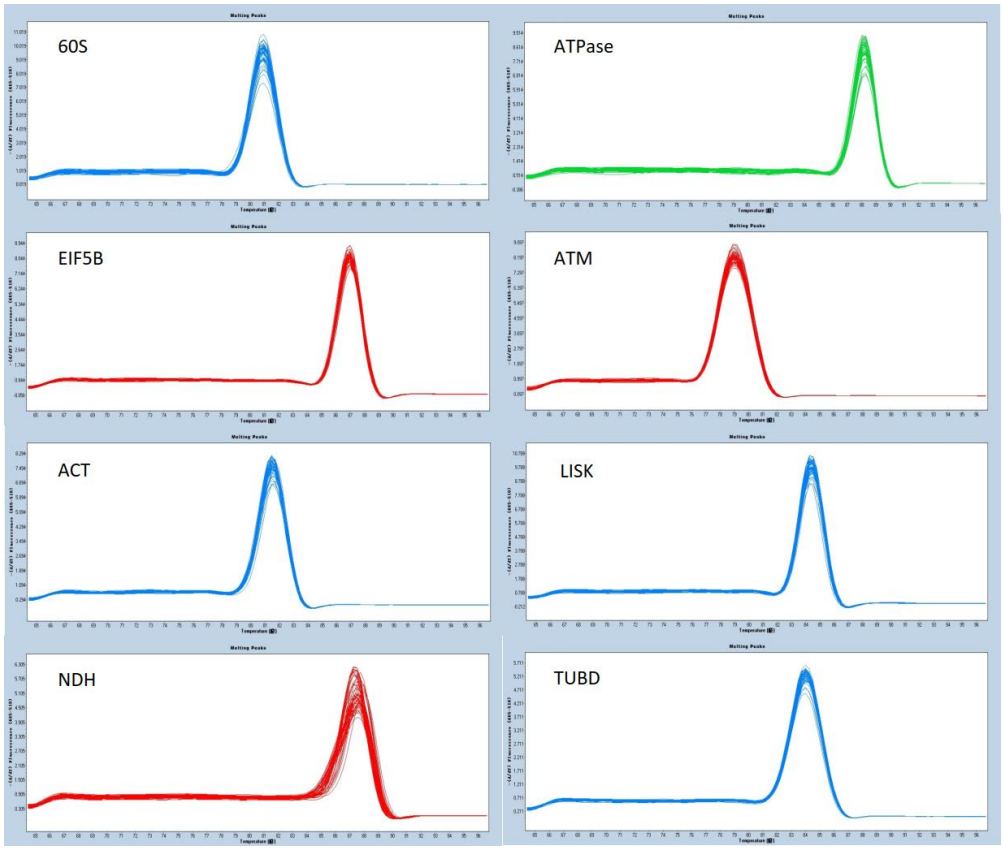

Supplementary Figure 2. qPCR melting curves of the eight candidate reference genes.

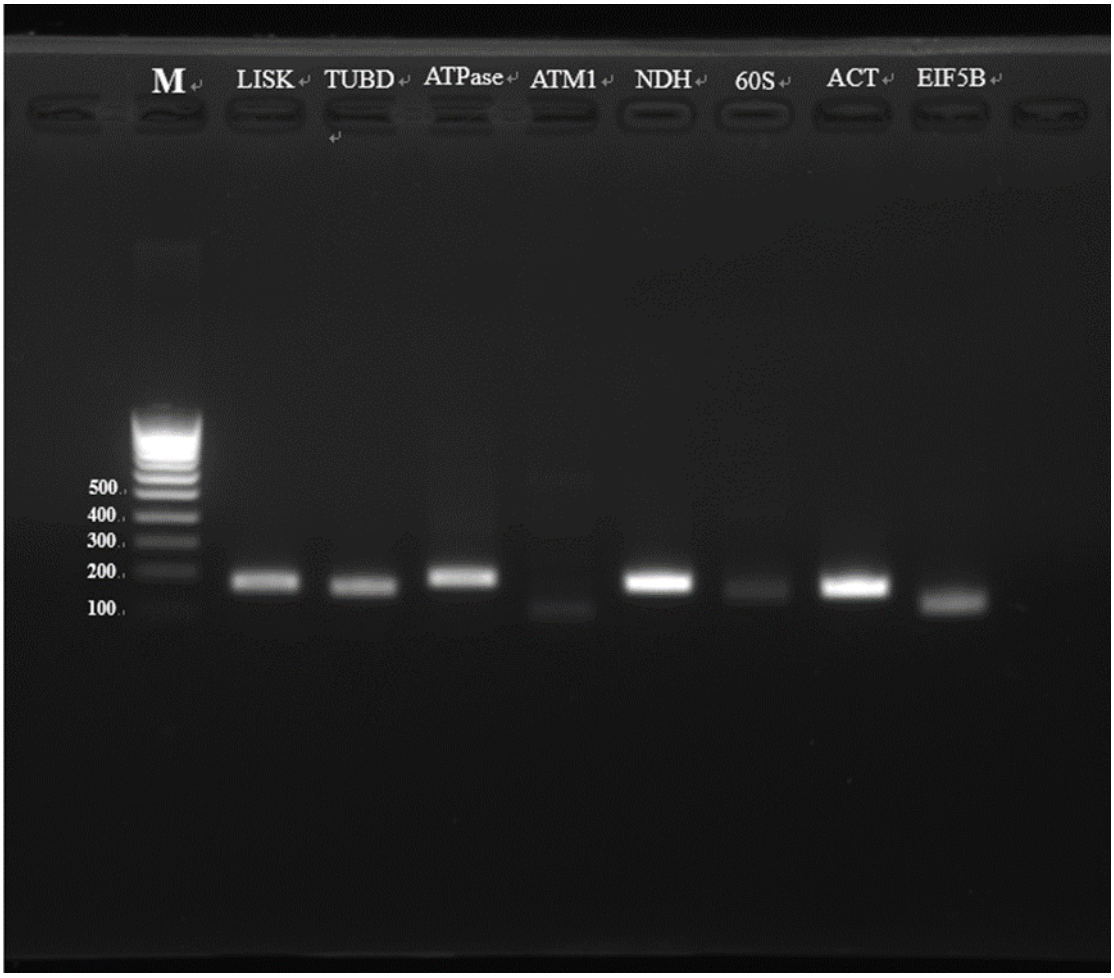

Supplementary Figure 3. Agarose gel electrophoresis of RT-PCR products of the 8 candidate reference genes.

Chapter II

Analysis of transcriptomic regulation in kelps during co-cultivation with *Laminarionema elsbetiae*, a filamentous brown algal endophyte

Chapter II. Analysis of transcriptomic regulation in kelps during co-cultivation with *Laminarionema elsbetiae*, a filamentous brown algal endophyte

Laminarionema elsbetiae, a filamentous brown algal endophyte, has the ability to infect many kelp species. It has been shown that *Saccharina latissima* is the main natural host of the endophyte *Laminarionema elsbetiae*, and that other kelps, such as *Laminaria digitata*, are occasional hosts. During the thesis of Miriam Bernard at Roscoff, a co-cultivation system was developed, based on laboratory-grown juvenile kelp sporophytes and filaments of the endophyte *L. elsbetiae*, to better understand the physiological and molecular bases of the interactions between kelps and encophytes and their specificities.

Bridging our two thesis projects, this chapter results from a collaborative work between Miriam Bernard and myself to compare the responses to the presence of the endophyte between *Saccharina latissima* and *Laminaria digitata* from two aspects: physiological responses and transcriptomic regulation. Therefore, some of the results in this joined manuscript in preparation were acquired by M. bernard and already presented in her thesis, such as the monitoring of the impact on the growth of plantlets and on photosynthesis rate within 15 days, and the infection rate using a previously developed qPCR-assay. My main contribution concerned the bioinformatic analysis of the RNA-seq datasets, acquired in the end of the Miriam Bernard's thesis, and the interpretation of these transcriptomic results. The aim was to compare the global transcriptomic regulations in two hosts, *S. latissima* and *L. digitata* after a short-term contact (24 and 48 hours) with *L. elsbetiae*, but also to analyze early regulation of genes potentially related to oxylipin signaling pathway.

Article in preparation

Early responses of Laminariales to an infection by *Laminarionema elsbetiae* provide insights about host specificity during kelp-endophyte interactions

Qikun Xing[1#], Miriam Bernard[1#], Sylvie Rousvoal[1], Erwan Corre[2], Gabriel V. Markov[1], Akira F. Peters[3], Catherine Leblanc[1]*

[1] Sorbonne Université, CNRS, UMR 8227, Integrative Biology of Marine Models, Station Biologique de Roscoff, Roscoff, France

[2] Sorbonne Université, CNRS, FR2424, Analysis and Bioinformatics for Marine Science, Station Biologique de Roscoff (SBR), Roscoff, France

[3] Bezhin Rosko, 29250 Santec, France

# These authors contributed equally to the work

* Author for correspondence. Catherine Leblanc, Email: catherine.leblanc@sb-roscoff.fr; Tel.: +33 2 98 29 23 62

Abstract

The filamentous algal endophyte *Laminarionema elsbetiae* is highly prevalent in European populations of the brown alga *Saccharina latissima*, but has also been found occasionally in the other kelp species *Laminaria digitata*. The presence of *L. elsbetiae* coincides with morphological changes in the hosts such as twisted stipes and deformed blades, however, little is known about the molecular bases of these algal host-endophyte interactions. Using a co-cultivation experiment, we showed that the physiological responses and later endophyte prevalences are different between the main and the occasional host. A comparative transcriptomic approach conducted on the two kelps during the first contact with the endophyte *L. elsbetiae* revealed a stronger and faster transcriptomic regulation in the occasional host *L. digitata* after 24 hours of cocultivation. During the first two days of cocultivation, only 21 differentially expressed genes (DEGs) were common in both kelps, indicating a crucial difference between the molecular responses of the two hosts. By functional annotation, we identified DEGs related to host-endophyte recognition, defense response and cell wall modification. Our results suggest that expression pattern differences between the two kelps related to the recognition of the endophyte and subsequent defense reactions could explain the variability of natural infection patterns.

Key words : Laminariales, Endophyte, Defense response, RNA-seq, Physiology

1. Introduction

Kelps – including large brown macroalgae of the order Laminariales – are major components of rocky intertidal and subtidal habitats (Wynne & Bold, 1985). They do not only serve as food source or habitats for animals, but also provide a substratum for smaller organisms growing on (epiphytes) or inside (endophytes) of their thalli, such as fungi, oomycetes or filamentous algae (Bartsch et al., 2008, Gachon et al., 2010). The prevalence of the latter can be very high, reaching up to 100% of infected individuals in natural kelp population (Lein et al., 1991, Ellertsdottir & Peters, 1997, Bernard et al., 2018). Furthermore, filamentous algal endophytes often coincide with disease symptoms in their hosts such as twisted stipes, crippled thalli or a reduced growth of the kelps (Peters, 1996, Gauna et al., 2009, Thomas et al., 2009), but the nature of endophytic relationships in different kelps species, from detrimental to neutral ones, is still an open question. As they have also been reported to lower the commercial value of infected kelps (Yoshida, 1979), endophytes represent a potential thread to the globally increasing seaweed aquaculture (Gachon et al., 2010).

Laminarionema elsbetiae is a filamentous brown alga, which is commonly found as an endophyte in the sugar kelp *Saccharina latissima* along European coasts (Ellertsdottir & Peters, 1997, Bernard et al., 2018, Bernard et al., 2019). Occasionally it also infects *Laminaria digitata*, although this kelp is more often associated to other endophyte species belonging to the genus *Laminariocolax* (Russell, 1964, Kornmann & Sahling, 1994). In Asia, *L. elsbetiae* has been described infecting the economically important *Saccharina japonica*, but none of the other kelp species in the direct vicinity, such as *Costaria costata* or *Undaria pinnatifida* (Kawai & Tokuyama, 1995). Similarly, kelps in Northern Brittany have shown significant variation in the prevalence of *L. elsbetiae* according to different host species (Bernard et al., 2018). It therefore seems that kelp-endophyte relationships underlie a certain specificity, but the molecular bases of the interaction between kelps and brown algal endophytes remain poorly understood.

In macroalgae, as for most eukaryotic organisms, the activation of defense responses and innate immunity relies on a successful recognition of the potential attacker. This may either involve the perception of exogenous elicitors, i.e. highly conserved patterns in the cell envelope or cell wall, which are found only on the attacker, but not on the host itself, or endogenous elicitors, such as

oligosaccharides deriving from the host's cell wall which are released following an enzymatic degradation during a biotic attack (Weinberger, 2007). This *non se* recognition is followed by different inducible defense reactions. A fast and common eukaryotic stress response is the so called oxidative burst, a release of reactive oxygen species (ROS). ROS do not only have direct cytotoxic effects on attackers, but are also involved in cell-wall strengthening and signalling processes (Hancock et al., 2001, Küpper et al., 2001, Küpper et al., 2002). Other defense pathways in kelps that may be activated during biotic interactions through gene expression regulation (Cosse et al., 2009) and involve the production of fatty acids and oxylipins and the emission of volatile halogenated organic compounds (Leblanc et al., 2006, La Barre et al., 2010).

A well-studied alga-endophyte pathosystem is the interaction between the red alga *Chondrus crispus* and the green algal endophyte *Ulvella operculata*. Sporophytes of *C. crispus* are regularly infected by *U. operculata*, but the endophyte cannot penetrate beyond the outer cell layers of the gametophyte of *C. crispus* (Correa & McLachlan, 1994). *U. operculata* expresses carrageenolytic activity to degrade and penetrate into the cell wall of *C.crispus* (Bouarab et al., 1999). Similarly, electronic microscopy observation suggested that the spores of *L. elsbetiae* penetrate the surface of *S. latissima* by locally dissolving the cell wall using alginolytic enzymes (Heesch & Peters, 1999). Oligosaccharides which are released during this interaction could act as endogenous elicitors that can be recognized by the kelp and trigger an activation of defense responses. However, further biochemical and molecular studies are necessary to confirm this hypothesis in kelps. Previous studies on *C. crispus* also suggest that the oxidative burst and the oxylipin pathway play an important role in the natural resistance of *C. crispus* gametophytes against *U. operculata* (Bouarab et al., 1999, Bouarab et al., 2004). This is in concordance with experiments showing that the resistance of *L. digitata* against the endophyte *Laminariocolax tomentosoides* was increased after an oxidative burst elicited by endogenous oligoalginate elicitors or by a pre-treatment with arachidonic acid, a polyunsaturated fatty acid (Küpper et al., 2002, Küpper et al., 2009). Thus, several different pathways may be involved in the inducible defense of kelps against algal endophytes. *In situ* surveys in Brittany have also shown that *S. latissima* sporophytes might be infected early in their life by *L. elsbetiae* and confirmed different prevalence according to host species (Bernard et al., 2018).

This paper aims at exploring the importance of both early recognition of endophytic presence and inducible defense responses in different kelp species, in relationship with specific infection

patterns observed in natural kelp populations. In this purpose, we investigated and compared the physiological and molecular responses of young sporophytes of the main host *S. latissima* and the occasional host *L. digitata* to an infection with *L. elsbetiae*. We developed a co-cultivation bioassay to measure the kelps' growth over 14 days in the presence of the endophyte and measured the production of H_2O_2 in kelp-endophyte co-cultures to follow the oxidative response of the kelps in the presence of endophytic algae. We tested pre-treatment with oligoalginates to explore *L. digitata* defense responses and resistance against *L. elsbetiae* endophyte, using the co-cultivation bioassay. To further understand the molecular bases of kelp-endophyte interaction and its specificity, a RNA sequencing analysis was conducted to compare the regulation of the gene expression of both kelp species during the first 2 days of contact with the endophyte *L. elsbetiae* in laboratory conditions.

2. Material and Methods

2.1. Biological material

Spores of fertile individuals of *S. latissima* and *L. digitata*, collected at Perharidy (near Roscoff, 48.73° N, 4.00° W) were released onto cover slips using the hanging-drop technique (WYNNE, 1969). The developing sporophytes were kept in Petri dishes with weekly changes of culture medium. For all cultures, filtered, autoclaved and natural seawater (FSW) was enriched with Provasoli solution (10mL Provasoli solution/L seawater) (Provasoli, 1968). After 4 weeks, the sporophytes were detached from the cover slips and transferred to 10 L bottles connected to an aeration system. Culture medium in the 10 L bottles was changed weekly. The kelp cultures were maintained at 14°C and 20µmol photons $s^{-1}m^{-2}$ with a 12 h light/dark cycle.

Cultures of the filamentous brown algae *L. elsbetiae*, *Laminariocolax tomentosoides* and *Microspongium tenuissimum* were obtained from the Bezhin Rosko culture collection. They were kept in Petri dishes at 14°C and 5 µmol photons $s^{-1}m^{-2}$ with monthly changes of culture medium.

2.2. Co-cultivation bioassay, growth and Chlorophyll fluorescence measurements

Both *S. latissima* and *L. digitata* species were co-cultivated with the endophyte for two weeks as described below.

Fifteen 2 L bottles were filled with 1.5 L sterile Provasoli-enriched FSW and connected to an aeriation system. A hole was punched in the kelp sporophytes at 1 cm distance from the basal meristem using a pipet tip. In the following experiment, the longitudinal growth of the sporophyte

blade was measured by monitoring the distance of the hole from the basal meristem with a ruler (Parke, 1948).The first measurement was done after 3-5 days to ensure that the growth behavior of all sporophytes was similar. Subsequently, a filament of *L. elsbetiae* or *M. tenuissimum* of similar size was added to 1 bottle, each containing one kelp sporophyte (N=5). *M. tenuissimum* – a filamentous brown alga which is not endophytic in *S. latissima* and *L. digitata* - was used as a control to test a nutrient competition effect. Nothing was added to the remaining 5 bottles (control cultures without endophyte).

After the addition of the filaments (day 0), growth of *S. latissima* was measured on days 3, 6, 9, 11. Growth of *L. digitata* was measured on days 3, 6, 10 and 14. To ensure a sufficient nutrient supply, an amount of 0.5 mL of Provasoli solution per day of experiment was added after each measurement. All co-cultivation experiments were performed at 14°C and 20 µmol photons $s^{-1}m^{-2}$ with a 12 h light/dark cycle.

The maximum quantum yield of photosystem II (Fv/Fm) was measured on the same days using a JuniorPAM (Walz, Germany). The sporophytes were dark-acclimated for 20 min prior to the measurement. The experiments with both kelp species were repeated twice for each species with similar results (data not shown). After the last measurement, the kelp sporophytes were frozen in liquid nitrogen and kept at -80°C for the molecular detection of the endophyte in the kelp tissue.

The growth curves and Fv/Fm graphs were drawn with GraphPad prism (GraphPad Prism Software, Inc., USA) and SPSS was used for statistical analyses (IBM Corp. Released 2015. IBM SPSS Statistics for Windows, Version 23.0. Armonk, NY: IBM Corp.). Normality of the data and homogeneity of variances were tested with the Shapiro-Wilk test and the Levene test, respectively. Subsequently, data were analyzed with one-way ANOVAs. Significant differences were evaluated with the Tukey post hoc test.

2.3. Infection ratio measurement

Kelps' DNA extraction and qPCR quantification of endophytes were performed as described previously (Bernard et al., 2018). In total, 15 individuals of *S. latissima* and 13 individuals of *L. digitata* from the co-cultivation bioassays with *L. elsbetiae* as well as 3 randomly chosen control sporophytes of each species were analyzed by qPCR for the quantification of *L. elsbetiae* DNA.

2.4. Oligoguluronates *L. digitata* pre-treatment and co-cultivation bioassay.

Sixteen *L. digitata* sporophytes raised in laboratory culture were transferred to small glass beakers, filled with 50 mL autoclaved FSW. 150 µg/ml of oligoguluronates blocks (GG, prepared from *L. hyperborea* according to Haug et al. (Haug et al., 1974) were added to 8 sporophytes . All beakers were placed on a shaker for 3h (100 rpm) and the occurrence of an oxidative burst was measured as described below. After the incubation, the sporophytes were washed by transferring them to new beakers containing 50 mL autoclaved FSW and shaking for another 15 minutes. This washing step was repeated twice. A hole was punched in 1 cm distance of the meristem in the kelps and they were transferred to 2 L bottles. The first measurement was done after 3 days to assure that growth behavior of all sporophytes (control and GG-treated) was similar. Then, filaments of *L. elsbetiae* were added to 4 of the GG pre-treated and to 4 of the untreated *L. digitata* sporophytes. Growth was measured as described above on days 3, 7, 10 and 14. Statistical analysis were performed as described above.

2.5. Oxidative response measurement

The net production of H_2O_2 in seawater surrounding kelp-endophyte co-cultures was determined using a luminol chemiluminescence method (Küpper et al., 2001). After measuring the fresh weight of young sporophytes of *S. latissima* and *L. digitata*, they were transferred to glass beakers containing 50 mL seawater and placed on a shaker (100rpm). The experimental set-up consisted of a control (only *S. latissima* or *L. digitata*), both kelps co-cultivated with the endophytes *L. elsbetiae* or *L. tomentosoides*, and 50 mL of seawater containing only filaments of *L. elsbetiae* or *L. tomentosoides*. As a positive control, 150 µg/mL of GG were added to another glass beaker containing 50mL of seawater and a sporophyte of either *S. latissima* or *L. digitata*.

150 µL of seawater were taken as samples for each measurement. Measurements were done before starting the treatment (t=0), and 2, 4, 6, 8, 10, 15, 20, 25 and 30 minutes after the addition of the endophytes or GG. For each measurement, 50 µL of 20 $U.mL^{-1}$ horseradish peroxidase, dissolved in pH 7.8 phosphate buffer, and 100 µL of 0.3 M luminol (5-amino-2,3-dihydro-1,4-phtalazinedione) were added automatically to the sample by two injectors of the GloMax 20/20 Luminometer (Promega, US). Chemiluminescence was measured immediately after the injection with a signal time of 1 s. A standard calibration curve from 0.1 µM to 20 mM H_2O_2 was drawn to determine the concentration of H_2O_2 in the seawater samples. H_2O_2 production by the kelp per g fresh weight was estimated by integrating the total amount of H_2O_2 monitored over 30 minutes

and expressed as log2-transformed fold changes between control and treatments. The experiment was repeated 3 times and a one-sample-t-test was used for statistical analysis.

2.6. RNA extraction for sequencing

For transcriptomic analysis, 16 bottles were filled with 1.5L autoclaved Provasoli enriched FSW and adapted to an aeriation system. One sporophyte of *S. latissima* (3-5 cm) was added to each bottle. After 24 h of acclimation time, filaments of *L. elsbetiae* were added to 12 of the bottles. Four individuals of the control group and 4 individuals co-cultivated with *L. elsbetiae* were taken after 24h and 48h. The kelp sporophytes were plotted dry with tissue paper, frozen in liquid nitrogen and stored in -80°C until RNA extraction. The same experimental set-up was used for *L. digitata* sporophytes.

RNA was extracted as described by Heinrich et al. (Heinrich et al., 2012) with a combination of a classical CTAB-based method and the RNeasy Mini kit (QIAGEN, Hilden, Germany) including an on-column DNA digestion. Quantity and purity of the extracted RNA were tested on a NanoDrop™ spectrophotometer (Thermo Fisher Scientific Inc., Waltham, US) and on a 2% agarose gel.

Based on the quality and concentration, 3 replicates of each condition and each kelp species were chosen for commercial library preparation and Illumina sequencing (HiSeq3000) at the Plateforme Génomique du Genopole Toulouse Midi-Pyrénées GeT (France).

2.7. *De novo* assembly of the transcriptome and identification of differentially expressed genes (DEGs)

The quality of the Illumina reads was checked using FastQC (Andrews, 2010). Reads were cleaned by removing adapters, low quality reads (Phred score <33) and short reads (< 50 nucleotides) with Trimmomatic (Bolger et al., 2014) and residual rRNA was removed with SortmeRNA (Kopylova et al., 2012). Another quality check was performed with FastQC on the processed reads to ensure that high quality reads were obtained through the cleaning steps. An additional cleaning step was done by removing reads of the endophyte by mapping to the transcriptome of *L. elsbetiae*, produced in the context of the Phaeoexplorer project (https://phaeoexplorer.sb-roscoff.fr/).

A *de novo* transcriptome assembly was created for both kelp species separately based on the pooled processed control reads using Trinity (Grabherr et al., 2011) with the default options. Transcript abundance was estimated by TPM implemented in Trinity. The quality of the transcriptome assemblies was evaluated by using BUSCO v2.0 (Simão et al., 2015) with eukaryote dataset and redundancy further reduced according to the TPM value. The quality of the assembly was assessed by re-mapping the cleaned reads using the bowtie2 aligner (Longmead & Salzberg, 2012).

Gene annotation was performed with a Blastx search against the NCBI-NR and the Uniprot databases with an E-value cut-off of 10^{-5}. Furthermore, genes were assigned to 2nd level GO subcategories within the three root categories molecular function, cellular component and biological process using Blast2GO (Conesa et al., 2005).

Differential gene expression between the control and the co-cultivation treatments was determined separately for the 24h and 48h samples using DESeq2 (Love et al., 2019). Log2 fold change values ≥ 0.7 and ≤ -0.7 with a p-value <0.01 were considered to be up- and downregulated, respectively. Heat maps were plotted using the R package pheatmap.

The genes that were differentially expressed in both species were compared with Blastn (E-value cut-off of 10^{-5}) against each other in order to identify common DEGs.

3. Results

3.1. The effect of co-cultivation with algal endophytes on kelp growth and infection

No significant differences in growth occurred within two weeks of co-cultivation of *S. latissima* with the non-endophytic *M. tenuissimum* and endophytic *L. elsbetiae* (Fig. 1A, Table S1).
In case of *L. digitata*, a significant difference between the treatments occurred 6 days after the addition of *L. elsbetiae* (Fig. 1B and Table S1). The growth of *L. digitata* was decreased significantly (Fig. 1B) as compared to the other treatments after 6 days of co-cultivation (Table S1, one-way ANOVA, p=0.013) and the difference persisted until the end of the experiment (Table S1). There was no significant effect of co-cultivation with *M. tenuissimum* on the growth of *L. digitata*.

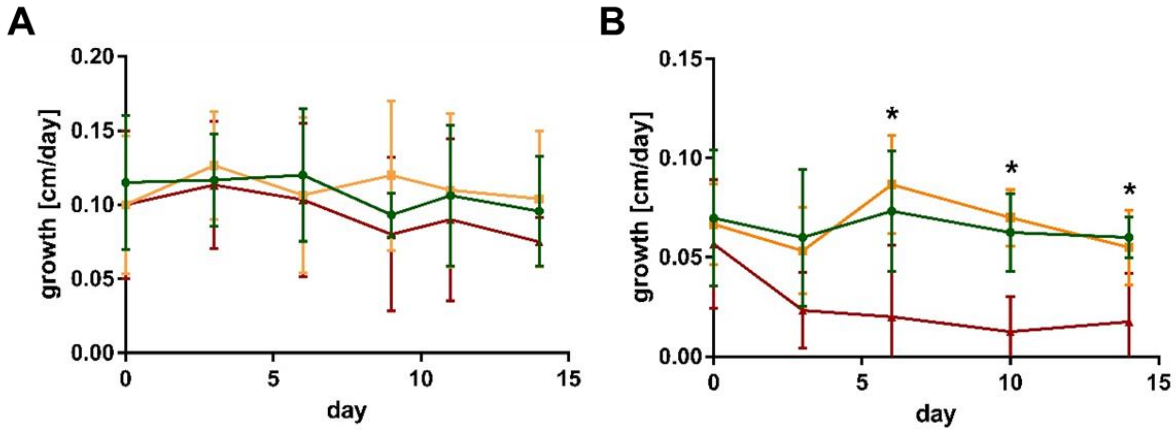

Figure 1. Growth of **A.** *S. latissima* and **B.** *L. digitata* in control conditions (green), in presence of the non-endophytic *M. tenuissimum* (yellow) and the endophyte *L. elsbetiae* (red). The presented values are mean values with standard deviation (N=5). Significant differences are indicated by asterisk (see Table 1).

No significant differences in the maximum quantum yield of photosystem II (Fv/Fm) occurred within *S. latissima* or *L. digitata* alone or in co-cultivation with *M. tenuissimum* and *L. elsbetiae* (Table S1).

At the end of the experiment after two weeks of co-cultivation, DNA of the endophyte was detected in 73.3% of the *S.latissima* samples using qPCR specific primers (11 out of 15 samples), whereas it was only detected in 30.8% of the *L. digitata* sporophytes (4 out of 13 samples). No *L. elsbetiae* DNA was detected in any of the controls by qPCR.

3.2. Oligoguluronates (GG) pre-treatment modified *L. digitata* responses towards algal endophytes

Co-cultivation of *L. digitata* sporophytes with the endophyte *L. elsbetiae* resulted in a significant decrease of growth from day 3 until day 14 (red line in Fig. 2, Table S2), as already described before (control as green line in Fig 2). However, the addition of *L. elsbetiae* did not have any effect on the growth of *L. digitata* sporophytes that had been pre-treated with GG 3 days before the co-cultivation was started (golden line, Fig. 2). There was no effect of the GG elicitation pre-treatment alone on the growth of *L. digitata* (grey line in Fig. 2).

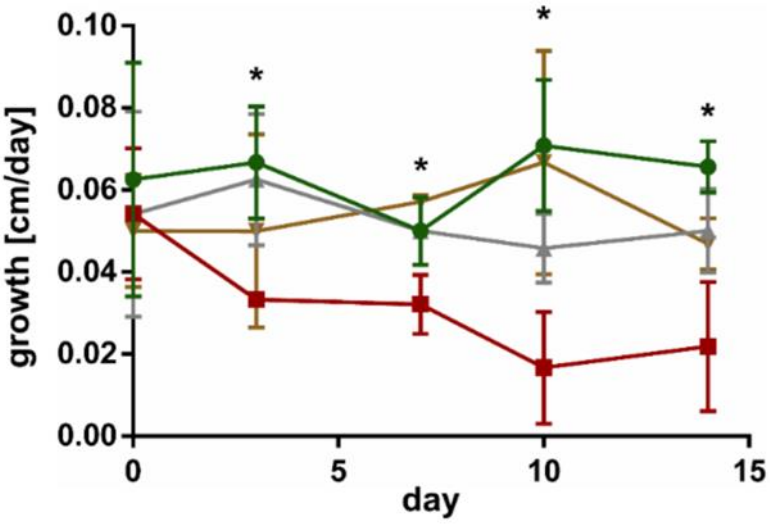

Figure 2. Growth of *L. digitata* without GG pre-treatment in control conditions (green) and in co-cultivation with *L. elsbetiae* (red) and of *L. digitata* with GG pre-treatment in control conditions (grey) and with *L. elsbetiae* (gold). Significant differences are indicated by asterisks (see table 2). The presented values are mean values with standard deviation (N=4).

3.3. Oxidative burst measurement

As already demonstrated by Küpper et al. (Küpper et al., 2001), oligoguluronates (GG) blocks triggered an oxidative burst in both kelp species, which is indicated by a significant fold change of H_2O_2 release as compared to the control (Table 1). *L. tomentosoides* and *L. elsbetiae* without kelp sporophytes did not lead to significant changes in H_2O_2 content in the surrounding seawater (data not shown).

The addition of *L. tomentosoides* to *S. latissima* resulted in a slight increase of H_2O_2 concentration in the seawater (log2FC = 0.21, one-sample t-test, p=0.09, Table 1). When added to *L. digitata*, on the other hand, *L. tomentosoides* caused a significant decrease of the H_2O_2 concentration in the

seawater (log2FC = -0.42, one-sample t-test, p=0.04, Table 1). No significant changes in the H_2O_2 concentration were observed after the addition of *L. elsbetiae* to both kelp species.

Table 1. Mean values of log2FC in H_2O_2 content monitored during 30 min in seawater surrounding the treated kelps as compared to the control (N=3) and results of the statistical analysis using a one-sample t-test. Ldig = *L. digitata*, GG = addition of oligoguluronates, Lels = *L. elsbetiae*, Ltom = *L. tomentosoides*, Slat = *S. latissima*.

Treatment	Mean log2FC	Stdev	t	Df	p-value
Ldig+GG	3.49	1.31	4.60	2	0.02*
Ldig+Lels	-0.61	0.26	-1.24	2	0.17
Ldig+Ltom	-0.42	0.07	-3.10	2	0.04*
Slat+GG	3.56	1.78	3.47	2	0.04*
Slat+Lels	-0.24	0.52	-0.78	2	0.26
Slat+Ltom	0.21	0.40	4.54	2	0.09

3.4. Global transcriptomic analysis of early kelp responses upon endophyte presence

The cleaned RNA sequencing reads of *S. latissima* and *L. digitata* were *de novo* assembled by Trinity and the general features of these two *de novo* transcriptomes are presented in Table S3. 90% of total expression was present in 24,733 and 34,251 transcripts, respectively. The results of the BUSCO analysis revealed a near-complete gene sequence information for two transcriptomes with 82.4% and 84.4% complete BUSCO matches in *S. latissima* and *L. digitata*, respectively.

Overall, the distribution of GO terms for the three root categories “Molecular Function”, “Cellular Component” and “Biological process” were very similar for the assembled transcriptomes of *S. latissima* and *L. digitata* (Fig. S1). Within the molecular function category, most hits were assigned to catalytic activity and binding. Within the biological process root, most genes belonged to metabolic and cellular processes (Fig. S1). Overall, 47.34% of the obtained genes of *S. latissima* could be annotated whereas the annotation rate was slightly lower in *L. digitata* (45.66%).

The comparison between control and co-cultivated conditions identified 107 and 155 DEG in *S. latissima* and *L. digitata*, respectively (Fig. S2). Only six differentially expressed genes (DEG) were detected in *S. latissima* in presence of *L. elsbetiae* after 24 h (Table S4), whereas 46 genes were significantly differentially expressed in *L. digitata* between control condition and co-culture

with the endophyte (Table S5). At this stage, the majority of DEGs were downregulated in both species (*S. latissima*, 5 genes, i.e. 83.33% of DEG, *L. digitata*: 29 DEG, i.e. 63%), with stronger repression for those identified in *S. latissima* and for 16 DEG of *L. digitata* (Fig. 3A). Unlike *S. latissima*, where only one gene was moderated up-regulated, 11 genes featured log2FC value above 5 compared to control in *L. digitata* (Fig. 3A). After 48 h, more changes in gene expression occurred and most detected DEG were up-regulated in both species (Fig. 3B).

In *S. latissima*, log2FC values of the 101 identified DEG ranged from 11.41 to -28.27 (Fig. 3B), but the majority (78.22%) showed moderate expression log2FC between 2 and -2 (Fig. 3B). In *L. digitata*, log2FC values of the 109 DEG ranged from 16.51 to -14.28 (log2-tranformed, Fig. 3B): 52 DEGs (47.71%) showed moderate log2FC between 2 and -2 and 29 DEGs (26.61%) were strongly up-regulated (log2FC > 6) (Fig. 3B). Among 262 DEGs identified in *S. latissima* and *L. digitata* in the 2-days cocultures with the endophyte, only 21 homologous genes were shared by both kelps.

Similarly to the whole transcriptome analysis, an important part of the differentially expressed genes of both kelp species (between 39.0 to 45.0 %) did not have a match through Blastx search in the available protein databases, as represented on Fig. 3. In case of *S. latissima*, after 24 h of co-cultivation with the endophyte, only one gene had a match through Blastx search as a conserved unknown *Ectocarpus* protein (Fig. 3a, Table S4). In *L. digitata*, among the 23 DEGs annotated based on at least on database after 24h of the addition of *L. elsbetiae* (Table S5), one putative respiratory burst oxidase homolog protein was strongly up-regulated (log2FC = 9.89), and 9 genes corresponded to conserved unknown or hypothetical proteins in *Ectocarpus* genome.

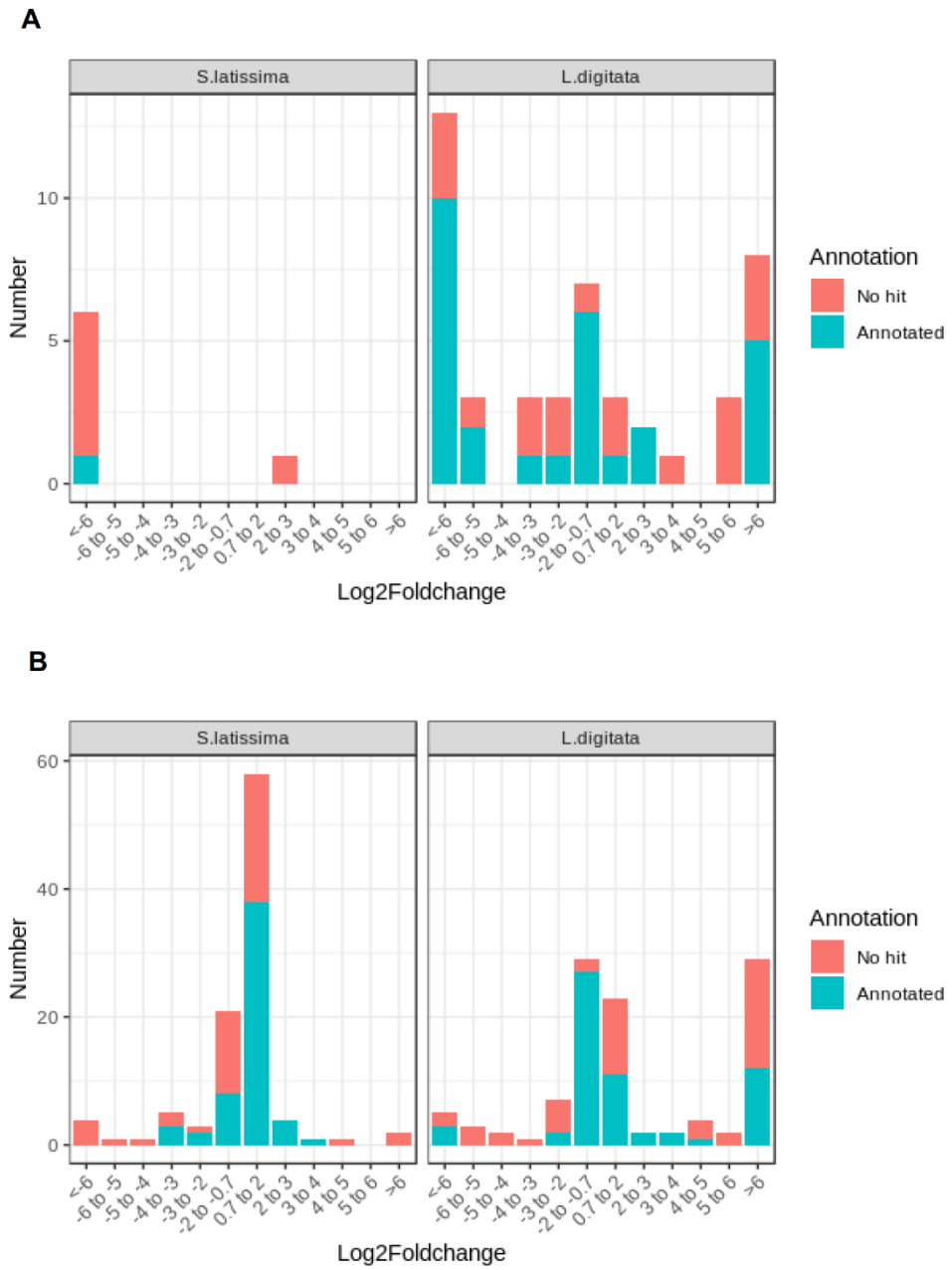

Figure 3. Frequency distribution of log2FC among DE genes in both species after **A.** 24h and **B.** 48 h of co-cultivation.

After 48 h of co-cultivation with the endophyte, 19 DEGs corresponded to conserved unknown or hypothetical *Ectocarpus* proteins. A functional putative annotation was retrieved for only 38 genes out of 101 DEG (see Table S6). Among the up-regulated DEGs, five mannuronan C-5-epimerases (log2FC = 0.92 to 1.58), two vanadium-dependent bromoperoxidases (log2FC = 1.60 and 1.32), an endo-1,3-beta-glucanase (log2FC = 2.92), an alginate lyase (log2FC = 1.09), a PAP2/haloperoxidase-like protein (log2FC = 0.92) and a putative respiratory burst oxidase homolog protein (log2FC = 0.99) were found. One putative LRR receptor-like serine/threonine-

protein kinase (log2FC = -1.84) was downregulated in the presence of *L. elsbetiae*. Further more, three genes that might be involved in oxylipin pathways, including two lipase genes (log2FC = 0.95 and 1.02) and one lipoxygenase gene (log2FC = 0.84), were found up-regulated at 48 h in *S. latissima*. In *L. digitata*, a putative annotation was obtained for 60 DEGs (Table S7). 31 DEG were annotated as conserved unknown or hypothetical *Ectocarpus* proteins whereas a putative functional annotation was retrieved for 25 DEGs (see Table S7). Among the up-regulated DEG putative annotations, there were two GDP-mannose dehydrogenase genes (log2FC = 1.38 and 0.76), a metacaspase gene (log2FC = 1.19), a serine carboxypeptidase-like gene (log2FC = 1.56), a photosystem II reaction center protein D1 gene (log2FC = 1.45), a carbohydrate 4-sulfotransferase gene (log2FC = 1.64) and a gene coding for a protein homologous to one of those up-regulated in the *Ectocarpus* imm mutant (log2FC = 13.49). Furthermore, a gene with high similarity to the *Ectocarpus* virus gene, encoding for a cystein-rich protein was strongly up-regulated in the co-cultivation treatment with *L. elsbetiae* (EsV 1-7, log2FC = 12.34). Among the downregulated DEG putative annotations, there were a long-chain acyl-CoA synthetase (log2FC = -1.21), a light harvesting protein lhcf6 (log2FC = -1.16), a carbonic anhydrase (log2FC = -1.48) and a cellulose synthase (log2FC = -1.66).

4. Discussion

In Brittany, *L. elsbetiae* is mainly found in *S. latissima*, whereas *L. digitata* is not only infected less frequently, but also with lower severity (Bernard et al., 2018, Bernard et al., 2019). However, until now, these endophytic interactions have rarely been studied apart from epidemiological surveys in natural kelp populations. This study provides a first insight into the bases of kelp-endophyte interactions on both physiological and molecular level and highlights the complex and specific cross-talk occurring after the recognition of endophytes by kelps which could explain host specificity.

4.1. The co-cultivation with *L. elsbetiae* only inhibited the growth of the occasional host, *L. digitata*

Previously, it was reported that algal endophytes can reduce the growth of their hosts by up to 70%, as it has been shown for the red algal endophyte *Hypneocolax stellaris* in its host, the rhodophyte *Hypnea musciformis* (Apt, 1984). Here we show that an effect on growth may be

dependent on the host species, as different physiological responses occurred in the two kelp species *S. latissima* and *L. digitata* towards a co-cultivation with the endophyte *L. elsbetiae*.
The growth of the main host *S. latissima* was not affected by the endophyte during the two weeks of co-cultivation, whereas *L. elsbetiae* DNA was detected in most of the sporophytes at the end of the experiment. Although this detection does not indicate that endophytic filaments were already growing inside of the kelp thallus, at least spores of the endophytes were likely to be attached to the kelp tissue by the end of the experiment. Thus, a direct and tiny contact between the endophyte and the kelp had been established, as already observed (Heesch & Peters, 1999), but without directly affecting the growth of *S. latissima*.

Oppositely, the growth of the occasional host *L. digitata* was significantly reduced after a few days of co-cultivation, when one third of the plantlets were shown to feature *L. elsbetiae* DNA contamination. As the filamentous brown alga *M. tenuissimum* did not have any effect on both kelps, nutrient competition could be excluded as a possible cause of the growth reduction. On transcriptome level, the expression of several growth-related genes in *L. digitata* was impacted by the co-cultivation with *L. elsbetiae*. One gene encoding a putative cellulose synthase was significantly down-regulated 48h after the addition of *L. elsbetiae*, and this might decrease cell elongation and division rate in young sporophytes. In *Arabidopsis thaliana*, lack of cellulose synthase resulted in a reduced cell growth rate of young seedlings (Hu et al., 2018). A gene coding for carbonic anhydrase, an essential enzyme for CO_2 fixation, was also down-regulated in *L. digitata*, suggesting an impact on carbon uptake and photosynthesis. It has been reported that endophytic pathogens can impair the efficiency of energy transfer from the light harvesting complexes to the reaction center of PS II in land plants (Luque et al., 1999, Guidi et al., 2007) and in the seagrass *Zostera marina* (Ralph & Short, 2002). In *L. digitata* cocutivated with the endophyte, we also observed differential expression of photosynthesis-related genes. The down-regulation of a light harvesting protein gene lhcf6 suggests a photoinhibition, which may be counteracted by the up-regulation of a photosystem II reaction center protein D1 gene as shown during the repairment of photosystem (Murata et al., 2007). Indeed, PAM measurements did not indicate any impact on the performance of photosystem II of the two kelp species, during the two weeks of cocultivation. According to our data, the presence of *L. elsbetiae* didn't strongly affect its main host, while it could impact more significantly photosynthesis and growth physiology of *L. digitata*, its occasional host.

4.2. *L. digitata* had a more rapid and efficient defense strategy than *S. latissima* against *L. elsbetiae*

In our study, the endophyte-detection results showed that the infection rate of *L. digitata* is much lower than *S. latissima* after two weeks of cocultivation, indicating different resistances to the infection with *L. elsbetiae* between the two kelp species. In addition to different regulations of growth or photosynthesis pathways, the RNA-seq data provide insights of the defense-related transcriptional mechanisms occurring during the first infection step. When a small portion (0.4%) of both transcriptomes showed significant expression differences, as already observed during the early steps of biotic interactions such as grazing in brown algae (Flöthe et al., 2014, Ritter et al., 2017a) or bacterial infection in red algae (de Oliveira et al., 2017), distinct transcriptomic regulation patterns appeared between the two kelps species, according to time and intensity of gene regulation. After 24 hours of co-cultivation with the endophyte, only few genes were differentially regulated in *S. latissima*, whereas *L. digitata* already featured a stronger transcriptomic response. Although most of the DEGs were down-regulated in both species, a small portion of genes in *L. digitata* were already highly up-regulated after 24 hours. After 48 hours, almost the same amount of DEGs were found in both kelp species. Our results therefore suggest that the first contacts with the endophyte induced a faster and stronger transcriptomic response in the occasional host, *L. digitata*, as compared to the main host, *S. latissima*. The majority of differentially expressed genes were unique in the two kelp species and only twenty one genes were commonly differentially expressed in both kelps. This confirms that overall the two kelps react differently to the contact with the endophyte.

The overall rate of functional annotations was very low, as it is usually the case for non-model organisms (Armengaud et al., 2014). It is therefore difficult to fully understand the molecular responses of the two kelps toward an infection with *L. elsbetiae*, and further investigations will be necessary to characterize the functions of some conserved or specific unknown genes. However, some interesting gene candidates were annotated as related to defense responses. Putative respiratory burst oxidase homolog protein (rboh) genes were strongly up-regulated in the *L. digitata* samples after 24 hours of the additon of the endophyte (Fig. 4A), and in *S. latissima* after 48 hours, but with lower log2FC value (Fig. 4B). Rbohs are involved in oxidative bursts of plants (Torres & Dangl, 2005) and have been shown to be induced by elicitors and other stress conditions in some macroalgae (Luo et al., 2015, Wang et al., 2018). The local oxidative burst is known to be the earliest conserved response following recognition of the attack(er) in the plant and

macroalgal innate immunity systems and the reactive oxygen species produced by Rbohs act as toxic compounds and/or as defense signals (Potin et al., 2002). The comparison of the expression of the putative rboh genes in the two species suggests that the immunity responses in *L. digitata* could be much quicker and stronger than the one in *S. latissima* after the first contact with the endophyte. The 24-hours delay of transcriptomic regulations in *S. latissima* might due to the repression of the attack(er) recognition in this species. A gene encoding LRR receptor-like serine/threonine-protein kinase was indeed downregulated in *S. latissima*, and not in *L. digitata*, after 48 hours of the co-cultivation with *L. elsbetiae*. LRR receptor-like serine/threonine-protein kinases play a central role in the signaling of pathogen recognition (Afzal et al., 2008). It has been shown that viruses and bacteria have developed mechanisms to suppress the expression of genes involved in pathogen recognition in plants before an infection (Stack et al., 2005, Akira et al., 2006, Boller & He, 2009). The downregulation of this gene in *S. latissima* could result in an incomplete or inaccurate recognition of *L. elsbetiae* as an external biotic attack, avoiding the induction of immunity defense responses and leading to stronger infection. In *S. latissima*, no other putative known defense-related genes were found to be up-regulated. Based on transcriptomic regulations, a different scenario seems to occur in *L. digitata,* where several defense-related genes were up-regulated. For instance, a putative carbohydrate sulfotransferase gene, up-regulated after 48 hours, might have an effect on the recognition between host and endophyte. Carbohydrate sulfotransfereases act by adding sulfonyl groups from 3′ phosphoadenosine-5′phosphosulfate (PAPS) to a glycoside receptor and the sulfated carbohydrate can serve as a source of extracellular biological information to cells, influencing recognition events and signaling pathway(Bowman & Bertozzi, 1999). Metacaspase belong to a cysteine protease family and has an essential role in programmed cell death caused by the immunity response of plants (Spoel & Dong, 2012). The upregulation of this gene were also observed in terrestrial plants while encountering with pathogens (Jayaswall et al., 2016, Hoeberichts et al., 2003). Furthermore, a serine carboxypeptidase-like protein (SCPL) was up-regulated in *L. digitata.* SCPLs comprise a large family of protein hydrolyzing enzymes that play roles in multiple cellular processes. In addition, some SCPLs are involved in the biosynthesis of antimicrobial compounds and disease resistance in land plants(Liu et al., 2008, Mugford et al., 2009). So the SCPL we found might be also involved in the biosynthesis of defense-related compounds. Their strong upregulation in *L. digitata* suggests that - unlike *S. latissima* - *L. digitata* recognizes the endophyte as a thread and might activate defense reactions and efficient immunity responses, which could explain the lower infection patterns in natural *L. digitata* populations

(Bernard et al., 2018, Bernard et al., 2019). In young plantlets, the activation of defense reactions could consume plenty of energy, resulting in the decrease of growth rate during the first contacts with endophytes.

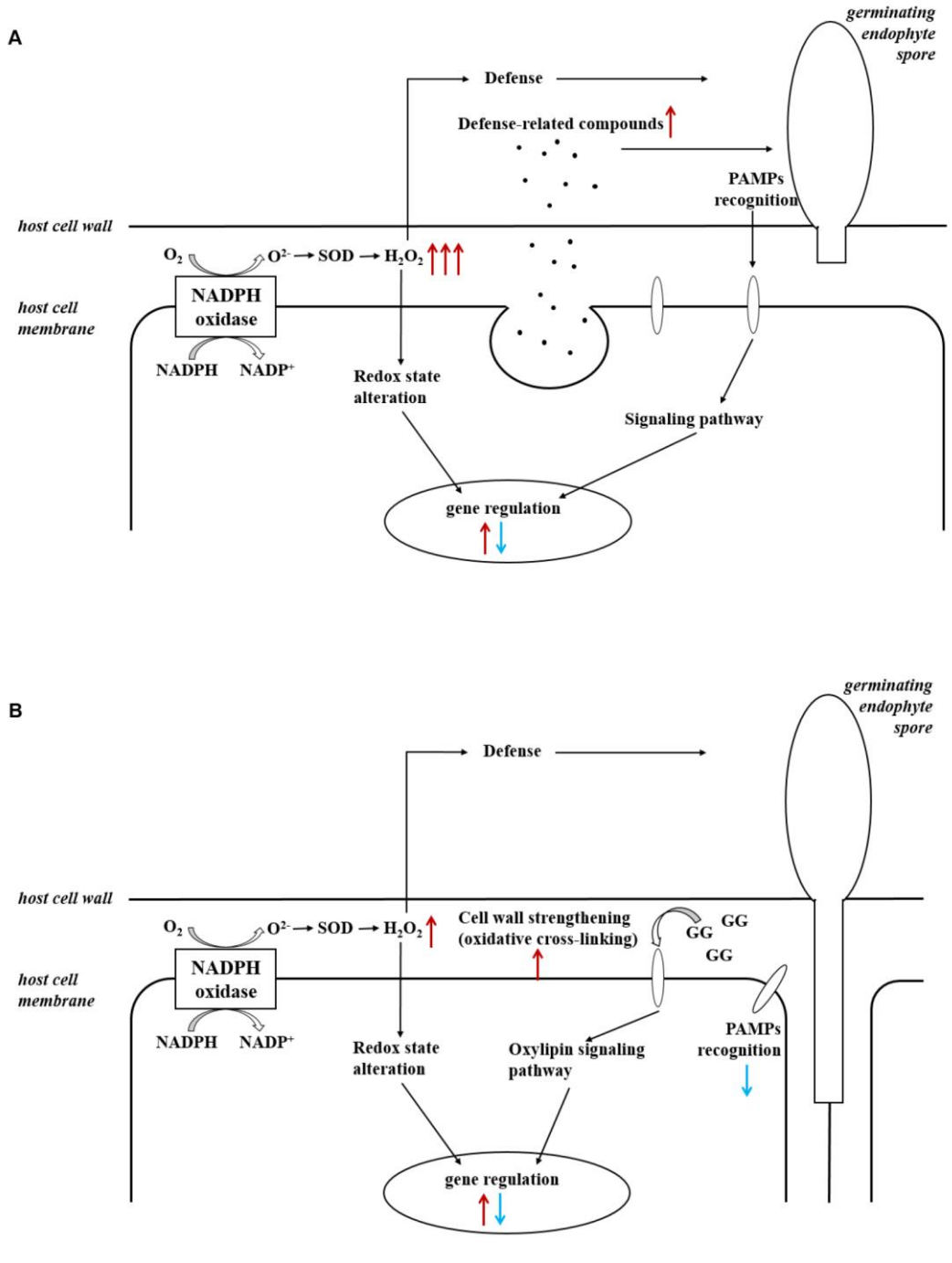

Figure 4. Summary of response of **A.** *L. digitata* and **B.** *S. latissima* during the interaction with endophyte.

4.3. Defense elicitation can modify the physiological response of *L. digitata* towards the algal endophyte

Above we hypothesized that the growth of *L. digitata* in the presence of *L. elsbetiae* was slowed down due to an activation of energy-costing defense reactions. Growth behaviour of *L. digitata* in co-cultivation with the endophyte after GG elicitation, however, was similar to the controls. An elicitation with GG has been shown to strongly induce defense-related genes in *L. digitata* (Cosse et al., 2009). The pre-treatment could therefore restore normal growth behaviour of the kelp in co-culture with the endophyte, due to the activation of the kelp defense reactions prior to the co-cultivation. Previously, resistance of *L. digitata* sporophytes against the filamentous algal endophyte *L. tomentosoides* has been induced by a GG pre-treatment (Küpper et al., 2002). The authors suggested that the oxidative burst caused by the addition of GG activated secondary, long-term defense mechanisms in the kelps that ultimately lead to a strengthening of their cell wall, thereby building up a mechanical barrier against the endophyte. In the field, the protection of juvenile sporophytes by GG elicitation was also observed in *S. latissima*, which reduced the density of endobionts and the number of bacterial cells on sporophytes (Wang et al., 2019).

Our experimental set-up, on the other hand, was rather monitoring the initial steps of kelp-endophyte interactions, mainly during the spore settlement and germination. The results suggest rapid and direct defense mechanisms that may have been enhanced through GG-induced priming effect, as already observed in *L. digitata* (Thomas et al., 2011). However, future studies using the qPCR bioassay could test a potential effect on long-term resistance of the kelp against the endophyte.

4.4. *S. latissima* gene expression responses were mainly related to the activation of cell wall metabolism

In the co-cultivation with *L. elsbetiae*, comparing to *L. digitata*, many cell wall modification related genes were up-regulated in *S. latissima.* Five mannuronan C-5 epimerase (MC5E) were up-regulated in *S. latissima*. MC5E is catalysing the last step of alginate biosynthesis, i.e. the conversion of mannuronic to guluronic acids (Michel et al., 2010). The upregulation of MC5E indicated the activation of alginate synthesis and modification of cell wall towards strenghtening in *S. latissima* upon the cocultivation (Fig. 4B). Other genes associated with cell wall metabolism were endo-1,3-beta-glucanase and alginate lyase. Endo-1,3-beta-glucanase catalyses the hydrolysis of 1,3-beta-D-glucosidic linkages in callose, laminarin, and various carbohydrates

found in the cell wall of plants (Casu et al., 2007). Alginate lyase can degrade alginate by cleaving the glycosidic bond through a β-elimination reaction, generating an oligomer with a 4-deoxy-L-erythro-hex-4-enepyranosyluronate at the nonreducing end (Kim et al., 2011). The functions of both genes are related to the degradation of cell wall. So the fact that these enzymes were up-regulated 48 hours after the infection with the endophyte suggests an enhanced activity of either decomposing the host cell wall or degrading the endophyte cell wall. Two DEGs in *S. latissima*, imm up-regulated 3 and EsV 1-7, were previously identified as members of a putative regulatory cascade with their potential life-cycle-related roles in *E. siliculosus* (Peters et al., 2008, Macaisne et al., 2017). The strong up-regulation of these two genes might lead to the regulation of cell-cycle for replacing the broken cell wall, which was also observed in the wounding responses of land plants (Dombrowski et al., 2020). The other gene regulations occurring after 48 hours could be related to the accumulation and perception of cell wall degradation products, such as oligoalginates (Fig. 4B). Indeed, some stress-response related genes were up-regulated in *S. latissima* such as vanadium dependent bromoperoxidases (vBPO) and vanadium dependent iodoperoxidases (vIPO) involved in halide metabolism of brown algae and up-regulated during abiotic and biotic oxidative responses (Cosse et al., 2009, Strittmatter et al., 2016, Salavarría et al., 2018). Others up-regulated genes were putatively involved in calcium and oxylipin signaling pathways, two key pathways activated upon biotic and abiotic stress (Zhang et al., 2014, Knight, 1999, Eckardt, 2008). For oxylipin pathways, only few genes were up-regulated at 48 h in *S. latissima* and no DEGs were detected in *L. digitata*. These results suggest that either the activation of the oxylipin pathways didn't need some transcriptomic regulation, or this regulation occurs earlier after pathogen recognition.

5. Conclusion

During the biotic interaction, an endophyte's fitness is defined by its ability to infect whereas the kelps fitness is defined by its ability to resist the infection. Therefore, both partners are underlying a strong selective pressure which is driving and accelerating co-evolution. The comparison of interactions between brown algal endophyte *L. elsbetiae* and its different kelp hosts provides an interesting system to study of defense response in kelps and co-evolution of endophyte and hosts. The results presented in this study demonstrate that the main host *S. latissima* and the occasional host *L. digitata* both react to the endophyte *L. elsbetiae* on a physiological and a transcriptomic level, showing that the interactions with the endophyte were not neutral, but their reactions show

crucial different patterns. We propose that differences in the early recognition and subsequent induced defense reactions could be a possible explanation for the occurrence of different natural endophyte infection patterns in the two host kelps.

6. Supplementary Material

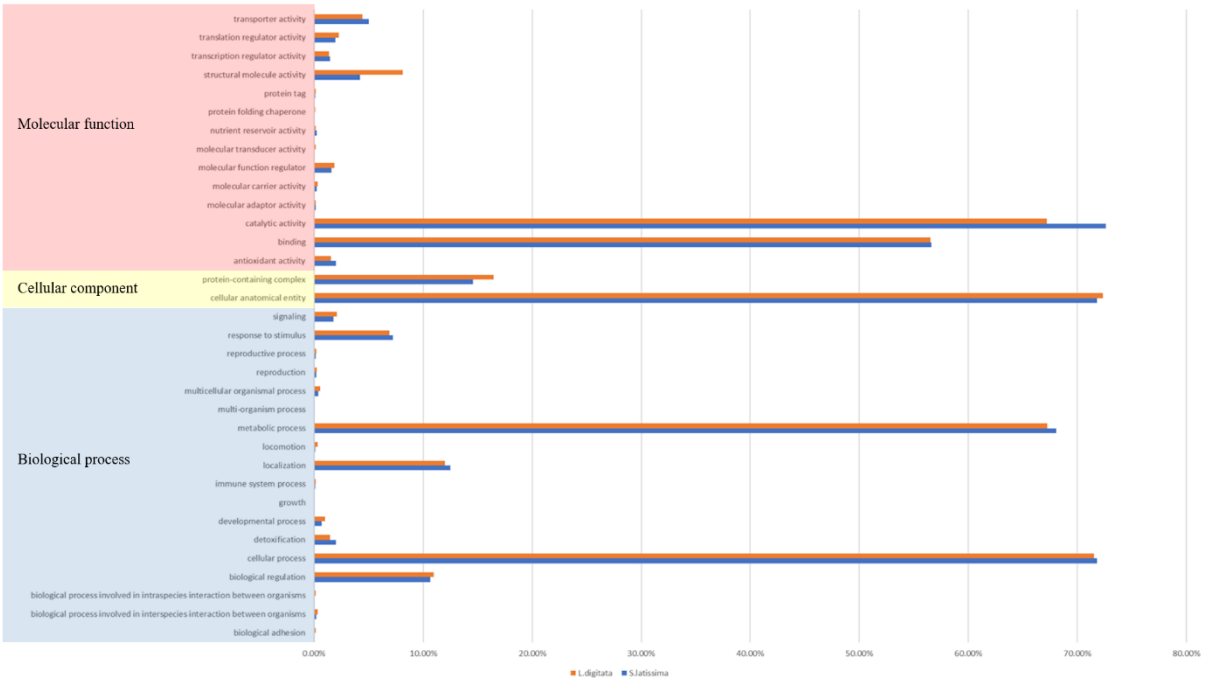

Figure S1. Distribution of the functional categories derived from Gene Ontology terms obtained by Blast2GO hits of genes from the *S. latissima* and the *L. digitata* transcriptome.

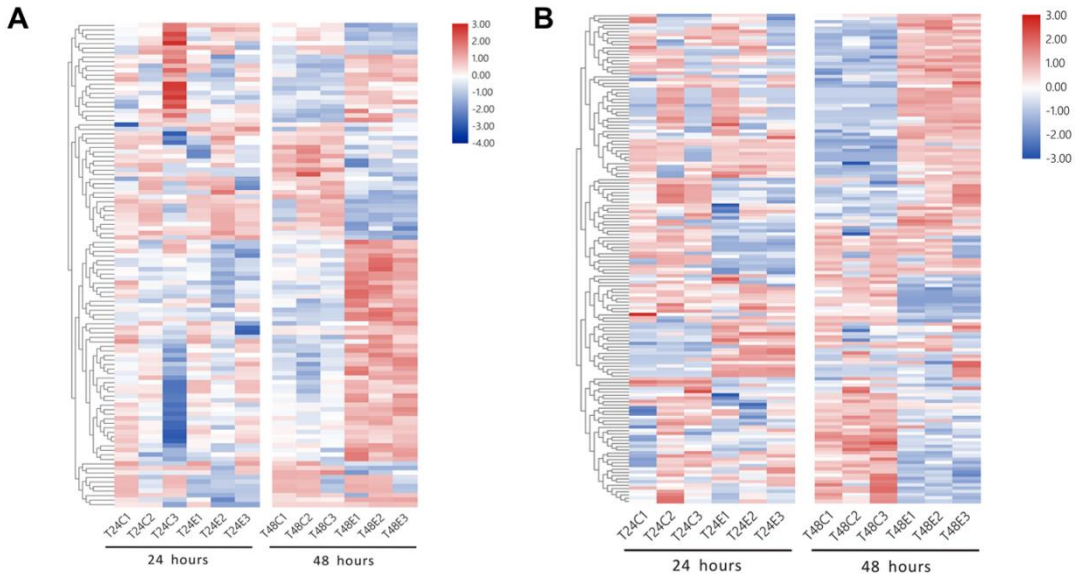

Figure S2. Differentially expressed genes in **A.** *S. latissima* and **B.** *L. digitata* after 24h and 48h of co-culture.

Table S1. Statistical analysis of the co-cultivation bioassay. Significant p-values are marked by asterisks.

		Growth			Fv/Fm		
Experiment	One-Way ANOVA	F	Df	p-value	F	Df	p-value
S. latissima	Day 0	0.17	2	0.85	0.47	2	0.64
Co-cultivation	Day 3	0.17	2	0.84	0.11	2	0.9
	Day 6	0.15	2	0.86	0.59	2	0.57
	Day 9	1.14	2	0.35	0.07	2	0.93
	Day 11	0.2	2	0.82	0.39	2	0.68
	Day 14	0.63	2	0.55	0.04	2	0.96
L. digitata	Day 0	0.26	2	0.77	0.06	2	0.94
Co-cultivation	Day 3	2.82	2	0.1	0.27	2	0.77
	Day 6	6.37	2	0.01*	0.02	2	0.98
	Day 10	16.17	2	>0.01*	0.04	2	0.96
	Day 14	7.58	2	>0.01*	0.29	2	0.75

Table S2. Statistical analysis of the co-cultivation bioassay with GG pre-treatment. Significant p-values are marked by asterisks.

Experiment	One-Way ANOVA	F	df	p-value
L. digitata +	Day 0	0.24	3	0.87
GG pre-treatment	Day 3	3.61	3	0.04*
	Day 7	9.73	3	>0.01*
	Day 10	7.85	3	>0.01*
	Day 14	12.21	3	>0.01*

Table S3. Summary of the Trinity assembly and annotation for *S. latissima* and *L. digitata*.

	S. latissima	*L. digitata*
Total number of reads	986,800,000	1,001,600,000
Number of used reads	900,200,999	910,400,000
Number of assembled transcripts	24,733	34,251
GC content	55.03	54.31
N50 length (bp)	1,856	1,733
Average mapping rate	93.23%	90.12%
Annotation rate	47.34%	45.66%

Table S4. Log2Foldchange values and annotations of DEGs in *S. latissima* after 24 h of co-cultivaiton

ID	LOG2FoldChange	Annotation
TRINITY_DN5615_c1_g1_i1	-8.43	conserved unknown protein [Ectocarpus siliculosus]
TRINITY_DN776_c3_g1_i10	-28.44	NA
TRINITY_DN776_c3_g1_i13	-9.74	NA
TRINITY_DN7708_c0_g1_i10	2.57	NA
TRINITY_DN1587_c1_g1_i2	-9.66	NA
TRINITY_DN3653_c2_g3_i1	-12.35	NA

Table S5. Log2Foldchange values and annotations of DEGs in *L.digitata* after 24 h of co-cultivaiton

ID	LOG2FoldChange	Annotation
TRINITY_DN3439_c0_g1_i19	-28.45	putative lipoprotein [Ectocarpus siliculosus]
TRINITY_DN1792_c1_g1_i2	-28.39	unnamed protein product [Ectocarpus sp. CCAP 1310/34]
TRINITY_DN78_c0_g1_i3	-23.04	RME1L2, RME1-like GTPase/ATPase without a C-terminal EH domain [Ectocarpus siliculosus]
TRINITY_DN810_c0_g2_i4	-22.45	NA
TRINITY_DN7657_c0_g1_i1	-10.94	NA
TRINITY_DN7386_c0_g1_i10	-10.13	hypothetical protein Lal_00013077 [Lupinus albus]
TRINITY_DN2980_c0_g1_i2	-9.71	NA
TRINITY_DN2315_c0_g1_i4	-9.29	unnamed protein product [Ectocarpus sp. CCAP 1310/34]
TRINITY_DN26_c0_g2_i1	-9.14	hypothetical protein ENHYD8BJ_140222 [Enhydrobacter sp. 8BJ]
TRINITY_DN9413_c0_g1_i9	-8.96	hypothetical protein Lal_00001024 [Lupinus albus]
TRINITY_DN624_c0_g2_i4	-8.87	unnamed protein product [Ectocarpus sp. CCAP 1310/34]
TRINITY_DN4004_c0_g1_i3	-7.43	hypothetical protein A15U_04539, partial [Escherichia coli KTE210]
TRINITY_DN8479_c1_g1_i2	-7.04	conserved unknown protein [Ectocarpus siliculosus]
TRINITY_DN26_c0_g1_i13	-5.91	hypothetical protein Lal_00015017 [Lupinus albus]
TRINITY_DN239_c2_g1_i2	-5.49	NA
TRINITY_DN26_c0_g1_i16	-5.43	hypothetical protein Lal_00015017 [Lupinus albus]
TRINITY_DN5565_c0_g1_i2	-3.81	NA
TRINITY_DN6395_c2_g1_i8	-3.73	NA
TRINITY_DN8564_c0_g1_i5	-3.09	unnamed protein product [Ectocarpus sp. CCAP 1310/34]
TRINITY_DN8961_c1_g1_i5	-2.67	NA
TRINITY_DN2423_c0_g1_i9	-2.49	Unsaturated glucuronyl hydrolase, family GH88 [Ectocarpus siliculosus]
TRINITY_DN9297_c1_g1_i8	-2.11	NA
TRINITY_DN2505_c0_g4_i2	-1.80	NA
TRINITY_DN1782_c2_g1_i3	-1.55	unnamed protein product [Ectocarpus sp. CCAP 1310/34]
TRINITY_DN3778_c3_g3_i1	-1.54	NA
TRINITY_DN193_c0_g4_i2	-1.32	NA
TRINITY_DN7410_c0_g1_i2	-1.17	NA
TRINITY_DN1341_c1_g1_i7	-1.01	NA
TRINITY_DN21167_c0_g1_i3	-0.99	NA
TRINITY_DN2165_c1_g1_i15	1.45	unnamed protein product [Ectocarpus sp. CCAP 1310/34]
TRINITY_DN1887_c0_g1_i1	1.83	NA
TRINITY_DN2550_c0_g1_i7	1.83	NA
TRINITY_DN223_c0_g2_i3	2.07	fibronectin type III domain-containing protein [Ectocarpus siliculosus]
TRINITY_DN2165_c1_g1_i2	2.17	expressed unknown protein [Ectocarpus siliculosus]
TRINITY_DN6180_c0_g1_i11	3.74	NA

TRINITY_DN8710_c1_g1_i2	5.35	NA
TRINITY_DN2487_c0_g1_i2	5.74	NA
TRINITY_DN499_c0_g2_i2	5.95	NA
TRINITY_DN44264_c0_g1_i1	6.55	NA
TRINITY_DN2199_c0_g3_i2	7.01	conserved unknown protein [Ectocarpus siliculosus]
TRINITY_DN11732_c0_g1_i4	7.12	NA
TRINITY_DN9297_c1_g1_i2	9.33	NA
TRINITY_DN1341_c1_g1_i6	9.89	putative respiratory burst oxidase homolog protein [Ectocarpus siliculosus]
TRINITY_DN9444_c0_g1_i5	12.04	unnamed protein product [Ectocarpus sp. CCAP 1310/34]
TRINITY_DN2326_c0_g1_i15	13.06	conserved unknown protein [Ectocarpus siliculosus]
TRINITY_DN6727_c3_g1_i4	27.25	Light harvesting complex protein [Ectocarpus siliculosus]

Table S6. Log2Foldchange values and annotations of DEGs in *S. latissima* after 48 h of co-cultivaiton

ID	LOG2FoldChange	Annotation
TRINITY_DN19169_c0_g2_i4	-28.27	NA
TRINITY_DN16571_c0_g1_i1	-11.59	NA
TRINITY_DN16450_c2_g1_i1	-10.55	NA
TRINITY_DN12328_c0_g1_i3	-9.39	NA
TRINITY_DN118290_c0_g1_i1	-5.16	NA
TRINITY_DN2679_c0_g1_i7	-4.58	NA
TRINITY_DN632_c5_g1_i1	-4.00	NA
TRINITY_DN1601_c3_g1_i1	-3.75	unnamed protein product [Ectocarpus sp. CCAP 1310/34]
TRINITY_DN872_c0_g1_i5	-3.68	unnamed protein product [Ectocarpus sp. CCAP 1310/34]
TRINITY_DN564_c0_g3_i2	-3.55	conserved unknown protein [Ectocarpus siliculosus]
TRINITY_DN459_c0_g1_i2	-3.49	NA
TRINITY_DN7461_c0_g1_i1	-2.29	NA
TRINITY_DN11370_c0_g2_i11	-2.13	Glucokinase [Ectocarpus siliculosus]
TRINITY_DN446_c0_g1_i1	-2.12	expressed unknown protein [Ectocarpus siliculosus]
TRINITY_DN10_c0_g1_i8	-1.88	NA
TRINITY_DN26666_c0_g1_i1	-1.87	NA
TRINITY_DN16536_c0_g1_i5	-1.84	LRR receptor-like serine/threonine-protein kinase FEI 2 OS=Arabidopsis thaliana
TRINITY_DN2115_c3_g2_i1	-1.64	NA
TRINITY_DN1573_c0_g1_i1	-1.52	NA
TRINITY_DN10853_c1_g1_i1	-1.46	NA
TRINITY_DN1943_c0_g2_i2	-1.35	NA
TRINITY_DN16914_c0_g1_i3	-1.24	unnamed protein product, partial [Ectocarpus sp. CCAP 1310/34]
TRINITY_DN1276_c3_g1_i1	-1.18	mannuronan C-5-epimerase, partial [Laminaria digitata]
TRINITY_DN1737_c0_g1_i5	-1.15	pleiotropic drug resistance transporter [Ectocarpus siliculosus]
TRINITY_DN31811_c0_g3_i2	-1.12	NA
TRINITY_DN4854_c2_g1_i1	-1.10	NA
TRINITY_DN1128_c2_g1_i2	-1.10	NA
TRINITY_DN6654_c0_g2_i1	-1.08	NA
TRINITY_DN6659_c0_g4_i1	-0.95	NA
TRINITY_DN6534_c0_g1_i3	-0.92	NA
TRINITY_DN8480_c2_g1_i1	-0.92	conserved unknown protein [Ectocarpus siliculosus]
TRINITY_DN4238_c0_g1_i1	-0.90	kinesin K39 [Ectocarpus siliculosus]

TRINITY_DN619_c1_g1_i5	-0.89	Glutaredoxin glutaredoxin/malate transporter fusion protein [Ectocarpus siliculosus]
TRINITY_DN1138_c0_g3_i1	-0.80	unnamed protein product [Ectocarpus sp. CCAP 1310/34]
TRINITY_DN202_c0_g1_i8	-0.77	similar to activating transcription factor 6 [Ectocarpus siliculosus]
TRINITY_DN109_c5_g1_i2	0.72	unnamed protein product [Ectocarpus sp. CCAP 1310/34]
TRINITY_DN1247_c1_g2_i1	0.73	beta-lactamase domain protein [Ectocarpus siliculosus]
TRINITY_DN14163_c0_g1_i3	0.73	NA
TRINITY_DN8750_c0_g1_i1	0.73	unnamed protein product [Ectocarpus sp. CCAP 1310/34]
TRINITY_DN36125_c0_g3_i2	0.75	unnamed protein product [Ectocarpus sp. CCAP 1310/34]
TRINITY_DN11804_c0_g1_i1	0.76	NA
TRINITY_DN834_c8_g1_i1	0.76	conserved unknown protein [Ectocarpus siliculosus]
TRINITY_DN210_c0_g1_i2	0.77	adenylate kinase [Ectocarpus siliculosus]
TRINITY_DN121104_c0_g1_i1	0.79	long chain acyl-coA synthetase [Ectocarpus siliculosus]
TRINITY_DN5961_c0_g2_i3	0.80	unnamed protein product [Ectocarpus sp. CCAP 1310/34]
TRINITY_DN2608_c0_g1_i6	0.80	NA
TRINITY_DN13058_c1_g1_i3	0.81	NA
TRINITY_DN282_c0_g1_i3	0.81	NA
TRINITY_DN9040_c0_g2_i2	0.82	conserved unknown protein [Ectocarpus siliculosus]
TRINITY_DN396_c0_g1_i2	0.82	Ca2+/calmodulin-dependent protein kinase II [Ectocarpus siliculosus]
TRINITY_DN14686_c0_g1_i3	0.83	NA
TRINITY_DN3970_c0_g3_i1	0.83	conserved unknown protein [Ectocarpus siliculosus]
TRINITY_DN6827_c0_g1_i1	0.84	Lipoxygenase [Ectocarpus siliculosus]
TRINITY_DN107_c0_g1_i1	0.86	NA
TRINITY_DN1018_c4_g1_i1	0.86	NA
TRINITY_DN1666_c0_g1_i1	0.88	NA
TRINITY_DN14617_c2_g1_i1	0.90	NA
TRINITY_DN1914_c2_g2_i1	0.92	Mannuronan C-5-epimerase [Ectocarpus siliculosus]
TRINITY_DN1135_c0_g3_i1	0.92	PAP2/haloperoxidase-like protein [Chondrus crispus]
TRINITY_DN104485_c0_g1_i1	0.94	NA
TRINITY_DN12343_c0_g1_i1	0.94	conserved unknown protein [Ectocarpus siliculosus]
TRINITY_DN1527_c2_g1_i1	0.95	lipase [Ectocarpus siliculosus]
TRINITY_DN1173_c1_g1_i6	0.96	conserved unknown protein [Ectocarpus siliculosus]
TRINITY_DN116805_c0_g1_i1	0.97	NA
TRINITY_DN625_c1_g1_i3	0.98	Sulfotransferase [Ectocarpus siliculosus]
TRINITY_DN2842_c0_g4_i1	0.99	putative deacetylase sulfotransferase [Ectocarpus siliculosus]
TRINITY_DN619_c1_g1_i1	0.99	Glutaredoxin glutaredoxin/malate transporter fusion protein [Ectocarpus siliculosus]
TRINITY_DN1424_c0_g2_i1	1.00	putative respiratory burst oxidase homolog protein [Ectocarpus siliculosus]
TRINITY_DN125220_c0_g1_i1	1.01	Glutamyl-tRNA Synthetase [Ectocarpus siliculosus]
TRINITY_DN1928_c0_g1_i5	1.02	2-Isopropylmalate synthase [Ectocarpus siliculosus]
TRINITY_DN1527_c2_g2_i1	1.03	lipase [Ectocarpus siliculosus]
TRINITY_DN1094_c1_g3_i1	1.05	MEP13 [Ectocarpus sp. CCAP 1310/34]
TRINITY_DN14241_c0_g1_i7	1.07	NA
TRINITY_DN1408_c0_g1_i1	1.09	imm upregulated 3 [Ectocarpus siliculosus]
TRINITY_DN3341_c0_g2_i1	1.09	alginate lyase [Saccharina japonica]
TRINITY_DN1252_c0_g1_i3	1.10	mannuronan C-5-epimerase [Laminaria digitata]
TRINITY_DN4841_c0_g1_i1	1.12	unnamed protein product [Ectocarpus sp. CCAP 1310/34]

TRINITY_DN471_c0_g1_i8	1.22	NA
TRINITY_DN389_c4_g2_i1	1.29	mannuronan C-5-epimerase [Laminaria digitata]
TRINITY_DN2447_c1_g1_i2	1.33	vanadium-dependent bromine peroxidase [Saccharina japonica]
TRINITY_DN16536_c0_g1_i3	1.34	NA
TRINITY_DN558_c0_g1_i9	1.42	NA
TRINITY_DN4658_c1_g2_i1	1.46	conserved unknown protein [Ectocarpus siliculosus]
TRINITY_DN3555_c1_g2_i1	1.48	NA
TRINITY_DN2358_c0_g4_i1	1.51	NA
TRINITY_DN87_c0_g1_i1	1.53	EsV-1-163 [Ectocarpus siliculosus]
TRINITY_DN15412_c0_g1_i2	1.56	Mannuronan C-5-epimerase [Ectocarpus siliculosus]
TRINITY_DN3462_c3_g1_i1	1.58	Mannuronan C-5-epimerase [Ectocarpus siliculosus]
TRINITY_DN867_c7_g1_i1	1.60	EsV-1-163 [Ectocarpus siliculosus]
TRINITY_DN2339_c0_g1_i4	1.60	unnamed protein product [Ectocarpus sp. CCAP 1310/34]
TRINITY_DN717_c4_g1_i1	1.60	putative vanadium-dependent iodoperoxidase 3 [Laminaria digitata]
TRINITY_DN5976_c0_g1_i2	1.69	NA
TRINITY_DN6951_c0_g3_i1	1.98	NA
TRINITY_DN169_c1_g1_i5	2.26	von Willebrand A domain containing protein [Ectocarpus siliculosus]
TRINITY_DN449_c0_g1_i6	2.55	von Willebrand A domain containing protein [Ectocarpus siliculosus]
TRINITY_DN449_c0_g1_i5	2.77	similar to integrin alpha Hr1 precursor-like [Ectocarpus siliculosus]
TRINITY_DN6095_c0_g3_i2	2.93	Endo-1,3-beta-glucanase, family GH81 [Ectocarpus siliculosus]
TRINITY_DN3555_c0_g1_i9	3.57	hypothetical protein Esi_0425_0022 [Ectocarpus siliculosus]
TRINITY_DN6452_c0_g1_i6	4.85	NA
TRINITY_DN6025_c0_g1_i2	6.17	NA
TRINITY_DN7912_c1_g1_i2	11.41	NA

Table S7. Log2Foldchange values and annotations of DEGs in *L.digitata* after 48 h of co-cultivaiton

ID	LOG2FoldChange	Annotation
TRINITY_DN14831_c0_g3_i2	-14.28	Inositol 2-dehydrogenase [Ectocarpus siliculosus]
TRINITY_DN1081_c1_g1_i4	-11.36	unnamed protein product [Ectocarpus sp. CCAP 1310/34]
TRINITY_DN5786_c0_g1_i5	-9.91	putative vanadium-dependent iodoperoxidase 3 [Laminaria digitata]
TRINITY_DN5448_c4_g1_i1	-8.72	NA
TRINITY_DN11189_c1_g1_i2	-6.51	NA
TRINITY_DN12588_c0_g2_i1	-5.74	NA
TRINITY_DN40415_c0_g1_i1	-5.38	NA
TRINITY_DN1233_c1_g1_i3	-5.05	NA
TRINITY_DN3397_c1_g1_i2	-4.90	NA
TRINITY_DN2213_c0_g1_i5	-4.14	NA
TRINITY_DN882_c3_g1_i1	-3.44	NA
TRINITY_DN19415_c1_g1_i1	-2.92	NA
TRINITY_DN74078_c1_g1_i5	-2.69	NA
TRINITY_DN882_c3_g1_i2	-2.64	NA
TRINITY_DN24127_c0_g1_i2	-2.58	unnamed protein product [Ectocarpus sp. CCAP 1310/34]
TRINITY_DN11409_c0_g1_i1	-2.48	NA
TRINITY_DN523_c2_g1_i1	-2.44	Leucine rich repeat carbohydrate binding protein [Ectocarpus siliculosus]
TRINITY_DN21226_c0_g1_i1	-2.06	NA
TRINITY_DN250_c1_g3_i1	-1.88	unnamed protein product [Ectocarpus sp. CCAP 1310/34]
TRINITY_DN1850_c10_g1_i1	-1.86	unnamed protein product [Ectocarpus sp. CCAP 1310/34]

TRINITY_DN390_c0_g1_i15	-1.80	glucose sorbosone dehydrogenase [Ectocarpus siliculosus]
TRINITY_DN3431_c4_g1_i2	-1.66	Cellulose synthase (UDP-forming), family GT2 [Ectocarpus siliculosus]
TRINITY_DN2737_c0_g1_i7	-1.59	unnamed protein product [Ectocarpus sp. CCAP 1310/34]
TRINITY_DN7206_c0_g2_i1	-1.56	NA
TRINITY_DN12949_c0_g1_i9	-1.48	unnamed protein product [Ectocarpus sp. CCAP 1310/34]
TRINITY_DN2426_c0_g1_i5	-1.48	carbonic anhydrase [Saccharina japonica]
TRINITY_DN1166_c0_g1_i3	-1.43	hypothetical protein Esi_0117_0034 [Ectocarpus siliculosus]
TRINITY_DN1517_c4_g2_i1	-1.38	NA
TRINITY_DN874_c0_g1_i5	-1.29	polymorphic outer membrane protein [Ectocarpus siliculosus]
TRINITY_DN4308_c2_g1_i1	-1.21	long-chain acyl-CoA synthetase [Ectocarpus siliculosus]
TRINITY_DN13634_c0_g1_i2	-1.20	unnamed protein product [Ectocarpus sp. CCAP 1310/34]
TRINITY_DN5597_c0_g1_i4	-1.19	Related to G-protein coupled receptors [Ectocarpus siliculosus]
TRINITY_DN3648_c0_g1_i7	-1.18	GT18 [Ectocarpus sp. CCAP 1310/34]
TRINITY_DN20532_c0_g1_i9	-1.16	light harvesting protein lhcf6 [Saccharina latissima]<>chloroplast light harvesting protein lhcf6 [Saccharina japonica]
TRINITY_DN2737_c0_g1_i4	-1.14	unnamed protein product [Ectocarpus sp. CCAP 1310/34]
TRINITY_DN2115_c0_g1_i1	-1.10	expressed unknown protein [Ectocarpus siliculosus]
TRINITY_DN755_c0_g1_i2	-1.02	unnamed protein product [Ectocarpus sp. CCAP 1310/34]
TRINITY_DN2940_c0_g1_i5	-1.02	unnamed protein product [Ectocarpus sp. CCAP 1310/34]
TRINITY_DN8405_c0_g1_i1	-0.88	conserved unknown protein [Ectocarpus siliculosus]
TRINITY_DN677_c0_g1_i4	-0.86	Triose phosphate/phosphate translocator, non-green plastid, chloroplast precursor (CTPT), C-terminal [Ectocarpus siliculosus]
TRINITY_DN1734_c0_g3_i14	-0.85	unnamed protein product [Ectocarpus sp. CCAP 1310/34]
TRINITY_DN9803_c0_g1_i1	-0.82	hypothetical protein Esi_0065_0030 [Ectocarpus siliculosus]
TRINITY_DN6338_c0_g1_i1	-0.78	conserved unknown protein [Ectocarpus siliculosus]
TRINITY_DN1620_c6_g1_i1	-0.77	unnamed protein product [Ectocarpus sp. CCAP 1310/34]
TRINITY_DN4375_c1_g1_i2	-0.77	Polymorphic membrane protein [Ectocarpus siliculosus]
TRINITY_DN1344_c3_g1_i1	-0.77	chitinase-domain containing protein [Ectocarpus siliculosus]
TRINITY_DN723_c2_g1_i1	-0.72	unnamed protein product [Ectocarpus sp. CCAP 1310/34]
TRINITY_DN545_c0_g1_i5	0.77	GDP-mannose dehydrogenase 2 [Saccharina japonica]
TRINITY_DN6853_c3_g1_i1	0.86	NA
TRINITY_DN26454_c0_g1_i5	0.90	NA
TRINITY_DN3531_c0_g1_i1	0.93	NA
TRINITY_DN27878_c3_g1_i1	0.98	NA
TRINITY_DN2905_c1_g2_i1	1.00	unnamed protein product [Ectocarpus sp. CCAP 1310/34]
TRINITY_DN11332_c0_g1_i1	1.02	conserved unknown protein [Ectocarpus siliculosus]
TRINITY_DN2059_c1_g1_i2	1.06	NA
TRINITY_DN919_c1_g3_i1	1.09	NA
TRINITY_DN7898_c1_g1_i1	1.11	NA
TRINITY_DN27884_c0_g1_i2	1.12	NA
TRINITY_DN2038_c0_g1_i2	1.19	Metacaspase[Ectocarpus siliculosus]
TRINITY_DN2429_c0_g4_i3	1.22	conserved unknown protein [Ectocarpus siliculosus]
TRINITY_DN2850_c2_g1_i3	1.36	NA
TRINITY_DN545_c0_g1_i4	1.38	GDP-mannose dehydrogenase 2 [Saccharina japonica]
TRINITY_DN1874_c0_g3_i1	1.40	NA
TRINITY_DN7036_c0_g2_i2	1.43	unnamed protein product [Ectocarpus sp. CCAP 1310/34]
TRINITY_DN25753_c0_g1_i1	1.45	photosystem II reaction center protein D1 [Saccharina japonica]
TRINITY_DN39_c0_g1_i4	1.56	Serine Carboxypeptidase-like [Ectocarpus siliculosus]

TRINITY_DN688_c0_g1_i3	1.65	carbohydrate 4-sulfotransferase 8 [Fistulifera solaris]
TRINITY_DN35903_c0_g1_i1	1.69	ribulose-1,5-bisphosphate carboxylase/oxygenase large subunit [Laminaria digitata]
TRINITY_DN101866_c0_g1_i2	1.83	NA
TRINITY_DN254_c1_g4_i1	1.93	NA
TRINITY_DN4168_c1_g1_i2	2.35	expressed unknown protein [Ectocarpus siliculosus]
TRINITY_DN8266_c0_g1_i4	2.89	expressed unknown protein [Ectocarpus siliculosus]
TRINITY_DN455_c2_g2_i2	3.41	expressed unknown protein [Ectocarpus siliculosus]
TRINITY_DN6153_c0_g1_i3	3.95	unnamed protein product [Ectocarpus sp. CCAP 1310/34]
TRINITY_DN8825_c0_g1_i8	4.26	NA
TRINITY_DN3366_c1_g1_i8	4.28	NA
TRINITY_DN9269_c4_g2_i1	4.40	Tim50 homolog, mitochondrial inner membrane protein of TIM23 complex [Ectocarpus siliculosus]
TRINITY_DN12586_c0_g1_i8	4.60	NA
TRINITY_DN3968_c0_g1_i7	5.35	NA
TRINITY_DN7495_c0_g1_i1	5.64	NA
TRINITY_DN26_c0_g1_i16	6.15	hypothetical protein Lal_00015017 [Lupinus albus]
TRINITY_DN4443_c0_g1_i1	6.51	NA
TRINITY_DN8095_c5_g1_i1	6.63	NA
TRINITY_DN3873_c1_g1_i2	6.97	NA
TRINITY_DN45640_c0_g2_i2	7.48	NA
TRINITY_DN4004_c0_g1_i3	7.93	hypothetical protein A15U_04539, partial [Escherichia coli KTE210]
TRINITY_DN3080_c1_g2_i2	8.65	NA
TRINITY_DN3837_c0_g1_i2	9.76	NA
TRINITY_DN26_c0_g2_i1	9.82	hypothetical protein ENHYD8BJ_10132 [Enhydrobacter sp. 8BJ]
TRINITY_DN9413_c0_g1_i9	9.90	hypothetical protein Lal_00001024 [Lupinus albus]
TRINITY_DN2737_c0_g1_i8	10.13	unnamed protein product [Ectocarpus sp. CCAP 1310/34]
TRINITY_DN10816_c1_g3_i2	10.19	NA
TRINITY_DN943_c0_g6_i1	10.96	NA
TRINITY_DN1158_c4_g2_i1	11.14	unnamed protein product [Ectocarpus sp. CCAP 1310/34]
TRINITY_DN1056_c6_g1_i2	11.47	DEAD box helicase [Ectocarpus siliculosus]
TRINITY_DN3337_c1_g1_i4	11.58	conserved unknown protein [Ectocarpus siliculosus]
TRINITY_DN1483_c0_g2_i4	11.69	NA
TRINITY_DN3976_c2_g1_i2	11.84	NA
TRINITY_DN371_c2_g1_i1	12.35	EsV-1-7 [Ectocarpus siliculosus]
TRINITY_DN1531_c0_g1_i4	12.37	unnamed protein product [Ectocarpus sp. CCAP 1310/34]
TRINITY_DN17_c0_g2_i1	12.50	NA
TRINITY_DN4671_c0_g1_i2	12.60	NA
TRINITY_DN559_c0_g1_i1	12.66	unnamed protein product [Ectocarpus sp. CCAP 1310/34]
TRINITY_DN6020_c0_g1_i4	13.05	NA
TRINITY_DN1022_c1_g1_i2	13.41	NA
TRINITY_DN1297_c0_g5_i2	13.49	imm upregulated 3 [Ectocarpus siliculosus]
TRINITY_DN907_c1_g1_i2	13.59	NA
TRINITY_DN5523_c1_g1_i6	13.86	NA
TRINITY_DN1483_c0_g2_i3	16.51	NA

Chapter III

Transcriptomic and metabolomic response of *Saccharina latissima* to oligoguluronates elicitation provide insights into oxylipin pathways in kelps

Chapter III. Transcriptomic and metabolomic response of *Saccharina latissima* to oligoguluronates elicitation provide insights into oxylipin pathways in kelps

1. Introduction

Pathogen-induced molecular patterns (PIMPs) refer to endogenous elicitors induced by pathogen infection. Perception of PIMPs leads to the activation of defense responses in the infected host. For instance, oligogalacturonides (OGAs) are well-characterized cell wall-derived PIMPs, generated from enzymatic activity encoded by either the pathogen or the host, which activate immune responses in plants. Galletti et al. reported that OGAs induced the expression of NADPH oxidase gene and oxidative burst in *Arabidopsis thaliana* (Galletti et al., 2008). Furthermore, OGAs also induced the gene regulation of several signaling pathways, such as Ca^{2+} signaling, MAPK signaling and oxylipin pathways (Galletti et al., 2011, Moscatiello et al., 2006, Denoux et al., 2008). Other defense-related genes were also induced by OGAs, including genes encoding enzymes involved in the biosynthesis of defense-related compounds (Denoux et al., 2008, Ferrari et al., 2003).

Like OGA-induced oxidative burst and pathogen responses in plants, kelps perceived cell wall degradation products that activate similar defense responses. Oligoguluronate (GG) is the oligomeric degradation products of alginate, the key component of marine brown algal cell walls. Küpper et al. (2001) have found that GG induced a strong release of H_2O_2 within 10 minutes in *Laminaria digitata*. At the same time, a strong potassium efflux was also detected during the GG elicitation, indicating some signaling pathways might be activated (Küpper et al., 2001). In later studies, several evidences have supported the hypothesis that the recognition of GG play a key role in the pathogen resistance of kelps. In 2002, it has been reported that GG pre-treatment significantly induced the resistance of *L. digitata* against the infection caused by the endophytic pathogen, *Laminariocolax tomentosoides* (Küpper et al., 2002). Similarly, GG pre-treatment also modified the physiological responses of *L. digitata* during the interaction with another endophytic pathogen *Laminarionema elsbetiae* (Bernard, 2018) (see also Chapter2). In other species of Laminariales, such as *Saccharina latissima*, the protection of juvenile sporophytes by GG

elicitation was also observed, which reduced the density of endobionts and the number of bacterial cells on sporophytes (Wang et al., 2019).

GG has been reported to induce some transcriptional regulation in plantlets of *L. digitata*. In this kelp, fifty genes were detected as differentially expressed genes in response to GG treatment (Cosse et al., 2009). Among those genes, some genes related to oxidative stress responses, such as glutathion-S-transferase (GST), thioredoxin (trx) and heat-shock protein (Hsp), were induced and related to the oxidative burst. The elicitor also triggered the expression of several vanadium-dependent haloperoxidase (vHPO) genes, which may produce volatile halocarbons by catalyzing the oxidation of halides in the presence of hydrogen peroxide. Moreover, genes encoding C5-epimerases were also identified in the differentially expressed genes and these enzymes are expected to convert nongelling mannuronic acid-rich alginates into GG-rich gelling polysaccharides, strengthening cell wall of the sporophytes. In addition to transcriptional regulation, GG also triggered the production of oxylipins and aldehydes in *L. digitata*. The GG elicitation induced release of various volatile aldehydes, such as (E)-4-hydroxyhex-2-enal (4-HHE), (E)-4-hydroxynon-2-enal (4-HNE) and 4-hydroxydodeca-2,6-dienal (4-HDDE). Then those aldehydes were tested on *L. digitata*. Only treatment with 4-HHE induced a later release of an oxylipin, 13s-hydroxy-9Z,11E,15Z-octadecatrienoic acid (13S)-HOTrE), suggesting that 4-HHE could activate the oxylipin signaling pathway leading to defense mechanisms in *L. digitata (Goulitquer et al., 2009).* In another study of *L. digitata*, the waterborne cues released by GG-elicited sporophytes induced similar transcriptional gene regulation in neighboring conspecifics, indicating that the signaling pathways activated by GG also participated in the long-distance communication between kelps (Thomas et al., 2011). Although these studies have provided some insights into the gene and metabolite regulation in response to GG treatment, in relationship with the activation of oxylipins pathway in *L. digitata*, the molecular effects caused by GG treatment are mainly undiscovered in other kelps species, where elicitation was likely to play a key role in induced resistance of sporophytes (Küpper, Müller et al. 2002).

Saccharina latissima is a common kelp species found in the north east Atlantic Ocean and the Pacific Ocean. Its sporophytes, with other kelp ones, are the major components of rocky intertidal and subtidal habitats. The aquaculture of this species is rapidly expanding in Europe. Due to its ecological and economic values, *S. latissima* has become a model of kelp biology and ecology

research fields. Recently, several studies reported on the global transcriptomic regulations occurring in *S. latissima* in response to various abiotic stress (Li et al., 2020a, Heinrich et al., 2015, Monteiro et al., 2019a, Li et al., 2020b). The genome of *S. latissima* will be soon available through Phaeoexplorer, a genomic project aiming at sequencing several genomes of main brown algal species. The availability of genomic resources will help to study the biological process in *S. latissima.*

In this chapter, we used *S. latissima* as a kelp model to investigate the molecular effects caused by GG elicitation, by developing global transcriptomic and metabolomic experimental approaches within a 12-hour time-course. For studying transcriptional responses, large-scale RNA-sequencing was performed on RNA from young sporophytes sampled at four time points (0.5h, 1h, 4.5h and 12h) after adding GG and compared to control samples. For metabolomic analysis, untargeted LC-MS was applied to detect metabolite changes at the same time points. The integration of these results helps us to better understand the elicitor-induced molecular responses in kelps, especially those derived from lipid oxidation signaling pathways.

2. Material and method

2.1. Biological material

Spores of *S. latissima* were released from fertile sporophytes collected at Perharidy (near Roscoff, 48.73° N, 4.00° W) using the hanging-drop technique (WYNNE, 1969). The male and female gametophytes were kept together in petri dishes to produce zygote. After the formation of developing sporophytes, they were kept in petri dishes with weekly changes of culture medium. For all cultures, natural seawater was filtered, autoclaved and enriched with Provasoli solution (10m Provasoli solution/L seawater) (Provasoli, 1968). After 4 weeks, the sporophytes were transferred to 2 L bottles connected to an aeration system with weekly changes of culture medium. The kelp cultures were maintained in 14°C and 20µmol photons $s^{-1}m^{-2}$ with a 12 h light/dark cycle.

2.2. Transcriptome analysis

2.2.1. GG treatment

Thirty-two *S. latissima* sporophytes cultivated in laboratory were placed in small glass beakers, filled with 30 mL autoclaved seawater. They were equally divided into two groups: control and treatment. For treatment group, oligoguluronates solution (GG, prepared from *L. hyperborea*) were added into seawater at a final concentration of 150µg/mL. The glass beakers were placed on a shaker incubated at 100rpm for 1 h in the cultivation condition. Then the sporophytes were rinsed several times with autoclaved seawater and transferred into clean glass bakers with 30 mL autoclave seawater. As shown in figure, samples for RNA sequencing were collected at four time points: 0.5h, 1h, 4.5h and 12h. And there were control and treatment groups with four biological replicates for each time points. These samples were frozen in liquid nitrogen and stored at -80°C.

2.2.2. RNA extraction, quality assessment and sequencing

RNA was extracted with the method described in chapter I. After the extraction, the quantity and quality of extracted RNA were tested on a NanoDrop™ spectrophotometer (Thermo Fisher Scientific Inc., Waltham, US) and on a 2% agarose gel. Then the RNA samples passed the quality assessment were used to perform sequencing library preparation and Illumina Novaseq S4 (PE 150bp) at the Plateforme Génomique du Genopole Toulouse Midi-Pyrénées GeT (France).

2.2.3. *De novo* assembly and annotation of the transcriptome

The quality control of raw data produced by sequencing was performed using FastQC (Andrews, 2010). Low quality reads (Phred score <33 or length < 50 nucleotides) and sequencing adapters were removed using Trimmomatic (Bolger et al., 2014) and residual rRNA was removed with SortmeRNA (Kopylova et al., 2012). The data cleaning step was followed by another quality check with FastQC to ensure the quality of data reach the requirements of downstream analysis.

A *de novo* transcriptome was assembled based on the pooled reads of all conditions using Trinity (Grabherr et al., 2011) with the default options. Then reads were mapped on the transcriptome to calculate the transcript abundance with Bowtie2 aligner and RSEM (Langmead & Salzberg, 2012, Li & Dewey, 2011a) and transcripts that represent 90% of reads were kept for downstream

analysis. After obtaining a transcriptome with low redundancy, reads were mapped to this new transcriptome with Bowtie 2 aligner and transcript abundance was estimated with RSEM.

Gene annotation was performed with a Blastx search against the NCBI-nr and the Uniprot database with an E-value cut-off of 10^{-5}. Gene ontology (GO) annotation and protein family (Pfam) analysis were performed using Blast2GO (Conesa et al., 2005). And KEGG annotation was performed on a web server, KEGG Automatic Annotation Server (KAAS) https://www.genome.jp/kegg/kaas/.

2.2.4. Differentially expressed gene analysis

Differentially expressed gene analysis between control and GG treatment was performed separately for samples of four time points using R package DESeq2 (Love et al., 2014). Transcripts with Log2Foldchange value $\geqslant$ 1 or $\leqslant$ -1 and adjusted p-value < 0.05 were considered as differentially expressed genes (DEGs). Then differentially expressed genes identified at four time points were used to perform GO and KEGG enrichment analysis.

2.3. Metabolic profiling of FFAs and their oxygenated derivatives

2.3.1. Treatments of algal samples

S. latissima sporophytes cultivated in laboratory were placed in small glass beakers, filled with 30 mL autoclaved seawater. The GG treatment was same with RNA sequencing experiment. For GC-MS analysis, two treatment groups (control and GG treatment) were collected at three time points (1, 4.5 and 12 h) and each treatment contained four biological replicates. For LC-MS analysis, two more groups pretreated with LOX inhibitors were added comparing to GC-MS analysis and they were pretreated with Salicylhydroxamic acid (SHAM) at 1 mM final concentration and n-propylgallate (n-PGal) at 100 µM final concentration, respectively, for 15 minutes before GG elicitation. Four treatment groups (control, GG, SHAM and n-PGal) were collected at four time points (0.5, 1, 4.5 and 12 h) with four biological replicates in each group. Collected samples were frozen in liquid nitrogen and stored at -80°C.

2.3.2. GC-MS analysis

For each algal treatment (control, GG) and sampling time (1, 4.5 and 12 h), FFAs and their derivatives were extracted from 10 mg freeze-dried powder with 1 mL ethyl acetate. In each sample, 1.25 µg.mL^{-1} 12-OH-lauric acid was added as an internal standard for extraction. The extraction lasted for at least 1 hour and then 1 mL ice-cold water was added to stop the reaction. The ethyl acetate phase was recovered and dried with SpeedVac vacuum concentrator. The extracts were dissolved in 100 µL ethanol and 0.1 mg.mL^{-1} tridecanoic acid was added as internal standard for derivatization. The derivatization was performed using Sylon (BSTFA/TMC 99:1). After the derivatization, the solvent was dried with SpeedVac vacuum concentrator and 100 µL Hexane was added to dissolve the extracts for GC-MS analysis.

Metabolites were analyzed by GC-MS using an Agilent GC 7890+ coupled to a 5975 quadrupole mass detector (Agilent, Les Ulis, France) and equipped with a DB/HP-5MS column (methyl phenyl siloxane: 30 m × 0.25 mm I.D. × 0.25 µm film thickness; J&W Scientific, Agilent) in the Electronic Impact (EI) mode at 70 eV. A sample (volume of 2 µL) was injected into the capillary column at 1 mL.min^{-1}, with a temperature of injection of 230°C. Then, the temperature gradient used was 60°C for 2 min, 60 to 290°C at 10°C.min^{-1} and stabilization at 290°C for 5 min. The range of masses analyzed were from 50 to 800 m/z.

2.3.3. LC-MS analysis

For each algal treatment (control, GG, n-PGal, SHAM) and sampling time (0.5, 1, 4.5 and 12 h), FFAs and their derivatives were extracted from 20 mg freeze-dried powder with 2 mL Ethyl acetate. In each sample, 1.25 µg.mL^{-1} 12-OH-lauric acid was added as an internal standard for analysis in the negative mode. The extraction lasted for at least 1 hour and then 1 mL ice-cold water was added to stop the reaction. The ethyl acetate phase was recovered and dried with SpeedVac vacuum concentrator. For metabolomic analysis, 100 µL EtOH:H_2O (8:2) were added to each sample and 50 µl of each extract

were used for analysis. Chemical compounds were first separated by ultrahigh-pressure liquid chromatography (UPLC) and analyzed by mass spectrometry (MS) on a Thermo Scientific LTQOrbitrap Discovery™ mass spectrometer (Thermo Scientific) equipped with an Electro Spray

Ionization (ESI) source running on the negative ionization mode, as described in Ritter et al. (2014) (Ritter et al., 2014). Metabolic samples were analyzed using a 1.9 µm Thermo Hypersil Gold C18 column (100 x 2.1 mm) and the mobile phase A was composed of 0.1% acetic acid in H_2O, and mobile phase B was 0.1% acetic acid in acetonitrile. The gradient, starting at 0% B, consisted of an initial hold at 60% mobile phase B from 1 to 3 min, followed by a gradient to 95% B in 12 min and a hold for 4 min, followed by re-equilibration for 4 min at 0% B, for a total run time of 23 min. Xcalibur 2.1 software was used for instrument control and data acquisition.

2.3.4. Data processing and statistical analysis

Metabolomic data obtained with Xcalibur software corresponded to a chromatogram and mass spectra for each sample. LC-MS data were processed by Galaxy-Workflow4Metabolomics (W4M) on the online version (Giacomoni et al., 2015), after conversion of raw spectra to mzXML format using MSConvert. In W4M pipeline, data processing was performed using centWave method for the peak picking, with a maximum deviation of 10 ppm. The signal/noise threshold was fixed at 8, the prefilter at 3,100 and the noise filter at 5000. For the first group step, density method was used, with the band width set at 30 and the minimum fraction of samples necessary at 0.25. For correction of retention time, the obiwarp method was used and a step size of 0.1 m/z. The second group step was performed using density method and a band width of 10. Fillpeaks step was used with the chrom filling method. Finally, annotation by CAMERA was set using a max ion charge of 2, a general ppm error of 5 and a precision of 4 decimals of m/z values. After the conversion of raw spectra to CDF format, the GC-MS data were analyzed using free software MS-DIAL 4.24 (Tsugawa et al., 2015) with default parameters. The final table of LC- and GC-MS data analysis contained ions abundances in samples, which corresponded to peak areas. Then the contamination was removed using blank samples and normalization was performed by dividing the area of the internal standard in the sample. Principal Component Analysis (PCA) and Orthogonal Partial Least Squared – Discriminant Analysis (OPLS-DA) were performed to select significantly different ions (VIP > 1). These ions were further annotated by comparing to Metlin (Smith et al., 2005) and NIST 14 databases. And t-test was performed on ions with interests to prevent the false positive.

3. Results

3.1. Transcriptome assembly and analysis of differentially expressed genes (DEGs)

The clean reads of all treatments were assembled by Trinity into 27,904 transcripts with an average contig length of 1,424 bp. The average GC content of this *de novo* transcriptome from *S. latissima* was 54.7%. The results of the BUSCO analysis revealed a near-complete gene sequence information for this *S. latissima* transcriptome with 80.2% complete BUSCO matches.

After 0.5 h of GG elicitation, a small fraction of genes (0.8%, i.e. 224 genes) showed significant expression differences between samples from control and GG treatments, in which 133 genes were upregulated and 91 genes were downregulated. The number of differential expressed genes (DEGs) started increasing after 1 hour, reaching 5.2% of the total transcriptome: 1,451 genes (1,040 upregulated genes and 411 downregulated genes) were identified as DEGs. During the time-course, the number of DEGs reached the summit at 4.5 h with 17% of the total genes, and among these DEGs, 48.6% were downregulated (2,314 genes) and 51.4% upregulated (2,447 genes) (Figure 1A). Then the amount of DEGs decreased to 6.2%, with 1,732 genes in total, and more genes were downregulated (58.6%) at 12 h.

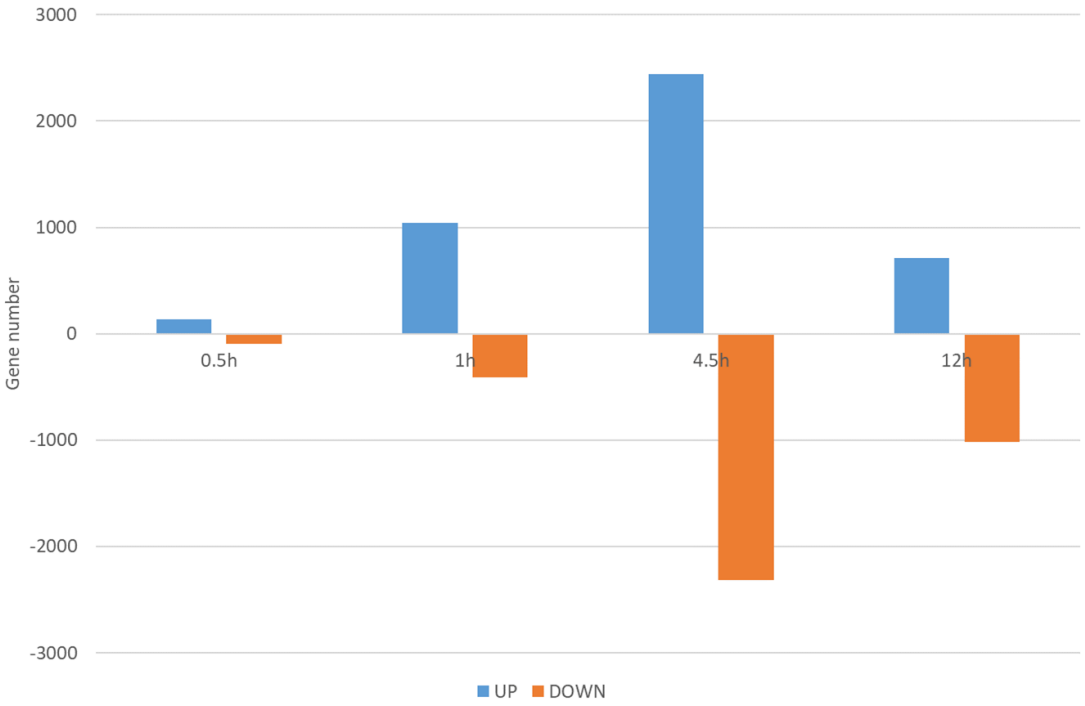

Fig. 1 Number of up-regulated (blue) and down-regulated (orange) genes at four time points

Among the differentially expressed genes identified at the four time points of the GG treatment, most DEGs were specifically expressed at one time point. Only 5 upregulated genes (Figure 2A) and 1 downregulated gene (Figure 2B) were shared by all four time points. More common genes were found between two adjacent time points.

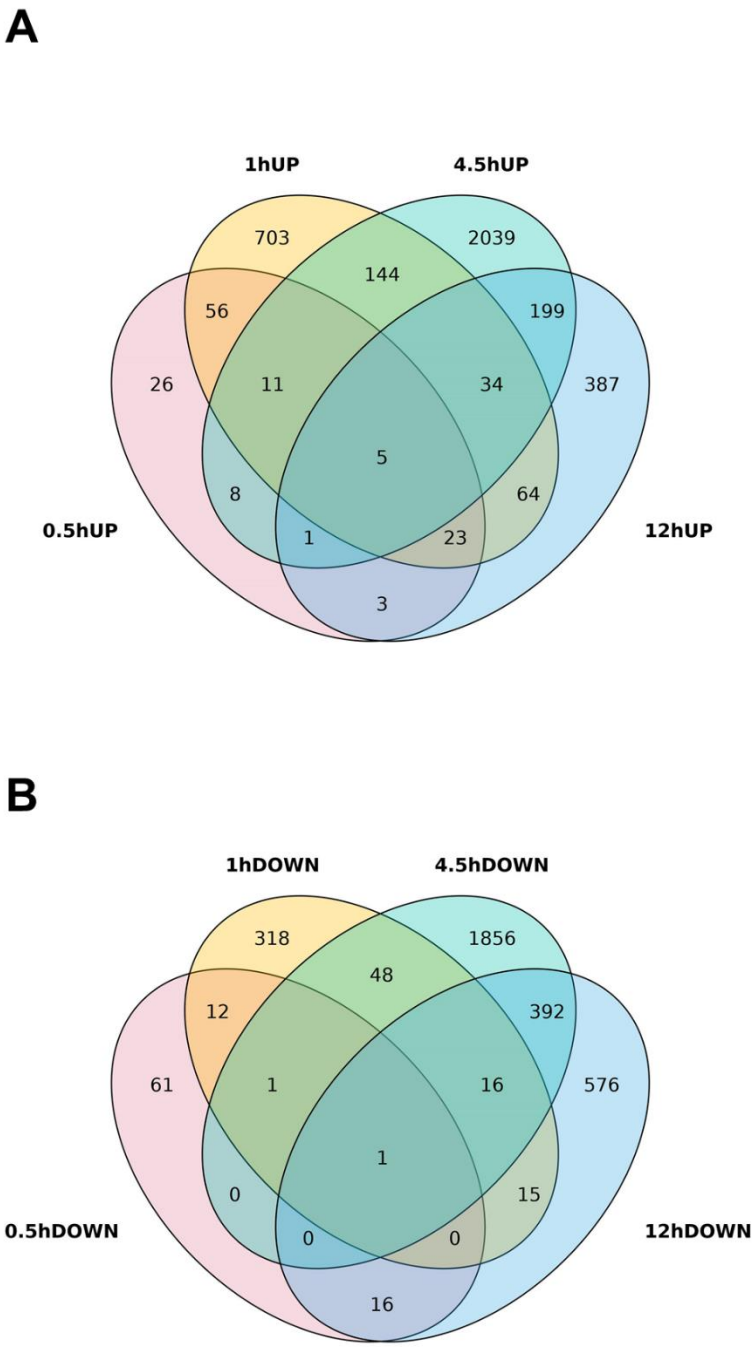

Fig. 2 A: Venn diagram of up-regulated genes of four time points. B: Venn diagram of down-regulated genes of four time points.

3.2. KEGG enrichment analysis of differentially expressed genes

A KEGG enrichment analysis was conducted to identify particular metabolic pathways which could be regulated upon GG elicitation, based on DEG's annotation information. Globally, the results showed two very distinct patterns according to up- or down-regulated DEGs (Figure 3). For the up-regulated DEGs, the most significantly enriched pathway names were related to lipid metabolism, such as linoleic acid metabolism, arachidonic acid metabolism and Lipid metabolism (Figure 3A). Then the terms corresponding to the metabolisms of amino acids and glutathione were also enriched with low q-value under 0.05. Interestingly, other two categories, Plant-pathogen interaction and Plant hormone signal transduction, also appeared in the list of top 30 enriched pathways.

In the down-regulated differentially expressed genes, the enriched pathway names were mostly related to the basic biological processes, such as Photosynthesis, DNA replication and Glycolysis (Figure 3B).

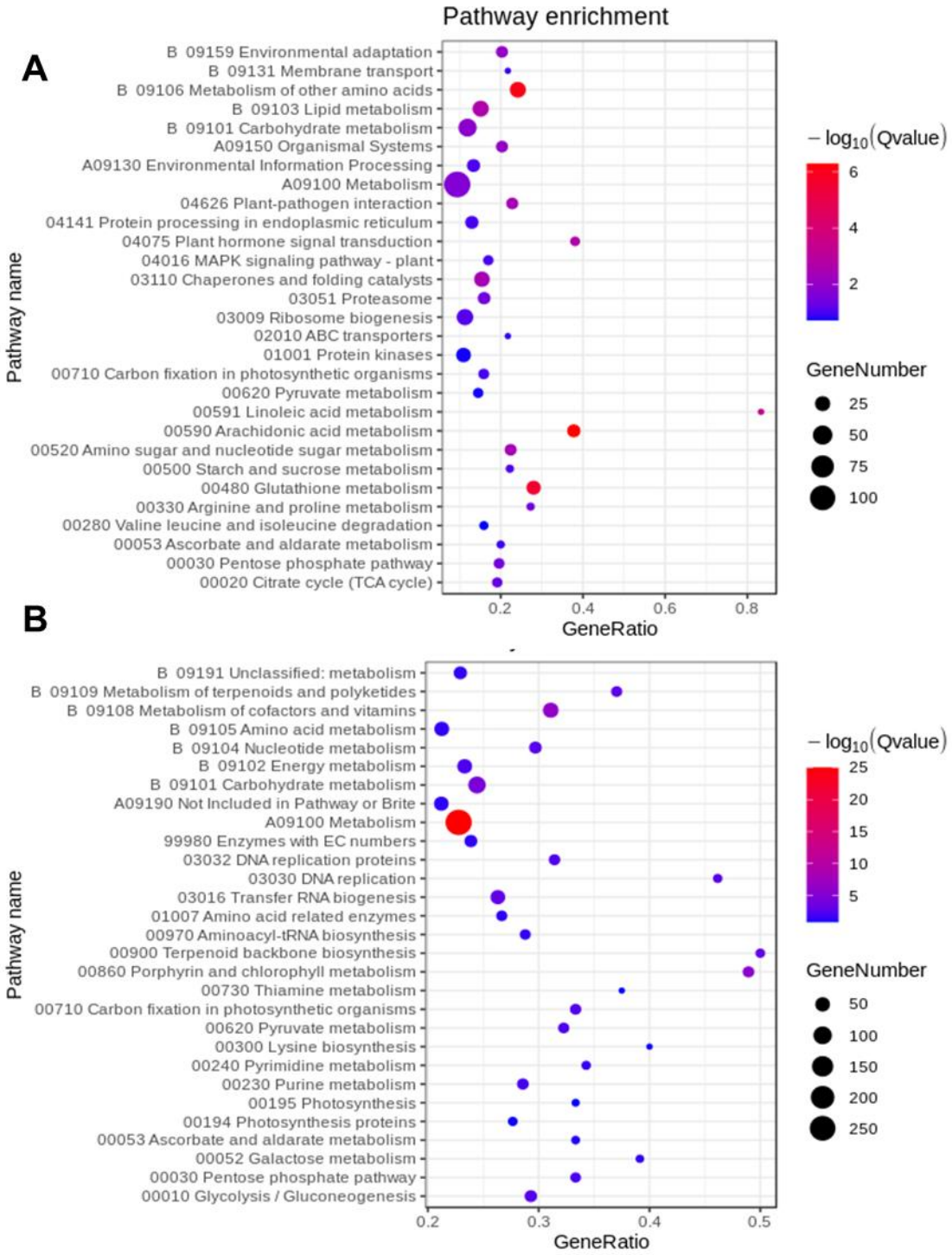

Fig. 3 A: KEGG enrichment of up-regulated genes. B: KEGG enrichment of down-regulated genes.

3.3. Expression analysis of biological processes and metabolic pathways of interest based on functional annotation of differentially expressed genes at four time points

3.3.1. DEGs classified in Lipid-associated and -derived metabolism pathways

Based on KEGG enrichment analysis, in lipid metabolism pathways, including linoleic acid metabolism and arachidonic acid metabolism, fifty-six genes were identified as significantly up-regulated genes. Among those genes, twenty-two genes were annotated as lipase-encoding genes and they had very diverse expression patterns. Only two of them featured a slight increase already after 30 minutes, when most had their strongest expression after 1hour, some showed another expression peak after 12h. Other lipase-encoding genes are significantly upregulated only after 4.5 h or 12 h (Figure 4). Sixteen DEGs encoding glutathione S-transferases were mainly up-regulated after 4.5 h, and some are still overexpressed after 12 h (Figure 4). In relation to downstream lipid metabolism and signaling cascades, i.e. Linoleic acid and Arachidonic acid metabolisms, six lipoxygenase (LOX) genes and four cytochrome P450 (CYP) genes were significantly up-regulated at 4.5 h or 12 h and one of the CYP genes was induced twice (at 1 h and 12 h) during the whole process.

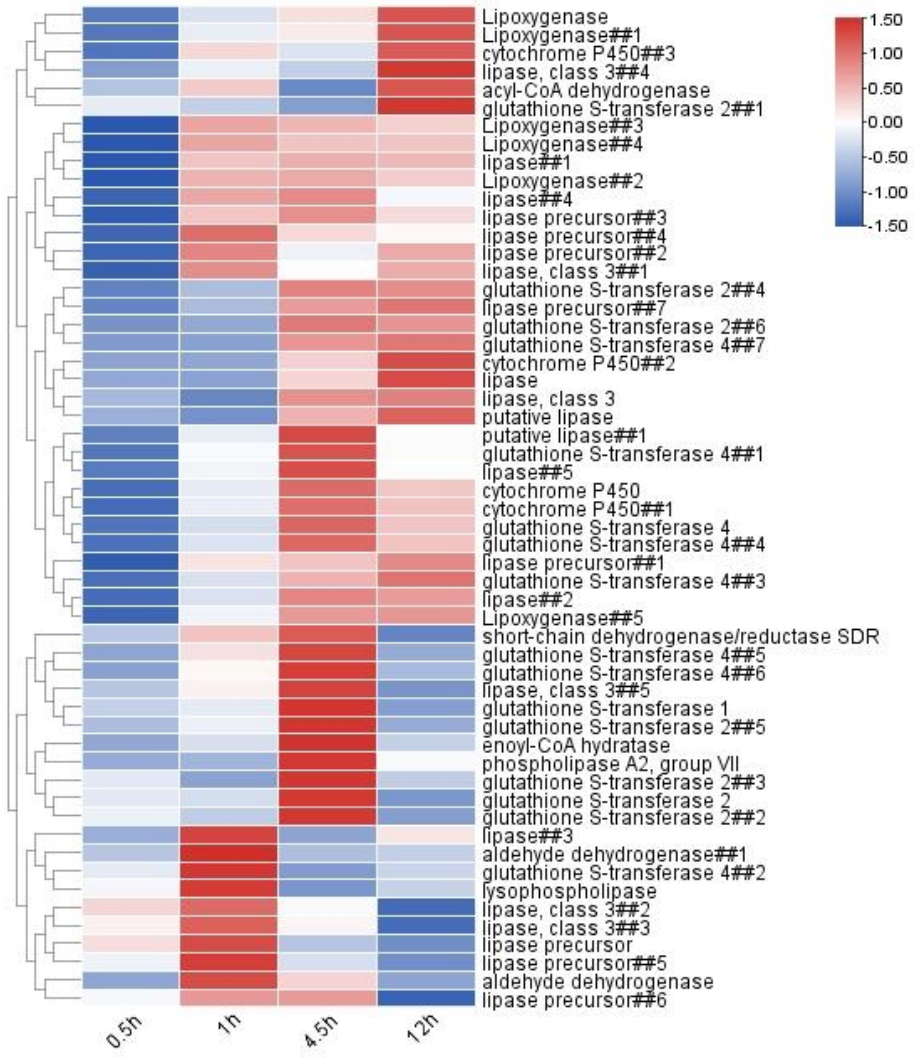

Fig. 4 Heatmap of DEGs expression related to lipid metabolism according to scaled Log2Foldchange values and time-course. Each line corresponds to one DEG.

3.3.2. DEGs of Plant-pathogen interaction category

Three DEGs potentially involved in calcium signaling pathway were found in the KEGG category called plant-pathogen interaction, including two calcium/calmodulin-dependent protein kinase genes and one calmodulin gene. These genes were induced at very early stages after GG treatment (1 h) (Figure 5). In the same category, two genes annotated as heat shock protein 90 (HSP90) and two putative genes encoding NB-ARC and TPR repeat-containing protein were up-regulated at 4.5 h. A gene encoding LRR-containing GTPases of the ROCO family was also up-regulated at 4.5 h. Additionally, a gene encoding pathogenesis-related protein were also induced by GG treatment after 1 h and the up-regulation of this gene were also found at 4.5 h and 12 h.

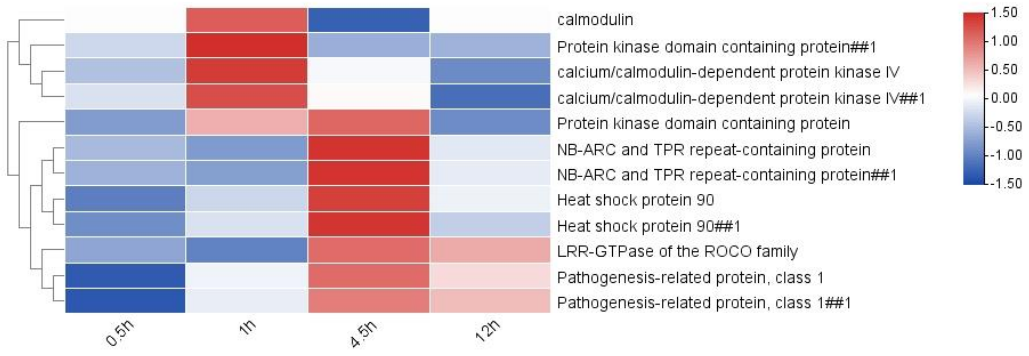

Fig. 5 Heatmap of 12 DEGs expression related to plant-pathogen interaction category according to scaled Log2Foldchange values and time-course. Each line corresponds to one DEG.

3.3.3. DEGs related to cell wall modification

GG treatment induced transcriptional regulation of the cell wall modification process in *S. latissima*. Fifty-three DEGs were found related to this category and a large fraction corresponded to forty-one putative mannuronan C-5-epimerase (ME) genes, which also featured diverse expression patterns within 12 h. The expression of eleven genes putatively encoding another enzyme involved in carbohydrate metabolism, an endo-1,3-beta-glucanase, were repressed at early stages (0.5 h and 1 h) and started increasing only after 4.5 h (Figure 6).

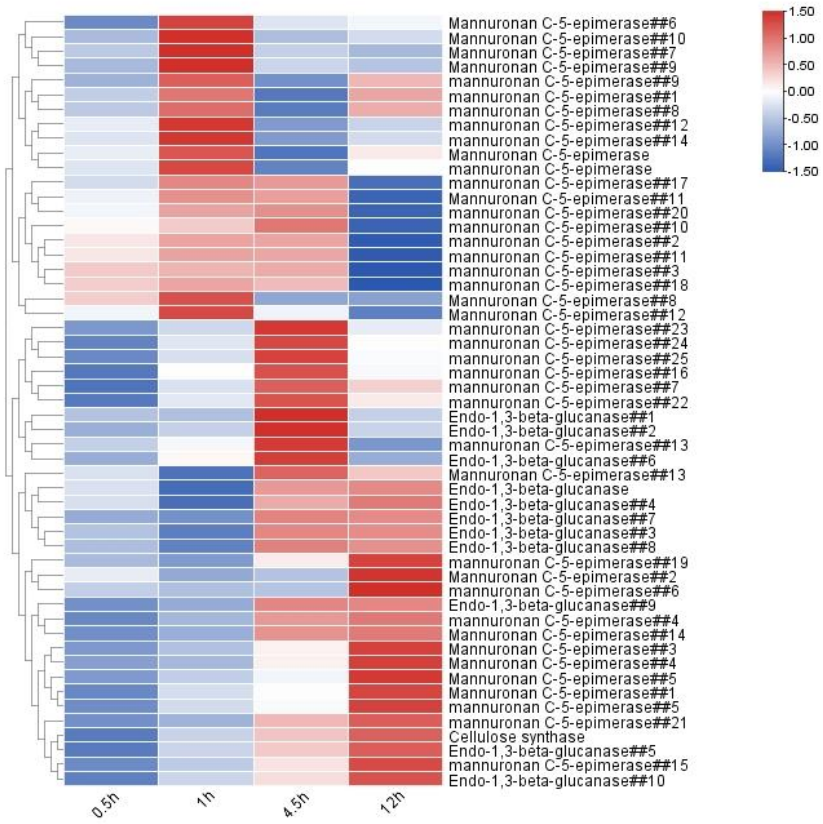

Fig. 6 Heatmap of 54 DEGs expression related to cell wall metabolism according to scaled Log2Foldchange values and time-course. Each line corresponds to one DEG.

3.3.4. DEGs related to oxidative responses

Many genes annotated as coding for proteins related to oxidative responses were regulated under GG treatment. For instance, forty-nine genes putatively encoding vanadium-dependent bromoperoxidase (vBPO), likely to be involved in antioxidant protection in brown algae appeared down-regulated at 0.5 h and up-regulated at 1 h, 4.5 h and 12 h (Figure 7). The up-regulation of other putative ROS detoxifying enzyme genes were also observed at 4.5 h, including a thioredoxin, a manganese superoxide dismutase, a ascorbate peroxidase and a glutathione reductase. Besides 4.5 h, the manganese superoxide dismutase gene was also up-regulated at other three time points. Finally, five genes annotated as genes encoding a putative respiratory burst oxidase homolog protein were up-regulated after 4.5 h.

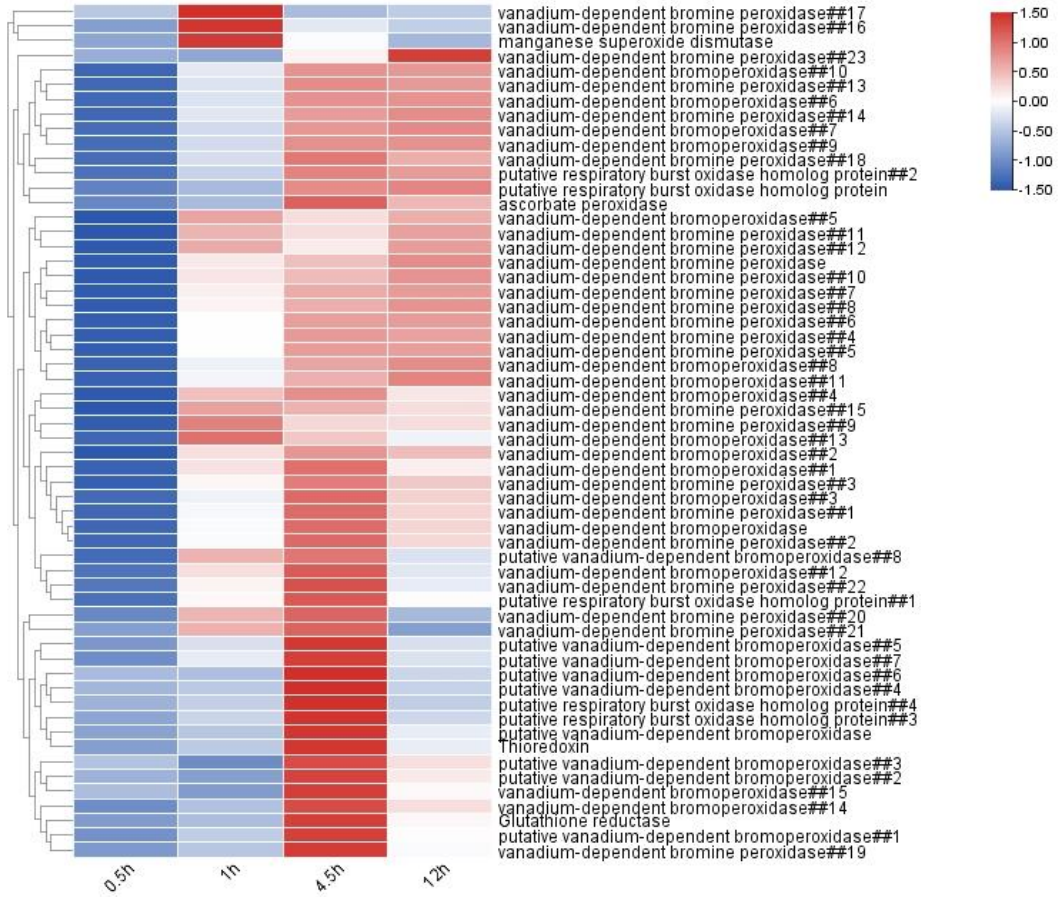

Fig. 7 Heatmap of 58 DEGs expression related to oxidative responses according to scaled Log2Foldchange values and time-course. Each line corresponds to one DEG.

3.3.5. DEGs annotated as putative Transcription regulators

Our study identified eight up-regulated and four down-regulated genes annotated as putative transcription regulators. Most of them were differentially expressed very early, at 0.5 h and 1 h (Figure 8). During the short-term GG treatment, gene up-regulation were observed in genes annotated as potentially coding for three heat shock transcription factors, a pathogenesis-related transcriptional factor, two zinc finger transcriptional factors and a histone-like transcription factor. A gene encoding NIN-like transcription factor were down-regulated at 1 h. Additionally, the down-regulation in longer term responses (4.5 h and 12 h) were found in another pathogenesis-related transcriptional factor, a heat shock transcription factor and a histone-like transcription factor.

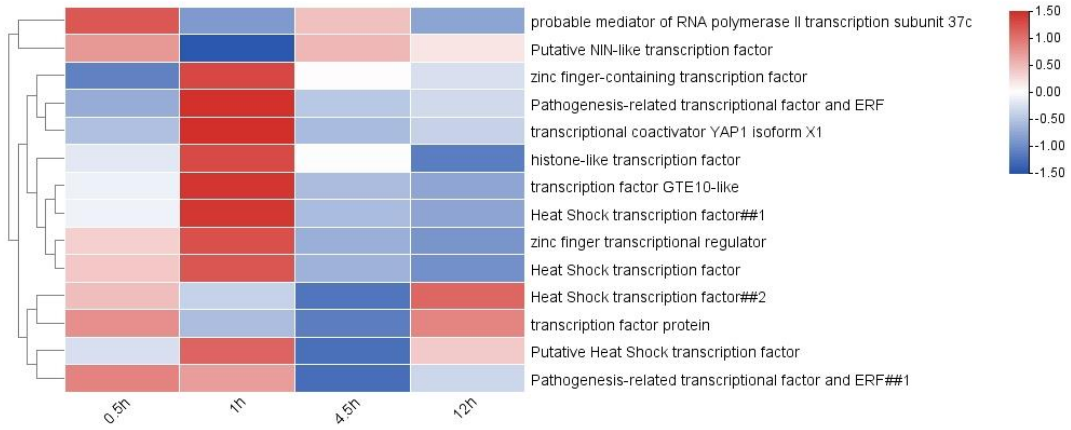

Fig. 8 Heatmap of 14 DEGs expression annotated as transcription regulators according to scaled Log2Foldchange values and time-course. Each line corresponds to one DEG.

3.4. Analysis of metabolic changes upon GG elicitation

3.4.1. Metabolic profiling by GC-MS

After GC-MS analysis of all algal extracts, obtained from the control and GG-elicited plantlets after 1 h, 4.5 h and 12 h, the spectra data were analyzed using MSDIAL pipeline. The full metabolic dataset contained 612 features, corresponding to identified peaks, that were used for statistical testing. Principal component analysis (PCA) of the dataset for *S. latissima* explained 22.85% of the observed variation and the differences between GG-treatment and control sample groups at 1 h were the most significant among the three time points (Figure 9). Then the orthogonal partial least squares discriminant analysis (OPLS-DA) identified 227 metabolites with significant differences (VIP > 1) between control and GG-treated samples at 1 h (R2X = 0.316, R2Y = 0.83, Q2 = 0.654). 126 and 106 metabolites featured significant differences (VIP > 1) were found after 4.5 h (R2X = 0.182, R2Y = 0.759, Q2 = 0.303) and 12 h (R2X = 0.156, R2Y = 0.651, Q2 = 0.112), respectively. However, none of these metabolites potentially involved in GG-induced metabolic responses showed a robust annotation through the NIST database search.

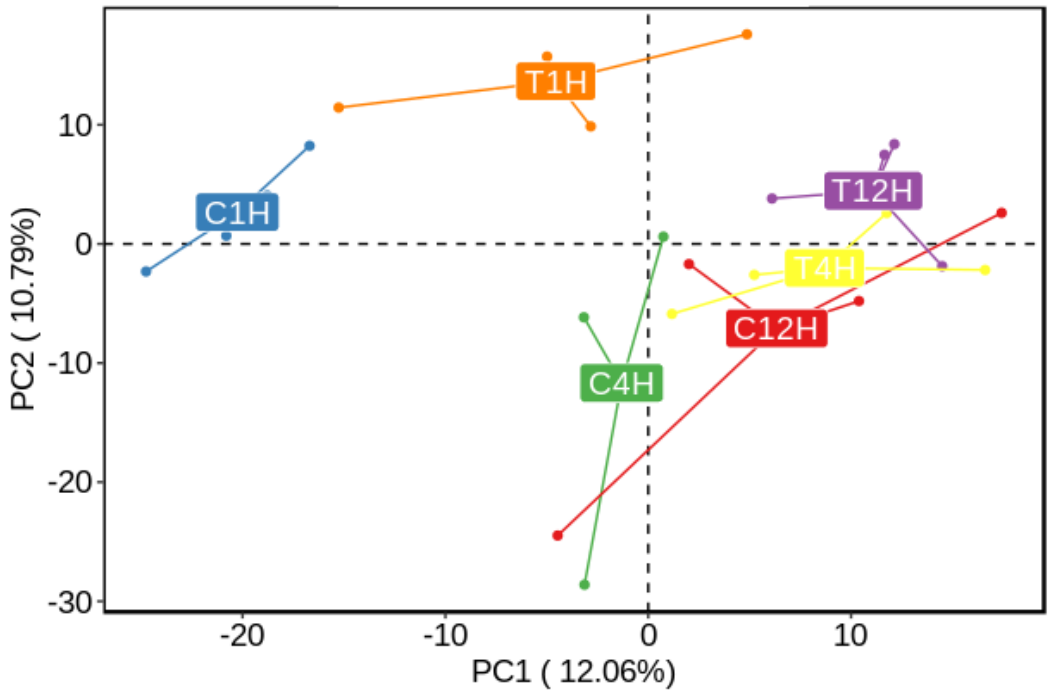

Fig. 9 PCA plot of GC-MS analysis at three time points. C1H: control at 1 h (colored in blue); T1H: GG treatment at 1 h (orange); C4H: control at 4.5 h (green); T4H: GG treatment at 4.5 h (yellow); C12H: control at 12 h (red); T12H: GG treatment at 12 h (purple) (N=4).

Additionally, 6 free fatty acids, myristic acid (C14), palmitic acid (C16), α-linolenic acid (C18:3), 5,8,11-Eicosatrienoic acid (C20:3), arachidonic acid (C20:4) and eicosapentaenoic acid (C20:5), were selected from *in silico* annotation using NIST database and searched into the full metabolic dataset to follow their metabolic changes upon GG-treatment (Figure 10). At 1 h, palmitic acid peak intensity was slightly decreased in GG-treated comparing to control samples. The intensities of α-linolenic acid and arachidonic acid peaks increased at 1 h and decreased at 12 h. However, none of these changes were significant.

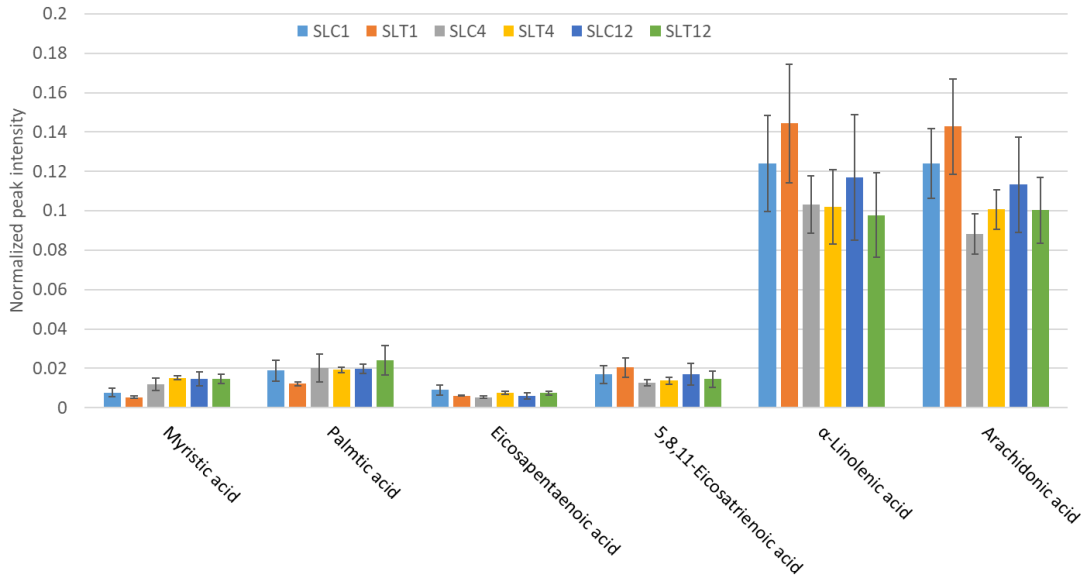

Fig. 10 Normalized peak intensity of 6 FFAs from GC-MS data at three time points. SLC1: control at 1 h; SLT1: GG treatment at 1 h; SLC4: control at 4.5 h; SLT4: GG treatment at 4 h; SLC12: control at 12 h; SLT12: GG treatment at 12 h (N=4).

3.4.2. Metabolite profiling by LC-MS

To obtain more information about global metabolic changes upon GG elicitation, and those related to the oxylipin pathway, high-resolution LC-MS analysis were performed on algal extracts, obtained from control and GG-elicited plantlets after 0.5 h, 1 h, 4.5 h and 12 h. In addition, two groups of algal samples were pretreated with potential LOX inhibitors, SHAM and n-PGal, before GG elicitation, to analyze metabolic changes related to LOX activity. The LC-MS data were analyzed for each time point, independently, using the Workflow4Metabolomics pipeline.

At 0.5 h, the metabolic dataset contained 2,213 features, corresponding to identified peaks, that were used for statistical testing. The PCA result explained 24.04% of the observed variation and showed the most significant difference between four groups among four time points (Figure 11A). The OPLS-DA identified 550, 947 and 888 metabolites with significant differences (VIP > 1) in GG-treated (R2X = 0.163, R2Y = 0.842, Q2 = 0.123), n-PGal-pretreated (R2X = 0.237, R2Y = 0.731, Q2 = 0.467) and SHAM-pretreated groups (R2X = 0.235, R2Y = 0.841, Q2 = 0.557), respectively, comparing to the control group. At 1 h, the metabolic dataset contained 1,757 features. The PCA result explained 25.19% of the observed variation (Figure 11B). The OPLS-

DA identified 412, 210 and 322 metabolites featuring significant differences (VIP > 1) in GG-treated (R2X = 0.157, R2Y = 0.754, Q2 = -0.0213), n-PGal-pretreated (R2X = 0.109, R2Y = 0.62, Q2 = -0.449) and SHAM-pretreated groups (R2X = 0.134, R2Y = 0.729, Q2 = -0.00387) comparing to the control group. At 4.5 h, the metabolic dataset contained 2,335 features. The PCA result explained 22.29% of the observed variation (Figure 11C). The OPLS-DA identified 404, 991 and 822 metabolites featured significant differences (VIP > 1) in GG-treated (R2X = 0.129, R2Y = 0.903, Q2 = 0.0838), n-PGal-pretreated (R2X = 0.229, R2Y = 0.766, Q2 = 0.501) and SHAM-pretreated groups (R2X = 0.215, R2Y = 0.82, Q2 = 0.457) comparing to the control group. At 12 h, the metabolic dataset contained 2,341 features. The PCA result explained 42.19% of the observed variation (Figure 11D). The OPLS-DA identified only 51, 163 and 123 metabolites with significant differences (VIP > 1) between GG-treated (R2X = 0.075, R2Y = 0.22, Q2 = -0.118), n-PGal-pretreated (R2X = 0.147, R2Y = 0.285, Q2 = -0.228) and SHAM-pretreated groups (R2X = 0.117, R2Y = 0.406, Q2 = -0.211) comparing to the control group.

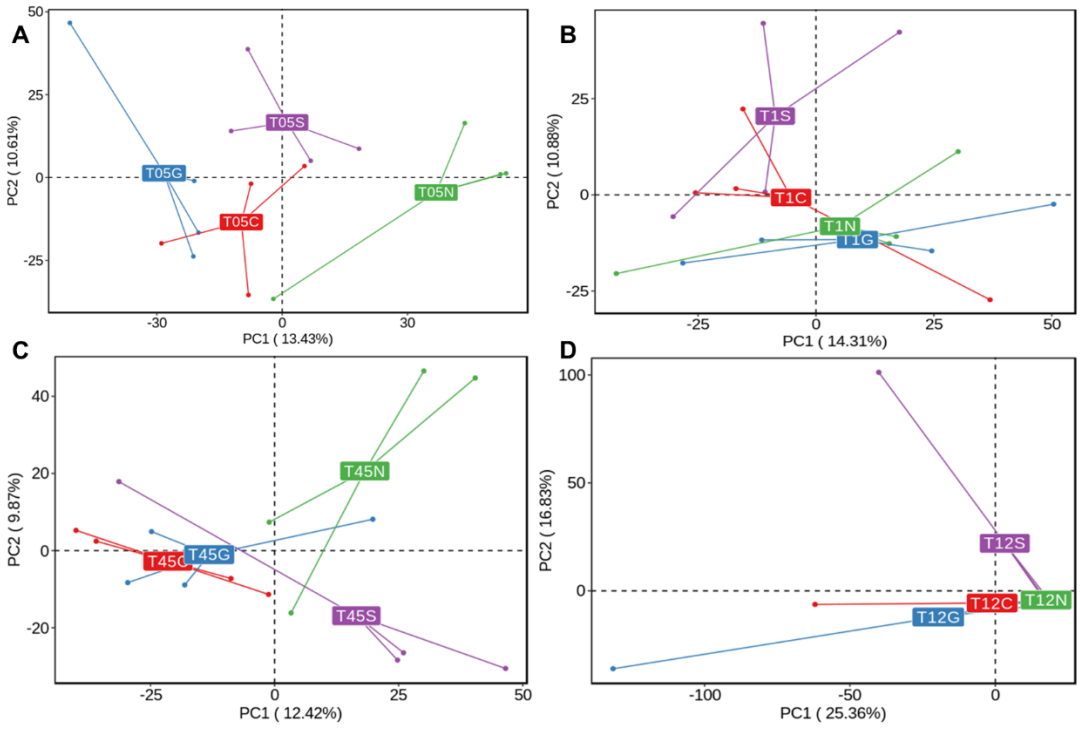

Fig. 11 PCA plot of LC-MS analysis at four time points. **A:** T05C: control (colored in red) at 0.5 h; T05G: GG treatment (blue) at 0.5 h; T05N: n-PGal treatment (green) at 0.5 h; T05S: SHAM treatment (purple) at 0.5 h; **B:** T1C: control (red) at 1 h; T1G: GG treatment (blue) at 1 h; T1N: n-PGal treatment (green) at 1 h; T1S: SHAM treatment (purple) at 1 h; **C:** T45C: control (red) at 4.5 h; T45G: GG treatment (blue) at 4.5 h; T45N: n-PGal treatment (green) at 4.5 h; T45S: SHAM treatment (purple) at 4.5 h; **D:** T12C: control (red) at 12 h; T12G: GG treatment (blue) at 12 h; T12N: n-PGal treatment (green) at 12 h; T12S: SHAM treatment (purple) at 12 h (N=4)

According to the *in silico* annotation of significant different ions in LC-MS profiling, the significant changes of putative free fatty acids (FFAs) and their oxidized derivatives were only detected at 0.5 h. Therefore we mainly focused on the analysis of metabolic profiling at 0.5 h. The intensity of a peak corresponding to FFA, stearic acid (C18), was significantly decreased at 0.5 h (t-test, adjusted p-value < 0.05) (Figure 12). Two putative downstream oxidized derivatives of C18 oxylipin pathway, 4-oxo-9Z,11Z,13E,15E-octadecatetraenoic acid and 12-oxophytodienoic acid (12-OPDA), were significantly accumulated at 0.5 h (t-test, adjusted p-value < 0.05). The down-regulation was also observed for a putative oxidized derivative of myristic acid (C14), the 7-oxo-11E-tetradecenoic acid.

In the GG-elicited sample group pretreated with SHAM, unlike in control GG-treatment, up-regulation of 12-OPDA and down-regulation of stearic acid were not shown at 0.5h (Figure 12). Similarly, three other putative oxylipins, 4-oxo-9Z,11Z,13E,15E-octadecatetraenoic acid, 12-oxo-14,18-dihydroxy-9Z,13E,15Z-octadecatrienoic acid and 7-oxo-11E-tetradecenoic acid showed the opposite trends to GG-treatment. Moreover, the 14-carbon FFA, myristic acid, was significantly decreased in the SHAM treated group (t-test, adjusted p-value < 0.05) comparing to control. In addition to C18 FFA-derived compounds, several metabolites involved in C20 oxylipin pathway were detected in the two inhibitors-treated groups. Among those compounds, one putative 20-carbon polyunsaturated fatty acid, 4,8,12,16-eicosatetraenoic acid, was significantly up-regulated (t-test, adjusted p-value < 0.05) in the group pretreated with SHAM comparing to GG-elicited control (Figure 12). Two C20 FFA-derived oxylipins amounts, prostaglandin E3 and J2, were significantly increased in the SHAM treated group comparing to GG-treatment group (Figure 12).

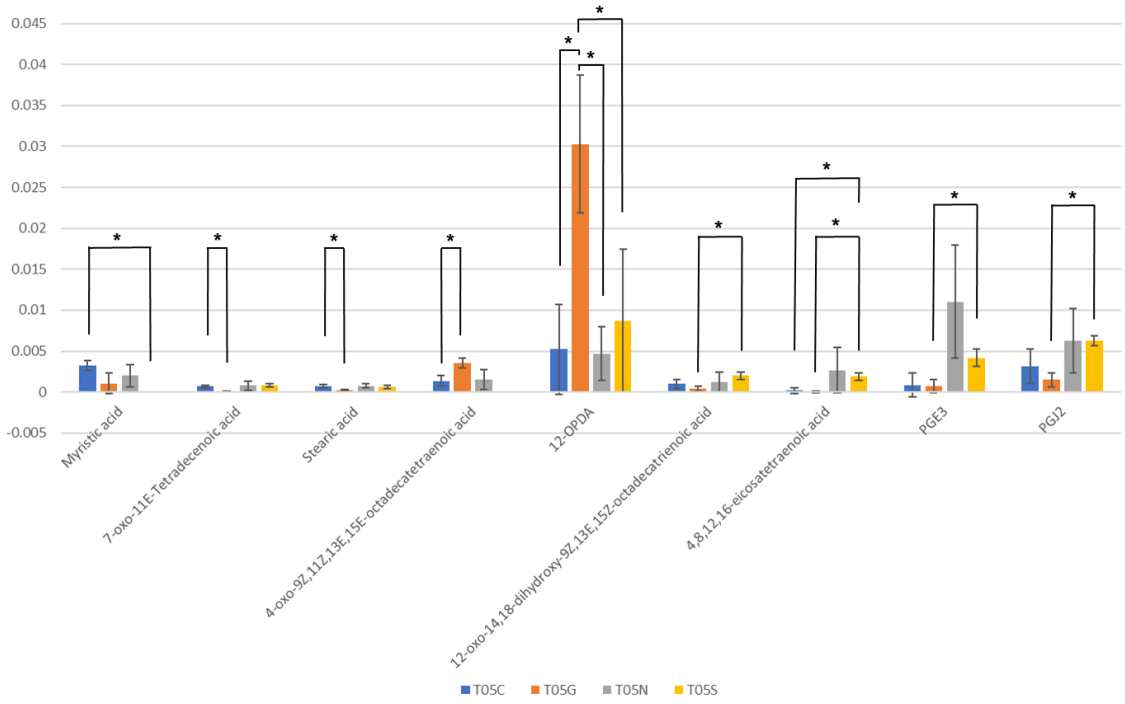

Fig. 12 Normalized peak intensity of 9 metabolites, identified through in silico annotation from LC-MS datasets at 0.5 h. T05C: control; T05G: GG treatment; T05N: n-PGal pre-treatment and GG elicitation; T05S: SHAM pre-treatment and GG elicitation; *: t-test adjusted p-value < 0.05.

4. Discussion

GG is known as a defense elicitor in kelps and induces physiological responses, such as oxidative burst, pathogen resistance and oxylipin production, as well as transcriptional regulation. In our study, we obtained the transcriptome-wide gene regulation at early stages after GG treatment in *S. latissima* by performing a time-course RNA sequencing. In plants, the defense elicitors are known to activate the defense-related genes through specific signaling pathways (Vidhyasekaran, 2016). Following GG elicitation in *S. latissima*, we observed that three genes involved in calcium signaling pathways were up-regulated at 1 h. In land plants, previous studies have demonstrated that Ca^{2+} acts as an important second messenger during the defense responses and that some Ca^{2+} binding protein, such as calmodulin and Ca^{2+}-dependent protein kinase, interpret the signal into appropriate molecular and biochemical responses (Zhang et al., 2014). Two genes encoding kinase domain containing protein were also up-regulated at 1 h, indicating a potential signaling function during GG treatment. Transcription factors (TFs) are also important regulators in the transcriptomic responses. In land plants, there are six major families of TFs involved in defense responses: basic leucine zipper containing domain proteins (bZIP), TFs containing amino-acid sequence WRKYGQK (WRKY), myelocytomatosis related proteins (MYC), myeloblastosis

related proteins (MYB), APETALA2/ETHYLENE-RESPONSIVE ELEMENT BINDING FACTORS (AP2/EREBP) and the NAC family grouping together those three factors: no apical meristem (NAM), Arabidopsis transcription activation factor (ATAF), and cup-shaped cotyledon (CUC) (Alves et al., 2014, Ng et al., 2018). Among those families, only one, the NAC are late innovations that are not conserved at the level of the whole Archaeplastida lineage (de Mendoza & Sebé-Pedrós, 2019, Wilhelmsson et al., 2017) , and are not expected to be present in brown algae or other stramenopiles. Among stramenopiles, there are only a few TFs for which functional data are available: a TALE-domain TF is known to regulate life cycle transitions in brown algae (Arun et al., 2019), whereas in diatoms, there are functional data for two bZIP TFs (Matthijs et al., 2017, Mann et al., 2020) and one bHLH-PAS (Annunziata et al., 2019). Here our data point toward the differential expression of other TF families. We observed that GG-treated *S. latissima* up-regulated a gene encoding pathogenesis-related transcriptional factor at 1 h, which belongs to AP2 family according to the conserved domain search. This up-regulation might be related to the transcriptomic activation of downstream defense-related responses. At the same time, the up-regulation was also detected in genes encoding several putative heat shock transcription factors (HSFs), which belongs to a huge gene family, conserved in most eukaryotes, and that are involved in coping with various environmental stresses (Nishizawa et al., 2006). Previous studies showed that HSFs were also involved in the immune response of land plants and animals (Singh & Aballay, 2006, Wei et al., 2018). This up-regulation of several genes putatively involved in calcium signaling pathway and transcription factors indicates that GG elicitation might induce the regulation of defense responses at early stage in *S. latissima*.

Oxylipin pathways seems to have important roles in the signaling process during GG-triggered defense responses. In our study, many genes putatively involved in lipid metabolism were identified as DEGs and most of them were annotated as lipase. The up-regulation of these lipase genes was dependent on induction time (1 h, 4.5 h and 12 h), and the diverse expression patterns of them might indicate their functional differences. Previous studies demonstrated that lipases catalyzed membrane lipid into FFAs, which could be used as substrate for oxylipin biosynthesis (Wasternack & Feussner, 2018). However, in GG-elicited *S. latissima*, significant accumulation of FFAs has not been observed through metabolomic analysis, following the up-regulation of lipase genes. This result might be due to the rapid conversion of FFAs into oxylipins by downstream enzymes, such as LOX, following the oxidative burst (Cosse et al., 2007).

Interestingly, putative LOXs encoding genes were detected up-regulated after 4.5 h. Another gene family involved in oxylipin pathway, CYPs, was shown to be highly diverse according to their enzymatic function, such as allene oxide synthase, hydroperoxide lyase/isomerase, epoxyalcohol synthase and divinyl ether synthase (Wasternack & Feussner, 2018). In our study, the differentially expressed CYP genes, like lipase-annotated genes, were also up-regulated depending on the induction time. Interestingly, one of the putative CYP genes was up-regulated twice at 1 h and 12 h, suggesting that there might be two successive inductions of oxylipin pathways within 12 h after the GG elicitation. The long-term monitoring of H_2O_2 in the surrounding of *S. lattissima* didn't detect any second oxidative burst, after the first one recorded within 30 minutes, just after the application of GG (data not shown), suggesting the second induction of oxylipin pathways was different from the first one. In agreement with these results, LC-MS analysis showed that GG treatment induced significant and rapid changes of metabolites in C18 oxylipin pathways. A significant decrease was observed for C18 FFA, stearic acid after 30 minutes, and, in parallel, the contents of two oxidized derivatives in C18 oxylipin pathways, 12-OPDA and 4-oxo-9Z,11Z,13E,15E-octadecatetraenoic acid, showed an upward trend, suggesting an early activation of C18 oxylipin pathway and a transformation from FFA to oxylipins through enzymatic cascades (Figure 13). 12-OPDA is considered as an important signal molecule and participates in many biological processes, such as seed germination, drought tolerance and defense response (Dave et al., 2011, Savchenko et al., 2014, Wasternack & Feussner, 2018). The accumulation of 12-OPDA was also observed during copper stress in *Laminaria digitata* (Ritter et al., 2008). In land plants, previous study has shown that 12-OPDA induced the up-regulation of TF genes, such as zinc finger transcription factors, and genes involved in calcium signaling pathway (Taki et al., 2005). Therefore, upon GG elicitation, the accumulation of 12-OPDA after 0.5 h might lead to the transcriptomic up-regulation of TF genes and calcium signaling pathway we observed after 1 h, suggesting 12-OPDA might act a key role in the regulation of gene expression in response to biotic interactions. To better understand the oxylipin pathway regulation in *S. latissima* in this context, we used two LOX inhibitors, SHAM and n-PGal, to pretreat algal samples before GG elicitation. In SHAM and n-PGal treatment groups, there was no significant accumulation of 12-OPDA and 4-oxo-9Z,11Z,13E,15E-octadecatetraenoic acid, suggesting that the C18 oxylipin biosynthesis pathway was blocked. Interestingly, the content of another C18 FFA derived oxylipin, the 12-oxo-14,18-dihydroxy-9Z,13E,15Z-octadecatrienoic acid, was increased comparing to GG-treated group, accumulating in SHAM pretreated condition at 0.5 h. Moreover, the increase of several metabolites involved in C20 oxylipin pathway, such as

4,8,12,16-eicosatetraenoic acid, prostaglandin E3 and J2, was also observed in SHAM pretreated group comparing to GG treatment, suggesting the activation of C20 oxylipin pathway when LOX activity was inhibited. Similar to 12-OPDA, prostaglandins are cyclopentenone-type compounds and participate in the immune response in animals (Funk, 2001). Accumulation of many prostaglandins were also induced by copper stress in *L. digitata* (Ritter et al., 2008). Previous studies showed that prostaglandin A2 can induce the oxidative burst and the increase of one oxylipin, the 15-hydroxyeicosatetraenoic acid in *L. digitata* (Zambounis et al., 2012b), suggesting the possibility for prostaglandins acting as defense inducer. In our study, the accumulation of these prostaglandins only appears when LOXs were inhibited, leading to the hypothesis that C20 oxylipin pathway could be a sort of backup of C18 FFA-derived pathway in response to GG elicitation. In that case, there might be some other enzymes instead of LOX to catalyze the first step of oxylipin biosynthesis in *S. latissima*.

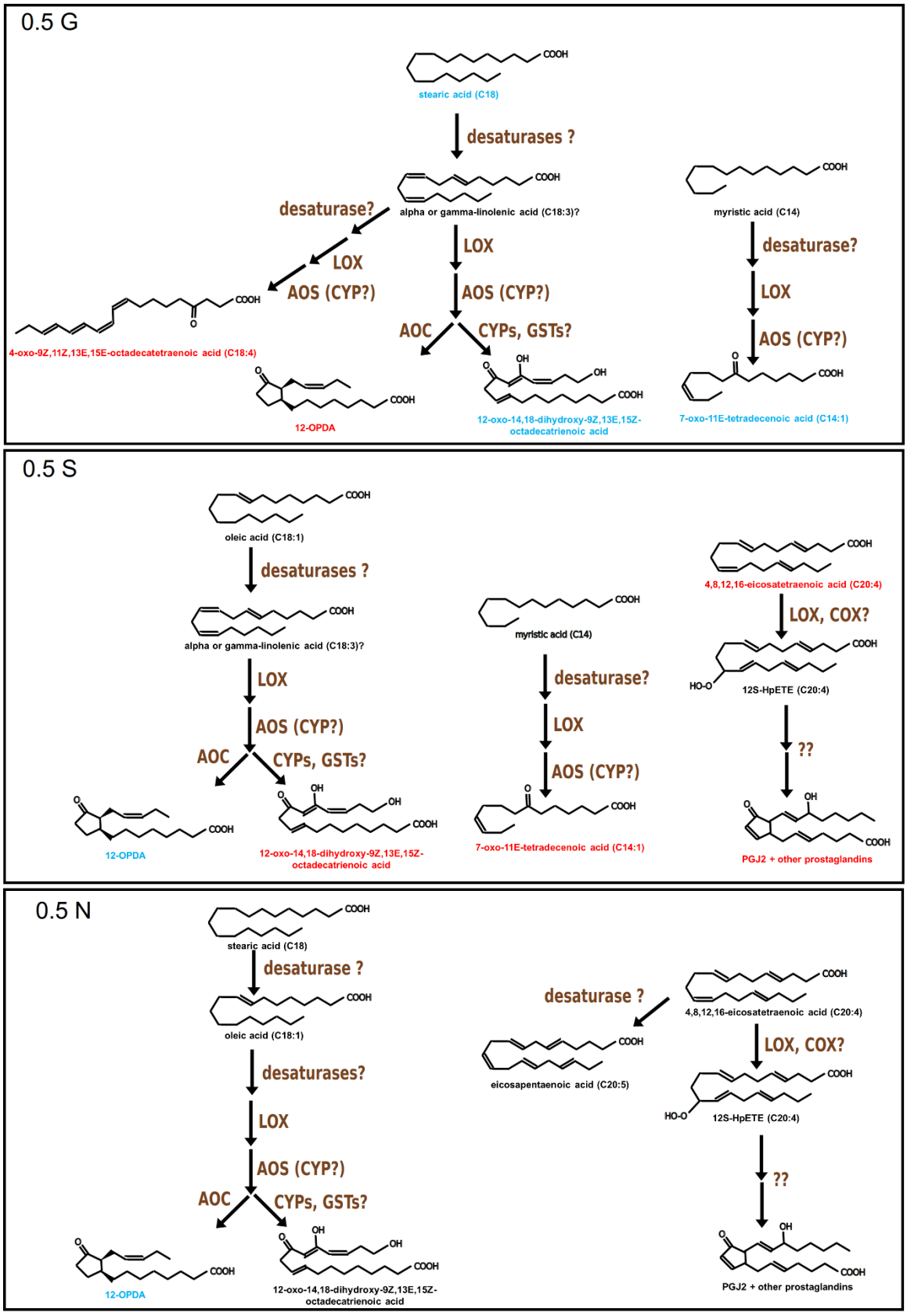

Fig. 13 Partially reconstructed oxylipin pathways in *S. latissima* based on the LC-MS data of three treatments at 0.5 hour. 0.5G: GG treatment compared to control samples; 0.5S: SHAM pre-treatment group compared to GG treatment; 0.5N: n-PGal pretreatment group compared to GG treatment. The significantly accumulated compounds were colored

in red and significantly decreased compounds were colored in blue. 12-OPDA: 12-Oxo-phytodienoic acid; PGJ2 prostaglandin J2; 12S-HpETE: (5Z,8Z,10E,12S,14Z)-12-hydroperoxyicosa-5,8,10,14-tetraenoic acid LOX: lipoxygenase; AOC: allene oxide cyclase; AOS: allene oxide synthase; CYP: cytochrome P450; GST: Glutathione S-transferase; COX: Cyclooxygenase.

After the signal transduction, the downstream defense-related genes were activated. In our study, several genes that could be involved in defense response were up-regulated after 4.5 h. Among those genes, one gene was annotated as pathogenesis-related protein, which regulated the defense responses and enhance the resistance of plants to pathogens (Alexander et al., 1993, Lakhssassi et al., 2020, Peng et al., 2017). At the same time, two genes putatively encoding HSP 90 were also up-regulated. HSP 90s always participate in defense response in land plants. For instance, HSP 90 regulated the defense response in *Arabidopsis* by interacting directly with the immune receptor, rpp4 (Bao et al., 2014). Similarly, in rice, HSP 90 facilitates the maturation of the pattern recognition receptor of pathogen-associated molecular patterns (Chen et al., 2010). In this scenario, the up-regulation of HSP 90 genes at 4.5 h might contribute to the perception of pathogens. Another gene encoding receptor, LRR-containing GTPases of the ROCO family, was also up-regulated at 4.5 h. The ROCO family is thought to be involved in pathogen perception of *Ectocarpus* immune responses (Zambounis et al., 2012a). Besides the perception of pathogens, production of reactive oxygen species (ROS) is also a defense strategy in many macroalgae and ROS may have direct cytotoxic effects on pathogen (Cosse et al., 2007). In our study, four genes encoding a putative respiratory burst oxidase homolog protein were up-regulated after 4.5 h. At the same time, many genes involved in ROS detoxification were up-regulated, such as thioredoxin, manganese superoxide dismutase, ascorbate peroxidase, glutathione reductase, vBPOs and glutathione S-transferases (GST). Additionally, forty-one putative mannuronan C-5-epimerase (ME) genes were induced by GG elicitation, which contribute to the cell wall strengthening by epimerizing D-mannuronate residues into L-guluronate during alginate biosynthesis. Moreover, eleven genes putatively encoding endo-1,3-beta-glucanase and one cellulose synthase were up-regulated at 4.5 h and 12 h. Consequently, we hypothesized that the synergetic up-regulation of MC5E, endo-1,3-beta-glucanase and cellulose genes might facilitate the strengthening of cell walls after GG perception.

5. Conclusion

The results presented in this study demonstrate that GG treatment induced massive gene regulation in brown algae *S. latissima*, including signaling pathway, transcription regulators, oxidative stress response and defense response. The expression pattern of genes involved in oxylipin pathways suggested that more than one induction of oxylipin pathway during the GG elicitation in *S. latissima*. The metabolite profiling of free fatty acid and oxylipins further proved that the first induction of oxylipin pathway happened at very early stage. These results provided insights into the defense-related responses induced by GG treatment in *S. latissima*.

Chapter IV

Studies of potential signaling and biological roles of oxylipins and aldehydes in two kelp model species.

Chapter IV. Studies of potential signaling and biological roles of oxylipins and aldehydes in two kelp model species.

1. Introduction

Volatile organic compounds (VOCs) produced by land plants are considered as an important group of signal or defense molecules. Their ecological roles have been widely investigated in plant-herbivore interactions. The common VOCs in land plant are so-called "Green Leaf Volatiles" (GLVs), including (E)-2-hexenal, (Z)-3-hexenal, n-hexanal and their corresponding alcohols or esters, which are derived from the 13-hydroperoxides of linoleic or linolenic acid after processing by fatty acid hydroperoxide lyases (HPL). GLVs produced by damaged plant tissues by grazers can activate the defense responses in intact plants (Matsui, 2006). It has been reported that (E)-2-hexenal, (Z)-3-hexenol or (Z)-3-hexenyl acetate induced the expression of several defense-related genes like pathogenesis-related proteins (PRs) and phenylalanine ammonia lyase (PAL) genes. In *Arabidopsis thaliana*, treatment with (E)-2-hexenal triggered the oxylipin pathway by inducing the expression of allene oxide synthase (AOS) and lipoxygenase 2 (LOX2) (Kishimoto et al., 2005). Similarly, the activation of oxylipin pathways were also observed in *Citrus jambhiri* in response to (E)-2-hexenal (Gomi et al., 2003).

Besides GLVs, several oxylipins have been proven to induce the defense responses in plants. For instance, methyl jasmonate, the volatile analog of jasmonic acid, has been tested on wide range of land plants and it can induce defense response cascade as an elicitor (Belhadj et al., 2006, Franceschi et al., 2002, Wu et al., 2008). In the jasmonic acid biosynthesis pathway, the intermediate, 12-Oxo-phytodienoic acid (12-OPDA), has been identified as an important signal in the symbiont-induced systemic resistance (Carella, 2020). It regulates diverse biological processes, leading to the resistance to herbivores. For example, the exogenous application of OPDA enhanced the resistance to corn leaf aphids in maize (Varsani et al., 2019). Similarly, the arachidonic acid-derived oxylipins, prostaglandins (PGs), have been identified as immuno-active lipids, which regulate the immune response in invertebrates and vertebrates (Harris et al., 2002) , and volatile aldehydes, such as 4-hydroxynonenal, are important mediators in cellular pathways related to oxidative stress (Zhang & Forman, 2017).

Like land plants and animals, brown macroalgae have developed a sophisticated innate immunity. The first phase of innate immunity is the perception of biotic attacks, which could trigger an oxidative burst, specific gene regulation (Küpper et al., 2001, Cosse et al., 2009, Ritter et al., 2017a), and the release of various fatty acid-derived volatile compounds. In *Laminaria digitata*, the application of oligoguluronate (GG), the component of brown algal cell wall, also induced the release of various aldehydes, such as (E)-4-hydroxyhex-2-enal (4-HHE), (E)-4-hydroxynon-2-enal (4-HNE) and (E,E)-dodeca-2,4-dienal (Goulitquer et al., 2009). These aldehydes were also detected in the seawater of tide pool during low-tide, where *L. digitata* was exposed to multiple abiotic stresses, such as UV, salinity and temperature (Goulitquer et al., 2009). In a later study, Thomas et al. reported that waterborne signal molecules released from *L. digitata* after oligoguluronates (GG) treatment were able to induce some defense-related genes in other sporophytes maintained in the same seawater. These results suggested that these waterborne cues might participate in the distance signaling and shape the response in the neighboring conspecifics (Thomas et al., 2011). The 4-HHE treatment of *L. digitata* was later shown to reduce its consumption by *P. pellucida*, suggesting the potential function of 4-HHE as defense signal molecule (Cabioch, 2016). In addition to aldehydes, several oxylipins, including prostaglandins and 12-OPDA, were induced by copper stress in *L. digitata* (Ritter et al., 2008). These findings suggest that kelps developed a complex signaling system in response to biotic and abiotic stresses, which might include signaling pathways with similarities with those of both animals and land plants. However, the biological function of these oxylipin-derived compounds is still unclear in brown algae.

In this chapter, we compared the global transcriptomic regulation of 4HHE and GG treatments in *L. digitata*. 4HHE was also applied in *S. latissima* to analyze metabolomic changes using untargeted GC-MS metabolite profiling. Additionally, several genes involved in the oxylipin pathways were used as marker genes to screen aldehydes and oxylipins that could serve as signal molecules in *S. latissima*. These results provide insights into the function of oxylipin pathway-derived compounds in kelp algal species.

2. Material and method

2.1. Biological material

Fertile sporophytes of *S. latissima* and *L. digitata* were collected at Perharidy (near Roscoff, 48.73° N, 4.00° W) and the spores releasing and zygote production were performed using the same method described in chapter 3. The juvenile sporophytes of *S. latissima* and *L. digitata* were kept in 2 L bottles connected to an aeration system with weekly changes of culture medium. The kelp cultures were maintained in 14°C and 20µmol photons $s^{-1}m^{-2}$ with a 12 h light/dark cycle.

2.2. Transcriptomic analysis of 4-HHE and GG treatments in *L. digitata*

Sporophytes of *L. digitata* cultivated in laboratory were placed in small glass beakers, filled with 30 mL autoclaved seawater. For GG treatment, oligoguluronates solution (GG, prepared from *L. hyperborea*) were added into seawater at a final concentration of 150µg/mL. The glass beakers were placed on a shaker incubated at 100rpm for 1 h in the cultivation condition. For 4-HHE treatment, the 4-HHE solution were added into seawater at a final concentration of 100ng/mL. The glass beakers were placed on a shaker incubated at 100rpm for 4 h in the cultivation condition. Then the sporophytes were rinsed several times with autoclaved seawater and transferred into clean glass bakers with 30 mL autoclave seawater. The three groups (GG, 4-HHE and control) were collected at 12 h. These samples were frozen in liquid nitrogen and stored at -80°C.

RNA of these samples was extracted with the method described in chapter I. After the extraction, the RNA sequencing and data analysis were performed with the methods described in chapter III.

2.3. GC-MS analysis of 4-HHE treatment in *S. latissima*

Sporophytes of *S. latissima* cultivated in laboratory were placed in small glass beakers, filled with 30 mL autoclaved seawater. The 4-HHE solution were added into seawater at a final concentration of 100ng/mL. The glass beakers were placed on a shaker incubated at 100rpm for 4 h in the cultivation condition. Then the sporophytes were rinsed several times with autoclaved seawater and transferred into clean glass bakers with 30 mL autoclave seawater. The two groups (4-HHE and control) were collected at 4 h, 12 h and 24 h. These samples were frozen in liquid nitrogen

and stored at -80°C. The metabolites extraction, GC-MS and data analysis were performed as described in chapter III.

2.4. Phylogenetic analysis of LOX and CYP genes

Two groups of key genes in oxylipin pathways, LOXs and CYPs, were firstly chosen as candidates. The HMMER3 software (Eddy, 2010) with default parameters was used to search CYP and LOX domains in the genome-translated proteomes of three brown alga species (*Ectocarpus siliculosus*, *Cladosiphon okamuranus* and *S. japonica*). These sequences with DEG sequences of LOX or CYP genes form chapter III were aligned using CLUSTAL Omega (Sievers & Higgins, 2014). The alignment files were used as input for MEGA 7.0 (Kumar et al., 2016) to build the Maximum-likelihood (ML) phylogenetic trees. The phylogenetic tree of CYP genes was built with Whelan-Goldman(WAG) + Gamma distributed with Invariant sites (G+I) + Freqs. (F) model. And the phylogenetic tree of LOX genes was built with WAG + G model. bootstrap with 1000 replicates was performed to obtain the confidence support level.

2.5. Targeted gene expression analysis using RT-qPCR

Sporophytes of *S. latissima* cultivated in laboratory were placed in small glass beakers, filled with 30 mL autoclaved seawater. For oxylipin and aldehyde treatment, the solution of three oxylipins (12-OPDA, 13-HpOTre and 15-HEPE) and three aldehydes (4-HHE, 4-HNE and Dodecadienal) were added into seawater at a final concentration of 100ng/mL. The glass beakers were placed on a shaker incubated at 100rpm for 4 h in the cultivation condition. Then the sporophytes were collected, frozen in liquid nitrogen and stored at -80°C. RNA extraction and RT-qPCR were performed using two reference genes, ATP and EIF5B, as described in chapter I. The primer sequences of LOX and CYP genes were listed in Table 1. The statistical analysis was performed using one-way ANOVA followed by LSD post-hoc test.

Table.1 Primer sequences of Lipoxygenase and cytochrome P450 genes used in RT-qPCR.

ID	Annotation	Primer sequences:
TRINITY_DN7381_c0_g1_i1	Lipoxygenase	**Forward:** GGACAGACTTCAGGCGAACA

	[Ectocarpus siliculosus]	**Reverse:** AGTTCCTCCTTGGTAACGCC
TRINITY_DN2016_c0_g1_i1	Lipoxygenase [Ectocarpus siliculosus]	**Forward:** TCGTGGCGTCCTTCTTGTC **Reverse:** TGCTCGGGTCTGTCTACCA
TRINITY_DN2920_c0_g3_i2	epoxyalcohol synthase CYP5164B1 [Ectocarpus siliculosus]	**Forward:** GTGAGTCGAGAATGCCGATG **Reverse:** CTTGGCCAGATGGACGAGC
TRINITY_DN2920_c1_g3_i3	epoxyalcohol synthase CYP5164B1 [Ectocarpus siliculosus]	**Forward:** ATGGACCTCCTCGTCCCTAC **Reverse:** GGGAAACCGTAAGCGAAGAC

2.6. H_2O_2 measurement

Sporophytes of *S. latissima* cultivated in laboratory were placed in small glass beakers, filled with 30 mL autoclaved seawater. The solution of three oxylipins (12-OPDA, 13-HpOTre and 15-HEPE) were added into seawater at a final concentration of 100ng/mL. And three concentration (10ng/mL, 100ng/mL and 1μg/mL) were tested in treatments with aldehydes (4-HHE, 4-HNE, Hexanal and Dodecadienal). H_2O_2 emission was measured before and during 1 h incubation in control and all treatments using method described in chapter II.

3. Result and discussion

3.1. Comparative transcriptome analysis of *L. digitata* treated with 4-HHE and GG

In previous study, the 4-HHE treatment significantly reduced the algal consumption by gastropod grazers belonging to the *P. pellucida* species and induced the production of several free fatty acid-derived compounds in *L. digitata*, suggesting the 4-HHE might induce defense responses by activating the oxylipin pathway (Cabioch, 2016). To investigate biosynthesis pathways induced by 4-HHE and compare them to those induced during defense elicitation, a transcriptome analysis was performed on young *L. digitata* sporophytes treated by 4-HHE or GG comparing to control group after 12 hours in laboratory controlled conditions.

The clean reads for all treatments were assembled by Trinity into 34,032 transcripts with an average contig length of 1,226 bp. The average GC content of this *de novo* transcriptome from *L. digitata* was 54.8%. The results of the BUSCO analysis revealed a near-complete gene sequence information for the transcriptome with 78.5% complete BUSCO matches.

After 12 h of 4-HHE treatment, a small fraction of genes (1.05%, including 163 up-regulated and 197 down-regulated DEGs) showed significant expression differences comparing to control group. For GG treatment, 787 genes were up-regulated and 629 genes were down-regulated after 12 h, when compared to control samples. The comparison of differentially expressed genes showed that 115 up-regulated genes (Figure 1A) and 24 down-regulated genes (Figure 1B) were shared between 4-HHE and GG treatment.

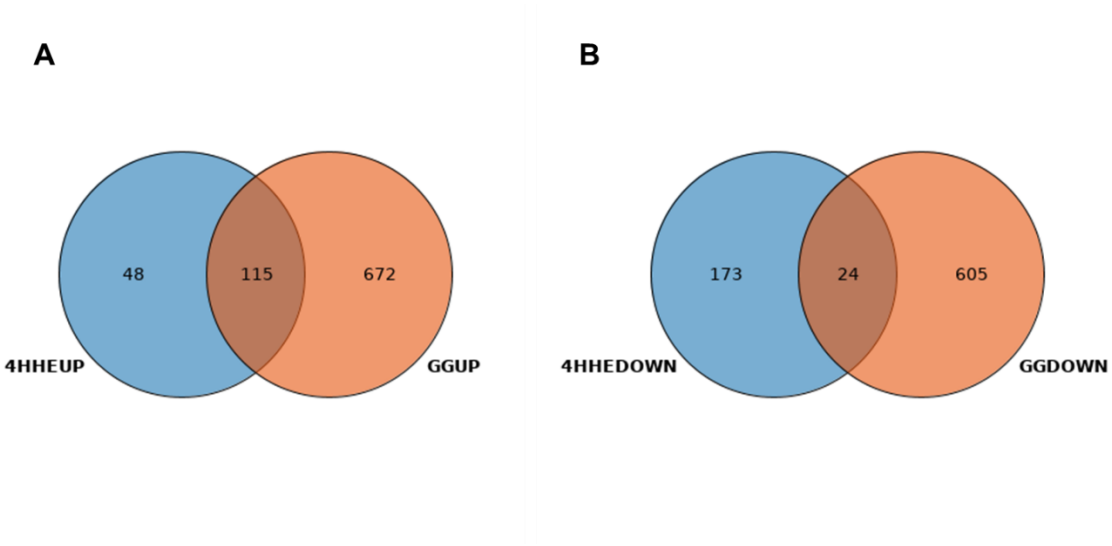

Fig. 1 Venn diagram of **A.** up-regulated genes of 4-HHE and GG treatment and **B.** down-regulated genes after 12h of 4-HHE and GG treatment comparing to control samples

Then the gene expression was analyzed on the DEGs whose functional annotations belong to five categories: calcium signaling pathway, transcription regulator, oxylipin pathway, defense response and oxidative response.

Five genes encoding calcium dependent kinases were up-regulated in response to GG elicitation after 12 h in *L. digitata* (Table 1). Calcium dependent kinases (CDKs) are important Ca^{2+} censor proteins in the calcium signaling pathways which play key roles during various abiotic and biotic stress in most eukaryotic organisms (Batistič & Kudla, 2012). The up-regulation of these five putative CDK genes indicated a massive signal transduction following GG treatment. Among those putative CDK genes, only one gene (TRINITY_DN2829_c1_g1_i1) was also induced by 4-

HHE treatment at 12 h, suggesting that 4-HHE might induce more specific molecular responses compared to GG elicitation.

Five genes encoding putative transcription regulators were up-regulated in response to GG treatment. Two of them were annotated as MYB transcription factors, which belong to a large family and are involved in gene regulations in response to biotic and abiotic stresses (Ambawat et al., 2013). In *Arabidopsis*, a MYB transcription factor, MYB15, was shown to control the lignification of cell wall appositions, which is a basal defense response (Chezem et al., 2017). The wheat R2R3-MYB transcription factor TaRIM1 increased the resistance of host against pathogen by enhancing the expression of five defense-related genes (Shan et al., 2016). Two other genes were annotated as heat shock transcription factors, which might also participate in the regulation of defense response. None of these four transcription factor genes was found to be differentially expressed in 4-HHE treatment. Only one gene encoding putative a RNA polymerase sigma factor SigD was up-regulated in both 4-HHE and GG treatments (Table 2).

Table. 2 Log2Foldchange value of genes involved in calcium signaling pathways and transcription regulators, significantly up-regulated genes are highlight with red color

ID	Annotation	4HHE	GG
TRINITY_DN351_c0_g2_i1	Calcium-dependent protein kinase 2	-0.51	1.80
TRINITY_DN9292_c0_g1_i1	calcium-dependent protein kinase	0.93	1.25
TRINITY_DN336_c2_g1_i1	calcium-dependent protein kinase	0.74	1.43
TRINITY_DN8143_c0_g1_i5	calcium-dependent protein kinase	0.84	1.47
TRINITY_DN2829_c1_g1_i1	calcium/calmodulin-dependent protein kinase	1.71	1.86
TRINITY_DN485_c7_g1_i1	myb-like DNA-binding protein	0.83	1.50
TRINITY_DN659_c4_g2_i1	Heat Shock transcription factor	0.92	1.65
TRINITY_DN10087_c0_g1_i2	Transcriptional activator Myb	0.52	1.15
TRINITY_DN4325_c4_g1_i1	Putative Heat Shock transcription factor	0.46	1.35
TRINITY_DN657_c0_g1_i2	RNA polymerase sigma factor SigD	1.15	1.37

Several genes putatively involved in oxylipin pathway were differentially expressed in *L. digitata* under both treatments. In GG treatment, two putative phospholipase genes and one lipoxygenase gene were up-regulated after 12 h, suggesting a late activation of oxylipin pathway in *L. digitata*.

Furthermore, 4-HHE treatment repressed the expression of two cytochrome P450 genes, suggesting 4-HHE might negatively regulated the oxylipin pathway in *L. digitata* after 12 h (Table 3).

GG and 4-HHE treatments also induced some defense-related genes (Table 2). For instance, a gene encoding LanC lantibiotic synthetase component C-like 2 (LanCL) was up-regulated in both treatment groups. LanCL proteins are homologous to bacterial LanC and involved in the biosynthesis of antimicrobial peptides (Willey & van der Donk, 2007). In tomatoes, the up-regulation of one LanCL gene were detected during wounding and after methyl-JA treatment, suggesting LanCL may play a role in the jasmonate-mediated plant protection against biotic stress (Liu, 2004). A pathogen-related gene was only induced by GG treatment and a homologous gene was also shown to be upregulated upon GG elicitation in *S. latissima*. Furthermore, 4-HHE also induced a specific defense-related gene, a putative metacaspase gene, which encodes a cysteine-dependent protease. A recent study showed that the damage on plants triggered the release of immunomodulatory signal peptide produced by metacaspase (Hander et al., 2019).

Seven genes related to oxidative responses were significantly up-regulated in both treatments. Among those genes, two glutathione S-transferase genes and one catalase gene were up-regulated in 4-HHE and GG treatment at 12 h. Two putative vanadium-dependent bromoperoxidase genes and one L-ascorbate peroxidase gene were only induced following GG treatment. Another putative L-ascorbate peroxidase encoding gene was specifically up-regulated in response to 4-HHE treatment.

Table. 3 Log2Foldchange value of genes involved in oxylipin pathways, defense response and oxidative response, significantly up-regulated genes and down-regulated genes are highlighted with red color and blue color, respectively

ID	Annotation	4HHE	GG
TRINITY_DN19539_c0_g1_i1	calcium-independent phospholipase a2-gamma	0.85	1.87
TRINITY_DN9021_c0_g1_i1	Putative phospholipase	0.58	1.28
TRINITY_DN5135_c0_g1_i4	Lipoxygenase	0.34	1.10
TRINITY_DN8748_c0_g1_i1	cytochrome P450	-3.52	-0.38
TRINITY_DN9178_c0_g1_i2	cytochrome P450	-3.43	-0.48

TRINITY_DN4799_c9_g1_i1	LanC lantibiotic synthetase component C-like 2	1.08	1.38
TRINITY_DN1741_c0_g1_i1	Pathogenesis-related protein	0.33	3.21
TRINITY_DN1232_c1_g1_i3	Metacaspase	1.02	0.95
TRINITY_DN957_c0_g2_i1	vanadium-dependent bromoperoxidase 1	0.45	1.02
TRINITY_DN5130_c1_g1_i1	vanadium-dependent bromoperoxidase 1	0.46	1.32
TRINITY_DN679_c1_g3_i2	glutathione S-transferase	14.54	25.40
TRINITY_DN46310_c0_g2_i2	glutathione S-transferase	2.40	4.33
TRINITY_DN1585_c3_g1_i2	Catalase	1.66	2.01
TRINITY_DN13_c0_g2_i2	L-ascorbate peroxidase	1.30	0.65
TRINITY_DN13_c2_g1_i1	L-ascorbate peroxidase	-0.05	1.09

Altogether, 4-HHE had a smaller impact on the transcriptomic regulation and induced some common gene regulation in *L. digitata* compared to *L. digitata* treated with GG. It is possible that part of the gene regulation in *L. digitata* treated with GG were induced by 4-HHE, considering the previous study in which GG treatment triggered the release of 4-HHE in *L. digitata* (Goulitquer et al., 2009). However, 4-HHE also induced some different gene regulation that were not detected in *L. digitata* treated with GG. It could be due to the production of other oxylipins or aldehydes in *L. digitata* during GG treatment, which also had an impact on the regulation of these genes. These results suggested that studying the gene regulation induced by oxylipins and aldehydes could help us to decipher the complex gene regulation mechanism in *L. digitata* during the GG treatment.

3.2. GC-MS metabolite profiling of *S. latissima* treated with 4-HHE

To further analyze and compare the metabolic pathways activated by 4HHE treatment, we performed a time course GC-MS metabolic profiling in our model species, *S. latissima*. After GC-MS analysis of all algal extracts, obtained from the control and GG-elicited plantlets after 4 h, 12 h and 24 h, the mass spectra data were analyzed using MSDIAL pipeline. The full metabolic dataset contained 1,047 features, corresponding to identified peaks, that were used for statistical testing. Principal component analysis (PCA) of the dataset explained 18.67% of the observed variation and the differences between 4HHE-treatment and control were significant at 12 h among three time points (Figure 2). Then the orthogonal partial least squares discriminant analysis (OPLS-DA) identified 167 metabolites featured significant differences (VIP > 1) between control

and 4-HHE-treated samples at 4 h (R2X = 0.174, R2Y = 0.869, Q2 = 0.308). 177 and 118 metabolites featured significant differences (VIP > 1) were found in 12 h (R2X = 0.198, R2Y = 0.883, Q2 = 0.436) and 24 h (R2X = 0.137, R2Y = 0.809, Q2 = -0.0989), respectively.

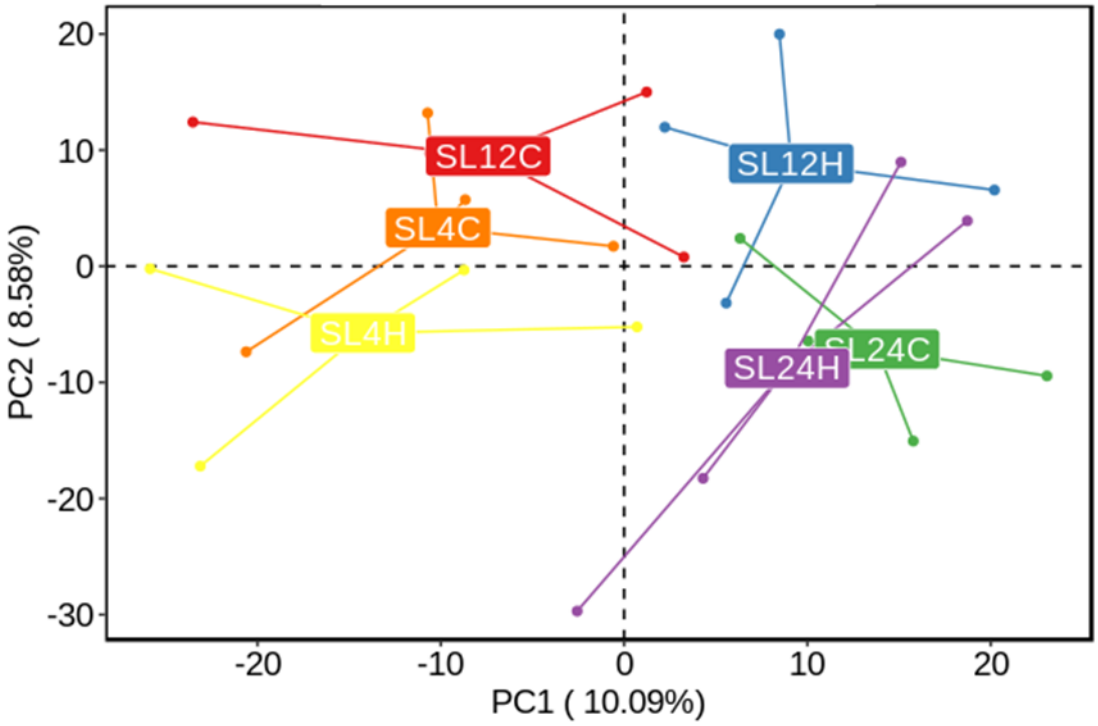

Fig. 2 PCA plot of GC-MS analysis at three time points. SL4C: control (colored in orange) at 4 h; SL4H: 4-HHE treatment (yellow) at 4 h; SL12C: control (red) at 12 h; SL12H: 4-HHE treatment (blue) at 12 h; SL24C: control (green) of 24 h; SL24H: 4-HHE treatment (purple) of 24 h (N=4).

Among those ions, six of them were annotated as methyl esters of free fatty acid by the NIST database, including methyl myristate, methyl linoleate, methyl linolenate, methyl palmitate, methyl arachidonate and 5,8,11,14,17-Eicosapentaenoic acid, methyl ester. Two of them, annotated as methyl myristate and methyl palmitate, were significantly accumulated (FDR < 0.05) after 12 h (Figure 3). In previous studies, methyl myristate and methyl palmitate have been proven to be effective deterrent against herbivores (Henderson et al., 1991). Methyl palmitate was identified in the extract of walnut, *Juglans regia* L., and it showed strong insecticidal activities (97.9% mortality) against adults of *Tetranychus cinnabarinus* at 10 mg/ml (Wang et al., 2009a). As mentioned above, in another kelp, *L. digitata*, the pre-treatment of 4-HHE significantly reduced the consumption by the herbivores, *P. pellucida* (Cabioch, 2016). If signaling pathways are conserved in these two closely-related species, we could hypothesize that a 2-fold accumulation of methyl myristate and methyl palmitate could be one of the defense reactions induced by 4-HHE.

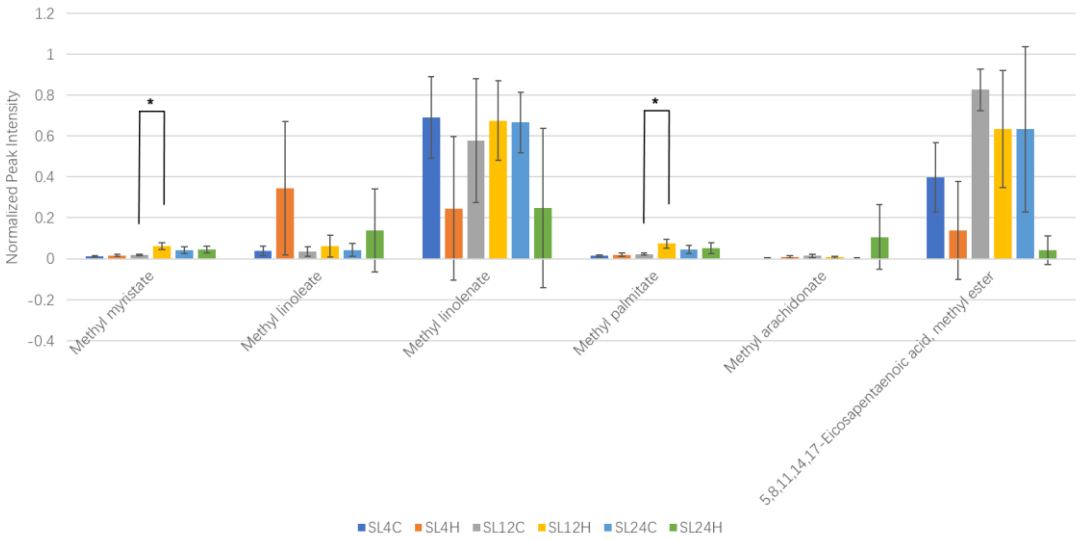

Fig. 3 Normalized peak intensity of 6 methyl esters of free fatty acid from GC-MS at three time points. SL4C: control (colored in dark blue) at 4 h; SL4H: 4-HHE treatment (orange) at 4 h; SL12C: control (grey) at 12 h; SL12H: 4-HHE treatment (yellow) at 12 h; SL24C: control (light blue) at 24 h; SL24H: 4-HHE treatment (green) at 24 h (N=4); *: t-test adjusted p-value < 0.05.

Then other ions were annotated by NIST database to search for the putative precursor of these methyl esters. Six free fatty acids were also detected in the GC-MS dataset, such as palmitic acid, α-linolenic acid, arachidonic acid, eicosapentaenoic acid, myristic acid and oleic acid (Figure 4). No significant change was observed in these free fatty acids. However, slight increase trends were found in 4-HHE treated group of all free fatty acids at 4 h compared to control. The relative amount of all free fatty acids was slightly decreased in 4-HHE treated groups at 12 h. These results suggested that there might be a release of free fatty acids at 4 h and then fatty acids could be converted into methyl esters and other oxidative derivatives. And the genes encoding fatty acid methyltransferases could be potential defense-related genes.

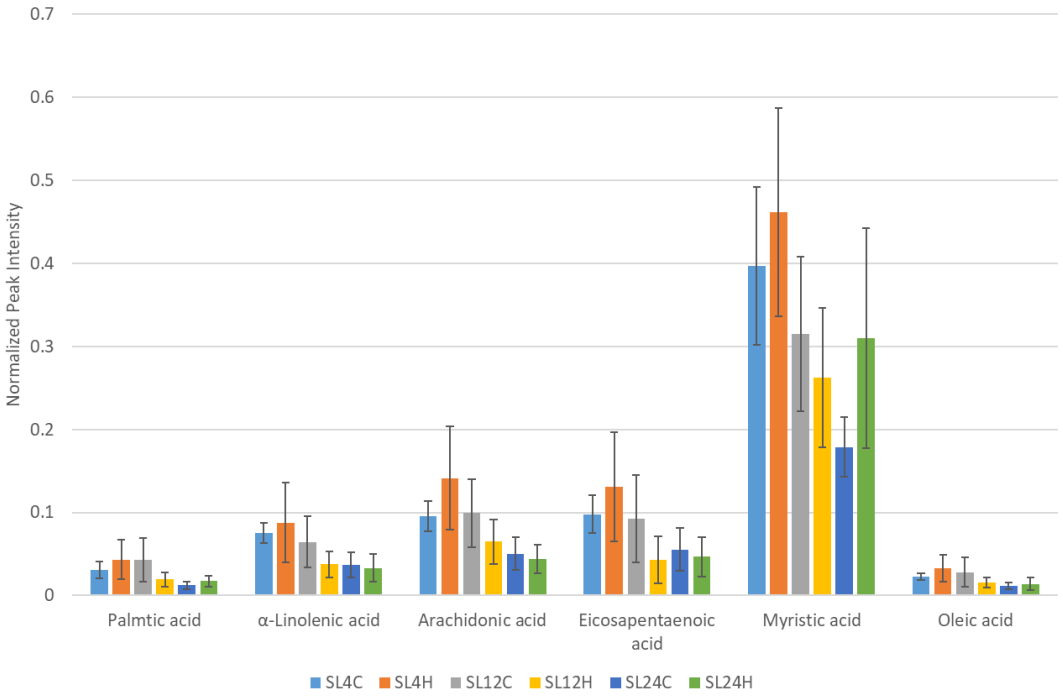

Fig. 4 Normalized peak intensity of 6 free fatty acids from GC-MS at three time points. SL4C: control (colored in light blue) at 4 h; SL4H: 4-HHE treatment (orange) at 4 h; SL12C: control (grey) at 12 h; SL12H: 4-HHE treatment (yellow) at 12 h; SL24C: control (dark blue) at 24 h; SL24H: 4-HHE treatment (green) at 24 h (N=4).

3.3. Screening of putative biological signals among other oxylipins and their derivatives in *S. latissima*

In previous studies, it has been proven that signal molecules released by the sporophytes of the other kelp species, *L. digitata*, after GG elicitation induced gene regulation in neighboring sporophyte (Thomas et al., 2011). And many volatile aldehydes have been detected in the surrounding seawater of *L. digitata* after GG elicitation and multiple abiotic stresses, such as temperature, light and drought stress (Goulitquer et al., 2009). Based on these finding, it has been assumed that oxylipins and their derivatives might act as biological signals during stresses. The aim of this section was to screen some oxylipins and aldehydes that could activate oxylipin pathway without inducing an oxidative burst in our model species, *S. latissima*. We selected four aldehydes (4-HHE, 4-HNE, Hexanal and Dodecadienal) and three oxylipins (12-OPDA, 13-HpOTre and 15-HEPE) that were produced by brown algae during GG elicitation or copper stress (Goulitquer et al., 2009, Ritter et al., 2014, Ritter et al., 2008). Firstly, the H_2O_2 measurement was performed. Four aldehydes were used to treat *S. latissima* at three concentrations (1μg/mL, 100ng/mL and 10ng/mL). And three oxylipins were used to treat *S. latissima* at 100ng/mL. As shown in figure 5, no significant H_2O_2 accumulation was detected in surrounding seawater of *S.*

latissima treated with these oxylipins and aldehydes at different concentrations. This result is similar to the results obtained in *L. digitata* (Cabioch, 2016). In kelps, the oxidative burst seems to be an essential component of innate immunity as the GG-induced oxidative burst significantly decreased the infection rate by endophytic pathogens (Küpper et al., 2002). Our results suggested that, unlike GG, these oxylipins and aldehydes do not induce the release of ROS in *S. latissima*.

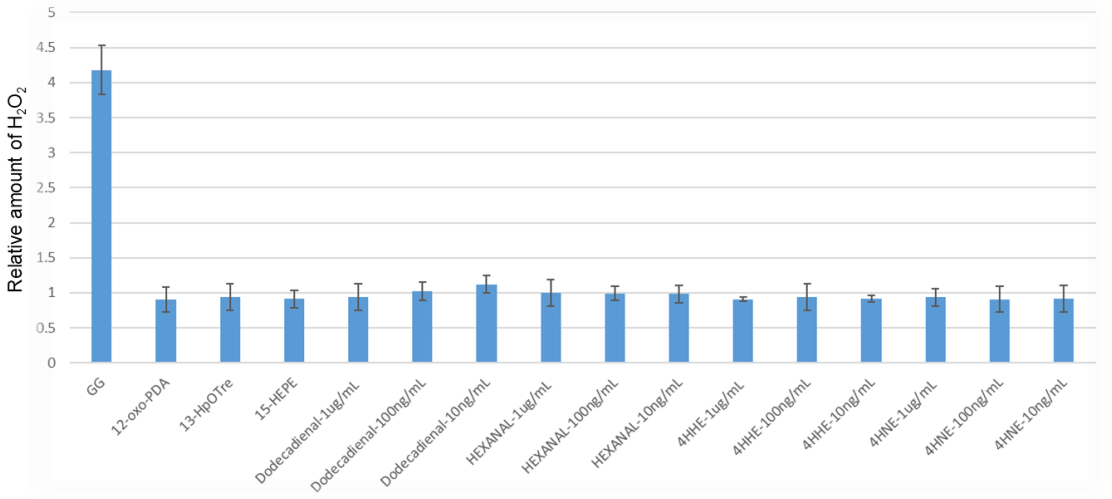

Fig. 5 Relative amount of H_2O_2 production by *S. latissimi* during 60 minutes after an incubation with different oxylipins and aldehydes compared to control (N=4).

In chapter III, several differentially expressed LOX and CYP genes were detected in response to GG elicitation, which could be used as marker gene for detecting the activation of oxylipin pathways in *S. latissima*. To select suitable marker genes from these LOX and CYP genes, two phylogenetic trees were constructed using the full-length protein sequences of LOX and CYP genes in four brown algae (*Ectocarpus siliculosus*, *Cladosiphon okamuranus*, *S. japonica* and *S. latissima*) (Figure 6). In the CYP tree, those protein sequences were divided into seven clans (CYP51, CYP5161, CYP5163, CYP5164, CYP5162, CYP5160 and CYP97), according to previous analyses (Teng et al., 2019). The CYP51 clan is common between plants and animals and is involved in sterol synthesis. The CYP97 clan is also conserved in plants and involved in carotenoid hydroxylation. In the CYP5164 clan, one CYP5164B1 gene from *E. siliculosus* was expressed in *E. coli* and the recombinant protein exhibited the activity of epoxyalcohol synthase (EsEAS), converting linoleate 9-hydroperoxide (9-HPOD) and linoleate 13-hydroperoxide (13-HPOD) into epoxyalcohols (Toporkova et al., 2017). Two differentially expressed CYP genes from *S. latissima* GG-elicited RNA-seq data, TRINITY_DN2920_c0_g3_i2 and TRINITY_DN2920_c1_g3_i3, were classified into the CYP5164 clan (Figure 6A), suggesting

that these two CYP genes might also be involved in oxylipin pathway. The different expression pattern of these two genes (Figure 6A) might be due to different functions. In LOX phylogenetic tree, protein sequences were divided into two groups (Figure 6B), corresponding to previously defined clades C1 and C2 (Teng et al., 2017). Two LOX genes with different expression patterns in *S. latissima* GG-elicited RNA-seq data (TRINITY_DN2016_c0_g1_i1 and TRINITY_DN7381_c0_g1_i1) belonged to different groups. In the end, two CYP genes and two LOX genes were selected as marker genes of oxylipin pathway regulation and used to screen oxylipins and aldehydes with potential signaling functionsin *S. latissima.*

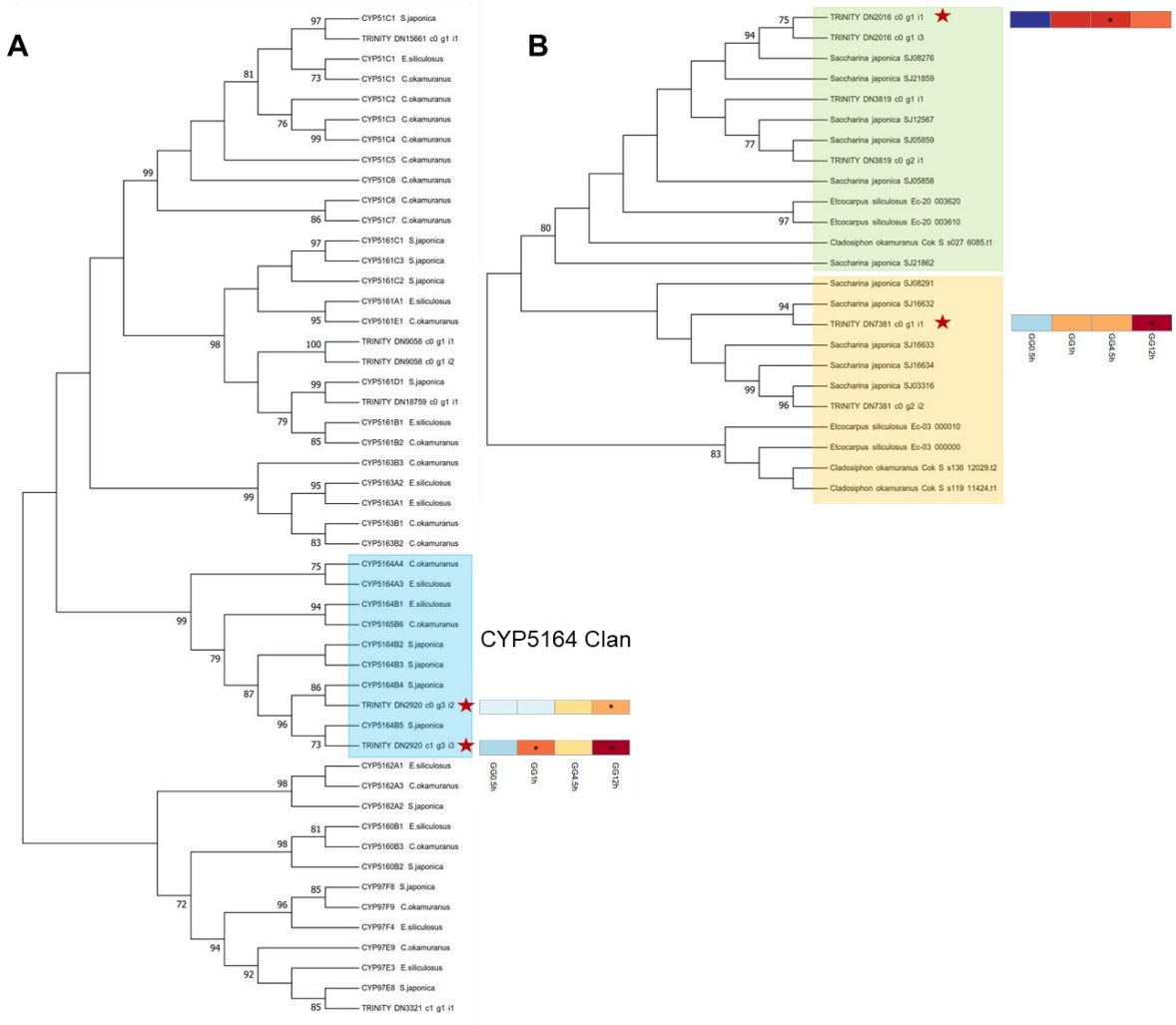

Fig. 6 Maximum-likelihood phylogenetic trees of **A**. cytochrome P450 genes and **B.** lipoxygenase genes, C1 clade is colored in green and C2 clade is colored in yellow, with expression data plotted for differentially expressed genes in chapter III. Bootstrap values above 70% are plotted on the trees.

The expression of LOX1 (TRINITY_DN7381_c0_g1_i1), LOX2 (TRINITY_DN2016_c0_g1_i1), CYP1 (TRINITY_DN2920_c0_g3_i2) and CYP2 (TRINITY_DN2920_c1_g3_i3), were analyzed in *S. latissima* treated with three oxylipins (12-

OPDA, 13-HpOTre and 15-HEPE) and three aldehydes (4-HHE, 4-HNE and Dodecadienal) after 4 hours. Only the CYP1 gene was significantly up-regulated (Log2Foldchange = 2.6, p-value < 0.05) in response to the treatment with 13-HpOTre, a precursor of jasmonic acid (Figure 7). The production of 13-HpOTre was already observed in *L. digitata* in response to copper stress (Ritter et al., 2008). Our result suggested that 13-HpOTre might act as a regulator of oxylipin pathway in *S. latissima*.

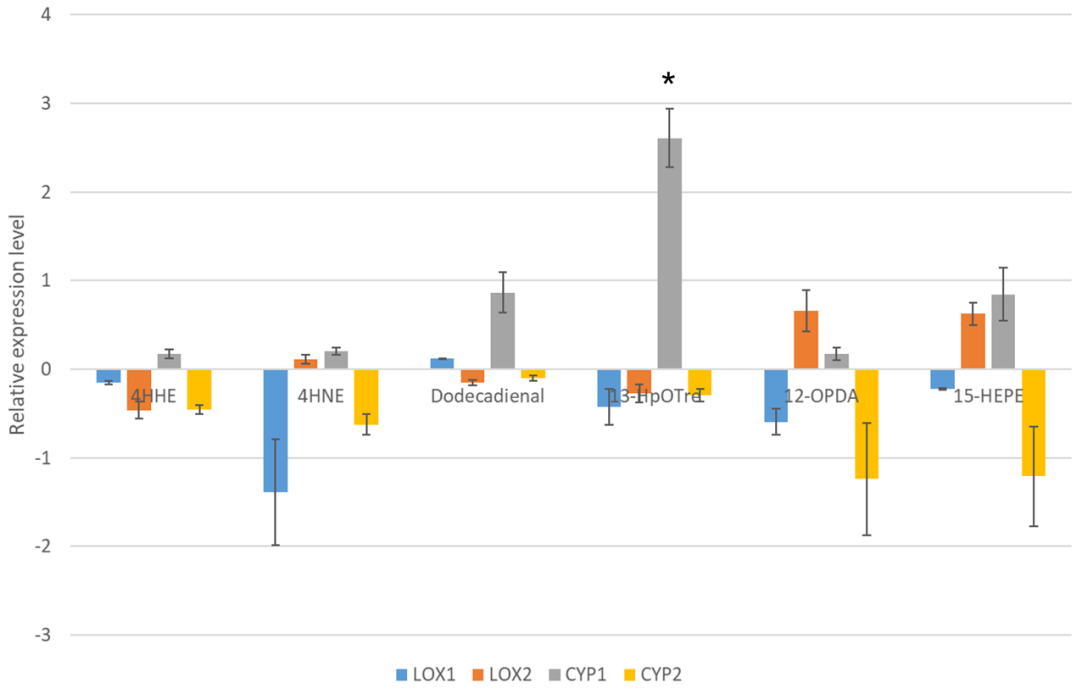

Fig. 7 Gene expression of four marker genes in *S. latissima* treated with three oxylipins and three aldehydes. *: One-way ANOVA p-value < 0.05.

4. Conclusion

In this study, the results of transcriptomic analysis demonstrated that 4-HHE induced the regulation of genes involved in signaling pathway and defense responses which were also detected in GG treatment at 12 h in *L. digitata*. However, less genes were differentially expressed in 4-HHE than GG treatment, suggesting that 4-HHE might induced specific gene regulation. The metabolite profiling of 4-HHE treatment detected the significantly accumulation of two putative defense-related compounds in *S. latissima*. The qPCR results showed that one oxylipin could induced the up-regulation of gene involved in oxylipin pathway. These results supported the hypothesis that oxylipins and aldehydes act as signal molecules during defense response in kelps.

Conclusions and perspectives

Conclusions and perspectives

The aim of this study was to explore oxylipin pathways and their regulation during defense responses in kelps. The results obtained in this thesis contribute to the current body of knowledge about defense-related responses in kelps. The global transcriptomic analysis provides first insight into the molecular basis of defense responses in two kelp species, *Saccharina latissima* and *Laminaria digitata*, to the algal endophyte *Laminarionema elsbetiae*. In addition to this study related to biotic interactions, the results of analyzing transcriptome in response to GG elicitation allow to draw a more precise picture of metabolic pathways regulated at the transcriptomic level during defense-related responses in *S. latissima*. The metabolic profiling of free fatty acid and their oxygenated derivatives completed these data by revealing the early regulation of oxylipin pathways upon GG elicitation. Furthermore, several oxylipins and aldehydes found in kelps were shown to induce gene regulation and metabolite changes in kelps, suggesting a direct role as signal molecules.

1. GG elicitation is an adequate experimental condition to study defense-related oxylipin pathways in *S. latissima*

To study the regulation of oxylipin pathways, the first step was to select a suitable experimental condition leading to the activation of this pathway. In a laboratory-controlled co-cultivation bioassay, *S. latissima*, the natural main host of *L. elsbetiae*, showed different physiological responses comparing to *L. digitata* which is the occasional host of *L. elsbetiae* in nature. The comparison of transcriptomic responses in the two hosts also showed different defense-related responses.

Within two days of the co-cultivation, one gene potentially involved in the recognition of endophytes was down-regulated in *S. latissima* and some defense-related responses were only activated after 48 hours. *L. digitata*, on the other hand, had a quicker and stronger transcriptional response and genes potentially related to defense responses, such as oxidative burst, were up-regulated after 24 hours. Later, after 48 hours, several upregulated genes might encode proteins involved in biosynthesis of specific defense compounds. Subsequently, the first contact with the

endophytes seems to activate in *L. digitata* more efficient defense responses than in *S. latissima*, leading to a stronger relative protection with a lower number of infected thalli after 2 weeks.

However, the co-cultivation with *L. elsbetiae* only induced the regulation of a small number of genes during 2 days in both kelps, and only a part of them were homologous of conserved genes with characterized functions in other eukaryotes. Contrary to what has been observed for biotic stresses in land plants (Vidhyasekaran, 2016), few genes potentially involved in oxylipin pathway were identified as differentially expressed genes. These results might suggest that the infection with *L. elsbetiae* spores only induce the regulation of specific defense-related genes. On the other hand, it could be due to some biases of the experimental set up: the timing of infection or the first contacts between spores and host surface are likely to be different in each biological replicate and it may be very difficult to synchronize the host responses, at the level of gene regulation, in this co-cultivation bioassay.

As a characterized defense elicitor in kelps, GG has been used to induce the regulation of some defense-related genes and the production of oxylipin-derived compounds in *L. digitata*. In this thesis, the transcriptome-wide gene regulation in response to GG elicitation was revealed in *S. latissima* for the first time. Based on this analysis, a schematic overview of the different induced pathways in *S. latissima* within 12 hours after GG elicitation was reconstructed and is presented in Fig.1. Unlike the co-cultivation with *L. elsbetiae*, GG elicitation induced massive gene regulation, leading to a more complete picture of defense-related patterns which are activated in the first hours after elicitor detection. An early transcriptional regulation was detected for genes potentially related to calcium signaling pathways and transcription regulators that might participate in early signaling and gene regulation up to 1 h. Then several genes related to defense and oxidative responses were up-regulated after 4.5 h and 12 h. Interestingly, many genes involved in oxylipin pathways were up-regulated and showed distinct expression patterns along the time-course. One of them, annotated as a cytochrome P450 gene, was up-regulated twice at 1 h and 12 h. These results suggested that GG elicitation induced a complex regulation of oxylipin pathways and some of these genes might be induced more than once within 12 hours. In addition, there were many unannotated genes that turned to be differentially expressed in response to GG elicitation and they might be related to defense responses specific to kelps. In the future, with the access to the *S. latissima* genome, these genes could be better annotated and their biological

function could be validated through crisper-cas9 gene editing system, recently developed in a brown algal model system (Badis and Cock, personal communication).

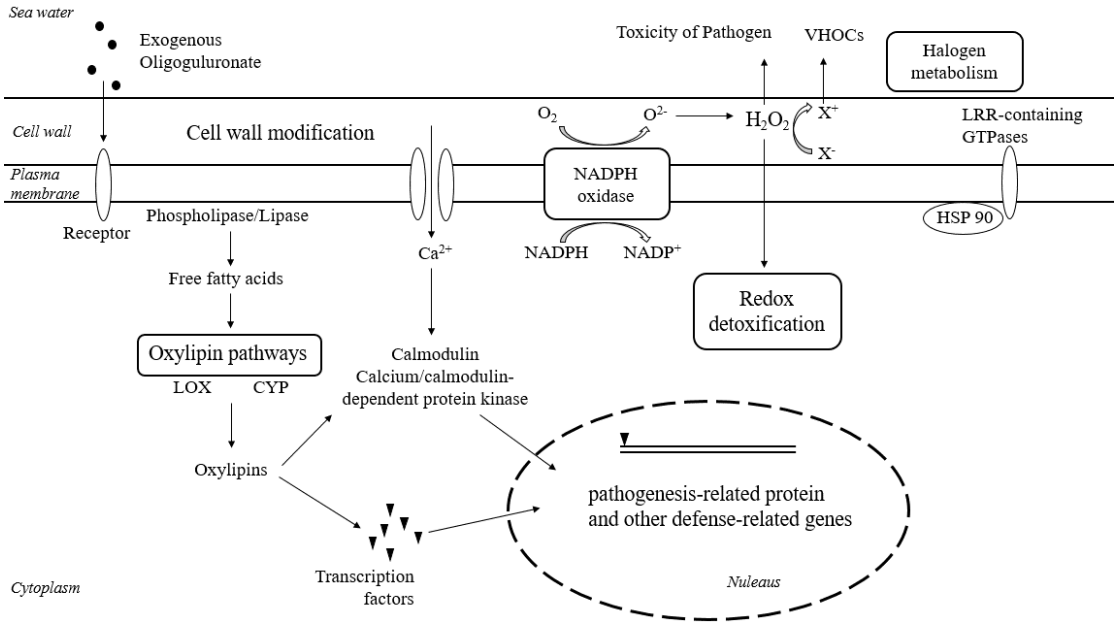

Fig.1 Representative scheme of defense-related pathways induced by GG elicitation in *S. latissima*, based on transcriptomic analysis. LOX, lipoxygenase; VHOCs, volatile halogenated organic compounds; CYP, cytochrome P450; HSP 90, heat shock protein 90

Compared to co-cultivation with *L. elsbetiae*, GG elicitation induced the regulation of more genes related to defense responses, especially those potentially related to enzymes of oxylipin pathways. GG treatment is easy to manipulate and can induce gene regulation in very short time and simultaneously in all algal surface cells. GG elicitation is therefore a powerful tool to study the very early stages of transcriptomic regulations, especially those related to transient or very specific transcript accumulation, in a context of defense responses. However, it still has some limits. For instance, GG treatment induced a strong oxidative burst and the regulation of many genes related to oxidative responses. Some defense-related responses specific to biotic stress may not be induced by GG. More bioassays still need to be established in the future for further studying algal-pathogen interactions or more generally biotic stress responses in kelps.

2. Oxylipin pathways in *S. latissima* seem to be activated several times upon GG elicitation

Based on the transcriptomic analysis, it has been suggested that oxylipin pathways were activated several times within 12 hours after GG elicitation in *S. latissima*. Metabolite profiling was performed to analyze the changes in oxylipin-derived metabolites during the same time-course after elicitation. These data on metabolic and transcriptomic regulations of oxylipin pathways during GG treatment in *S. latissima* have been integrated in Fig.2.

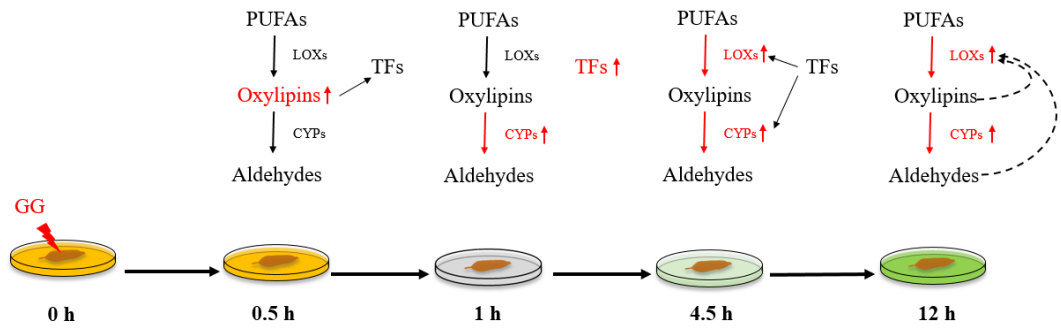

Fig.2 Simplified scheme of oxylipin pathways induced by GG treatment in *S. latissima*. PUFA: polyunsaturated fatty acids; LOX, lipoxygenase; CYP, cytochrome P450; TFs: transcription factors.

The significant increase of C18 free fatty acid-derived compounds was detected at 0.5 h. According to the gene expression data, no significant regulation of genes in oxylipin pathways was detected at that time, suggesting that the early production of these oxylipins was catalyzed by already present enzymes that may be activated by the release of substrates such as reactive oxygen species and polyunsaturated fatty acids (PUFAs). One of the early up-regulated metabolites related to oxylipin pathways was annotated as putative 12-OPDA and it might activate some signaling pathways and putative transcription regulators as detected after 1 h in *S. latissima* and already observed in plants (Taki et al., 2005). Similarly, the up-regulation of a putative CYP gene after 1 h could be induced directly by the oxylipins released after 0.5 h. Then two different groups of LOX and CYP genes were later up-regulated at 4.5 h and 12 h, respectively, suggesting that the induction of oxylipin pathway at these two time points might have different origins. The activation of oxylipin pathway at 4.5 h might be triggered by the transcription regulation induced at 1 h, leading to the production of various oxylipin-derived compounds. These compounds could act as signal molecules and later induce the up-regulation of oxylipin pathways at 12 h. However,

no significant accumulation of oxylipin-derived compounds was detected by metabolite profiling after 1 h. Maybe these signal molecules were immediately metabolized or rapidly diffused across membranes and only accumulated in surrounding seawater, being not detected in the endometabolome. Furthermore, the pharmacological approach suggested that C20 oxylipin pathways might be activated after GG treatment when the C18 oxylipin pathways were blocked, suggesting the putative alternative roles of C20 oxylipin pathway (Fig.3). In addition to further validate the chemical identities of compounds of interest by LC-MS/MS, it would be interested to include in metabolic profiling analyses the study of the exometabolome of GG-elicited plantlets, and some targeted gene regulation analyses by RT-qPCR to confirm some of these hypotheses.

3. Some oxylipin and aldehyde-induced transcriptomic regulation of defense-related genes and oxylipin pathways in kelps

To explore the hypothesis that oxylipin-derived compounds could act as intrinsic signal inductors of oxylipin pathways, several oxylipins and aldehydes have been tested in *L. digitata* and *S. latissima.* A volatile compound, 4-hydroxy Hexenal (4-HHE), was a first interesting compound because it was released by *L. digitata* after GG-treatment and abiotic stress and shown to reduce the consumption of *L. digitata* by grazers (thesis of L. Cabioch, unpublished data). In my thesis, the incubation with 4-HHE showed that, unlike GG, 4-HHE induced a small group of specific defense-related genes, without previous oxidative burst, in *L. digitata* and it seemed to have a negative effect on the regulation of oxylipin pathways by suppressing the expression of two CYP genes. In *S. latissima,* 4-HHE also induced some metabolic modifications, suggesting that 4-HHE could be a common signal perceived by the two kelps. No significant transcriptomic changes were detected for the four LOX and CYP genes after 4 h of 4-HHE treatment. Few other oxylipins and aldehydes were tested in *S. latissima* and one oxylipin, 13-HpOTre, induced the up-regulation of one CYP gene, suggesting that it could be a regulator of oxylipin pathways in kelps. However, these are still preliminary results. To complete this targeted gene expression analysis, more time points and more genes should be tested in the future. This could be combined with the screening of other potential signaling compounds. It is also possible that a single chemical compound would not be sufficient for triggering defense responses. Therefore, the application of a mixture of oxylipins and aldehydes could be an option for future experiments.

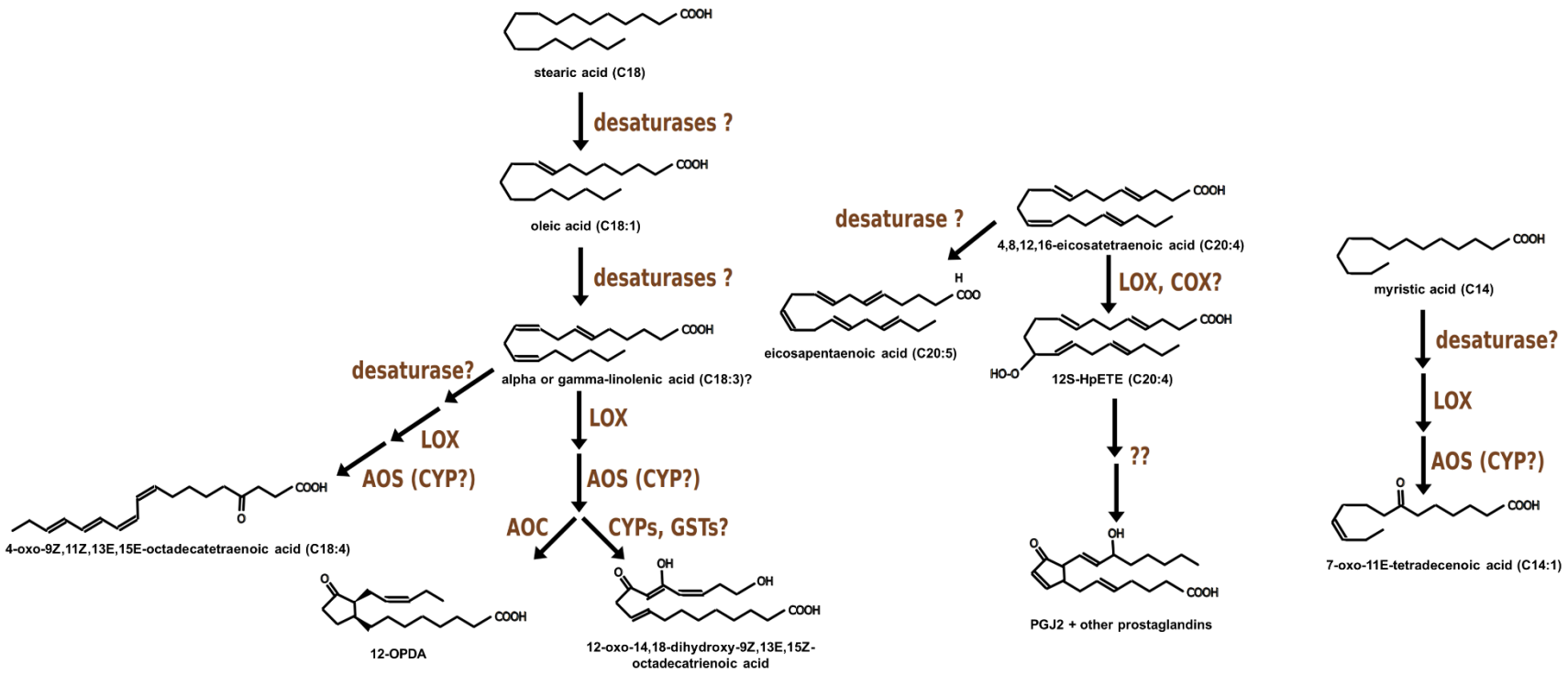

Fig. 3 Partially reconstructed oxylipin pathways in *S. latissima* based on the metabolic profiling data of three treatments at 0.5 hour. 12-OPDA: 12-Oxo-phytodienoic acid; PGJ2 prostaglandin J2; 12S-HpETE: (5Z,8Z,10E,12S,14Z)-12-hydroperoxyicosa-5,8,10,14-tetraenoic acid LOX: lipoxygenase; AOC: allene oxide cyclase; AOS: allene oxide synthase; CYP: cytochrome P450; GST: Glutathione S-transferase; COX: Cyclooxygenase.

4. Future directions for studying oxylipin pathway during defense responses in kelps

We obtained a large set of transcriptomic data, including data of GG treatment in *S. latissima,* 4-HHE and GG treatment in *L. digitata* and co-cultivation treatment with an endophyte for both kelps. The analysis of these data allows us to draw a more precise scheme of the molecular basis of defense response in kelps. With the increase of annotation ratio in brown algae, these data could be also used to identify more novel genes involved in defense responses and other biological processes. Some genes of interest could be functionally characterized in the future.

In this study, the combination of transcriptomic and metabolomic analysis significantly increased our knowledge about the regulation of oxylipin pathways during defense elicitation in *S. latissima*. The integration of these data helps us to partially reconstruct the oxylipin biosynthesis pathways and to propose some hypotheses about their regulation and roles, providing several directions for future studies on oxylipin pathways in kelps as follows:

Biochemical characterization of some enzymes could be conducted through heterologous expression of targeted genes. During the GG elicitation, genes involved in oxylipin pathways, such as LOX and CYP genes, showed highly diverse expression patterns, suggesting different functions between homologous genes. I initiated such approaches by performing the first step in the cloning of two CYP genes belonging to CYP5164 clan. One CYP gene belonging to this clan in *Ectocarpus siliculosus* was expressed in *E. coli* and the recombinant protein showed epoxyalcohol synthase when incubated with oxylipins (Toporkova et al., 2017). The biochemical characterization of these CYP and more enzymes will be performed, which will contribute to reconstruct the oxylipin pathways in kelps.

The regulation of defense-related compounds needs to be analyzed during experimental biotic interactions with multiple methods. The metabolic profiling using GG elicitation identified some metabolites that could be related to defense responses and the regulation of them in *S. latissima* during other biotic interactions still need to be explored. Our results also showed that single metabolic profiling method is not sufficient to analyze oxylipin-derived compounds due to their different chemical properties. Therefore, more metabolic analysis approaches, such as exometabolome, solid phase extraction for volatile compounds and MS imaging, should be used

to analyze the metabolic changes during infection and their localization around the infection sites in the future.

The biological roles of some compounds have to be further validated as defense signaling and on later protection of kelps, against endophyte infection for instance. Our preliminary results showed that some oxylipin-derived compounds, such as 4-HHE and 13HpOTre, were able to regulate the expression of oxylipin pathways and defense-related genes, suggesting that they could act as signal molecules during the defense responses. To confirm this hypothesis, these compounds need to be tested in other bioassays and at the same time, more oxylipin-derived compounds need to be screened to fully establish their involvement in the regulation of oxylipin biosynthesis pathways.

Reference

Affeldt, K. J., Brodhagen, M. & Keller, N. P. 2012. Aspergillus oxylipin signaling and quorum sensing pathways depend on G protein-coupled receptors. *Toxins* 4:695-717.

Afzal, A. J., Wood, A. J. & Lightfoot, D. A. 2008. Plant receptor-like serine threonine kinases: roles in signaling and plant defense. *Mol Plant-Microbe Interact* 21:507-17.

Akira, S., Uematsu, S. & Takeuchi, O. 2006. Pathogen recognition and innate immunity. *Cell* 124:783-801.

Alem, M. A. & Douglas, L. J. 2004. Effects of aspirin and other nonsteroidal anti-inflammatory drugs on biofilms and planktonic cells of Candida albicans. *Antimicrobial agents and chemotherapy* 48:41-47.

Alexander, D., Goodman, R. M., Gut-Rella, M., Glascock, C., Weymann, K., Friedrich, L., Maddox, D., Ahl-Goy, P., Luntz, T. & Ward, E. 1993. Increased tolerance to two oomycete pathogens in transgenic tobacco expressing pathogenesis-related protein 1a. *Proceedings of the National Academy of Sciences* 90:7327-31.

Allen, M. D., del Campo, J. A., Kropat, J. & Merchant, S. S. 2007. FEA1, FEA2, and FRE1, encoding two homologous secreted proteins and a candidate ferrireductase, are expressed coordinately with FOX1 and FTR1 in iron-deficient Chlamydomonas reinhardtii. *Eukaryot Cell* 6:1841-52.

Alves, M. S., Dadalto, S. P., Gonçalves, A. B., De Souza, G. B., Barros, V. A. & Fietto, L. G. 2014. Transcription factor functional protein-protein interactions in plant defense responses. *Proteomes* 2:85-106.

Ambawat, S., Sharma, P., Yadav, N. R. & Yadav, R. C. 2013. MYB transcription factor genes as regulators for plant responses: an overview. *Physiol Mol Biol Plants* 19:307-21.

Andersen, R. A. 2004. Biology and systematics of heterokont and haptophyte algae. *Am J Bot* 91:1508-22.

Andreou, A., Brodhun, F. & Feussner, I. 2009. Biosynthesis of oxylipins in non-mammals. *Progress in lipid research* 48:148-70.

Andrews, S. 2010. FastQC: a quality control tool for high throughput sequence data. Babraham Bioinformatics, Babraham Institute, Cambridge, United Kingdom.

Andrianarison, R.-H., Beneytout, J.-L. & Tixier, M. 1989. An enzymatic conversion of lipoxygenase products by a hydroperoxide lyase in blue-green algae (Oscillatoria sp.). *Plant Physiol* 91:1280-87.

Annunziata, R., Ritter, A., Fortunato, A. E., Manzotti, A., Cheminant-Navarro, S., Agier, N., Huysman, M. J., Winge, P., Bones, A. M. & Bouget, F.-Y. 2019. bHLH-PAS protein RITMO1 regulates diel biological rhythms in the marine diatom Phaeodactylum tricornutum. *Proceedings of the National Academy of Sciences* 116:13137-42.

Antón, R., Camacho, M., Puig, L. & Vila, L. 2002. Hepoxilin B3 and its enzymatically formed derivative trioxilin B3 are incorporated into phospholipids in psoriatic lesions. *Journal of investigative dermatology* 118:139-46.

Apt, K. E. 1984. EFFECTS OF THE SYMBIOTIC RED ALGA HYPNEOCOLAX STELLARIS ON ITS HOST HYPNEA MUSCIFORMIS (HYPNEACEAE, GIGARTINALES) 1. *J Phycol* 20:148-50.

Archibald, J. M. 2009. The puzzle of plastid evolution. *Curr Biol* 19:R81-R88.

Armengaud, J., Trapp, J., Pible, O., Geffard, O., Chaumot, A. & Hartmann, E. M. 2014. Non-model organisms, a species endangered by proteogenomics. *Journal of proteomics* 105:5-18.

Arun, A., Coelho, S. M., Peters, A. F., Bourdareau, S., Pérès, L., Scornet, D., Strittmatter, M., Lipinska, A. P., Yao, H. & Godfroy, O. 2019. Convergent recruitment of TALE homeodomain life cycle regulators to direct sporophyte development in land plants and brown algae. *Elife* 8:e43101.

Bao, F., Huang, X., Zhu, C., Zhang, X., Li, X. & Yang, S. 2014. Arabidopsis HSP90 protein modulates RPP4-mediated temperature-dependent cell death and defense responses. *New Phytol* 202:1320-34.

Barbosa, M., Valentão, P. & Andrade, P. B. 2016. Biologically active oxylipins from enzymatic and nonenzymatic routes in macroalgae. *Mar Drugs* 14:23.

Bartsch, I., Wiencke, C., Bischof, K., Buchholz, C. M., Buck, B. H., Eggert, A., Feuerpfeil, P., Hanelt, D., Jacobsen, S. & Karez, R. 2008. The genus Laminaria sensu lato: recent insights and developments. *Eur J Phycol* 43:1-86.

Batistič, O. & Kudla, J. 2012. Analysis of calcium signaling pathways in plants. *Biochimica et Biophysica Acta (BBA)-General Subjects* 1820:1283-93.

Beckers, G. J. & Conrath, U. 2007. Priming for stress resistance: from the lab to the field. *Curr Opin Plant Biol* 10:425-31.

Belhadj, A., Saigne, C., Telef, N., Cluzet, S., Bouscaut, J., Corio-Costet, M.-F. & Mérillon, J.-M. 2006. Methyl jasmonate induces defense responses in grapevine and triggers protection against Erysiphe necator. *J Agric Food Chem* 54:9119-25.

Belmonte, R., Wang, T., Duncan, G. J., Skaar, I., Mélida, H., Bulone, V., van West, P. & Secombes, C. J. 2014. Role of pathogen-derived cell wall carbohydrates and prostaglandin E2 in immune response and suppression of fish immunity by the oomycete Saprolegnia parasitica. *Infect Immun* 82:4518-29.

Bernard, M. 2018. *Molecular interactions between the kelp saccharina latissima and algal endophytes.* Sorbonne université.

Bernard, M., Rousvoal, S., Jacquemin, B., Ballenghien, M., Peters, A. F. & Leblanc, C. 2018. qPCR-based relative quantification of the brown algal endophyte Laminarionema elsbetiae in Saccharina latissima: variation and dynamics of host—endophyte interactions. *J Appl Phycol* 30:2901-11.

Bernard, M. S., Strittmatter, M., Murúa, P., Heesch, S., Cho, G. Y., Leblanc, C. & Peters, A. F. 2019. Diversity, biogeography and host specificity of kelp endophytes with a focus on the genera Laminarionema and Laminariocolax (Ectocarpales, Phaeophyceae). *Eur J Phycol* 54:39-51.

Bernart, M. & Gerwick, W. H. 1988. Isolation of 12-(S)-HEPE from the red marine alga Murrayella periclados and revision of structure of an acyclic icosanoid from Laurencia hybrida. Implications to the biosynthesis of the marine prostanoid hybridalactone. *Tetrahedron Lett* 29:2015-18.

Bernart, M. W. & Gerwick, W. H. 1994. Eicosanoids from the tropical red alga Murrayella periclados. *Phytochemistry* 36:1233-40.

Bernart, M. W., Whatley, G. G. & Gerwick, W. H. 1993. Unprecedented oxylipins from the marine green alga Acrosiphonia coalita. *J Nat Prod* 56:245-59.

Bolger, A. M., Lohse, M. & Usadel, B. 2014. Trimmomatic: a flexible trimmer for Illumina sequence data. *Bioinformatics* 30:2114-20.

Boller, T. & He, S. Y. 2009. Innate immunity in plants: an arms race between pattern recognition receptors in plants and effectors in microbial pathogens. *Science* 324:742-44.

Boonprab, K., Matsui, K., Akakabe, Y., Yotsukura, N. & Kajiwara, T. 2003. Hydroperoxy-arachidonic acid mediated n-hexanal and (Z)-3-and (E)-2-nonenal formation in Laminaria angustata. *Phytochemistry* 63:669-78.

Boonprab, K., Matsui, K., Akakabe, Y., Yotsukura, N. & Kajiwara, T. 2004. Arachidonic acid conversion by lipoxygenase in the brown alga, Laminaria angustata. *Agriculture and Natural Resources* 38:72-77.

Borchardt, S., Allain, E., Michels, J., Stearns, G., Kelly, R. & McCoy, W. 2001. Reaction of acylated homoserine lactone bacterial signaling molecules with oxidized halogen antimicrobials. *Appl Environ Microbiol* 67:3174-79.

Bouarab, K., Adas, F., Gaquerel, E., Kloareg, B., Salaün, J.-P. & Potin, P. 2004. The innate immunity of a marine red alga involves oxylipins from both the eicosanoid and octadecanoid pathways. *Plant Physiol* 135:1838-48.

Bouarab, K., Potin, P., Correa, J. & Kloareg, B. 1999. Sulfated oligosaccharides mediate the interaction between a marine red alga and its green algal pathogenic endophyte. *The Plant Cell* 11:1635-50.

Bowman, K. G. & Bertozzi, C. R. 1999. Carbohydrate sulfotransferases: mediators of extracellular communication. *Chem Biol* 6:R9-R22.

Brown, S. H., Zarnowski, R., Sharpee, W. & Keller, N. 2008. Morphological transitions governed by density dependence and lipoxygenase activity in Aspergillus flavus. *Appl Environ Microbiol* 74:5674-85.

Cabioch, L. 2016. *Chemical signaling and defense in brown algal kelps during interactions with herbivores.* Université Pierre et Marie Curie-Paris VI; Universidad católica de Chile.

Cantrell, C. L., Case, B. P., Mena, E. E., Kniffin, T. M., Duke, S. O. & Wedge, D. E. 2008. Isolation and identification of antifungal fatty acids from the basidiomycete Gomphus floccosus. *J Agric Food Chem* 56:5062-68.

Capra, V., Bäck, M., Barbieri, S. S., Camera, M., Tremoli, E. & Rovati, G. E. 2013. Eicosanoids and their drugs in cardiovascular diseases: focus on atherosclerosis and stroke. *Medicinal research reviews* 33:364-438.

Carella, P. 2020. Xylem-mobile oxylipins are critical regulators of induced systemic resistance in maize. Am Soc Plant Biol.

Casu, R. E., Jarmey, J. M., Bonnett, G. D. & Manners, J. M. 2007. Identification of transcripts associated with cell wall metabolism and development in the stem of sugarcane by Affymetrix GeneChip Sugarcane Genome Array expression profiling. *Functional & integrative genomics* 7:153-67.

Chehab, E. W., Kaspi, R., Savchenko, T., Rowe, H., Negre-Zakharov, F., Kliebenstein, D. & Dehesh, K. 2008. Distinct roles of jasmonates and aldehydes in plant-defense responses. *PloS one* 3:e1904.

Chen, L., Hamada, S., Fujiwara, M., Zhu, T., Thao, N. P., Wong, H. L., Krishna, P., Ueda, T., Kaku, H. & Shibuya, N. 2010. The Hop/Sti1-Hsp90 chaperone complex facilitates the maturation and transport of a PAMP receptor in rice innate immunity. *Cell Host & Microbe* 7:185-96.

Chezem, W. R., Memon, A., Li, F.-S., Weng, J.-K. & Clay, N. K. 2017. SG2-type R2R3-MYB transcription factor MYB15 controls defense-induced lignification and basal immunity in Arabidopsis. *The Plant Cell* 29:1907-26.

Choi, H., Proteau, P. J., Byrum, T. & Gerwick, W. H. 2012. Cymatherelactone and cymatherols A–C, polycyclic oxylipins from the marine brown alga Cymathere triplicata. *Phytochemistry* 73:134-41.

Cock, J. M. & Coelho, S. M. 2011. Algal models in plant biology. *J Exp Bot* 62:2425-30.

Cock, J. M., Sterck, L., Rouzé, P., Scornet, D., Allen, A. E., Amoutzias, G., Anthouard, V., Artiguenave, F., Aury, J.-M. & Badger, J. H. 2010. The Ectocarpus genome and the independent evolution of multicellularity in brown algae. *Nature* 465:617-21.

Coelho, S. M., Brownlee, C. & Bothwell, J. H. 2008. A tip-high, Ca 2+-interdependent, reactive oxygen species gradient is associated with polarized growth in Fucus serratus zygotes. *Planta* 227:1037-46.

Collén, J., Guisle-Marsollier, I., Léger, J. J. & Boyen, C. 2007. Response of the transcriptome of the intertidal red seaweed Chondrus crispus to controlled and natural stresses. *New Phytol* 176:45-55.

Conesa, A., Götz, S., García-Gómez, J. M., Terol, J., Talón, M. & Robles, M. 2005. Blast2GO: a universal tool for annotation, visualization and analysis in functional genomics research. *Bioinformatics* 21:3674-76.

Conrath, U. 2009. Priming of induced plant defense responses. *Adv Bot Res* 51:361-95.

Conrath, U., Pieterse, C. M. & Mauch-Mani, B. 2002. Priming in plant–pathogen interactions. *Trends Plant Sci* 7:210-16.

Correa, J. A. & McLachlan, J. 1994. Endophytic algae of Chondrus crispus (Rhodophyta). V. Fine structure of the infection by Acrochaete operculata (Chlorophyta). *Eur J Phycol* 29:33-47.

Cosse, A., Leblanc, C. & Potin, P. 2007. Dynamic defense of marine macroalgae against pathogens: from early activated to gene-regulated responses. *Adv Bot Res* 46:221-66.

Cosse, A., Potin, P. & Leblanc, C. 2009. Patterns of gene expression induced by oligoguluronates reveal conserved and environment-specific molecular defense responses in the brown alga Laminaria digitata. *New Phytol* 182:239-50.

Cristea, M. & Oliw, E. H. 2006. A G316A mutation of manganese lipoxygenase augments hydroperoxide isomerase activity: mechanism of biosynthesis of epoxyalcohols. *J Biol Chem* 281:17612-23.

Czechowski, T., Stitt, M., Altmann, T., Udvardi, M. K. & Scheible, W.-R. 2005. Genome-wide identification and testing of superior reference genes for transcript normalization in Arabidopsis. *Plant Physiol* 139:5-17.

d'Ippolito, G., Cutignano, A., Briante, R., Febbraio, F., Cimino, G. & Fontana, A. 2005. New C 16 fatty-acid-based oxylipin pathway in the marine diatom Thalassiosira rotula. *Organic & biomolecular chemistry* 3:4065-70.

d'Ippolito, G., Lamari, N., Montresor, M., Romano, G., Cutignano, A., Gerecht, A., Cimino, G. & Fontana, A. 2009. 15S-Lipoxygenase metabolism in the marine diatom Pseudo-nitzschia delicatissima. *New Phytol* 183:1064-71.

Dave, A., Hernández, M. L., He, Z., Andriotis, V. M., Vaistij, F. E., Larson, T. R. & Graham, I. A. 2011. 12-Oxo-phytodienoic acid accumulation during seed development represses seed germination in Arabidopsis. *The Plant Cell* 23:583-99.

de Mendoza, A. & Sebé-Pedrós, A. 2019. Origin and evolution of eukaryotic transcription factors. *Curr Opin Genet Dev* 58:25-32.

de Oliveira, L. S., Tschoeke, D. A., Lopes, A. C. R. M., Sudatti, D. B., Meirelles, P. M., Thompson, C. C., Pereira, R. C. & Thompson, F. L. 2017. Molecular mechanisms for microbe recognition and defense by the red seaweed Laurencia dendroidea. *Msphere* 2.

Dempsey, D. M. A. & Klessig, D. F. 2012. SOS–too many signals for systemic acquired resistance? *Trends Plant Sci* 17:538-45.

Deng, Y., Yao, J., Wang, X., Guo, H. & Duan, D. 2012. Transcriptome sequencing and comparative

analysis of Saccharina japonica (Laminariales, Phaeophyceae) under blue light induction. *PLoS One* 7:e39704.

Denoux, C., Galletti, R., Mammarella, N., Gopalan, S., Werck, D., De Lorenzo, G., Ferrari, S., Ausubel, F. M. & Dewdney, J. 2008. Activation of defense response pathways by OGs and Flg22 elicitors in Arabidopsis seedlings. *Molecular plant* 1:423-45.

Dheda, K., Huggett, J., Chang, J., Kim, L., Bustin, S., Johnson, M., Rook, G. & Zumla, A. 2005. The implications of using an inappropriate reference gene for real-time reverse transcription PCR data normalization. *Anal Biochem* 344:141-43.

Dittami, S. M., Scornet, D., Petit, J.-L., Ségurens, B., Da Silva, C., Corre, E., Dondrup, M., Glatting, K.-H., König, R. & Sterck, L. 2009. Global expression analysis of the brown alga Ectocarpus siliculosus (Phaeophyceae) reveals large-scale reprogramming of the transcriptome in response to abiotic stress. *Genome biology* 10:1-20.

Dombrowski, J. E., Kronmiller, B. A., Hollenbeck, V. & Martin, R. C. 2020. Transcriptome Analysis of Wounding in the Model Grass Lolium temulentum. *Plants* 9:780.

Eckardt, N. A. 2008. Oxylipin signaling in plant stress responses. Am Soc Plant Biol.

Eddy, S. 2010. HMMER3: a new generation of sequence homology search software. *URL:* http://hmmer. *janelia. Org*.

Egan, S., Fernandes, N. D., Kumar, V., Gardiner, M. & Thomas, T. 2014. Bacterial pathogens, virulence mechanism and host defence in marine macroalgae. *Environ Microbiol* 16:925-38.

Ellertsdottir, E. & Peters, A. F. 1997. High prevalence of infection by endophytic brown algae in populations of Laminaria spp.(Phaeophyceae). *Mar Ecol Prog Ser* 146:135-43.

Emeline, C. B., Ludovic, D., Laurent, V., Catherine, L., Kruse, I., Erwan, A. G., Florian, W. & Philippe, P. 2021. Induction of Phlorotannins and Gene Expression in the Brown Macroalga Fucus vesiculosus in Response to the Herbivore Littorina littorea. *Mar Drugs* 19:185.

Erb-Downward, J. R. & Noverr, M. C. 2007. Characterization of prostaglandin E2 production by Candida albicans. *Infect Immun* 75:3498-505.

Fan, F. & Roman, R. J. 2017. Effect of cytochrome P450 metabolites of arachidonic acid in nephrology. *Journal of the American Society of Nephrology* 28:2845-55.

Farmer, E. E. & Mueller, M. J. 2013. ROS-mediated lipid peroxidation and RES-activated signaling. *Annu Rev Plant Biol* 64:429-50.

Ferrari, S., Plotnikova, J. M., De Lorenzo, G. & Ausubel, F. M. 2003. Arabidopsis local resistance to Botrytis cinerea involves salicylic acid and camalexin and requires EDS4 and PAD2, but not SID2, EDS5 or PAD4. *The Plant Journal* 35:193-205.

Fiume, E. & Fletcher, J. C. 2012. Regulation of Arabidopsis embryo and endosperm development by the polypeptide signaling molecule CLE8. *The Plant Cell* 24:1000-12.

Flöthe, C. R., Molis, M. & John, U. 2014. Induced resistance to periwinkle grazing in the brown seaweed F ucus vesiculosus (P haeophyceae): molecular insights and seaweed-mediated effects on herbivore interactions. *J Phycol* 50:564-76.

Fonseca, S., Chini, A., Hamberg, M., Adie, B., Porzel, A., Kramell, R., Miersch, O., Wasternack, C. & Solano, R. 2009. (+)-7-iso-Jasmonoyl-L-isoleucine is the endogenous bioactive jasmonate. *Nat Chem Biol* 5:344-50.

Fontana, A., d'Ippolito, G., Cutignano, A., Miralto, A., Ianora, A., Romano, G. & Cimino, G. 2007a. Chemistry of oxylipin pathways in marine diatoms. *Pure and Applied Chemistry* 79:481-90.

Fontana, A., d'Ippolito, G., Cutignano, A., Romano, G., Lamari, N., Massa Gallucci, A., Cimino, G.,

Miralto, A. & Ianora, A. 2007b. LOX-induced lipid peroxidation mechanism responsible for the detrimental effect of marine diatoms on zooplankton grazers. *ChemBioChem* 8:1810-18.

Franceschi, V. R., Krekling, T. & Christiansen, E. 2002. Application of methyl jasmonate on Picea abies (Pinaceae) stems induces defense-related responses in phloem and xylem. *Am J Bot* 89:578-86.

Frankel, E. 1980. Lipid oxidation. *Progress in lipid research* 19:1-22.

Fu, Y., He, W., Wang, L. & Wei, Y. 2015. Selection of appropriate reference genes for quantitative real-time PCR in Oxytropis ochrocephala Bunge using transcriptome datasets under abiotic stress treatments. *Frontiers in plant science* 6:475.

Funk, C. D. 2001. Prostaglandins and leukotrienes: advances in eicosanoid biology. *science* 294:1871-75.

Gachon, C. M., Sime-Ngando, T., Strittmatter, M., Chambouvet, A. & Kim, G. H. 2010. Algal diseases: spotlight on a black box. *Trends Plant Sci* 15:633-40.

Galletti, R., Denoux, C., Gambetta, S., Dewdney, J., Ausubel, F. M., De Lorenzo, G. & Ferrari, S. 2008. The AtrbohD-mediated oxidative burst elicited by oligogalacturonides in Arabidopsis is dispensable for the activation of defense responses effective against Botrytis cinerea. *Plant Physiol* 148:1695-706.

Galletti, R., Ferrari, S. & De Lorenzo, G. 2011. Arabidopsis MPK3 and MPK6 play different roles in basal and oligogalacturonide-or flagellin-induced resistance against Botrytis cinerea. *Plant Physiol* 157:804-14.

Gao, D., Kong, F., Sun, P., Bi, G. & Mao, Y. 2018. Transcriptome-wide identification of optimal reference genes for expression analysis of Pyropia yezoensis responses to abiotic stress. *BMC Genomics* 19:251.

Gaquerel, E., Hervé, C., Labrière, C., Boyen, C., Potin, P. & Salaün, J.-P. 2007. Evidence for oxylipin synthesis and induction of a new polyunsaturated fatty acid hydroxylase activity in Chondrus crispus in response to methyljasmonate. *Biochimica et Biophysica Acta (BBA)-Molecular and Cell Biology of Lipids* 1771:565-75.

Garscha, U., Jernerén, F., Chung, D., Keller, N. P., Hamberg, M. & Oliw, E. H. 2007. Identification of dioxygenases required for Aspergillus development. *J Biol Chem* 282:34707-18.

Gauna, M. C., Parodi, E. R. & Cáceres, E. J. 2009. Epi-endophytic symbiosis between Laminariocolax aecidioides (Ectocarpales, Phaeophyceae) and Undaria pinnatifida (Laminariales, Phaeophyceae) growing on Argentinian coasts. *J Appl Phycol* 21:11-18.

Gerwick, W. H. 1994. Structure and biosynthesis of marine algal oxylipins. *Biochimica et biophysica acta* 1211:243-55.

Gerwick, W. H. 1996. Epoxy allylic carbocations as conceptual intermediates in the biogenesis of diverse marine oxylipins. *Lipids* 31:1215-31.

Gerwick, W. H., Åsen, P. & Hamberg, M. 1993a. Biosynthesis of 13R-hydroxyarachidonic acid, an unusual oxylipin from the red alga lithothamnion corallioides. *Phytochemistry* 34:1029-33.

Gerwick, W. H., Moghaddam, M. & Hamberg, M. 1991. Oxylipin metabolism in the red alga Gracilariopsis lemaneiformis: mechanism of formation of vicinal dihydroxy fatty acids. *Archives of biochemistry and biophysics* 290:436-44.

Gerwick, W. H., Proteau, P. J., Nagle, D. G., Wise, M. L., Jiang, Z. D., Bernart, M. W. & Hamberg, M. 1993b. Biologically active oxylipins from seaweeds. *Hydrobiologia* 260:653-65.

Giacomoni, F., Le Corguille, G., Monsoor, M., Landi, M., Pericard, P., Pétéra, M., Duperier, C.,

Tremblay-Franco, M., Martin, J.-F. & Jacob, D. 2015. Workflow4Metabolomics: a collaborative research infrastructure for computational metabolomics. *Bioinformatics* 31:1493-95.

Gomi, K., Yamasaki, Y., Yamamoto, H. & Akimitsu, K. 2003. Characterization of a hydroperoxide lyase gene and effect of C6-volatiles on expression of genes of the oxylipin metabolism in Citrus. *J Plant Physiol* 160:1219-31.

González-Pérez, A. B., Grechkin, A. & de Lera, Á. R. 2017. Rearrangement of vinyl allene oxide geometric isomers to cyclopentenones. Further computational insights with biologically relevant model systems. *Organic & biomolecular chemistry* 15:2846-55.

Gould, S. B., Waller, R. F. & McFadden, G. I. 2008. Plastid evolution. *Annu Rev Plant Biol* 59.

Goulitquer, S., Ritter, A., Thomas, F., Ferec, C., Salaün, J. P. & Potin, P. 2009. Release of volatile aldehydes by the brown algal kelp Laminaria digitata in response to both biotic and abiotic stress. *ChemBioChem* 10:977-82.

Graber, M. A., Gerwick, W. H. & Cheney, D. P. 1996. The isolation and characterization of agardhilactone, a novel oxylipin from the marine red alga Agardhiella subulata. *Tetrahedron Lett* 37:4635-38.

Grabherr, M. G., Haas, B. J., Yassour, M., Levin, J. Z., Thompson, D. A., Amit, I., Adiconis, X., Fan, L., Raychowdhury, R. & Zeng, Q. 2011. Trinity: reconstructing a full-length transcriptome without a genome from RNA-Seq data. *Nat Biotechnol* 29:644.

Gregson, R. P., Marwood, J. F. & Quinn, R. J. 1979. The occurrence of prostaglandins PGE2 and PGF2α in a plant-the red alga Gracilaria Lichenoides. *Tetrahedron Lett* 20:4505-06.

Guidi, L., Mori, S., Degl'Innocenti, E. & Pecchia, S. 2007. Effects of ozone exposure or fungal pathogen on white lupin leaves as determined by imaging of chlorophyll a fluorescence. *Plant Physiol Biochem* 45:851-57.

Hámberg, M., Gerwick, W. H. & Åsen, P. A. 1992. Linoleic acid metabolism in the red alga Lithothamnion corallioides: Biosynthesis of 11 (R)-hydroxy-9 (Z), 12 (Z)-octadecadienoic acid. *Lipids* 27:487-93.

Hörnsten, L., Su, C., Osbourn, A. E., Garosi, P., Hellman, U., Wernstedt, C. & Oliw, E. H. 1999. Cloning of linoleate diol synthase reveals homology with prostaglandin H synthases. *J Biol Chem* 274:28219-24.

Halliwell, B. & Gutteridge, J. M. 1985. Free radicals in biology and medicine. Pergamon.

Hamberg, M. 1986. Isolation and structures of lipoxygenase products from Saprolegnia parasitica. *Biochimica et Biophysica Acta (BBA)-Lipids and Lipid Metabolism* 876:688-92.

Hamberg, M. & Gerwick, W. 1993. Biosynthesis of vicinal dihydroxy fatty acids in the red alga Gracilariopsis lemaneiformis: identification of a sodium-dependent 12-lipoxygenase and a hydroperoxide isomerase. *Archives of Biochemistry and Biophysics* 305:115-22.

Hamberg, M., Zhang, L.-Y., Brodowsky, I. D. & Oliw, E. H. 1994. Sequential oxygenation of linoleic acid in the fungus Gaeumannomyces graminis: stereochemistry of dioxygenase and hydroperoxide isomerase reactions. *Archives of biochemistry and biophysics* 309:77-80.

Hancock, J., Desikan, R. & Neill, S. 2001. Role of reactive oxygen species in cell signalling pathways. Portland Press Ltd.

Hander, T., Fernández-Fernández, Á. D., Kumpf, R. P., Willems, P., Schatowitz, H., Rombaut, D., Staes, A., Nolf, J., Pottie, R. & Yao, P. 2019. Damage on plants activates Ca2+-dependent metacaspases for release of immunomodulatory peptides. *Science* 363.

Harðardóttir, S., Wohlrab, S., Hjort, D. M., Krock, B., Nielsen, T. G., John, U. & Lundholm, N. 2019. Transcriptomic responses to grazing reveal the metabolic pathway leading to the

biosynthesis of domoic acid and highlight different defense strategies in diatoms. *BMC Mol Biol* 20:1-14.

Harder, T., Campbell, A. H., Egan, S. & Steinberg, P. D. 2012. Chemical mediation of ternary interactions between marine holobionts and their environment as exemplified by the red alga Delisea pulchra. *J Chem Ecol* 38:442-50.

Harris, S. G., Padilla, J., Koumas, L., Ray, D. & Phipps, R. P. 2002. Prostaglandins as modulators of immunity. *Trends Immunol* 23:144-50.

Haug, A., Larsen, B. & Smidsrød, O. 1974. Uronic acid sequence in alginate from different sources. *Carbohydrate Research* 32:217-25.

Heesch, S. & Peters, A. F. 1999. Scanning electron microscopy observation of host entry by two brown algae endophytic in Laminaria saccharina (Laminariales, Phaeophyceae). *Phycol Res* 47:1-5.

Heil, M. 2008. Indirect defence via tritrophic interactions. *New Phytol* 178:41-61.

Heil, M. 2010. Plastic defence expression in plants. *Evol Ecol* 24:555-69.

Heinrich, S., Valentin, K., Frickenhaus, S., John, U. & Wiencke, C. 2012. Transcriptomic analysis of acclimation to temperature and light stress in Saccharina latissima (Phaeophyceae). *PLoS One* 7:e44342.

Heinrich, S., Valentin, K., Frickenhaus, S. & Wiencke, C. 2015. Temperature and light interactively modulate gene expression in Saccharina latissima (Phaeophyceae). *J Phycol* 51:93-108.

Heitz, T., Widemann, E., Lugan, R., Miesch, L., Ullmann, P., Désaubry, L., Holder, E., Grausem, B., Kandel, S. & Miesch, M. 2012. Cytochromes P450 CYP94C1 and CYP94B3 catalyze two successive oxidation steps of plant hormone jasmonoyl-isoleucine for catabolic turnover. *J Biol Chem* 287:6296-306.

Henderson, G., Wells, J. & Jeanne, R. 1991. Methyl palmitate and methyl myristate repel flies. *The Florida Entomologist* 74:365-68.

Herman, R. P. & Hamberg, M. 1987. Properties of the soluble arachidonic acid 15-lipoxygenase and 15-hydroperoxide isomerase from the oomycete Saprolegnia parasitica. *Prostaglandins* 34:129-39.

Hervé, C., Tonon, T., Collén, J., Corre, E. & Boyen, C. 2006. NADPH oxidases in Eukaryotes: red algae provide new hints! *Curr Genet* 49:190-204.

Higgs, M. & Mulheirn, L. 1981. Hybridalactone, an unusual fatty acid metabolite from the red alga Laurencia hybrida (Rhodophyta, Rhodomelaceae). *Tetrahedron* 37:4259-62.

Hoeberichts, F. A., Ten Have, A. & Woltering, E. J. 2003. A tomato metacaspase gene is upregulated during programmed cell death in Botrytis cinerea-infected leaves. *Planta* 217:517-22.

Hu, H., Zhang, R., Tao, Z., Li, X., Li, Y., Huang, J., Li, X., Han, X., Feng, S. & Zhang, G. 2018. Cellulose synthase mutants distinctively affect cell growth and cell wall integrity for plant biomass production in Arabidopsis. *Plant and Cell Physiology* 59:1144-57.

Ianora, A., Bastianini, M., Carotenuto, Y., Casotti, R., Roncalli, V., Miralto, A., Romano, G., Gerecht, A., Fontana, A. & Turner, J. T. 2015. Non-volatile oxylipins can render some diatom blooms more toxic for copepod reproduction. *Harmful Algae* 44:1-7.

Imbs, A. B., Vologodskaya, A. V., Nevshupova, N. V., Khotimchenko, S. V. & Titlyanov, E. A. 2001. Response of prostaglandin content in the red alga Gracilaria verrucosa to season and solar irradiance. *Phytochemistry* 58:1067-72.

Ishiguro, S., Kawai-Oda, A., Ueda, J., Nishida, I. & Okada, K. 2001. The DEFECTIVE IN ANTHER DEHISCENCE1 gene encodes a novel phospholipase A1 catalyzing the initial step of

jasmonic acid biosynthesis, which synchronizes pollen maturation, anther dehiscence, and flower opening in Arabidopsis. *The Plant Cell* 13:2191-209.

Jayaswall, K., Mahajan, P., Singh, G., Parmar, R., Seth, R., Raina, A., Swarnkar, M. K., Singh, A. K., Shankar, R. & Sharma, R. K. 2016. Transcriptome analysis reveals candidate genes involved in blister blight defense in tea (Camellia sinensis (L) Kuntze). *Scientific reports* 6:1-14.

Jensen, E. C., Ogg, C. & Nickerson, K. W. 1992. Lipoxygenase inhibitors shift the yeast/mycelium dimorphism in Ceratocystis ulmi. *Appl Environ Microbiol* 58:2505-08.

Jiang, Z.-D. & Gerwick, W. H. 1997. Novel oxylipins from the temperate red alga Polyneura latissima: evidence for an arachidonate 9 (S)-lipoxygenase. *Lipids* 32:231-35.

Jiang, Z. D. & Gerwick, W. H. 1991. Eicosanoids and other hydroxylated fatty acids from the marine alga Gracilariopsis lemaneiformis. *Phytochemistry* 30:1187-90.

Jiang, Z. D., Ketchum, S. O. & Gerwick, W. H. 2000. 5-Lipoxygenase-derived oxylipins from the red alga Rhodymenia pertusa. *Phytochemistry* 53:129-33.

Küpper, F. C., Gaquerel, E., Boneberg, E.-M., Morath, S., Salaün, J.-P. & Potin, P. 2006. Early events in the perception of lipopolysaccharides in the brown alga Laminaria digitata include an oxidative burst and activation of fatty acid oxidation cascades. *J Exp Bot* 57:1991-99.

Küpper, F. C., Gaquerel, E., Cosse, A., Adas, F., Peters, A. F., Müller, D. G., Kloareg, B., Salaün, J.-P. & Potin, P. 2009. Free fatty acids and methyl jasmonate trigger defense reactions in Laminaria digitata. *Plant and Cell Physiology* 50:789-800.

Küpper, F. C., Kloareg, B., Guern, J. & Potin, P. 2001. Oligoguluronates elicit an oxidative burst in the brown algal kelp Laminaria digitata. *Plant Physiol* 125:278-91.

Küpper, F. C., Müller, D. G., Peters, A. F., Kloareg, B. & Potin, P. 2002. Oligoalginate recognition and oxidative burst play a key role in natural and induced resistance of sporophytes of Laminariales. *J Chem Ecol* 28:2057-81.

Kanamoto, H., Takemura, M. & Ohyama, K. 2011. Identification of a cyclooxygenase gene from the red alga Gracilaria vermiculophylla and bioconversion of arachidonic acid to PGF 2α in engineered Escherichia coli. *Appl Microbiol Biotechnol* 91:1121-29.

Kawai, H. & Tokuyama, M. 1995. Laminarionema elsbetiae gen. et sp. nov.(Ectocarpales, Phaeophyceae), a new endophyte in Laminaria sporophytes. *Phycol Res* 43:185-90.

Kim, H. S., Lee, C.-G. & Lee, E. Y. 2011. Alginate lyase: structure, property, and application. *Biotechnology and bioprocess engineering* 16:843.

Kim, J. S., Kim, Y. H., Seo, Y. W. & Park, S. 2007. Quorum sensing inhibitors from the red alga, Ahnfeltiopsis flabelliformis. *Biotechnology and Bioprocess Engineering* 12:308-11.

Kishimoto, K., Matsui, K., Ozawa, R. & Takabayashi, J. 2005. Volatile C6-aldehydes and allo-ocimene activate defense genes and induce resistance against Botrytis cinerea in Arabidopsis thaliana. *Plant and Cell Physiology* 46:1093-102.

Knight, H. 1999. Calcium signaling during abiotic stress in plants. *Int Rev Cytol.* Elsevier, pp. 269-324.

Kock, J. L., Strauss, C. J., Pohl, C. H. & Nigam, S. 2003. The distribution of 3-hydroxy oxylipins in fungi. *Prostaglandins & other lipid mediators* 71:85-96.

Koeduka, T., Ishizaki, K., Mwenda, C. M., Hori, K., Sasaki-Sekimoto, Y., Ohta, H., Kohchi, T. & Matsui, K. 2015. Biochemical characterization of allene oxide synthases from the liverwort Marchantia polymorpha and green microalgae Klebsormidium flaccidum provides insight into the evolutionary divergence of the plant CYP74 family. *Planta* 242:1175-86.

Koeduka, T., Kajiwara, T. & Matsui, K. 2007. Cloning of lipoxygenase genes from a cyanobacterium, Nostoc punctiforme, and its expression in Eschelichia coli. *Curr Microbiol* 54:315-19.

Konotchick, T., Dupont, C. L., Valas, R. E., Badger, J. H. & Allen, A. E. 2013. Transcriptomic analysis of metabolic function in the giant kelp, M acrocystis pyrifera, across depth and season. *New Phytol* 198:398-407.

Koo, A. J., Cooke, T. F. & Howe, G. A. 2011. Cytochrome P450 CYP94B3 mediates catabolism and inactivation of the plant hormone jasmonoyl-L-isoleucine. *Proceedings of the National Academy of Sciences* 108:9298-303.

Kopylova, E., Noé, L. & Touzet, H. 2012. SortMeRNA: fast and accurate filtering of ribosomal RNAs in metatranscriptomic data. *Bioinformatics* 28:3211-17.

Kornmann, P. & Sahling, P.-H. 1994. Meeresalgen von Helgoland: Zweite Ergänzung. *Helgoländer Meeresuntersuchungen* 48:365-406.

Kousaka, K., Ogi, N., Akazawa, Y., Fujieda, M., Yamamoto, Y., Takada, Y. & Kimura, J. 2003. Novel oxylipin metabolites from the brown alga Eisenia bicyclis. *J Nat Prod* 66:1318-23.

Kowalczyk, N., Rousvoal, S., Hervé, C., Boyen, C. & Collén, J. 2014. RT-qPCR normalization genes in the red alga Chondrus crispus. *PloS one* 9.

Kumar, M., Kumari, P., Gupta, V., Anisha, P., Reddy, C. & Jha, B. 2010. Differential responses to cadmium induced oxidative stress in marine macroalga Ulva lactuca (Ulvales, Chlorophyta). *BioMetals* 23:315-25.

Kumar, M., Trivedi, N., Reddy, C. & Jha, B. 2011. Toxic effects of imidazolium ionic liquids on the green seaweed Ulva lactuca: oxidative stress and DNA damage. *Chem Res Toxicol* 24:1882-90.

Kumar, S., Stecher, G. & Tamura, K. 2016. MEGA7: molecular evolutionary genetics analysis version 7.0 for bigger datasets. *Mol Biol Evol* 33:1870-74.

Kumari, P., Kumar, M., Reddy, C. & Jha, B. 2013. Algal lipids, fatty acids and sterols. *Functional ingredients from algae for foods and nutraceuticals*. Elsevier, pp. 87-134.

Kumari, P., Kumar, M., Reddy, C. & Jha, B. 2014a. Nitrate and phosphate regimes induced lipidomic and biochemical changes in the intertidal macroalga Ulva lactuca (Ulvophyceae, Chlorophyta). *Plant and Cell Physiology* 55:52-63.

Kumari, P., Reddy, C. & Jha, B. 2015. Methyl jasmonate-induced lipidomic and biochemical alterations in the intertidal macroalga Gracilaria dura (Gracilariaceae, Rhodophyta). *Plant and Cell Physiology* 56:1877-89.

Kumari, P., Reddy, R. & Jha, B. 2014b. Quantification of selected endogenous hydroxy-oxylipins from tropical marine macroalgae. *Mar Biotechnol* 16:74-87.

Kuo, J.-M., Hwang, A., Hsu, H. H. & Pan, B. S. 1996. Preliminary identification of lipoxygenase in algae (Enteromorpha intestinalis) for aroma formation. *J Agric Food Chem* 44:2073-77.

Kuo, J.-M., Hwang, A. & Yeh, D.-B. 1997. Purification, substrate specificity, and products of a Ca2+-stimulating lipoxygenase from sea algae (Ulva lactuca). *J Agric Food Chem* 45:2055-60.

Kurata, K., Taniguchi, K., Shiraishi, K., Hayama, N., Tanaka, I. & Suzuki, M. 1989. Ecklonialactone-A and-B, two unusual metabolites from the brown alga Ecklonia stolonifera Okamura. *Chemistry Letters* 18:267-70.

Kurata, K., Taniguchi, K., Shiraishi, K. & Suzuki, M. 1993. Ecklonialactones-CF from the brown alga Ecklonia stolonifera. *Phytochemistry* 33:155-59.

Kustka, A. B., Shaked, Y., Milligan, A. J., King, D. W. & Morel, F. M. 2005. Extracellular production of superoxide by marine diatoms: Contrasting effects on iron redox chemistry and bioavailability. *Limnol Oceanogr* 50:1172-80.

Lüning, K. & Mortensen, L. 2015. European aquaculture of sugar kelp (Saccharina latissima) for

food industries: iodine content and epiphytic animals as major problems. *Bot Mar* 58:449-55.

López, M. A., Vicente, J., Kulasekaran, S., Vellosillo, T., Martínez, M., Irigoyen, M. L., Cascón, T., Bannenberg, G., Hamberg, M. & Castresana, C. 2011. Antagonistic role of 9-lipoxygenase-derived oxylipins and ethylene in the control of oxidative stress, lipid peroxidation and plant defence. *The Plant Journal* 67:447-58.

La Barre, S., Potin, P., Leblanc, C. & Delage, L. 2010. The halogenated metabolism of brown algae (Phaeophyta), its biological importance and its environmental significance. *Mar Drugs* 8:988-1010.

Lakhssassi, N., Piya, S., Bekal, S., Liu, S., Zhou, Z., Bergounioux, C., Miao, L., Meksem, J., Lakhssassi, A. & Jones, K. 2020. A pathogenesis - related protein GmPR08 - Bet VI promotes a molecular interaction between the GmSHMT08 and GmSNAP18 in resistance to Heterodera glycines. *Plant Biotechnol J* 18:1810.

Lamacka, M. & Sajbidor, J. 1998. The content of prostaglandins and their precursors in Mortierella and Cunninghamella species. *Lett Appl Microbiol* 26:224-26.

Lamari, N., Ruggiero, M. V., d'Ippolito, G., Kooistra, W. H., Fontana, A. & Montresor, M. 2013. Specificity of lipoxygenase pathways supports species delineation in the marine diatom genus Pseudo-nitzschia. *PLoS One* 8:e73281.

Lang, I. & Feussner, I. 2007. Oxylipin formation in Nostoc punctiforme (PCC73102). *Phytochemistry* 68:1120-27.

Lang, I., Göbel, C., Porzel, A., Heilmann, I. & Feussner, I. 2008. A lipoxygenase with linoleate diol synthase activity from Nostoc sp. PCC 7120. *Biochem J* 410:347-57.

Langmead, B. & Salzberg, S. L. 2012. Fast gapped-read alignment with Bowtie 2. *Nat Methods* 9:357.

Le Bail, A., Dittami, S. M., de Franco, P.-O., Rousvoal, S., Cock, M. J., Tonon, T. & Charrier, B. 2008. Normalisation genes for expression analyses in the brown alga model Ectocarpus siliculosus. *BMC Mol Biol* 9:75.

Leblanc, C., Colin, C., Cosse, A., Delage, L., La Barre, S., Morin, P., Fiévet, B., Voiseux, C., Ambroise, Y. & Verhaeghe, E. 2006. Iodine transfers in the coastal marine environment: the key role of brown algae and of their vanadium-dependent haloperoxidases. *Biochimie* 88:1773-85.

Lee, D.-S., Nioche, P., Hamberg, M. & Raman, C. 2008. Structural insights into the evolutionary paths of oxylipin biosynthetic enzymes. *Nature* 455:363-68.

Lee, H. J., Yoo, E. S., Hong, J., Choi, J. S. & Jung, J. H. 2010. The occurrence of 15-keto-prostaglandins in the red alga Gracilaria verrucosa. *Archives of pharmacal research* 33:1325-29.

Lee, J. H., Pestova, T. V., Shin, B.-S., Cao, C., Choi, S. K. & Dever, T. E. 2002. Initiation factor eIF5B catalyzes second GTP-dependent step in eukaryotic translation initiation. *Proceedings of the National Academy of Sciences* 99:16689-94.

Lee, W.-K., Namasivayam, P., Abdullah, J. O. & Ho, C.-L. 2017. Transcriptome profiling of sulfate deprivation responses in two agarophytes Gracilaria changii and Gracilaria salicornia (Rhodophyta). *Scientific reports* 7:1-14.

Lein, T. E., Sjøtun, K. & Wakili, S. 1991. Mass-occurrence of a brown filamentous endophyte in the lamina of the kelp Laminaria hyperborea (Gunnerus) Foslie along the southwestern coast of Norway. *Sarsia* 76:187-93.

Leliaert, F., Smith, D. R., Moreau, H., Herron, M. D., Verbruggen, H., Delwiche, C. F. & De Clerck,

O. 2012. Phylogeny and molecular evolution of the green algae. *Crit Rev Plant Sci* 31:1-46.

Leuti, A., Fazio, D., Fava, M., Piccoli, A., Oddi, S. & Maccarrone, M. 2020. Bioactive lipids, inflammation and chronic diseases. *Adv Drug Del Rev*.

Li, B. & Dewey, C. N. 2011a. RSEM: accurate transcript quantification from RNA-Seq data with or without a reference genome. *BMC Bioinformatics* 12:1-16.

Li, H., Monteiro, C., Heinrich, S., Bartsch, I., Valentin, K., Harms, L., Glöckner, G., Corre, E. & Bischof, K. 2020a. Responses of the kelp Saccharina latissima (Phaeophyceae) to the warming Arctic: from physiology to transcriptomics. *Physiol Plant* 168:5-26.

Li, H., Scheschonk, L., Heinrich, S., Valentin, K., Harms, L., Glöckner, G., Corre, E. & Bischof, K. 2020b. Transcriptomic responses to darkness and the survival strategy of the kelp Saccharina latissima in the early Polar night. *Frontiers in Marine Science*.

Lim, C. W., Han, S.-W., Hwang, I. S., Kim, D. S., Hwang, B. K. & Lee, S. C. 2015. The Pepper Lipoxygenase CaLOX1 Plays a Role in Osmotic, Drought and High Salinity Stress Response. *Plant and Cell Physiology* 56:930-42.

Lion, U., Wiesemeier, T., Weinberger, F., Beltrán, J., Flores, V., Faugeron, S., Correa, J. & Pohnert, G. 2006. Phospholipases and galactolipases trigger oxylipin-mediated wound-activated defence in the red alga Gracilaria chilensis against epiphytes. *ChemBioChem* 7:457-62.

Liu, F., Wang, W., Sun, X., Liang, Z. & Wang, F. 2014. RNA-Seq revealed complex response to heat stress on transcriptomic level in Saccharina japonica (Laminariales, Phaeophyta). *J Appl Phycol* 26:1585-96.

Liu, G. 2004. *Jasmonate regulation of defense responses in tomato (Lycopersicon esculentum).* Michigan State University,

Liu, H., Wang, X., Zhang, H., Yang, Y., Ge, X. & Song, F. 2008. A rice serine carboxypeptidase-like gene OsBISCPL1 is involved in regulation of defense responses against biotic and oxidative stress. *Gene* 420:57-65.

Liu, X., Guan, H., Song, M., Fu, Y., Han, X., Lei, M., Ren, J., Guo, B., He, W. & Wei, Y. 2018. Reference gene selection for qRT-PCR assays in Stellera chamaejasme subjected to abiotic stresses and hormone treatments based on transcriptome datasets. *PeerJ* 6:e4535.

Longmead, B. & Salzberg, S. 2012. Fast gapped-read alignment with Bowtie2.

Love, M., Anders, S. & Huber, W. 2014. DESeq2: Differential gene expression analysis based on the negative binomial distribution. Bioconductor.

Love, M. I., Anders, S. & Huber, W. 2019. Analyzing RNA-seq data with DESeq2.

Lowe, R., Shirley, N., Bleackley, M., Dolan, S. & Shafee, T. 2017. Transcriptomics technologies. *PLoS Comp Biol* 13:e1005457.

Lu, C., Shao, Z., Zhang, P. & Duan, D. 2020. Genome-wide analysis of the Saccharina japonica sulfotransferase genes and their transcriptional profiles during whole developmental periods and under abiotic stresses. *BMC Plant Biol* 20:1-20.

Luo, J., Wei, K., Wang, S., Zhao, W., Ma, C., Hettenhausen, C., Wu, J., Cao, G., Sun, G. & Baldwin, I. T. 2016. COI1-regulated hydroxylation of jasmonoyl-L-isoleucine impairs Nicotiana attenuata's resistance to the generalist herbivore Spodoptera litura. *J Agric Food Chem* 64:2822-31.

Luo, Q., Zhu, Z., Yang, R., Qian, F., Yan, X. & Chen, H. 2015. Characterization of a respiratory burst oxidase homologue from Pyropia haitanensis with unique molecular phylogeny and rapid stress response. *J Appl Phycol* 27:945-55.

Luque, J., Cohen, M., Savé, R., Biel, C. & Álvarez, I. F. 1999. Effects of three fungal pathogens on

water relations, chlorophyll fluorescence and growth of Quercus suber L. *Annals of Forest Science* 56:19-26.

Ma, R., Xu, S., Zhao, Y., Xia, B. & Wang, R. 2016. Selection and validation of appropriate reference genes for quantitative real-time PCR analysis of gene expression in Lycoris aurea. *Frontiers in plant science* 7:536.

Macaisne, N., Liu, F., Scornet, D., Peters, A. F., Lipinska, A., Perrineau, M.-M., Henry, A., Strittmatter, M., Coelho, S. M. & Cock, J. M. 2017. The Ectocarpus IMMEDIATE UPRIGHT gene encodes a member of a novel family of cysteine-rich proteins with an unusual distribution across the eukaryotes. *Development* 144:409-18.

Mann, M., Serif, M., Wrobel, T., Eisenhut, M., Madhuri, S., Flachbart, S., Weber, A. P., Lepetit, B., Wilhelm, C. & Kroth, P. G. 2020. The aureochrome photoreceptor PtAUREO1a is a highly effective blue light switch in diatoms. *Iscience* 23:101730.

Marshall, J.-A., Ross, T., Pyecroft, S. & Hallegraeff, G. 2005. Superoxide production by marine microalgae. *Mar Biol* 147:541-49.

Matsuda, Y., Beppu, T. & Arima, K. 1978. Circular dichroism of Fusarium lipoxygenase from Fusarium oxysporum. *Biochem Biophys Res Commun* 85:203-08.

Matsuda, Y., Satoh, T., Beppu, T. & Arima, K. 1976. Purification and properties of Co2+ requiring heme protein having lipoxygenase activity from Fusarium oxysporum. *Agric Biol Chem* 40:963-76.

Matsui, K. 2006. Green leaf volatiles: hydroperoxide lyase pathway of oxylipin metabolism. *Curr Opin Plant Biol* 9:274-80.

Matthijs, M., Fabris, M., Obata, T., Foubert, I., Franco-Zorrilla, J. M., Solano, R., Fernie, A. R., Vyverman, W. & Goossens, A. 2017. The transcription factor bZIP14 regulates the TCA cycle in the diatom Phaeodactylum tricornutum. *The EMBO journal* 36:1559-76.

Metting, F. 1996. Biodiversity and application of microalgae. *Journal of industrial microbiology* 17:477-89.

Meyer, N., Rettner, J., Werner, M., Werz, O. & Pohnert, G. 2018. Algal oxylipins mediate the resistance of diatoms against algicidal bacteria. *Mar Drugs* 16:486.

Michel, G., Tonon, T., Scornet, D., Cock, J. M. & Kloareg, B. 2010. The cell wall polysaccharide metabolism of the brown alga Ectocarpus siliculosus. Insights into the evolution of extracellular matrix polysaccharides in Eukaryotes. *New Phytol* 188:82-97.

Miralto, A., Barone, G., Romano, G., Poulet, S., Ianora, A., Russo, G., Buttino, I., Mazzarella, G., Laabir, M. & Cabrini, M. 1999. The insidious effect of diatoms on copepod reproduction. *Nature* 402:173-76.

Moghaddam, M., Gerwick, W. & Ballantine, D. 1989. Discovery of 12-(S)-hydroxy-5, 8, 10, 14-icosatetraenoic acid [12-(S)-HETE] in the tropical red alga Platysiphonia miniata. *Prostaglandins* 37:303-08.

Monte, I., Ishida, S., Zamarreño, A. M., Hamberg, M., Franco-Zorrilla, J. M., García-Casado, G., Gouhier-Darimont, C., Reymond, P., Takahashi, K. & García-Mina, J. M. 2018. Ligand-receptor co-evolution shaped the jasmonate pathway in land plants. *Nat Chem Biol* 14:480-88.

Monteiro, C., Heinrich, S., Bartsch, I., Valentin, K., Corre, E., Collén, J., Harms, L., Glöckner, G. & Bischof, K. 2019a. Temperature modulates sex-biased gene expression in the gametophytes of the kelp Saccharina latissima. *Frontiers in Marine Science* 6:769.

Monteiro, C. M. M., Li, H., Bischof, K., Bartsch, I., Valentin, K. U., Corre, E., Collén, J., Harms, L., Glöckner, G. & Heinrich, S. 2019b. Is geographical variation driving the transcriptomic

responses to multiple stressors in the kelp Saccharina latissima? *BMC Plant Biol* 19:1-15.

Montillet, J.-L., Leonhardt, N., Mondy, S., Tranchimand, S., Rumeau, D., Boudsocq, M., Garcia, A. V., Douki, T., Bigeard, J. & Lauriere, C. 2013. An abscisic acid-independent oxylipin pathway controls stomatal closure and immune defense in Arabidopsis. *PLoS Biol* 11:e1001513.

Moscatiello, R., Mariani, P., Sanders, D. & Maathuis, F. J. 2006. Transcriptional analysis of calcium-dependent and calcium-independent signalling pathways induced by oligogalacturonides. *J Exp Bot* 57:2847-65.

Mugford, S. T., Qi, X., Bakht, S., Hill, L., Wegel, E., Hughes, R. K., Papadopoulou, K., Melton, R., Philo, M. & Sainsbury, F. 2009. A serine carboxypeptidase-like acyltransferase is required for synthesis of antimicrobial compounds and disease resistance in oats. *The Plant Cell* 21:2473-84.

Murakami, N., Shirahashi, H., Nagatsu, A. & Sakakibara, J. 1992. Two unsaturated 9R-hydroxy fatty acids from the cyanobacteriumAnabaena flos-aquae f. flos-aquae. *Lipids* 27:776-78.

Murata, N., Takahashi, S., Nishiyama, Y. & Allakhverdiev, S. I. 2007. Photoinhibition of photosystem II under environmental stress. *Biochimica et Biophysica Acta (BBA)-Bioenergetics* 1767:414-21.

Nanjappa, D., d'Ippolito, G., Gallo, C., Zingone, A. & Fontana, A. 2014. Oxylipin diversity in the diatom family Leptocylindraceae reveals DHA derivatives in marine diatoms. *Mar Drugs* 12:368-84.

Newcomer, M. E. & Brash, A. R. 2015. The structural basis for specificity in lipoxygenase catalysis. *Protein Sci* 24:298-309.

Ng, D. W., Abeysinghe, J. K. & Kamali, M. 2018. Regulating the regulators: The control of transcription factors in plant defense signaling. *International journal of molecular sciences* 19:3737.

Niaz, Z., Sui, Z., Riaz, S., Liu, Y., Shang, E., Xing, Q., Khan, S., Du, Q. & Zhou, W. 2019. Identification of valid reference genes for the normalization of RT-qPCR gene expression data in Alexandrium catenella under different nutritional conditions. *J Appl Phycol* 31:1819-33.

Nishizawa, A., Yabuta, Y., Yoshida, E., Maruta, T., Yoshimura, K. & Shigeoka, S. 2006. Arabidopsis heat shock transcription factor A2 as a key regulator in response to several types of environmental stress. *The Plant Journal* 48:535-47.

Niu, M., Steffan, B. N., Fischer, G. J., Venkatesh, N., Raffa, N. L., Wettstein, M. A., Bok, J. W., Greco, C., Zhao, C. & Berthier, E. 2020. Fungal oxylipins direct programmed developmental switches in filamentous fungi. *Nature communications* 11:1-13.

Not, F., Siano, R., Kooistra, W. H., Simon, N., Vaulot, D. & Probert, I. 2012. Diversity and ecology of eukaryotic marine phytoplankton. *Adv Bot Res*. Elsevier, pp. 1-53.

Noverr, M. C., Erb-Downward, J. R. & Huffnagle, G. B. 2003. Production of eicosanoids and other oxylipins by pathogenic eukaryotic microbes. *Clin Microbiol Rev* 16:517-33.

Noverr, M. C., Phare, S. M., Toews, G. B., Coffey, M. J. & Huffnagle, G. B. 2001. Pathogenic yeasts Cryptococcus neoformans and Candida albicans produce immunomodulatory prostaglandins. *Infect Immun* 69:2957-63.

Nylund, G. M., Enge, S. & Pavia, H. 2013. Costs and benefits of chemical defence in the red alga Bonnemaisonia hamifera. *Plos One* 8:e61291.

Nylund, G. M., Weinberger, F., Rempt, M. & Pohnert, G. 2011. Metabolomic assessment of induced and activated chemical defence in the invasive red alga Gracilaria vermiculophylla. *PLoS One* 6:e29359.

Oliw, E. H. 2002. Plant and fungal lipoxygenases. *Prostaglandins & other lipid mediators* 68:313-23.

Paredes Juárez, G. A., Spasojevic, M., Faas, M. M. & de Vos, P. 2014. Immunological and technical considerations in application of alginate-based microencapsulation systems. *Frontiers in bioengineering and biotechnology* 2:26.

Parke, M. 1948. Studies on British laminariaceae. I. growth in Laminaria saccharina (l.) lamour. *J Mar Biol Assoc UK* 27:651-709.

Peng, Q., Su, Y., Ling, H., Ahmad, W., Gao, S., Guo, J., Que, Y. & Xu, L. 2017. A sugarcane pathogenesis-related protein, ScPR10, plays a positive role in defense responses under Sporisorium scitamineum, SrMV, SA, and MeJA stresses. *Plant Cell Rep* 36:1427-40.

Peters-Golden, M., Gleason, M. & Togias, A. 2006. Cysteinyl leukotrienes: multi-functional mediators in allergic rhinitis. *Clinical & Experimental Allergy* 36:689-703.

Peters, A. 1996. New record of the kelp endophyte Laminarionema elsbetiae (Phaeophyceae, Ectocarpales) at Helgoland and its life history in culture. *Nova Hedwigia* 62:341-9.

Peters, A. F., Scornet, D., Ratin, M., Charrier, B., Monnier, A., Merrien, Y., Corre, E., Coelho, S. M. & Cock, J. M. 2008. Life-cycle-generation-specific developmental processes are modified in the immediate upright mutant of the brown alga Ectocarpus siliculosus. *Development* 135:1503-12.

Pombo, M. A., Zheng, Y., Fei, Z., Martin, G. B. & Rosli, H. G. 2017a. Use of RNA-seq data to identify and validate RT-qPCR reference genes for studying the tomato-Pseudomonas pathosystem. *Scientific reports* 7:1-11.

Potin, P. 2008. Oxidative burst and related responses in biotic interactions of algae. *Algal chemical ecology.* Springer, pp. 245-71.

Potin, P., Bouarab, K., Salaün, J.-P., Pohnert, G. & Kloareg, B. 2002. Biotic interactions of marine algae. *Curr Opin Plant Biol* 5:308-17.

Powell, W. S. & Rokach, J. 2015. Biosynthesis, biological effects, and receptors of hydroxyeicosatetraenoic acids (HETEs) and oxoeicosatetraenoic acids (oxo-ETEs) derived from arachidonic acid. *Biochimica et Biophysica Acta (BBA)-Molecular and Cell Biology of Lipids* 1851:340-55.

Proteau, P. J. 1993. Oxylipins from temperate marine algae and a photoprotective sheath pigment from blue-green algae.

Proteau, P. J. & Gerwick, W. H. 1992. Cymathere ethers A and B: bicyclic oxylipins from the marine brown alga Cymathere triplicata. *Tetrahedron Lett* 33:4393-96.

Proteau, P. J., Rossi, J. V. & Gerwick, W. H. 1994. Absolute stereochemistry of neohalicholactone from the brown alga Laminaria sinclairii. *J Nat Prod* 57:1717-19.

Provasoli, L. 1968. Media and prospects for the cultivation of marine algae. *Cultures and Collections of Algae. Proceedings of US-Japan Conference, Hakone, September 1966.* Japan Society of Plant Physiology.

Ralph, P. J. & Short, F. T. 2002. Impact of the wasting disease pathogen, Labyrinthula zosterae, on the photobiology of eelgrass Zostera marina. *Mar Ecol Prog Ser* 226:265-71.

Ray, R., Li, D., Halitschke, R. & Baldwin, I. T. 2019. Using natural variation to achieve a whole-plant functional understanding of the responses mediated by jasmonate signaling. *The Plant Journal* 99:414-25.

Rempt, M., Weinberger, F., Grosser, K. & Pohnert, G. 2012. Conserved and species-specific oxylipin pathways in the wound-activated chemical defense of the noninvasive red alga Gracilaria chilensis and the invasive Gracilaria vermiculophylla. *Beilstein journal of organic chemistry*

8:283-89.

Reyes-Prieto, A., Weber, A. P. & Bhattacharya, D. 2007. The origin and establishment of the plastid in algae and plants. *Annu Rev Genet* 41:147-68.

Ribalet, F., Berges, J. A., Ianora, A. & Casotti, R. 2007. Growth inhibition of cultured marine phytoplankton by toxic algal-derived polyunsaturated aldehydes. *Aquat Toxicol* 85:219-27.

Ribalet, F., Intertaglia, L., Lebaron, P. & Casotti, R. 2008. Differential effect of three polyunsaturated aldehydes on marine bacterial isolates. *Aquat Toxicol* 86:249-55.

Ritter, A., Cabioch, L., Brillet-Guéguen, L., Corre, E., Cosse, A., Dartevelle, L., Duruflé, H., Fasshauer, C., Goulitquer, S. & Thomas, F. 2017a. Herbivore-induced chemical and molecular responses of the kelps Laminaria digitata and Lessonia spicata. *PLoS One* 12:e0173315.

Ritter, A., Dittami, S. M., Goulitquer, S., Correa, J. A., Boyen, C., Potin, P. & Tonon, T. 2014. Transcriptomic and metabolomic analysis of copper stress acclimation in Ectocarpus siliculosus highlights signaling and tolerance mechanisms in brown algae. *BMC Plant Biol* 14:1-17.

Ritter, A., Goulitquer, S., Salaün, J. P., Tonon, T., Correa, J. A. & Potin, P. 2008. Copper stress induces biosynthesis of octadecanoid and eicosanoid oxygenated derivatives in the brown algal kelp Laminaria digitata. *New Phytol* 180:809-21.

Romano, M., Cianci, E., Simiele, F. & Recchiuti, A. 2015. Lipoxins and aspirin-triggered lipoxins in resolution of inflammation. *Eur J Pharmacol* 760:49-63.

Ruocco, N., Albarano, L., Esposito, R., Zupo, V., Costantini, M. & Ianora, A. 2020a. Multiple roles of diatom-derived oxylipins within marine environments and their potential biotechnological applications. *Mar Drugs* 18:342.

Ruocco, N., Nuzzo, G., d'Ippolito, G., Manzo, E., Sardo, A., Ianora, A., Romano, G., Iuliano, A., Zupo, V. & Costantini, M. 2020b. Lipoxygenase Pathways in Diatoms: Occurrence and Correlation with Grazer Toxicity in Four Benthic Species. *Mar Drugs* 18:66.

Russell, G. 1964. Laminariocolax tomentosoides on the Isle of Man. *J Mar Biol Assoc UK* 44:601-12.

Russo, E., d'Ippolito, G., Fontana, A., Sarno, D., D'Alelio, D., Busseni, G., Ianora, A., von Elert, E. & Carotenuto, Y. 2020. Density-dependent oxylipin production in natural diatom communities: Possible implications for plankton dynamics. *The ISME journal* 14:164-77.

Saha, M., Rempt, M., Gebser, B., Grueneberg, J., Pohnert, G. & Weinberger, F. 2012. Dimethylsulphopropionate (DMSP) and proline from the surface of the brown alga Fucus vesiculosus inhibit bacterial attachment. *Biofouling* 28:593-604.

Salavarría, E., Paul, S., Gil-Kodaka, P. & Villena, G. K. 2018. First global transcriptome analysis of brown algae Macrocystis integrifolia (Phaeophyceae) under marine intertidal conditions. *3 Biotech* 8:185.

Sanders, P. M., Lee, P. Y., Biesgen, C., Boone, J. D., Beals, T. P., Weiler, E. W. & Goldberg, R. B. 2000. The Arabidopsis DELAYED DEHISCENCE1 gene encodes an enzyme in the jasmonic acid synthesis pathway. *The Plant Cell* 12:1041-61.

Savchenko, T., Kolla, V. A., Wang, C.-Q., Nasafi, Z., Hicks, D. R., Phadungchob, B., Chehab, W. E., Brandizzi, F., Froehlich, J. & Dehesh, K. 2014. Functional convergence of oxylipin and abscisic acid pathways controls stomatal closure in response to drought. *Plant Physiol* 164:1151-60.

Schena, M., Shalon, D., Davis, R. W. & Brown, P. O. 1995. Quantitative monitoring of gene expression patterns with a complementary DNA microarray. *Science* 270:467-70.

Schneider, C., Niisuke, K., Boeglin, W. E., Voehler, M., Stec, D. F., Porter, N. A. & Brash, A. R. 2007. Enzymatic synthesis of a bicyclobutane fatty acid by a hemoprotein–lipoxygenase fusion protein from the cyanobacterium Anabaena PCC 7120. *Proceedings of the National Academy of Sciences* 104:18941-45.

Schnitzler, I., Pohnert, G., Hay, M. & Boland, W. 2001. Chemical defense of brown algae (Dictyopteris spp.) against the herbivorous amphipod Ampithoe longimana. *Oecologia* 126:515-21.

Scholz, J., Brodhun, F., Hornung, E., Herrfurth, C., Stumpe, M., Beike, A. K., Faltin, B., Frank, W., Reski, R. & Feussner, I. 2012. Biosynthesis of allene oxides in Physcomitrella patens. *BMC Plant Biol* 12:1-15.

Schulze, A., Zimmer, M., Mielke, S., Stellmach, H., Melnyk, C. W., Hause, B. & Gasperini, D. 2019. Wound-induced shoot-to-root relocation of JA-Ile precursors coordinates Arabidopsis growth. *Molecular plant* 12:1383-94.

Scott, J. J., Oh, D.-C., Yuceer, M. C., Klepzig, K. D., Clardy, J. & Currie, C. R. 2008. Bacterial protection of beetle-fungus mutualism. *Science* 322:63-63.

Shan, T., Rong, W., Xu, H., Du, L., Liu, X. & Zhang, Z. 2016. The wheat R2R3-MYB transcription factor TaRIM1 participates in resistance response against the pathogen Rhizoctonia cerealis infection through regulating defense genes. *Scientific reports* 6:1-14.

Shim, W.-B. & Dunkle, L. D. 2002. Identification of genes expressed during cercosporin biosynthesisin Cercospora zeae-maydis. *Physiol Mol Plant Pathol* 61:237-48.

Shinozaki, K. & Yamaguchi-Shinozaki, K. 2007. Gene networks involved in drought stress response and tolerance. *J Exp Bot* 58:221-27.

Sievers, F. & Higgins, D. G. 2014. Clustal Omega, accurate alignment of very large numbers of sequences. *Multiple sequence alignment methods*. Springer, pp. 105-16.

Silveira, T. L., Domingues, W. B., Remião, M. H., Santos, L., Barreto, B., Lessa, I. M., Varela Junior, A. S., Martins Pires, D., Corcini, C. & Collares, T. 2018. Evaluation of reference genes to analyze gene expression in silverside Odontesthes humensis under different environmental conditions. *Frontiers in genetics* 9:75.

Simão, F. A., Waterhouse, R. M., Ioannidis, P., Kriventseva, E. V. & Zdobnov, E. M. 2015. BUSCO: assessing genome assembly and annotation completeness with single-copy orthologs. *Bioinformatics* 31:3210-12.

Singh, V. & Aballay, A. 2006. Heat-shock transcription factor (HSF)-1 pathway required for Caenorhabditis elegans immunity. *Proceedings of the National Academy of Sciences* 103:13092-97.

Smith, C. A., O'Maille, G., Want, E. J., Qin, C., Trauger, S. A., Brandon, T. R., Custodio, D. E., Abagyan, R. & Siuzdak, G. 2005. METLIN: a metabolite mass spectral database. *Therapeutic drug monitoring* 27:747-51.

Smith, W. L., Urade, Y. & Jakobsson, P.-J. 2011. Enzymes of the cyclooxygenase pathways of prostanoid biosynthesis. *Chemical reviews* 111:5821-65.

Spoel, S. H. & Dong, X. 2012. How do plants achieve immunity? Defence without specialized immune cells. *Nature reviews immunology* 12:89-100.

Stack, J., Haga, I. R., Schro¨der, M., Bartlett, N. W., Maloney, G., Reading, P. C., Fitzgerald, K. A., Smith, G. L. & Bowie, A. G. 2005. Vaccinia virus protein A46R targets multiple Toll-like–interleukin-1 receptor adaptors and contributes to virulence. *The Journal of experimental medicine* 201:1007-18.

Stintzi, A. 2000. The Arabidopsis male-sterile mutant, opr3, lacks the 12-oxophytodienoic acid

reductase required for jasmonate synthesis. *Proceedings of the National Academy of Sciences* 97:10625-30.

Strittmatter, M., Grenville-Briggs, L. J., Breithut, L., Van West, P., Gachon, C. M. & Küpper, F. C. 2016. Infection of the brown alga E ctocarpus siliculosus by the oomycete E urychasma dicksonii induces oxidative stress and halogen metabolism. *Plant, Cell Environ* 39:259-71.

Su, C. & Oliw, E. H. 1996. Purification and characterization of linoleate 8-dioxygenase from the fungus Gaeumannomyces graminis as a novel hemoprotein. *J Biol Chem* 271:14112-18.

Su, C. & Oliw, E. H. 1998. Manganese lipoxygenase: purification and characterization. *J Biol Chem* 273:13072-79.

Su, C., Sahlin, M. & Oliw, E. H. 1998. A protein radical and ferryl intermediates are generated by linoleate diol synthase, a ferric hemeprotein with dioxygenase and hydroperoxide isomerase activities. *J Biol Chem* 273:20744-51.

Sugimoto, K., Matsui, K., Iijima, Y., Akakabe, Y., Muramoto, S., Ozawa, R., Uefune, M., Sasaki, R., Alamgir, K. M. & Akitake, S. 2014. Intake and transformation to a glycoside of (Z)-3-hexenol from infested neighbors reveals a mode of plant odor reception and defense. *Proceedings of the National Academy of Sciences* 111:7144-49.

Taki, N., Sasaki-Sekimoto, Y., Obayashi, T., Kikuta, A., Kobayashi, K., Ainai, T., Yagi, K., Sakurai, N., Suzuki, H. & Masuda, T. 2005. 12-oxo-phytodienoic acid triggers expression of a distinct set of genes and plays a role in wound-induced gene expression in Arabidopsis. *Plant Physiol* 139:1268-83.

Teng, L., Fan, X., Nelson, D. R., Han, W., Zhang, X., Xu, D., Renault, H., Markov, G. V. & Ye, N. 2019. Diversity and evolution of cytochromes P450 in stramenopiles. *Planta* 249:647-61.

Teng, L., Han, W., Fan, X., Xu, D., Zhang, X., Dittami, S. M. & Ye, N. 2017. Evolution and expansion of the prokaryote-like lipoxygenase family in the brown alga Saccharina japonica. *Frontiers in plant science* 8:2018.

Thomas, D., Beltrán, J., Flores, V., Contreras, L., Bollmann, E. & Correa, J. A. 2009. LAMINARIOCOLAX SP.(PHAEOPHYCEAE) ASSOCIATED WITH GALL DEVELOPMENTS IN LESSONIA NIGRESCENS (PHAEOPHYCEAE) 1. *J Phycol* 45:1252-58.

Thomas, F., Cosse, A., Goulitquer, S., Raimund, S., Morin, P., Valero, M., Leblanc, C. & Potin, P. 2011. Waterborne signaling primes the expression of elicitor-induced genes and buffers the oxidative responses in the brown alga Laminaria digitata. *PLoS One* 6:e21475.

Thomas, F., Cosse, A., Le Panse, S., Kloareg, B., Potin, P. & Leblanc, C. 2014. Kelps feature systemic defense responses: insights into the evolution of innate immunity in multicellular eukaryotes. *New Phytol* 204:567-76.

Todd, J. S., Proteau, P. J. & Gerwick, W. H. 1993. Egregiachlorides AC: new chlorinated oxylipins from the marine brown alga Egregia menziesii. *Tetrahedron Lett* 34:7689-92.

Todd, J. S., Proteau, P. J. & Gerwick, W. H. 1994. The absolute configuration of ecklonialactones A, B, and E, novel oxylipins from brown algae of the genera Ecklonia and Egregia. *J Nat Prod* 57:171-74.

Toporkova, Y. Y., Ermilova, V. S., Gorina, S. S., Mukhtarova, L. S., Osipova, E. V., Gogolev, Y. V. & Grechkin, A. N. 2013. Structure–function relationship in the CYP74 family: conversion of divinyl ether synthases into allene oxide synthases by site-directed mutagenesis. *FEBS Lett* 587:2552-58.

Toporkova, Y. Y., Fatykhova, V. S., Gogolev, Y. V., Khairutdinov, B. I., Mukhtarova, L. S. & Grechkin, A. N. 2017. Epoxyalcohol synthase of Ectocarpus siliculosus. First CYP74-related enzyme of oxylipin biosynthesis in brown algae. *Biochimica et Biophysica Acta (BBA)-Molecular*

and Cell Biology of Lipids 1862:167-75.

Toporkova, Y. Y., Gogolev, Y. V., Mukhtarova, L. S. & Grechkin, A. N. 2008. Determinants governing the CYP74 catalysis: conversion of allene oxide synthase into hydroperoxide lyase by site-directed mutagenesis. *FEBS Lett* 582:3423-28.

Torres, M. A. & Dangl, J. L. 2005. Functions of the respiratory burst oxidase in biotic interactions, abiotic stress and development. *Curr Opin Plant Biol* 8:397-403.

Tsugawa, H., Cajka, T., Kind, T., Ma, Y., Higgins, B., Ikeda, K., Kanazawa, M., VanderGheynst, J., Fiehn, O. & Arita, M. 2015. MS-DIAL: data-independent MS/MS deconvolution for comprehensive metabolome analysis. *Nat Methods* 12:523-26.

Van Alstyne, K. L. & Houser, L. T. 2003. Dimethylsulfide release during macroinvertebrate grazing and its role as an activated chemical defense. *Mar Ecol Prog Ser* 250:175-81.

Van Alstyne, K. L., Nelson, A. V., Vyvyan, J. R. & Cancilla, D. A. 2006. Dopamine functions as an antiherbivore defense in the temperate green alga Ulvaria obscura. *Oecologia* 148:304-11.

Vance, R. E., Hong, S., Gronert, K., Serhan, C. N. & Mekalanos, J. J. 2004. The opportunistic pathogen Pseudomonas aeruginosa carries a secretable arachidonate 15-lipoxygenase. *Proceedings of the National Academy of Sciences* 101:2135-39.

Vardi, A., Formiggini, F., Casotti, R., De Martino, A., Ribalet, F., Miralto, A. & Bowler, C. 2006. A stress surveillance system based on calcium and nitric oxide in marine diatoms. *PLoS Biol* 4:e60.

Varsani, S., Grover, S., Zhou, S., Koch, K. G., Huang, P.-C., Kolomiets, M. V., Williams, W. P., Heng-Moss, T., Sarath, G. & Luthe, D. S. 2019. 12-Oxo-phytodienoic acid acts as a regulator of maize defense against corn leaf aphid. *Plant Physiol* 179:1402-15.

Vidhyasekaran, P. 2016. *Switching on plant innate immunity signaling systems*. Springer,

Vigor, C., Reversat, G., Rocher, A., Oger, C., Galano, J.-M., Vercauteren, J., Durand, T., Tonon, T., Leblanc, C. & Potin, P. 2018. Isoprostanoids quantitative profiling of marine red and brown macroalgae. *Food Chem* 268:452-62.

Wang, F., Lv, Y., Lin, L., Xu, N., Lu, K. & Sun, X. 2018. Characterization of a respiratory burst oxidase homolog from Gracilariopsis lemaneiformis (Rhodophyta) during stress and phytohormone treatments. *Bot Mar* 61:511-19.

Wang, G., Chang, L., Zhang, R., Wang, S., Wei, X., Rickert, E., Krost, P., Xiao, L. & Weinberger, F. 2019. Can targeted defense elicitation improve seaweed aquaculture? *J Appl Phycol* 31:1845-54.

Wang, K.-D., Borrego, E. J., Kenerley, C. M. & Kolomiets, M. V. 2020. Oxylipins other than jasmonic acid are xylem-resident signals regulating systemic resistance induced by Trichoderma virens in maize. *The Plant Cell* 32:166-85.

Wang, S., Zhao, F., Wei, X., Lu, B., Duan, D. & Wang, G. 2013. Preliminary study on flg22-induced defense responses in female gametophytes of Saccharina japonica (Phaeophyta). *J Appl Phycol* 25:1215-23.

Wang, Y., Wang, H., Shen, Z., Zhao, L., Clarke, S., Sun, J., Du, Y. & Shi, G. 2009a. Methyl palmitate, an acaricidal compound occurring in green walnut husks. *J Econ Entomol* 102:196-202.

Wang, Z., Gerstein, M. & Snyder, M. 2009b. RNA-Seq: a revolutionary tool for transcriptomics. *Nature reviews genetics* 10:57-63.

Wasternack, C. & Feussner, I. 2018. The oxylipin pathways: biochemistry and function. *Annu Rev Plant Biol* 69:363-86.

Wei, Y., Liu, G., Chang, Y., He, C. & Shi, H. 2018. Heat shock transcription factor 3 regulates plant

immune response through modulation of salicylic acid accumulation and signalling in cassava. *Mol Plant Pathol* 19:2209-20.

Weinberger, F. 2007. Pathogen-induced defense and innate immunity in macroalgae. *The Biological Bulletin* 213:290-302.

Weinberger, F. & Friedlander, M. 2000. Response of Gracilaria conferta (Rhodophyta) to oligoagars results in defense against agar-degrading epiphytes. *J Phycol* 36:1079-86.

Wilhelmsson, P. K., Mühlich, C., Ullrich, K. K. & Rensing, S. A. 2017. Comprehensive genome-wide classification reveals that many plant-specific transcription factors evolved in streptophyte algae. *Genome biology and evolution* 9:3384-97.

Willey, J. M. & van der Donk, W. A. 2007. Lantibiotics: peptides of diverse structure and function. *Annu Rev Microbiol* 61:477-501.

Wu, J., Wang, L. & Baldwin, I. T. 2008. Methyl jasmonate-elicited herbivore resistance: does MeJA function as a signal without being hydrolyzed to JA? *Planta* 227:1161-68.

WYNNE, M. 1969. Life history and systematic studies of some Pacific North American Phaeophyceae (brown algae). *Univ. Cal. Publ. Bot.* 50:1-88.

Wynne, M. J. & Bold, H. 1985. *Introduction to the Algae: Structure and Reproduction.* Prentice-Hall, Incorporated,

Xu, D., Brennan, G., Xu, L., Zhang, X. W., Fan, X., Han, W. T., Mock, T., McMinn, A., Hutchins, D. A. & Ye, N. 2019. Ocean acidification increases iodine accumulation in kelp-based coastal food webs. *Global Change Biol* 25:629-39.

Yang, C., Pan, H., Noland, J. E., Zhang, D., Zhang, Z., Liu, Y. & Zhou, X. 2015. Selection of reference genes for RT-qPCR analysis in a predatory biological control agent, Coleomegilla maculata (Coleoptera: Coccinellidae). *Scientific reports* 5:18201.

Ye, N., Zhang, X., Miao, M., Fan, X., Zheng, Y., Xu, D., Wang, J., Zhou, L., Wang, D. & Gao, Y. 2015. Saccharina genomes provide novel insight into kelp biology. *Nature communications* 6:1-11.

Yokomizo, T., Nakamura, M. & Shimizu, T. 2018. Leukotriene receptors as potential therapeutic targets. *The Journal of clinical investigation* 128:2691-701.

Yoshida, T. 1979. Streblonema (Phaeophyceae) infection in the frond of cultivated Undaria (Phaeophyceae). *Proc. Int. Seaweed Symp.*, pp. 219-23.

Yuzuru, M., Teruhiko, B. & Kei, A. 1978. Crystallization and positional specificity of hydroperoxidation of Fusarium lipoxygenase. *Biochimica et Biophysica Acta (BBA)-Lipids and Lipid Metabolism* 530:439-50.

Zambounis, A., Elias, M., Sterck, L., Maumus, F. & Gachon, C. M. 2012a. Highly dynamic exon shuffling in candidate pathogen receptors··· what if brown algae were capable of adaptive immunity? *Mol Biol Evol* 29:1263-76.

Zambounis, A., Gaquerel, E., Strittmatter, M., Salaün, J.-P., Potin, P. & Küpper, F. C. 2012b. Prostaglandin A2 triggers a strong oxidative burst in Laminaria: a novel defense inducer in brown algae? *Algae* 27:21-32.

Zhan, A., Huang, X. & Li, S. 2019. Genome-wide identification and evaluation of new reference genes for gene expression analysis under temperature and salinity stresses in Ciona savignyi. *Frontiers in genetics* 10:71.

Zhang, H. & Forman, H. J. 2017. 4-hydroxynonenal-mediated signaling and aging. *Free Radical Biol Med* 111:219-25.

Zhang, L., Du, L. & Poovaiah, B. 2014. Calcium signaling and biotic defense responses in plants. *Plant signaling & behavior* 9:e973818.

Zhang, Y., Peng, X., Liu, Y., Li, Y., Luo, Y., Wang, X. & Tang, H. 2018. Evaluation of suitable reference genes for qRT-PCR normalization in strawberry (Fragaria× ananassa) under different experimental conditions. *BMC Mol Biol* 19:8.

Zhang, Y., Wang, X., Shan, T., Pang, S. & Xu, N. 2019. Transcriptome profiling of the meristem tissue of Saccharina japonica (Phaeophyceae, Laminariales) under severe stress of copper. *Marine genomics* 47:100671.

Zhao, Y., Dong, W., Zhang, N., Ai, X., Wang, M., Huang, Z., Xiao, L. & Xia, G. 2014. A wheat allene oxide cyclase gene enhances salinity tolerance via jasmonate signaling. *Plant Physiol* 164:1068-76.

List of abbreviations

ANOVA: analysis of variance

Fv/Fm: maximum quantum yield of photosystem II

GST: glutathione-S-transferase

HSP: heat-shock protein

LRR: leucine-rich-repeats

MAMPs: microbe-associated molecular pattern

MC5E: mannuronan C 5 epimerase

ML: maximum likelihood analysis

PAMPs: pathogen-associated molecular pattern

PCR: polymerase chain reaction

qPCR: quantitative polymerase chain reaction

RNA: ribonucleic acid

RNAseq: RNA sequencing

DNA: deoxyribonucleic acid

ROS: reactive oxygen species

VHOCs: volatile halogenated organic compounds

vBPO: vanadium-dependent bromoperoxidase

vHPO: vanadium-dependent haloperoxidase

GG: homopolymeric guluronate blocks

MG: alternating mannuronate and guluronate blocks

MM: homopolymeric mannuronate blocks

Appendix I : Oral presentation

- Annual meeting of the French Phycological Society (online) on 15th December 2020: "Deciphering molecular mechanism of kelp defenses upon biotic stress."(Xing Q., Rousvoal S., Corre E., Markov G., Peters AF., Leblanc C)

- 12th International Phycological Congress (online) from 22nd to 26th March 2021: "Deciphering molecular mechanism of kelp defenses upon biotic stress."(Xing Q., Rousvoal S., Corre E., Markov G., Peters AF., Leblanc C)

Appendix II: Presented posters

12th Congress of the International Plant Molecular Biology, 5-10 August 2018

Comparative transcriptomic analysis of the interaction between an algal endophyte and two kelp species

XING Qikun[1], BERNARD Miriam[1], ROUSVOAL Sylvie [1], CORRE Erwan[2], PETERS Akira F.[3], LEBLANC Catherine[1]

1- Sorbonne Université, CNRS, UMR8727, Integrative Biology of Marine Models Laboratory, Station Biologique de Roscoff, France
2- Sorbonne Université, CNRS, FR2424, Analysis and Bioinformatics for Marine Science, Station Biologique de Roscoff, France
3- Bezhin Rosko, Santec, France

Background

The algal endophyte *Laminarionema elsbetiae* is highly prevalent in European populations of the large brown alga, *Saccharina latissima*, but has also been found occasionally in the other kelp *Laminaria digitata*. Its presence coincides with morphological changes in the hosts such as twisted stipes and deformed blades, however, little is known about the molecular bases of this interaction. Using a co-cultivation experiment, we revealed that the growth of *L. digitata* was significantly affected by the presence of the endophyte after 6 days, but not that of *S. latissima*.

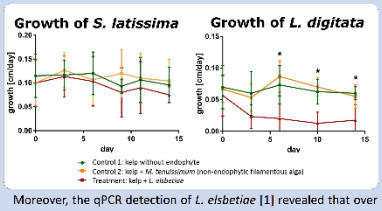

Moreover, the qPCR detection of *L. elsbetiae* [1] revealed that over 70% samples of *S. latissima* could be infected by *L. elsbetiae* after 2 weeks of co-culture, when only 30% of *L. digitata* showed an endophytic signal to endophyte interaction. These results suggested that physiological and defense responses are different according to the host species.

In this context, a comparative transcriptomic analysis was performed to get further insight into the molecular mechanisms induced in the two kelp hosts after the first contact with the endophyte.

Methods

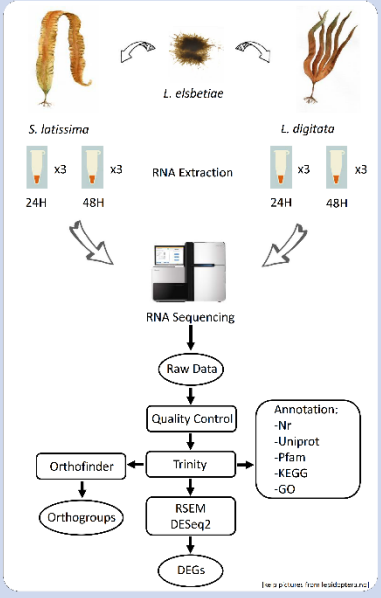

Fig.1 Treatment and sampling of co-cultivation samples and workflow of transcriptome analysis. Control samples are treated in the same process without co-cultivation of *L. elsbetiae*.

References

1. Bernard, Miriam, et al. "qPCR-based relative quantification of the brown algal endophyte *Laminarionema elsbetiae* in *Saccharina latissima*: variation and dynamics of host–endophyte interactions." Journal of Applied Phycology (2017): 1-11.
2. Grabherr, Manfred G., et al. "Trinity: reconstructing a full-length transcriptome without a genome from RNA-Seq data." Nature biotechnology 29.7 (2011): 644.
3. Emms, David M., and Steven Kelly. "OrthoFinder: solving fundamental biases in whole genome comparisons dramatically improves orthogroup inference accuracy." Genome biology 16.1 (2015): 157.

Results

Table1.Summary of the Trinity assembly and annotation for *S. latissima* and *L. digitata de novo* transcriptomes.

	S. latissima	*L. digitata*
Total number of reads	988,800,000	1,001,600,000
Number of used reads	900,200,999	910,400,000
Number of Trinity transcripts	23,049	28,766
Total size of the transcriptome (bp)	33,040,961	35,985,095
GC content	55.03	54.21
N50 length (bp)	1,869	1,562
Average contig length (bp)	1,433.51	1,250.96
Average mapping rate	92.13%	89.22%
Annotation rate (Blastx)	47.06%	42.28%

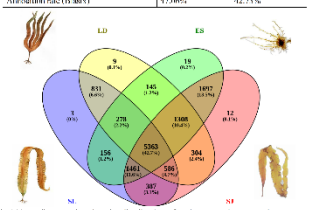

Fig.2 Venn diagram showing the distribution of orthogroups between the transcriptomes of four brown algae: *S. latissima* (SL), *L. digitata* (LD), *L. siliculosus* (LS) and *S. japonica* (SJ).

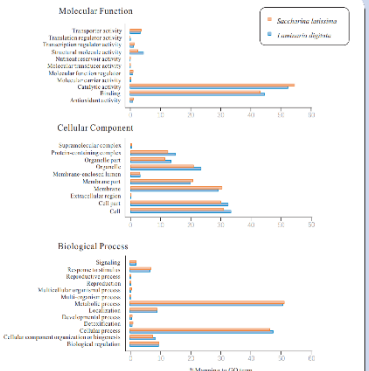

Fig.3 Distribution of the functional categories derived from Gene Ontology terms obtained by Blast2GO hits of genes from the *S. latissima* and the *L. digitata* transcriptome.

- According to the average transcripts length and mapping rate(Table.1), these two kelp de novo transcriptomes feature good quality in completeness of assembly.

- Orthogroups analysis among four brown algae species(Fig.2) showed a high proportion of common orthogroups comparing to available brown algal data, which showed a good coverage in gene content.

- The distribution of GO terms for the three root categories "Molecular Function", "Cellular Component" and "Biological process"(Fig.3) were very similar for the assembled transcriptomes of *S. latissima* and *L. digitata*.

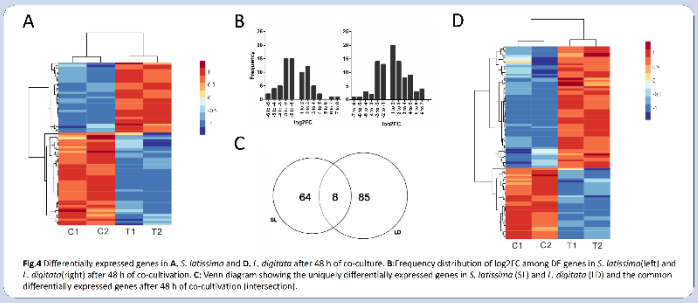

Fig.4 Differentially expressed genes in A. *S. latissima* and D. *L. digitata* after 48 h of co-culture. B:Frequency distribution of log2FC among DE genes in *S. latissima*(left) and *L. digitata*(right) after 48 h of co-cultivation. C: Venn diagram showing the uniquely differentially expressed genes in *S. latissima* (SL) and *L. digitata* (LD) and the common differentially expressed genes after 48 h of co-cultivation (intersection).

-Differential expression gene analysis showed that the transcriptional regulation occurred in both kelp species in response to the endophyte *L. elsbetiae*. However most of differential expressed genes (DEGs) were only detected in both kelp species after 48h(Fig.4 A+D).

-There were only 8 common DEGs between two species after 48h of co-cultivation(Fig.4C). Most of DEGs have lower fold changes compared to control condition(Fig.4B).

-Some host defense-related gene were found in DEGs.

In *L. digitata*, 93 DEGs in total. 58 upregulated genes, 35 downregulated genes.
Upregulated DEGs: NB-ARC and TPR repeat-containing protein, aryl sulfotransferase, EsV 1-7, Malic enzyme, Ubiquitin carboxyl-terminal hydrolase, Enoyl-CoA hydratase, etc.
Downregulated DEGs: Glutamate synthase, PR1-like metalloprotease, Beta-lactamase hydrolase, Carbonyl reductase, Proline iminopeptidase, etc.

In *S. latissima*, 72 DEGs in total. 32 genes upregulated, 40 genes downregulated.
Upregulated DEGs: Glutathione S-transferase, FAD linked oxidase, Methionine aminopeptidase, Mannuronan C-5 epimerase, Cathepsin H, etc.
Downregulated DEGs: Methionine-R-sulfoxide reductase, Guanylyl cyclase, LRR-GTPase of the ROCO family, FF2, Urease accessory protein ureG, Lipase, etc.

Conclusions

This first insight into host transcriptional regulation in kelp-endophyte interactions demonstrated that there are crucial differences between reaction of the main host *S. latissima* and occasional host *L. digitata* in response to the endophyte *L. elsbetiae*. For example, the early recognition process, strengthen of cell wall, oxidative burst, etc. We propose that these difference of early transcriptional regulation between two kelp species could be a possible explanation for the occurrence of different natural infection patterns.

Regulatory Oxylipins conference, 1-4 April 2019, GHENT, BELGIUM

Studies of the oxylipin pathway regulation in brown algal kelps

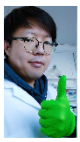

XING Qikun[1], MARKOV Gabriel [1], ROUSVOAL Sylvie [1], LEROUX Cédric [2], POTIN Philippe [1], LEBLANC Catherine [1]

1- Sorbonne Université, CNRS, UMR8727, Integrative Biology of Marine Models Laboratory, Station Biologique de Roscoff, France
2- Sorbonne Université, CNRS, FR2424, Metabomer-Corsaire, Station Biologique de Roscoff (SBR), Roscoff, France

1 Background

Among the Stramenopiles lineage, multicellular brown algae show simple filamentous, such in Ectocarpales, to very differentiated thalli, the largest and most complex ones belonging to the order of Laminariales (commonly known as kelps). Kelps form the largest marine community along the rocky coastal line and are involved in various biotic interactions with associated micro- and macro-organisms.

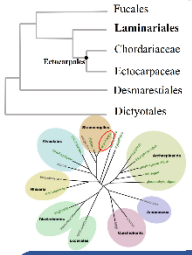

Similarly to land plants and animals, brown algal kelps featured inducible responses upon abiotic and biotic stress, such as the release of free polyunsaturated fatty acids (PUFAs), oxidized derivatives from both C18- and C20- PUFAs, and aldehydes. However, in the brown algal lineage, their biosynthesis pathway has been hardly explored neither their biological roles in the induction of defense or signaling metabolic responses.

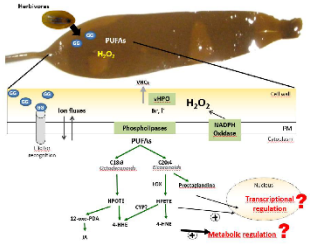

2 Method

Phylogenetic analysis of P450 and LOX genes

The HMMER3 software with default parameters was used to search P450 and LOX domains in the genome-translated proteomes of each species. Redundant sequences were discarded from the data set to obtain unique P450 and LOX genes. These sequences were aligned using CLUSTAL Omega. The alignment files were used as input for MEGA 7.0 to build the ML phylogenetic trees.

Oxidative response measurement and LC-MS metabolic profiling

The net production of H_2O_2 was determined in seawater surrounding aldehyde- or oxylipin-treated kelps, using a luminol chemiluminescence method (Glazener et al. 1991).
Ethyl acetate metabolic extracts of *Saccharina latissima* and *Laminaria digitata* were prepared after 4 hours of 4-HHE treatment and analyzed by LC-MS on the Metabomer plateform. The LC-MS data were analyzed using the Workflow4Metabo pipeline (Giacomoni et al. 2014).

3 Phylogenetic analysis

Phylogenetic analysis of LOX genes

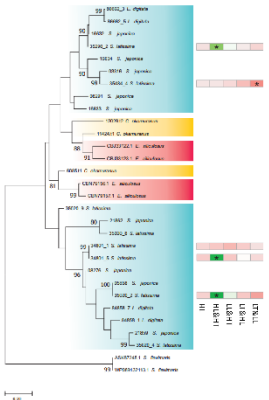

Fig1. Phylogenetic tree of LOX genes in selected brown algae.

The phylogenetic analysis revealed a recent duplication of LOX genes in Laminariales. In addition, differential expression analysis based on previous microarray data (Heinrich et al. 2012) showed diverse expression patterns of LOX homologs in *S. latissima*, upon abiotic stress, suggesting different biological functions in this complex multigenic family.

Phylogenetic analysis of P450 genes

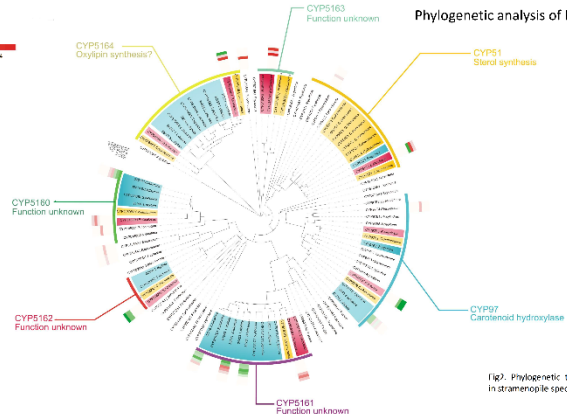

Fig2. Phylogenetic tree of P450s in stramenopile species.

Similarly, the phylogenetic analysis supported the high diversity of P450s in Stramenopiles, P450s were devided into seven major groups. In group CYP5161 and CYP5164, the phylogenetic tree showed gene duplication of P450s in Laminariales. These genes have different patterns under abiotic stress, which also indicated different biological functions. The biochemical functions of four groups are still unknown, and could be related to the oxylipin pathway.

4 Preliminary results on oxylipin pathway regulation analysis

H_2O_2 measurement

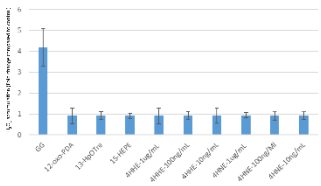

Fig3. H_2O_2 accumulation over 1 hour, in surrounding seawater of *S. saccharina* after the incubation with different aldehydes, oxylipins and oligoalginates (GG) for 4 hours. 4HHE:4-hydroxy-hexenal, 4-HNE:4-hydroxy-nonenal ; 13-HpOTre 13-hydroperoxy-9,11E,15Z-octadecatrienoic acid; 15-HLPL (±)-15-hydroxy-5Z,8Z,11Z,13E,17Z-eicosapentaenoic acid

At the contrary of oligoalginates elicitation, oxylipin-related compounds do not trigger an oxidative burst in *S. latissima* plantlets.

Metabolomic changes analyzed by LC-MS

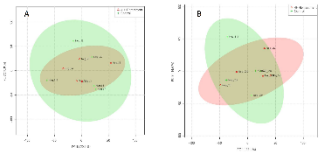

Fig4. PCA plot of the control and 4-HHE treatment samples in *S. latissima*(A) and *L. digitata*(B).

No significant change of metabolic patterns was observed after four hours of 4-HHE treatment in *S. latissima*, while in *L. digitata*, 12 differentially expressed ions were detected. Among those ions, two compounds were annotated as compounds which potentially related to defense reactions against herbivores.

5 Conclusions & future work

Kelps show more gene duplications and complex expression profiles compared to Ectocarpales, in both LOX and P450s families, suggesting different functions. Additional expression and biochemical studies will be necessary to better understand their involvement in oxylipin pathway.
Preliminary results have shown that some oxylipin-related compounds such as 4-HHE might trigger metabolic regulation and defense reactions in kelps, but without inducing any oxidative burst.
The annotation of differentially-expressed compounds will be validated using LC-MS/MS analysis.
Other oxylipin-related compounds will be tested on the regulation of metabolic pathways using LC-MS and of gene expression by transcriptomic analysis.

References

Glazener et al. "An improved method for monitoring active oxygen in bacteria-treated suspension cells using luminol-dependent chemiluminescence." Physiological and Molecular Plant Pathology 39.2 (1991): 123-133.
Heinrich et al. "Transcriptomic analysis of acclimation to temperature and light stress in *Saccharina latissima* (Phaeophyceae)." PLoS One 7.8 (2012): e44342.
Giacomoni et al. "Workflow4Metabolomics: a collaborative research infrastructure for computational metabolomics." Bioinformatics 31.9 (2014): 1493-1495.

Résumé

Les oxylipines sont des composés oxygénés dérivés d'acides gras polyinsaturés (AGPI), présents dans de nombreux organismes. Chez les plantes et les animaux, ils ont des rôles signaux dans la croissance et en réponse à divers stress. Les algues brunes ont développé des voies de biosynthèse des oxylipines uniques, à partir des AGPI de types C18 et C20. Cependant, le rôle et la régulation de ces voies sont encore peu connus chez les algues brunes, notamment pendant les réponses de défense. Au cours de ma thèse, j'ai mené des analyses transcriptomiques à large échelle afin de déchiffrer les régulations moléculaires chez deux espèces d'algues brunes, *Saccharina latissima* et *Laminaria digitata*, lors d'interactions biotiques, en relation avec l'induction des voies des oxylipines. La co-culture avec un endophyte a montré de faibles effets sur la transcription des gènes à un stade précoce, chez ces deux espèces, mais des schémas de régulation distincts. Seuls trois gènes liés à la biosynthèse d'oxylipines étaient surexprimés chez *S. latissima*, co-cultivée avec l'endophyte. Pour explorer plus avant la régulation de ces voies, des sporophytes de *S. latissima* ont été traités avec des oligoguluronates (GG) pour analyser les changements transcriptomiques et métabolomiques au cours du temps suite à l'élicitation des défenses. Parmi les gènes différentiellement exprimés, plusieurs gènes pourraient être liés aux voies des oxylipines. Un gène codant potentiellement pour un cytochrome P450 (CYP) est surexprimé à 1 h et 12 h, suggérant une induction séquentielle des voies des oxylipines chez *S. latissima*. Plusieurs oxylipines, issues de la voie des AGPI en C18, seraient accumulées après 0,5 h, montrant une production précoce de ces signaux potentiels. De plus, l'inhibition des lipoxygénases supprime cette production suite à l'élicitation par les GG et conduit à l'accumulation de métabolites liés aux composés dérivés des AGPI en C20, suggérant le rôle alternatif de cette voie. Enfin, le rôle biologique de plusieurs oxylipines et aldéhydes a été étudié. Parmi ces composés, le 4-hydroxy hexénal (4-HHE) et le 13-HpOTrE ont induit la surexpression de certains gènes, comme un gène codant une CYP, et l'accumulation de composés putatifs de défense chez *L. digitata* ou *S. latissima*. Ces résultats suggèrent que le 4-HHE et le 13-HpOTrE pourraient agir comme des molécules signal chez ces espèces. Les résultats de ces travaux ont permis de reconstruire partiellement les voies des oxylipines et de mieux comprendre leur régulation lors des réponses de défense chez les grandes algues brunes.

Abstract

Oxylipins are oxygenated compounds derived from polyunsaturated fatty acids (PUFAs), found in many organisms. In land plants and animals, they are known to have regulating roles in growth and in response to various stresses. Brown algae have developed unique oxylipin pathways, using both C18- and C20- type PUFAs. However, the role and regulation of oxylipin pathways during defense responses are largely unclear in brown algae. In my PhD thesis, I conducted large transcriptomic analyses in order to decipher the molecular responses of two kelps species, *Saccharina latissima* and *Laminaria digitata* during biotic interactions, in relationships with the induction of oxylipin pathways. First a co-cultivation with an endophyte showed small impacts on the transcriptomic regulation in both kelps at early stage, but with different patterns. Only three genes related to oxylipin pathways were up-regulated in *S. latissima* co-cultivated with the endophyte. To further explore the regulation of oxylipin pathways, oligoguluronates were used to analyze the time-course of transcriptomic and metabolomic changes in *S. latissima* sporophytes upon defense elicitation. Among differentially expressed genes, several genes putatively involved in oxylipin pathways were identified with diverse expression patterns. One putative cytochrome P450 (CYP)-encoding gene was induced at 1 h and 12 h, suggesting that oxylipin pathways in *S. latissima* might be induced at least two times. Several putative oxylipins, derived from C18 oxylipin pathways, were accumulated at 0.5 h, showing an early production of these potential signaling compounds. In addition, the inhibition of lipoxygenases before GG elicitation suppressed this production and led to the accumulation of metabolites related to C20-PUFAs derived compounds at 0.5 h, suggesting the putative alternative role of C20 oxylipin pathways. Finally, the biological function of several oxylipins and aldehydes were tested on targeted gene or metabolite inductions in S. latissima and L. digitata. Altogether, these results led to the partial reconstruction of oxylipin pathways and provide a better understanding of their regulation during defense responses in kelps.